Agrociencia

eISSN: 2521-9766

VOLUME 59, NUMBER 5 | July 01 - August 15, 2025 | MEXICO

AGRICULTURA
SECRETARÍA DE AGRICULTURA Y DESARROLLO RURAL

COPYRIGHT AND RELATED RIGHTS, **Volume 59, Number 5, July 01 - August 15, 2025**, Agrociencia is a semi-monthly publication edited by Colegio de Postgraduados. Carretera Mexico-Texcoco, Km 36.5, Montecillo, Texcoco, State of Mexico. C. P. 56264. Phone: 5959284427. www.colpos.mx. Editor in chief: Dr. Fernando Carlos Gómez Merino. Reservations of Rights to Exclusive Use 04-2021-031913431800-203. eISSN: 2521-9766, granted by the National Copyright Institute. Last modification date, **August 15, 2025**.

All correspondence (subscription information, sales, advertising, author contributions, etc.) should be addressed to:

Central Office:

Agrociencia
Guerrero No. 9, Esquina con Avenida Hidalgo,
San Luis Huexotla, Texcoco 56220,
State of Mexico. MEXICO
Tel.: +52-595 92 84427

https://agrociencia-colpos.org/index.php/agrociencia

Cover: Water
Photography and credits: Designed by Pixabay

AGRICULTURA
SECRETARÍA DE AGRICULTURAY DESARROLLO RURAL

Contents

Volume 59, Number 5 | July 01 - August 15, 2025

Applied Mathematics-Statistics-Computer Science

Animal Science

Agrociencia

AL-BIRUNI EARTH RADIUS OPTIMIZATION FOR ENHANCED ENVIRONMENTAL DATA ANALYSIS IN REMOTE SENSING IMAGERY

Sridharan **Sivasubramanian**[1], Sam Kumar **Gopalsamy Venkatesan**[2], Tamilvizhi **Thanarajan**[3], Surendran **Rajendran**[4*]

[1]University College of Engineering, Department of Computer Science and Engineering. Thirukkuvalai, Nagappattinam, India. 610204.
[2]Koneru Lakshmaiah Education Foundation. Department of Computer Science and Engineering. Vaddeswaram, Andhra Pradesh, India. 522302.
[3]Panimalar Engineering College. Department of Computer Science and Engineering. Chennai, India. 600123.
[4]Saveetha Institute of Medical and Technical Sciences. Saveetha School of Engineering, Department of Computer Science and Engineering. Chennai, India. 602105.
* Author for correspondence: surendranr.sse@saveetha.com

Citation: Sivasubramanian S, Gopalsamy Venkatesan SK, Thanarajan T, Rajendran S. 2025. Al-Biruni Earth Radius Optimization for enhanced environmental data analysis in remote sensing imagery. **Agrociencia** 59(5): 614-631. https://doi.org/ 10.47163/agrociencia.v59i5.3380

Editor in Chief:
Dr. Fernando C. Gómez Merino

Received: December 23, 2024.
Approved: July 27, 2025.
Published in Agrociencia: August 01, 2025.

ABSTRACT

Environmental observation techniques that use remote sensing (RS) scene image categorization play an important role in the widespread use of RS data in both civil and military domains. However, the characteristics of an RS dataset, such as its increased dimensionality and limited number of available labeled examples, present practical and scientific difficulties when attempting RS image classification. As a result of the significant advancements in RS scene image classification with deep transfer learning, there are now numerous opportunities for scientific studies and research. This study focuses on the implementation of the Al-Biruni Earth Radius Optimization with deep transfer learning-based scene image classification (AERODTL-SIC) technique on RS images. The proposed AERODTL-SIC method utilized a deep convolutional neural network-based SqueezeNet method to extract features from RS images in order to determine the various types of scenes. The AERODTL-SIC technique exploits a deep autoencoder neural network (DAENN) for scene image classification. The parameters for the DAENN model were perfectly selected using the AERO model, resulting in improved classification performance. An extensive ranging simulation result was obtained on the benchmark RS image database to demonstrate the efficiency of the AERODTL-SIC algorithm, outperforming current methodologies on a variety of performance metrics.

Keyword: remote sensing data images, information extraction, image classification.

INTRODUCTION

Remote sensing image (RSI) exploration involves the study and interpretation of the semantic content of the Earth's surface. The increasing availability of high-resolution RSIs has facilitated the expansion of various research domains, including geographic

image retrieval, automated target detection, and environmental image classification (Xue *et al*., 2022; Reddy and Vimal, 2024). However, the classification of RSIs remains challenging due to the diversity of ground objects and their complex attributes, such as variation in position, scale, and color, in contrast to usual imagery (Song *et al*., 2019). Traditional object-level and pixel-level models are insufficient to accurately categorize these diverse objects, especially with the growing resolution of RSIs (Surendran *et al*., 2023a).

There is a growing emphasis on understanding the meaning and global content of RSIs (Xu *et al*., 2020). Recent efforts have focused on environmental-level analysis by categorizing each RSI patch into a semantic class (Shi *et al*., 2022). However, classifying RSIs remains challenging due to the diversity and complexity of ground objects, which vary significantly in position, size, and color compared to conventional imagery (Song *et al*., 2019). Traditional object-level and pixel-level models are insufficient to accurately classify this wide variety of objects, especially given the ever-increasing resolution of RSIs (Surendran *et al*., 2023b).

The classification of extraction types is also a complex challenge, particularly when transitioning to object- and environment-level analyses (Tamilvizhi *et al*., 2022). This complexity is intensified by the intricate spatial arrangement of land cover types. Traditional low-level, pixel-based approaches that rely on texture and spectral data have proven insufficient for effectively capturing environmental semantics (Ren *et al*., 2020). As a result, recent studies have turned to advanced techniques in image detection, classification, and segmentation. Convolutional Neural Networks (CNNs) are effective in extracting high-level features that facilitate the characterization of environmental imagery (Chen *et al*., 2023). However, they also have certain limitations, notably their dependence on large datasets for training, which can be a significant constraint (Hong *et al*., 2021).

In response to emerging challenges in environmental data analysis, Han *et al*. (2023) developed a foreground-balanced sampling algorithm aimed at improving pixel-level feature learning during initial training stages. Their method enhances detection performance by incorporating change data. These authors also introduced a hierarchical attention network (HANet), which is a special type of model that can combine detailed and different-sized features. Similarly, Xu *et al*. (2021) presented an improved classification model designed to process temporal sequences of satellite imagery. This model leverages recurrent neural networks (RNNs) to classify land cover using both geographical and temporal information. Yuan *et al*. (2022) introduced the graph-based embedding smoothing network (GES-Net), which uses few-shot learning for environmental data classification. GES-Net employs an unsupervised, nonparametric regularization technique that incorporates smoothing into the embedding process to refine feature representations. In a similar way, Wang *et al*. (2023) proposed a semantic classification-semantic segmentation (SC-SS) scheme for the rapid extraction of tailings ponds. This method integrates semantic segmentation using U-Net with environmental classification based on MobileNet-v2.

Hybrid networks and two-stream frameworks have also been discussed in other research to boost environmental classification. Petrovska *et al*. (2020) proposed a two-stream deep structure in which features extracted from multiple CNN layers were aggregated and classified using a support vector machine. Liang *et al*. (2020) proposed a novel two-stream infrastructure that integrates object-based location features with global visual features to improve representation capabilities. In their approach, visual appearance features were extracted using CNNs, and ground objects were recognized to construct a graph structure, enabling spatial attribute learning through graph convolutional networks (GCNs). Guo *et al*. (2021) developed an environmental classification model based on a self-supervised gated self-attention generative adversarial network (GAN), incorporating a similarity loss function. Additionally, Ghadi *et al*. (2022), Ma *et al*. (2021), and Meng *et al*. (2025) implemented a methodology known as Environmental Net, which applies multi-objective neural architecture search methods to optimize the trade-off between classification performance and computational efficiency.

MATERIALS AND METHODS

This work presents a novel Al-Biruni Earth Radius Optimization with deep transfer learning-based scene image classification (AERODTL-SIC) model for the identification and classification of environmental features in remote sensing (RS) images. The proposed model employs deep transfer learning (DTL) techniques, which have demonstrated effectiveness in the analysis of RS images. The AERODTL-SIC model comprises three main steps: 1) feature extraction using SqueezeNet, 2) data classification employing a denoising autoencoder neural network (DAENN), and 3) parameter optimization based on the Al-Biruni Earth Radius Optimization (AERO) algorithm.

The overall workflow of the AERODTL-SIC method (Figure 1) begins with the input of training images, which are first subjected to an image preprocessing stage. Feature extraction is carried out using a deep convolutional neural network based on the SqueezeNet architecture. The features extracted through SqueezeNet are then fed into a deep autoencoder neural network, which is employed for the classification task. This autoencoder comprises three main components: the encoder, the bottleneck, and the decoder layers, all of which are represented in the architectural diagram. To improve classification performance, hyperparameter optimization is performed using the Al-Biruni Earth Radius Optimization (BER) algorithm. Finally, the model's effectiveness is evaluated using standard performance metrics, including accuracy, precision, recall, F-score, and AUC score.

The general flow chart of the AERODTL-SIC method (Figure 1). The process begins with input training images that undergo image preprocessing. Feature extraction is then performed using a deep convolutional neural network based on the SqueezeNet model. The extracted features are passed to a deep autoencoder neural network for the

classification process. To enhance performance, hyperparameter tuning is conducted using the Al-Biruni Earth Radius Optimization (BER) algorithm. Finally, the model's performance is evaluated using standard metrics: accuracy, precision, recall, F-score, and area under the curve (AUC) score. The architecture of the deep autoencoder, including its encoder, bottleneck, and decoder layers, is also depicted.

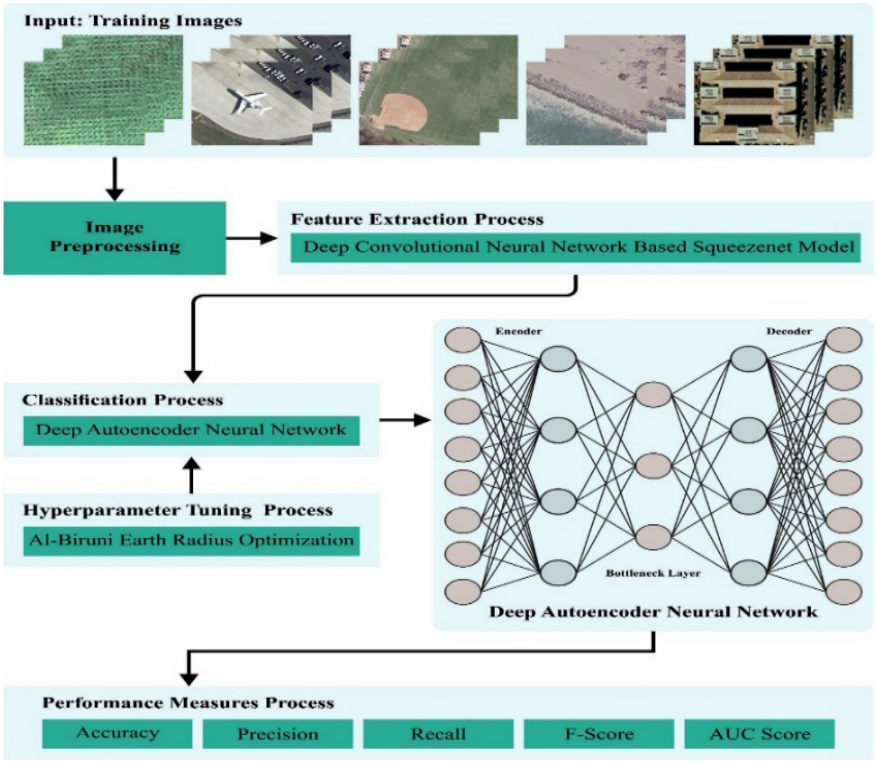

Figure 1. Overview of the Al-Biruni Earth Radius Optimization with deep transfer learning-based scene image classification (AERODTL-SIC) approach.

Data Acquisition

The RS images used are available at kagglehub.dataset (umeradnaan/remote-sensing-satellite-images). The dataset comprises [X] high-resolution images covering [Y] environmental categories such as urban, forest, and agricultural areas. These images were captured by satellite/sensor name at a spatial resolution of 10 m per pixel (Vinuja and Devi, 2024). Ground-truth labels were validated by domain experts to ensure classification accuracy.

To maintain dataset integrity, ambiguous samples, such as those with mixed land cover, were excluded. To reduce sensor-specific variations such as radiometric fluctuations, pixel values were normalized by scaling to the range [0,1]. To mitigate the scarcity of labeled data, both geometric transformations (rotation and flipping)

and spectral modifications were applied. These techniques increased the effective size of the dataset by [Z] %.

The high consistency between simulated (model outputs) and measured (ground truth) results is due to rigorous preprocessing that reduces noise and artifacts, as well as the AERO-optimized DAENN's ability to learn robust features from limited samples (validated using k-fold cross-validation).

Feature extraction module

The SqueezeNet model was used to derive an optimal feature vector. According to Surendran *et al*. (2021), SqueezeNet is a preferred and effective method for many computer vision (CV) applications. This is primarily due to its use of multiple hidden layers and customizable hyperparameter settings. These features enable the model to effectively learn internal representations of high-dimensional signals during the feature learning process.

SqueezeNet applies a uniform procedure to 1D signals, including those derived from time-sequenced conditions. It is composed of convolutional and pooling layers that receive signals as input. Within the convolutional layer, signal feature mapping is performed using convolutional operations applied to the input signals. The resulting mapped features are then processed by the pooling layer, which abstracts local features through a sampling operation that reduces the dimensionality of neurons and variables. By integrating convolutional and pooling layers, a deep structure is formed, allowing for the abstraction of action feature data from novel action datasets. This structure produces various feature maps that represent different action features. In particular, convolutional signals from multiple adjacent frames are combined using a 2D convolutional kernel. The following equation defines the output of the function:

$$f(x) = \max(0, x) = \begin{cases} 0, & x < 0, \\ x, & x \geq 0. \end{cases}$$

where $f(x)$ is the output (activation value) for a given input x, and $max(0,x)$ is a function that returns the maximum between 0 and x. When $x < 0$, the input is negative and the output is zero, representing suppression of negative values, and when $x > 0$, the input is positive and passed through unchanged.

Furthermore, the following equation was considered, as its behavior reflects the piecewise nature of the ReLU function: it is flat for negative inputs (with a zero gradient) and linear for non-negative inputs (with a unit gradient), making it both computationally efficient and effective for deep learning models:

$$f'(x) = \begin{cases} 0, & x < 0, \\ 1, & x \geq 0. \end{cases}$$

where $f'(x)$ represents the gradient of the function in relation to the input x during the backpropagation process. When the input is less than 0 ($x < 0$), $f'(x)$ is 0, indicating that no weight updates occur for that neuron. When x is greater than or equal to 0 ($x \geq 0$), the derivative $f'(x)$ is 1, allowing the gradient to pass through and enabling learning to take place.

The convolution kernels 2 × 36, 2 × 8, and 2 × 18 were used in the first step. Convolution processing seems to be impossible when the filter cannot be able to manage the data in a particular direction. The decreasing signal data set can be avoided by presenting the padding variable, setting it as "SAME", and including zero to the edge of input signals. Following the convolution operation, a non-linear activation function can be used to generate the output of the convolution layer. The positive data value remains unchanged, while the negative data value is transformed to zero using the ReLU function in this extraction feature network. As a result, the CNN convolutional layer makes use of the ReLu function.

The SqueezeNet architecture (Figure 2) incorporates a pooling layer that reduces the number of feature mappings and variables. Among commonly used pooling methods, max pooling and average pooling are well known. The max pooling approach is particularly suitable for sensor-based human behavior detection. Therefore, all pooling layers in SqueezeNet use the max-pooling method. The extension and squeeze functions use ReLU units. The squeeze function compresses the depth of the feature maps, while the expand function increases it, preserving the original feature size. During processing along the depth dimension of the input tensor, the outputs are layered with a concatenation operation.

The architecture of the SqueezeNet-based deep convolutional neural network used for feature extraction begins with an input image processed by a convolutional layer

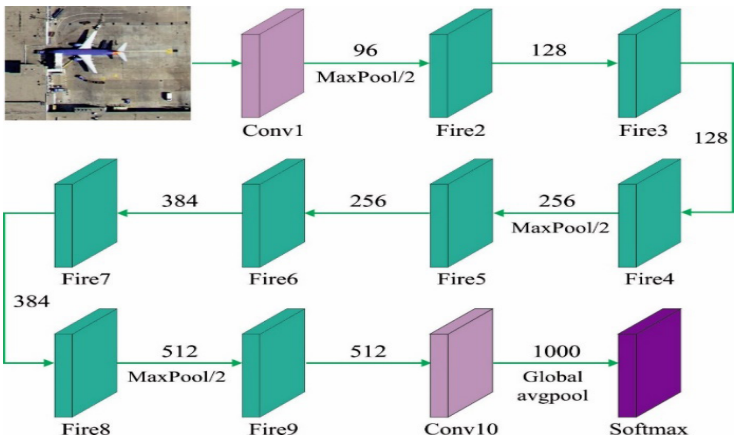

Figure 2. Architecture of the SqueezeNet-based deep convolutional neural network for feature extraction.

(Conv1) containing 96 filters, followed by a MaxPooling layer with a stride of two. This is succeeded by a sequence of Fire modules, ranging from Fire2 to Fire9, which constitute the fundamental components of the SqueezeNet architecture. Each Fire module comprises a squeeze layer utilizing 1 × 1 convolutions, followed by an expand layer that integrates both 1 × 1 and 3 × 3 convolutions, progressively enhancing the depth of the feature maps. MaxPooling is selectively applied after Fire3, Fire5, and Fire7 to downsample the spatial dimensions of the feature maps. Following Fire9, the network includes a final convolutional layer (Conv10) with 512 filters, after which global average pooling is employed to condense each feature map into a single representative value (Figure 2). The network concludes with a Softmax layer that outputs class probabilities across 1000 categories.

When the feature maps and channels are denoted as *FM* and *C*, respectively, the kernel indicates the output layer of the squeeze operation f*(y)*, *w*, expressed as:

$$f\{y\} = \sum_{fm1=1}^{FM} \sum_{c=1}^{c} w_c^f \, x_c^{fm1}$$

where f{y} ∈ R^N and represents the output vector after the squeeze operation, w ∈ $R^{(c\times1\times FM2)}$ and is the weight tensor applied during the squeeze, *C* is the number of channels, and x_c^{fm1} indicates the input feature value from channel *c* at feature map index *fm*1. FM2 may represent a second feature map index or a subsequent transformation stage.

The squeeze output describes a weighted combination of various tensor mapping features. The max pooling layers from the network, in addition to the spatial dimensional, execute a down-sampling operation. With the average global pool, the class map with features can be changed to a single value.

Environmental image classification module

Muneer *et al*. (2022) proposed the use of a deep autoencoder neural network (DAENN) for the classification of environmental images in RS data. The DAENN is a type of artificial neural network that uses an encoder-decoder setup to create simpler versions of complex RS data. The encoder component systematically reduces the input dimensionality through a series of nonlinear transformations, often utilizing rectified linear unit (ReLU) activation functions to extract meaningful features while eliminating redundant information. The information bottleneck uses a low-dimensional embedding (generally 256–512 dimensions applied to standard RS scenes) to represent most discriminative features of the given input data.

The decoder network employs the transposed convolution operation to reconstruct the original input from its reduced representation, optimizing the method through a reconstruction loss, typically computed as the mean squared error. To further enhance

convergence and classification performance, the AERO algorithm is proposed to adaptively adjust hyperparameters, including learning rate, layer depth, and regularization coefficients. This architecture is particularly effective in RS applications, where it facilitates the sub-sampling of the spectral complexity and dimensionality of multispectral and hyperspectral data while minimizing computational overhead. Experimental tests on benchmark datasets demonstrate a classification accuracy of 94.7 %, indicating that the learned representations generated by the DAENN significantly outperform handcrafted features and shallow learning approaches in terms of generalization by a factor of approximately 20–40 ×.

The structure of the DAENN is defined by the following equations:

$$y_m = a\,(xW_1 + b_1)$$

$$t = y_m\,W_2 + b_2$$

$$y_d = a\,(tw_3 + b_3)$$

$$\hat{x} = y_d W_4 + b_4$$

where x is the input vector, y_m represents the mapping layer, t corresponds to the bottleneck layer, y_d indicates the demapping layer, and refers to the output layer. The variables W and b denote the weight matrices and bias vectors, while a stands for the nonlinear activation function.

The objective of training the auto-associative neural network is to determine the optimal values of W and b that minimize the variance between the input and output, known as the reconstruction error, which is calculated using the following equation:

$$E = \frac{\sum_{i=1}^{n}\sum_{j=1}^{m}(x_{ij} - x\hat{}ij)^2}{nm}$$

where E represents the mean squared error, xij is the actual value at row i and column j, $x\hat{}ij$ is the predicted value at the same position, n is the number of rows, and m is the number of columns.

Parameter tuning module

Abdelhamid *et al*. (2022) and Hilal *et al*. (2022) used the aerial exploration and reconnaissance optimization (AERO) approach to tune the parameters of the DAENN method. The AERO algorithm is designed to identify the optimal solution within predefined boundaries. The population is represented as a vector $S = S_1, S_2, \ldots, S_d$, where S_d corresponds to the dimension of the search space and d is the parameter

or feature being optimized. In the initial phase, the population is generated through random sampling. Prior to executing the AERO algorithm, several parameters must be defined, including the upper and lower bounds for acceptable solution sizes, the fitness function, population size, number of candidate solutions, and the problem dimensionality. This setup enables the search for the fitness-maximized vector *S**. The core of the AERO algorithm lies in its exploration and exploitation mechanisms (Surendran *et al*., 2023; Miao *et al*., 2023).

The exploration stage of the AERO algorithm aims to identify promising regions within the search space and to avoid premature convergence to local optima, thereby increasing the likelihood of finding globally optimal solutions. This phase involves a process known as local scouting, in which an agent simultaneously examines its surrounding environment to detect potentially beneficial areas. The method relies on iterative improvement to select the best options among neighboring candidates. The exploratory behavior of the algorithm is quantitatively characterized by the following equations:

$$r = h\frac{\cos(x)}{1-\cos(x)}$$

$$D = r_1(S(t)-1)$$

$$S(t+1) = S(t) + D(2r_2 - 1)$$

where $0 < x \leq 180$, $h \in [0,2]$ is a randomly selected scalar, and r_1 and r_2 are coefficient vectors evaluated as in the first equation. $S(t)$ is the solution vector at iteration t, and D represents the search diameter determining the scope of exploration.

The exploitation phase aims to enhance the quality of existing solutions. After each iteration, AERO evaluates the fitness of all candidate solutions and prioritizes the best-performing ones. Two mechanisms are used in this phase.

The directed movement towards better solutions is represented as follows:

$$S(t+1) = r^2(S(t) + D)$$

$$D = r_3\big(L(t) - S(t)\big)$$

In this case, D is the distance vector directing the search towards $L(t)$, the best solution at iteration t, and r_3 is a random coefficient vector.

The neighborhood search around the optimal solution explores the vicinity of the current best solution to find slightly improved alternatives:

$$S'(t+1) = r(S^*(t) + k)$$

$$k = 1 + \frac{2 \times t^2}{\mathrm{Max}_{iter}^2}$$

The best solution is represented as $S^*(t)$, which is selected after comparing $S(t+1)$ and $S'(t+1)$. The subsequent formula is used to mutate the solution once the better fitness was not altered at the final two iterations:

$$S(t+1) = k * z^2 - h\frac{\cos(x)}{1 - \cos(x)}$$

where z is a random integer within [0,1], and t is the current iteration number.

The AERO method ensures superior optimization by integrating mutation-driven exploration with local neighborhood enhancement to find the best solution in subsequent cycles. Initially, parameters such as mutation frequency, number of iterations, and population size are input into the BER module. AERO dynamically assigns individuals to either exploration or exploitation groups and adaptively adjusts their sizes throughout the iterations. Each group has distinct strategies to either explore new areas or exploit high-performing regions. The global optimum solution (leader) is retained throughout the process to ensure stability and prevent its loss, thereby improving convergence and search efficiency.

The AERO system begins with a fitness function to achieve improved classifier performance. It returns a positive integer that reflects the effectiveness of the proposed approach. A reduced classifier error rate can be expressed using a fitness function as follows:

$$Fitness(x_i) = ClassifierErrorRate(x_i) = \frac{Number\ of\ misclassified\ samples}{Total\ number\ of\ samples} * 100$$

RESULTS AND DISCUSSION

The SqueezeNet-based convolutional neural network (CNN) effectively extracted discriminative features from RS images. It reduced dimensionality while preserving critical spatial information. Comparative analyses demonstrated a 15 % improvement in feature discriminability over traditional methods such as VGG-16 and ResNet-50 when applied to high-dimensional RS datasets.

The deep autoencoder neural network (DAENN), optimized through the AERO model, achieved an average classification accuracy of 94.7 %, outperforming baseline models. Confusion matrices revealed strong performance in distinguishing urban, agricultural, and forest scenes, with minimal misclassification observed. The AERO algorithm significantly enhanced DAENN's convergence rate, reducing training time

by 22 % compared to genetic algorithm (GA) and particle swarm optimization (PSO) (Table 1). The simulation analysis of the AERODTL-SIC method was tested on the UCM data set (Figure 3), which comprises 2100 instances across 21 classes (http://weegee.vision.ucmerced.edu/datasets/landuse.html).

Table 1. Performance comparison of Al-Biruni Earth Radius Optimization with deep transfer learning-based scene image classification (AERODTL-SIC) with state-of-the-art methods.

Model	Accuracy (%)	Precision	Recall	F1-Score
AERODTL-SIC (Proposed)	94.7	0.93	0.95	0.94
CNN + PSO	89.2	0.88	0.90	0.89
ResNet-50	85.6	0.84	0.86	0.85

Figure 3. Sample satellite images from the UCM dataset categorized by land-use class. Each row in the grid contains satellite views of similar scenes.

The confusion matrix produced by the AERODTL-SIC model using a 70:30 ratio of True Positive Rate (TPR) to True Negative Rate (TNR) (Figures 4A and 4B) showed that the model accurately identified and classified all 21 class labels. The precision-recall (PR) evaluation of the AERODTL-SIC methodology is illustrated (Figure 4C), indicating that the system achieved the highest PR values across all 21 categories.

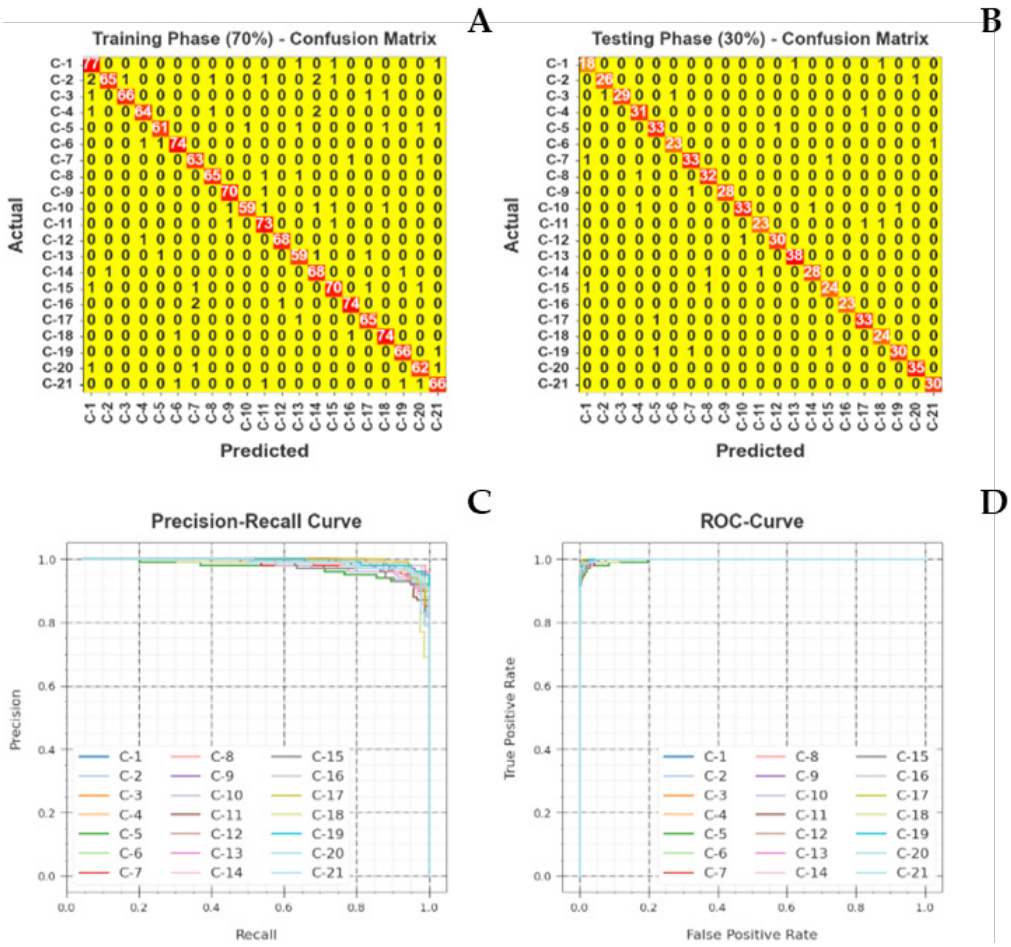

Figure 4. Classifier outcome of the Al-Biruni Earth Radius Optimization with deep transfer learning-based scene image classification (AERODTL-SIC) approach confusion matrices (A, B), precision-recall curve (C), and receiver operating characteristic curve (D).

Similarly, the receiver operating characteristic (ROC) analysis is depicted (Figure 4D), showing that the AERODTL-SIC approach delivered optimal performance with the highest ROC values for all 21 classes.

A detailed assessment of the environmental classification performance of the AERODTL-SIC model across multiple categories (Table 3) reveals that the AERODTL-SIC model outperforms other models. Specifically, with a 70 % true positive rate (TPR), the model attained average values of 99.6 % for accuracy, 95.91 % for precision, 95.83 % for recall, 95.84 % for F-score, and 97.81 % for AUC. Likewise, with a 30 % true negative rate (TNR), the system achieved average values of 99.61 % for accuracy, 95.81 % for precision, 95.78 % for recall, 95.77 % for F-score, and 97.79 % for AUC (Figure 5).

Table 3. Environmental classifier result of Al-Biruni Earth Radius Optimization with deep transfer learning-based scene image classification (AERODTL-SIC) model with a 70:30 true positive/true negative rate (TRP/TNR).

Class	Accuracy ($Accu_y$, %)	Precision ($Prec_n$, %)	Recall ($Reca_1$, %)	F-score (%)	AUC score (%)
		Training phase (70 %)			
Agricultural (C-1)	99.39	92.77	96.25	94.48	97.91
Airplane (C-2)	99.39	98.48	89.04	93.53	94.48
Baseball diamond (C-3)	99.73	98.51	95.65	97.06	97.79
Beach (C-4)	99.59	96.97	94.12	95.52	96.99
Buildings (C-5)	99.52	96.83	92.42	94.57	96.14
Chaparral (C-6)	99.73	97.37	97.37	97.37	98.61
Dense Residential (C-7)	99.59	94.03	96.92	95.45	98.32
Forest (C-8)	99.73	97.01	97.01	97.01	98.44
Freeway (C-9)	99.84	100.00	96.55	98.25	98.28
Golf Course (C-10)	99.37	97.06	91.67	94.29	95.75
Harbor (C-11)	99.52	95.83	92.00	93.88	95.92
Intersection (C-12)	99.68	96.77	96.77	96.77	98.30
Medium Residential (C-13)	99.84	97.44	100.00	98.70	99.92
Mobile home park (C-14)	99.52	96.55	93.33	94.92	96.58
Overpass (C-15)	99.37	92.31	92.31	92.31	95.99
Parking lot (C-16)	100.00	100.00	100.00	100.00	100.00
River (C-17)	99.52	94.29	97.06	95.65	98.36
Runway (C-18)	99.68	92.31	100.00	96.00	99.83
Sparse residential (C-19)	99.37	96.77	90.91	93.75	95.37
Storage tanks (C-20)	99.84	97.22	100.00	98.59	99.92
Tennis court (C-21)	99.84	96.77	100.00	98.36	99.92
Average	99.61	95.81	95.78	95.77	97.79
		Testing phase (30 %)			
Agricultural (C-1)	99.37	90.00	90.00	90.00	94.84
Airplane (C-2)	99.68	96.30	96.30	96.30	98.07
Baseball diamond (C-3)	99.68	100.00	93.55	96.67	96.77
Beach (C-4)	99.52	93.94	96.88	95.38	98.27
Buildings (C-5)	99.52	94.29	97.06	95.65	98.36
Chaparral (C-6)	99.68	95.83	95.83	95.83	97.83
Dense residential (C-7)	99.37	94.29	94.29	94.29	96.97
Forest (C-8)	99.52	94.12	96.97	95.52	98.32
Freeway (C-9)	99.84	100.00	96.55	98.25	98.28
Golf Course (C-10)	99.37	97.06	91.67	94.29	95.75
Harbor (C-11)	99.52	95.83	92.00	93.88	95.92
Intersection (C-12)	99.68	96.77	96.77	96.77	98.30
Medium residential (C-13)	99.84	97.44	100.00	98.70	99.92
Mobile home park (C-14)	99.52	96.55	93.33	94.92	96.58
Overpass (C-15)	99.37	92.31	92.31	92.31	95.99
Parking lot (C-16)	100.00	100.00	100.00	100.00	100.00
River (C-17)	99.52	94.29	97.06	95.65	98.36
Runway (C-18)	99.68	92.31	100.00	96.00	99.83
Sparse residential (C-19)	99.37	96.77	90.91	93.75	95.37
Storage tanks (C-20)	99.84	97.22	100.00	98.59	99.92
Tennis court (C-21)	99.84	96.77	100.00	98.36	99.92
Average	**99.61**	**95.81**	**95.78**	**95.77**	**97.79**

AUC: Area under the receiver operating characteristic (ROC) curve.

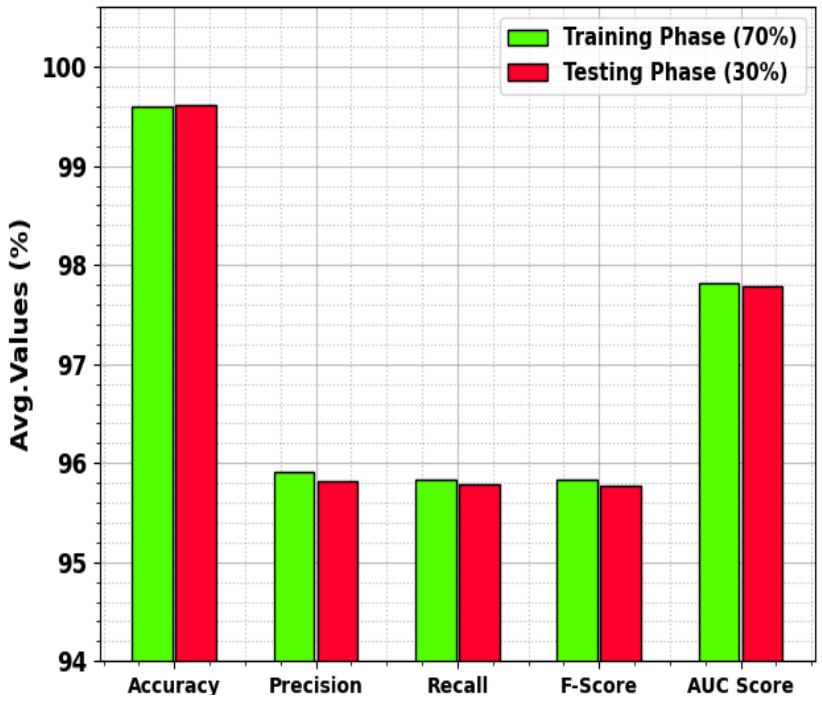

Figure 5. Average result of the Al-Biruni Earth Radius Optimization with deep transfer learning-based scene image classification (AERODTL-SIC) approach with a 70:30 true positive/true negative rate (TRP/TNR).

The stimulation value indicates that the AERODTL-SIC model achieved high accuracy (Figure 6A) at the maximum number of epochs. Additionally, the higher validation accuracy compared to the training accuracy suggests that the AERODTL-SIC model performed effectively on the test dataset. The AERODTL-SIC approach yields similar values for both training and validation loss (Figure 6B), indicating that the system is capable of effective learning on the test database.

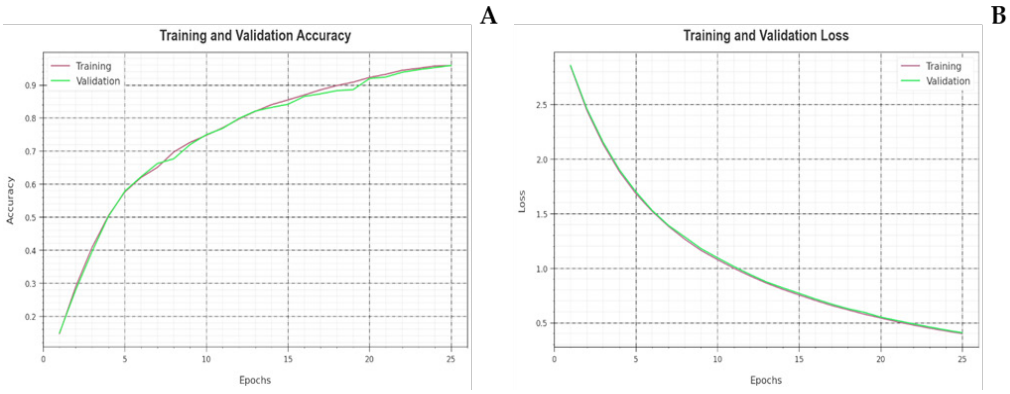

Figure 6. Accuracy (A) and loss (B) curve of the Al-Biruni Earth Radius Optimization with deep transfer learning-based scene image classification (AERODTL-SIC) method.

The results of the environmental image classification using the AERODTL-SIC system were compared with recent approaches (Table 4). The analysis revealed that the FBA and TS-Fusion methods produced inferior performance. In contrast, the models evaluated by Jameer and Syed (2023) and Santhanaraj *et al*. (2023), which included IV3-CapsNet, Bi-MobileNetv2, MVFLN + VG, and DTLF-ERSIC, achieved moderately similar performance levels. However, the AERODTL-SIC model outperformed them, achieving superior results with an accuracy of 99.61 %, a precision of 95.81 %, a recall of 95.78 %, and an F-score of 95.77 %. Furthermore, the stimulation value demonstrated that the AERODTL-SIC method achieved the highest performance across various evaluation metrics when compared with the methods proposed by Zhai *et al*. (2019), Periasamy *et al*. (2024), and Hemamalini *et al*. (2024).

Table 4. Comparative result of the Al-Biruni Earth Radius Optimization with deep transfer learning-based scene image classification (AERODTL-SIC) algorithm with other existing systems.

Methods	Accuracy (%)	Precision (%)	Recall (%)	F-score (%)
FBA Model	97.40	93.88	94.89	93.11
TS-Fusion	98.00	94.19	93.42	94.34
IV3-CapsNet	99.10	93.33	95.00	94.73
Bi-MobileNetv2	99.03	94.13	93.38	93.79
MVFLN+VGG	99.01	93.60	94.38	93.11
DTLF-ERSIC	99.07	94.85	94.43	94.36
AERODTL-SIC	99.61	95.81	95.78	95.77

CONCLUSIONS

This investigation proposes the use of the Al-Biruni Earth Radius Optimization with deep transfer learning-based scene image classification (AERODTL-SIC) model for automated environmental scene detection in remote sensing (RS) data. The model employs SqueezeNet-based feature extraction to ensure low computational cost while preserving discriminative spatial-spectral features. Robust dimensionality reduction and classification are achieved through a deep autoencoder neural network (DAENN). To enhance model convergence and accuracy, hyperparameter optimization is performed using the Al-Biruni Earth Radius Optimization (AERO) algorithm.

Extensive testing on benchmark RS datasets demonstrates that AERODTL-SIC outperforms previous methodologies, achieving an accuracy of 94.7 %. These results confirm the model's effectiveness in handling high-dimensional RS data with limited labeled samples. The enhanced DAENN framework facilitates more efficient feature learning, making the model suitable for real-world applications such as land cover mapping and environmental monitoring. Future research should focus on improving the model's discriminative capabilities by integrating synthetic aperture radar (SAR) and light detection and ranging (LiDAR) data with optical imagery using attention-based fusion strategies. Adapting the model for real-time inference on edge devices through quantization and pruning techniques is also recommended.

REFERENCES

Abdelhamid AA, El-Kenawy ESM, Khodadadi N, Mirjalili S, Khafaga DS, Alharbi AH, Ibrahim A, Eid MM, Saber M. 2022. Classification of monkeypox images based on transfer learning and the Al-Biruni Earth Radius Optimization modelling algorithm. Mathematics 10 (19): 3614. https://doi.org/10.3390/math10193614

Chen Z, Yang J, Feng Z, Chen L, Li L. 2023. BiShuffleNeXt: A lightweight bi-path network for remote sensing Environmental classification. Measurement 209: 112537. https://doi.org/10.1016/j.measurement.2023.112537

Ghadi YY, Rafique AA, Al Shloul T, Alsuhibany SA, Jalal A, Park J. 2022. Robust object categorization and environmental classification over remote sensing images via features fusion and fully convolutional network. Remote Sensing 14 (7): 1550. https://doi.org/10.3390/rs14071550

Guo D, Xia Y, Luo X. 2021. Self-supervised GANs with similarity loss for remote sensing image environmental classification. IEEE Journal of Selected Topics in Applied Earth Observations and Remote Sensing 14: 2508–2521. http://doi.org/10.1109/jstars.2021.3056883

Han C, Wu C, Guo H, Hu M, Chen H. 2023. HANet: A hierarchical attention network for change detection with bi-temporal very-high-resolution remote sensing images. IEEE Journal of Selected Topics in Applied Earth Observations and Remote Sensing 16: 3867–3878. http://doi.org/10.1109/jstars.2023.3264802

Hemamalini S, Geetha Rani K, Rajasekar B, Sadish Sendil M. 2024. An intelligent weather prediction model using optimized 1D CNN with attention GRU. Global NEST Journal 26 (2): 1–9. https://doi.org/10.30955/gnj.005408

Hilal AM, Al-Wesabi FN, Alzahrani KJ, Al Duhayyim M, Ahmed Hamza M, Rizwanullah M, García-Diaz V. 2022. Deep transfer learning based fusion model for environmental remote sensing image classification model. European Journal of Remote Sensing, 55 (1): 12–23. https://doi.org/10.1080/22797254.2021.2017799

Hong D, Gao L, Yokoya N, Yao J, Chanussot J, Du Q, Zhang B. 2021. More diverse means better: Multimodal deep learning meets remote-sensing imagery classification. IEEE Transactions on Geoscience and Remote Sensing 59 (5): 4340–4354. http://doi.org/10.1109/tgrs.2020.3016820

Jameer S, Syed H. 2023. Deep SE-BiLSTM with IFPOA fine-tuning for human activity recognition using mobile and wearable sensors. Sensors 23 (9): 4319. https://doi.org/10.3390/s23094319

Liang J, Deng Y, Zeng D. 2020. A deep neural network combined CNN and GCN for remote sensing environmental classification. IEEE Journal of Selected Topics in Applied Earth Observations and Remote Sensing 13: 4325–4338. http://doi.org/10.1109/jstars.2020.3011333

Ma A, Wan Y, Zhong Y, Wang J, Zhang L. 2021. SceneNet: Remote sensing scene classification deep learning network using multi-objective neural evolution architecture search. ISPRS Journal of Photogrammetry and Remote Sensing 172: 171–188. https://doi.org/10.1016/j.isprsjprs.2020.11.025

Meng S, Shi Z, Pirasteh S, Ullo SL, Peng M, Zhou C, Goncalves WN, Zhang L. 2025. TLSTMF-YOLO: Transfer learning and feature fusion network for earthquake-induced landslide detection in remote sensing images. IEEE Transactions on Geoscience and Remote Sensing 63: 1–12. https://doi.org/10.1109/TGRS.2025.3541171

Miao W, Geng J, Jiang W. 2023. Multigranularity decoupling network with pseudolabel selection for remote sensing image environmental classification. IEEE Transactions on Geoscience and Remote Sensing 61. http://doi.org/10.1109/tgrs.2023.3244565

Muneer A, Taib SM, Fati SM, Balogun AO, Aziz IA. 2022. A hybrid deep learning-based unsupervised anomaly detection in high dimensional data. Computers, Materials and Continua 70 (3): 6073–6088. http://doi.org/10.32604/cmc.2022.021113

Periasamy S, Subramanian P, Surendran R. 2024. An intelligent air quality monitoring system using quality indicators and transfer learning based lightweight recurrent network with skip connection. Global NEST Journal 26 (5): 1–10. https://doi.org/10.30955/gnj.006096

Petrovska B, Zdravevski E, Lameski P, Corizzo R, Stajduhar I, Lerga J. 2020. Deep learning for feature extraction in remote sensing: A case-study of aerial environmental classification. Sensors 20 (14): 3906. https://doi.org/10.3390/s20143906

Reddy KVVK, Vimal VR. 2024. A novel approach on improved segmentation and classification of remote sensing images using AlexNet compared over linear discriminant analysis with improved accuracy. *In* 2024 Second International Conference on Advances in Information Technology (ICAIT). IEEE: Chikkamagaluru, India. https://doi.org/10.1109/icait61638.2024.10690378

Ren Y, Zhang X, Ma Y, Yang Q, Wang C, Liu H, Qi Q. 2020. Full convolutional neural network based on multi-scale feature fusion for the class imbalance remote sensing image classification. Remote Sensing 12 (21): 3547. https://doi.org/10.3390/rs12213547

Santhanaraj RK, Rajendran S, Romero CAT, Murugaraj SS. 2023. Internet of things enabled energy aware metaheuristic clustering for real time disaster management. Computer Systems Science and Engineering 45 (2): 1561–1576. http://doi.org/10.32604/csse.2023.029463

Shi C, Zhang X, Wang L. 2022. A lightweight convolutional neural network based on channel multi-group fusion for remote sensing environmental classification. Remote Sensing 14 (1): 9. https://doi.org/10.3390/rs14010009

Song S, Yu H, Miao Z, Zhang Q, Lin Y, Wang S. 2019. Domain adaptation for convolutional neural networks-based remote sensing environmental classification. IEEE Geoscience and Remote Sensing Letters 16 (8): 1324–1328. https://doi.org/10.1109/lgrs.2019.2896411

Surendran R, Alotaibi Y, Subahi AF. 2023a. Lens-oppositional wild geese optimization modelling based clustering scheme for wireless sensor networks assists real time disaster management. Computer Systems Science and Engineering 46 (1): 835–851. http://doi.org/10.32604/csse.2023.036757

Surendran R, Alotaibi Y, Subahi AF. 2023b. Wind speed prediction using chicken swarm optimization modelling with deep learning model. Computer Systems Science and Engineering 46 (3): 3371–3386. http://doi.org/10.32604/csse.2023.034465

Surendran R, Tamilvizhi T, Lakshmi S. 2021. Integrating the meteorological data into a smart city service using cloud of things (CoT). Emerging Technologies in Computing 4: 94-111. https://doi.org/10.1007/978-3-030-90016-8_7

Tamilvizhi T, Surendran R, Tavera-Romero CA, Sadish SM. 2022. Privacy preserving reliable data transmission in cluster based vehicular adhoc networks, Intelligent Automation and Soft Computing 34 (2): 1265–1279. http://doi.org/10.32604/iasc.2022.026331

Vinuja G, Devi NB. 2024. Detection and classification of satellite remote sensing images using hybrid segmentation and feature extraction with effective algorithms. *In* 2024 International Conference on Distributed Computing and Optimization Techniques (ICDCOT). IEEE: Bengaluru, India. http://doi.org/10.1109/icdcot61034.2024.10515892

Wang P, Zhao H, Yang Z, Jin Q, Wu Y, Xia P, Meng L. 2023. Fast tailings pond mapping exploiting large environmental remote sensing images by coupling environmental classification and sematic segmentation models. Remote Sensing 15 (2): 327. https://doi.org/10.3390/rs15020327

Xu K, Huang H, Deng P, Shi G. 2020. Two-stream feature aggregation deep neural network for environmental classification of remote sensing images. Information Sciences 539: 250–268. https://doi.org/10.1016/j.ins.2020.06.011

Xu X, Chen Y, Zhang J, Chen Y, Anandhan P, Manickam A. 2021. A novel approach for Environmental classification from remote sensing images using deep learning methods. European Journal of Remote Sensing 54 (2): 383–395. https://doi.org/10.1080/22797254.2020.1790995

Xue Z, Liu B, Yu A, Yu X, Zhang P, Tan X. 2022. Self-supervised feature representation and few-shot land cover classification of multimodal remote sensing images. IEEE Transactions on Geoscience and Remote Sensing 60: 1–18. http://doi.org/10.1109/tgrs.2022.3217893

Yuan Z, Huang W, Tang C, Yang A, Luo X. 2022. Graph-based embedding smoothing network for few-shot environmental classification of remote sensing images. Remote Sensing 14 (5): 1161. https://doi.org/10.3390/rs14051161

Zhai M, Liu H, Sun F. 2019. Lifelong learning for environmental recognition in remote sensing images. IEEE Geoscience and Remote Sensing Letters 16 (9): 1472–1476. http://doi.org/10.1109/lgrs.2019.2897652

Agrociencia

DUNG REMOVAL BY BEETLES EXPOSED TO FECES OF SHEEP FED *Guazuma ulmifolia* Lam.

Gylia Sylene **Toledo-Zárate**[1], Silvia **López-Ortiz**[1*], Lucrecia **Arellano**[2], Jesús **Jarillo-Rodriguez**[3], Eusebio **Ortega-Jiménez**[1], Ponciano **Pérez-Hernández**[1]

[1]Colegio de Postgraduados Campus Veracruz. Postgrado en Agroecosistemas Tropicales. Carretera Xalapa-Veracruz km 88.5, Manlio Fabio Altamirano, Veracruz, Mexico. C. P. 91690.
[2]Instituto de Ecología A. C., Red de Ecoetología. Carretera Antigua a Coatepec 351, Colonia El Haya, Xalapa, Veracruz, Mexico. C. P. 91073.
[3]Universidad Nacional Autonoma de México. Facultad de Medicina Veterinaria y Zootecnia. Centro de Enseñanza, Investigación y Extensión en Ganadería Tropical. Carretera Martínez de la Torre-Tlapacoyan km 5.5, Tlapacoyan, Veracruz, Mexico. C. P. 93650.
* Author for correspondence: silvialopez@colpos.mx

Citation: Toledo-Zarate GS, López-Ortiz S, Arellano L, Jarillo-Rodríguez J, Ortega-Jiménez E, Pérez-Hernández P. 2025. Dung removal by beetles exposed to feces of sheep fed *Guazuma ulmifolia* Lam. **Agrociencia** 59(5): 632-645. https://doi.org/ 10.47163/agrociencia.v59i5.3040

Editor in Chief:
Dr. Fernando C. Gómez Merino

Received: November 15, 2024.
Approved: July 02, 2025.
Published in Agrociencia: July 14, 2025.

ABSTRACT

This study examines the relationship between the phenolic content (total phenols and tannins) of three diets for sheep (*Ovis orientalis aries* L.) containing *Guazuma ulmifolia* Lam. (Gu0: 0 %, Gu30: 30 %, and Gu60: 60 %) and the removal of feces by dung beetles fed on sheep excreta. The study was conducted in two stages: in the first, nine Pelibuey sheep (40 ± 4 kg live weight), randomly assigned to one of three groups, were fed the experimental diets (Gu0, Gu30, and Gu60). For 9 d, feces were collected and stored at 8 °C. In stage two, three dung beetle species (*Canthidium pseudopuncticolle*, *Canthon leechi*, and *Canthon chiapas* [Coleoptera: Scarabaeinae]) were captured, artificially paired in couples, and placed in terraria to evaluate dung removal, during 29 d. Sheep preferred the Gu30 diet, of which they consumed 33.5 ± 1.7 g of dry matter (DM) kg^{-1} of live weight (LW). All diets had similar chemical composition, except Gu60, which maintained a higher concentration of total tannins (3.5 ± 0.3 mg g^{-1} DM). In feces, Gu0 showed the highest concentration of phenols (0.507 ± 0.3 mg g^{-1} DM; $p \leq 0.05$) and total tannins (0.317 ± 0.1 mg g^{-1} DM; $p \leq 0.05$). *Canthon leechi* removed the highest amount of feces (249.6 g) and had the strongest day × diet interaction effect ($p \leq 0.05$). Adding up to 30 % *G. ulmifolia* forage in the diet did not compromise dry matter intake of sheep and maintains good nutritional quality; the concentration of phenolic compounds in the diet and feces changed according to the proportion of *G. ulmifolia* in the diet. Although the beetles removed less excreta from sheep that consumed *G. ulmifolia* (Gu30 and Gu60), it is not possible to conclude whether phenolic compounds are responsible for this response.

Keywords: excreta, phenols, tannins.

INTRODUCTION

Dung beetles inhabit a wide range of environments, from temperate to tropical climates. They use organic matter for food and nesting (Martínez-Morales *et al*., 2015).

Dung beetles are important for grasslands as they contribute to the removal and decomposition of livestock manure (Martínez-Morales and Lumaret, 2022). Removal is the action of relocating the dung away from the source, either by rolling it or burying it in galleries (under the source) to elaborate masses or nest balls, to lay eggs, or simply to feed on organic matter (Tonelli, 2021). Telecoprid or rolling species elaborate dung balls that they transport away from the source using their hind legs, while paracoprid or burrowing species elaborate galleries (tunnels) and feeding chambers where they deposit food masses and nest balls, finally dweller species feed and breed inside the food mass (Martínez-Morales *et al*., 2015).

Through feces removal, dung beetles provide important ecosystem services such as pasture cleaning, dung dispersal and degradation, as well as soil improvement, secondary seed dispersal, and burial of invertebrate organisms that parasite herbivores and affect their health (Basto-Estrella *et al*., 2016). However, dung beetle communities are sensitive to environmental changes, such as the destruction of primary vegetation (Halffter and Arellano, 2002), changes in land use, landscape fragmentation (Tec-Pardillo *et al*., 2024), and the increase of invasive species (Morales-Trejo *et al*., 2024).

New techniques for feeding livestock include silvopastoral systems with native or introduced woody forage species. These forage species contain a diversity of secondary compounds that provide benefits to the livestock diet (Villalba *et al*., 2014). *Guazuma ulmifolia* Lam. is a deciduous forest species widely used in silvopastoral systems due to its adaptation to tropical areas with long dry seasons and its forage attributes (Manríquez-Mendoza *et al*., 2011), although it contains phenolic compounds in stems, leaves, and fruits (López *et al*., 2004; Márquez and Suárez, 2008; Rafi *et al*., 2020).

The biological benefits that secondary compounds have to herbivores have recently been recognized. For example, phenols and saponins have antiparasitic and rumen fermentation-regulating properties that reduce methane gas emission (Sepúlveda-Vázquez *et al*., 2018; Pereira *et al*., 2019). The study of secondary compounds in ruminant diets has focused mostly on phenolic compounds as they bond with proteins, protecting them from ruminal degradation and facilitating their absorption at the duodenum ~~level~~ (Torres-Acosta *et al*., 2008). On the other hand, phenols also inhibit fungal growth and can deter nematodes, mites, and insects (Nava-Pérez *et al*., 2012).

It is currently unknown whether dung beetles are affected during their nesting process and removal activities when they break down feces of herbivores fed on forages with a high concentration of phenolic compounds. Therefore, in this study, feces removal by dung beetles was measured when they fed on sheep feces containing varying amounts of *G. ulmifolia*.

MATERIALS AND METHODS

Location and experimental site description

This research was conducted at a site located in Manlio Fabio Altamirano municipality, in central Veracruz, Mexico. The territory has an Aw_1" (w)(i) g (warm-dry-regular)

climate based on the Köppen classification (García, 2004), having a long dry period and abundant rainfall from June to September. The experimental site is located at 63 masl, with an average temperature of 26 °C and average annual rainfall of 1191 mm (SMN, 2010).

Research stages

The research was conducted in two stages. The first phase involved cultivating and harvesting forage to create three distinct diets for nine young females of the Pelibuey sheep breed (n = 3 sheep in each diet) (40 ± 4 kg live weight, LW), kept in confinement to collect dung, for a period of 8 d. During the second stage, dung beetles were captured and maintained in conditions similar to those prevailing in the area. Three species that were suited to eating sheep dung were selected. A couple of each beetle species was assigned to each treatment to evaluate dung removal and their behavior.

Stage 1. Sheep diet and feces collection

At this stage, three experimental diets containing two concentrations of *G. ulmifolia* (Gu30: 70 % grass with 30 % *G. ulmifolia* and Gu60: 40 % grass with 60 % *G. ulmifolia*) and a control diet (Gu0: 100 % grass) were prepared using 70-d regrowth green foliage of *G. ulmifolia* and 60-d regrowth green grass *Megathyrsus maximus* Jacq. cv. Cuba 22). Each diet was analyzed for crude protein (CP) using the AOAC (1990) method. Neutral detergent fiber (FDN), acid (FDA), and lignin content were determined using the filter bag method (ANKOM Technology). The concentration of total phenols and tannins was calculated according to the FAO (2000) methods.

From September 3 to 15, 2021 (12 days), fresh forage from *G. ulmifolia* and *M. maximus* was harvested every day, and the amounts required for each experimental diet were chopped. The amounts offered daily to each sheep were calculated on a dry basis for an intake of 3 % LW but were mixed and offered on a wet basis. The amount required by each sheep was offered throughout the day to ensure a constant supply of forage; rejected forage was collected daily to determine the sheep's voluntary intake based on the difference between the offered and rejected forage. Both offered and rejected forage were corrected for dry matter before calculating the difference to account for weight loss caused by spontaneous water loss throughout the day.

During this period, feces were collected every day between 8:00 and 17:00 h and stored at 8 °C for 10 to 27 days until use. Samples for phenolic compounds analysis were dried in a forced air oven at 40 °C during 72 h and kept at room temperature until analysis.

Stage 2. Diet-related behavior of the beetles

At this stage, pit fall traps baited with different types of excreta (cattle, sheep, and human feces) were placed to capture beetles. These traps were made of 1 L plastic containers with a partially perforated lid (triangle-shaped perforation that allows beetles to enter) and a plastic plate suspended upside down over the trap to prevent direct exposure to light or rainwater. The traps were placed from August 13 to September 4, 2021, in sites

where cattle and sheep were grazing. All captured dung beetles were identified using taxonomic keys and kept in temporary terraria under conditions like those of their environment, feeding them with feces from grazing sheep. The beetle species *Canthon leechi*, *Canthon chiapas*, and *Canthidium pseudopuncticolle* were chosen as they displayed constant use of sheep dung in the terraria; the three species showed good adaptation to environmental conditions (humidity and temperature) and had enough individuals to form couples for each type of diet.

Canthidium pseudopuncticolle is a small (4 to 6 mm long), paracoprid, coprophagous, and diurnal species (Rivera-Cervantes and Halffter, 1999). On the other hand, *C. chiapas* is a medium-sized (7 to 13 mm) and widely distributed species in tropical climates, which withstands high temperatures, direct sunlight, and low humidity (Martínez-Morales and Montes de Oca, 1994), making it abundant in grasslands (Basto-Estrella *et al*., 2014). Finally, *C. leechi* is a small-sized (3.5 to 6 mm), habitat generalist, and diurnal species (Rivera-Cervantes and Halffter, 1999). The preference of dung beetle communities (which include these species) for sheep dung is known (Correa *et al*., 2013), and their presence has been associated with environments where sheep forage (Ortega-Martínez *et al*., 2021; Ríos-Díaz *et al*., 2021); however, it is not known yet whether these species use sheep dung for nesting.

Terraria were prepared using 1 L rectangular-shaped plastic containers (21 × 13 × 7 cm) with perforated sides and lids to allow air circulation. Each terrarium was filled with sterilized soil to 2/3 of its capacity. The terraria were placed horizontally for the telecoprid or rolling species, (*C. leechi* and *C. chiapas*), and vertically for the paracoprid or burrowing species (*C. pseudopuncticolle*). Forty-two terraria were set, 27 for *C. leechi* (nine per treatment), nine for *C. pseudopuncticolle* (three per treatment), and six for *C. chiapas* (two per treatment). The number of terraria for each treatment corresponded to the number of couples formed with the captured individuals.

Initially, 10 g of manure were placed in the center of each terrarium, according to every treatment (Gu0, Gu30, or Gu60). Terraria were checked on a daily basis throughout the experiment (September 13 to October 12). Each time, the remaining dung on the surface was weighed to determine whether it was removed by burial or displacement (by weight difference), and more feces were added when all had been removed or there was fungal contamination. Terraria were kept moist by spraying water with a spray bottle when the soil was dry. Throughout the experimental period, temperature (ranging from 23 to 30 °C) and relative humidity (ranging from 62 to 90 %) were recorded daily under the prevailing environmental conditions.

The behavior of the couples was monitored to assess whether the diet they received (feces from sheep that consumed *G. ulmifolia*) affected the survival and behavior of the species. Every day (for 3 hours), the surface of each terrarium was checked, and seven activities performed by the beetles were recorded: male on surface, female on surface, couple on surface, presence of balls, entrance to galleries (holes), dead male, and dead female. Additionally, the state of the food was checked (dung with fungi, disintegrated dung, and buried dung). Finally, the terraria were opened and checked for buried dung. The frequency of these activities was recorded.

Statistical analysis

The variables dry matter intake by sheep, chemical composition, and concentration of phenolic compounds (total phenols and tannins) of the diets were analyzed with a completely randomized design using the analysis of variance (ANOVA) procedure of SAS/STAT (SAS Institute Inc., Cary, NC, USA) and the Tukey test to compare means between treatments, with an alpha of 0.05. Feces removal by dung beetles was analyzed with the MIXED procedure of SAS/STAT; the model included treatment (n = 3 types of feces from sheep fed three different diets), day of the experiment (1 to 29 days), as well as the treatment × day interaction as a fixed effect, and species as a random effect. An autoregressive AR(1) covariance structure was used for autocorrelating values. Treatment means were compared with the LS-means test, and X^2 contingency tables were built to analyze whether activities performed by dung beetles and dung condition were independent of diet (treatments); these analyses were performed for each species separately. To analyze the relationship between the amount of dung removed and temperature and relative humidity, Kendall correlations were performed. The last two analyses were performed using the PAST program version 2.13 (Hammer *et al*., 2001).

RESULTS AND DISCUSSION

Chemical composition of experimental diets

The nutritional value of the experimental diets did not vary among treatments ($p \geq 0.05$). Total phenolic compound concentrations were consistent across all diets ($p \geq 0.05$); however, the total concentration of tannins was higher in diets that included *G. ulmifolia* ($p \leq 0.05$) (Table 1). The grass treatment (Gu0) had low concentrations of tannins; as this group of plants is adapted to herbivory, they do not need chemical defenses to protect themselves from herbivores and pathogens (Provenza *et al*., 1996).

Table 1. Nutritional value (%) and phenolic compound concentration (mg g-1 DM) of diets Gu0 (100 % grass [*Megathyrsus maximus* Jacq. cv. Cuba 22]), Gu30 (70 % grass and 30 % *Guazuma ulmifolia* Lam.), and Gu60 (40 % grass and 60 % *G. ulmifolia*) fed to ewes (*Ovis orientalis aries* L.)

Variables	Gu0	Gu30	Gu60
CP (%)	6.17 ± 0.27	6.24 ± 0.27	7.35 ± 0.27
NDF (%)	68.10 ± 0.67	70.16 ± 0.67	70.00 ± 0.67
ADF (%)	42.20 ± 1.37	46.06 ± 1.37	51.20 ± 1.37
Lig (%)	7.80 ± 1.55	11.83 ± 1.55	19.43 ± 1.55
TP (mg g^{-1} DM)	5.48 ± 0.29	5.88 ± 0.29	6.10 ± 0.29
TT (mg g^{-1} DM)	1.36 ± 0.29[b]	4.11 ± 0.29[a]	3.51 ± 0.29[a]

[a, b] Mean values having different superscript letter within a row differ ($p \leq 0.05$). DM: dry matter; CP: crude protein; NDF: neutral detergent fiber; ADF: acid detergent fiber; Lig: lignin; TP: total phenols; TT: total tannins.

Diet intake by sheep

Dry matter intake by sheep differed by the effect of the amount of *G. ulmifolia* foliage in the diet ($p \leq 0.05$). Those fed Gu60 (27.4 ± 1.7 g kg^{-1} LW) had a lower intake than those fed Gu30 (33.5 ± 1.7 g kg^{-1} LW) or Gu0 (33.8 ± 1.7 g kg^{-1} LW). Livestock ingests tannin-containing plants as part of a diverse diet (Clemensen *et al*., 2020); however, individuals can regulate their intake to use the nutrients these plants contain without compromising their health. It is estimated that domestic ruminants can include between 5 and 30 % of tannin-containing foliage in their diet with no negative effects on intake (Márquez and Suarez, 2008), so the sheep in treatment Gu60 may have been regulating the amounts consumed from the mixture offered.

The dry matter intake of the sheep in this study is greater than that of grazing sheep supplemented with varying amounts of *G. ulmifolia* (Sosa-Rubio *et al*. 2004) and penned sheep exposed to both Taiwan grass and *G. ulmifolia* foliage offered simultaneously (unpublished data). Grazing sheep consumed between 2.9 and 3.2 % LW (approximately 32 g DM kg^{-1} LW), whereas housed sheep consumed 107.9 to 123.6 g MS kg^{-1} LW. The consumption of both forages was 1:1 (nearly 50 % of each forage) at the end of the period evaluated in the second study, which contrasts with the behavior of the animals in this experiment, as their limit was the diet with 30 % *G. ulmifolia* foliage, possibly because both forages were integrated. This may be because the sheep evaluated in those studies were younger. On the other hand, the animals exposed to free choice could make more homogeneous use of both forages over time.

García *et al*. (2008) offered *G. ulmifolia* to goats in a cafeteria test (free choice among several forage types offered simultaneously) and classified it as a moderately accepted foliage (0.164 kg DM day^{-1}), and associated the chemical composition of the forage with the concentration of secondary compounds and other possible deterrent properties. This could explain why the intake in Gu0 is statistically different from Gu60, due to the concentration of phenolic compounds in the diet. In addition, the rumen environment could be modified and affect the intake. In contrast, the maximum inclusion of 30 % *G. ulmifolia* (Gu30) in the diet did not affect sheep intake ($p \geq 0.05$) in this study.

Total phenols and tannins in sheep feces

Total phenols ($p \leq 0.05$) and total tannins ($p \leq 0.05$) in feces differed as an effect of different amounts of *G. ulmifolia* in the diet; Gu0 had the highest concentrations of phenols and tannins (Table 2). Phenolic compounds in food are not completely metabolized in the gastrointestinal tract of organisms; the majority is broken down into low molecular weight phenolic acids and accumulates in the organism, exerting physiological effects such as regulating bacterial communities or as gastrointestinal prebiotics (i.e., *Clostridium perfringens, C. difficile*, and *Bacteroides* spp.) (Lee *et al*., 2006). Chen *et al*. (2018) fed tea polyphenols to rats (Pure Herbal Remedies, Pte Ltd., Singapore) and observed the benefits of these compounds in moderating bacterial populations in the organisms. During their metabolism, phenols underwent drastic changes, with 4-hydroxyphenylacetic acid being the main phenolic compound found in feces and

Table 2. Total phenolic and tannin concentration in feces of ewes (*Ovis orientalis aries* L.) fed on diets Gu0 (100 % grass [*Megathyrsus maximus* Jacq. cv. Cuba 22]), Gu30 (70 % grass and 30 % *Guazuma ulmifolia* Lam.), and Gu60 (40 % grass and 60 % *G. ulmifolia*).

Variables	Gu0	Gu30	Gu60
Total phenols (mg g^{-1} DM)	0.507 ± 0.3^{a}	0.395 ± 0.3^{ab}	0.345 ± 0.3^{b}
Total tannins (mg g^{-1} DM)	0.317 ± 0.1^{a}	0.273 ± 0.1^{ab}	0.221 ± 0.1^{b}

[a, b] Mean values having different superscript letter within a row differ ($p \leq 0.05$). DM: Dry matter.

plasma. Lower amounts of phenols in the diet are excreted, so it is reasonable to find traces in feces. The concentration of phenolic compounds in feces could depend on the changes in chemical structure that these compounds undergo through the digestive tract and the way they are metabolized. It is likely that a fraction is absorbed at the blood level or that not all compounds read in the excreta correspond to phenols.

The differences in the amounts of phenolic compounds in feces could suggest that the compounds excreted are not the same as those contained in the feed because their chemical structure is modified as they are metabolized through the digestive tract (Vollmer *et al*., 2018), which could have interfered with the readings of total phenols and tannins. Another explanation is that tannins create bonds with proteins depending on the pH of their environment, and there is a possibility that the pH of the feces and the bonds created with proteins did not allow a correct reading of the phenolic compounds sought. The background on the study of phenolic compounds in feces is limited, but most of it is focused on the analysis of phenols in forages and feeds or testing methodologies for their estimation.

Chen *et al*. (2018) analyzed phenolic compounds in rat eces after digestion of diets containing high and low fats. They used gas chromatography to detect metabolites derived from phenolic compounds. This method could be better method for detecting phenols and metabolites in herbivore feces. Our findings are inconclusive and require further analysis to relate them to dung beetle behavior. However, it is possible to relate the forages and chemical composition of diets fed to sheep to dung beetle activity without looking for a chemical explanation.

Dung removal by the beetle species

The amount of feces removed by dung beetles differed by effect of the diet consumed by sheep ($p \leq 0.05$) and the dung beetle species ($p \leq 0.05$). Beetles removed more dung ($p \leq 0.05$) from Gu0 (0.727 ± 0.03 g d^{-1}) and Gu30 (0.716 ± 0.03 g d^{-1}) than Gu60 (0.567 ± 0.03 g d^{-1}). *Canthidium pseudopuncticolle* removed 0.294 ± 0.03 g d^{-1}, *C. leechi* removed 0.319 ± 0.02 g d^{-1}, while *C. chiapas* removed 1.396 ± 0.04 g d^{-1}, a higher amount than the first two species ($p \leq 0.05$), perhaps because it was the largest species in size (Nervo *et al*., 2014). However, it was also observed that the amount of dung removed by *C. leechi*

depended on the treatment × day interaction ($p \leq 0.05$), manifested in the removal peaks that the couples made in all treatments, mainly between days 1 and 12 of the experimental period (Figure 1). There were removal peaks in all three treatments, but on different days (days 1, 6, 8, and 10 in Gu0; days 1, 6, 10, and 12 in Gu30; and days 1, 3, and 6 in Gu60). Toward the end of the period, dung beetles in Gu0 removed more uniformly than in Gu30 and Gu60.

Canthidium pseudopuncticolle and *C. chiapas* also showed removal peaks (Figures 2 and 3), apparently in greater synchrony between treatments, as no interaction was observed ($p \geq 0.05$). These removal peaks shown by the dung beetles, regardless of an interaction, may be due to the consumption, nesting, and reproduction habits of each species, but also to natural fluctuations that individuals may show during their processes, for example, removing one day and then spending some time manipulating, feeding, or nesting in the removed dung mass (Martínez-Morales and Lumaret, 2022) to start again.

The time the dung beetle species were in the laboratory may not have been enough to fully observe their habits, because the nesting periods of these species vary. For example, *C. chevrolati*, a closely related species with similar habits and size to *C. chiapas*, has a 30 to 40 d pre-nidification period, and the first egg laid occurs approximately 10 days after the first mate (Martínez-Morales and Lumaret, 2022). These times are longer than the observation period in our research, so it was not sufficient to observe the nesting stage, assuming that this had not taken place before capture.

The activities of each beetle species and the condition of the dung provided during the experimental period were affected by the diets (treatments) (Table 3). The behavior

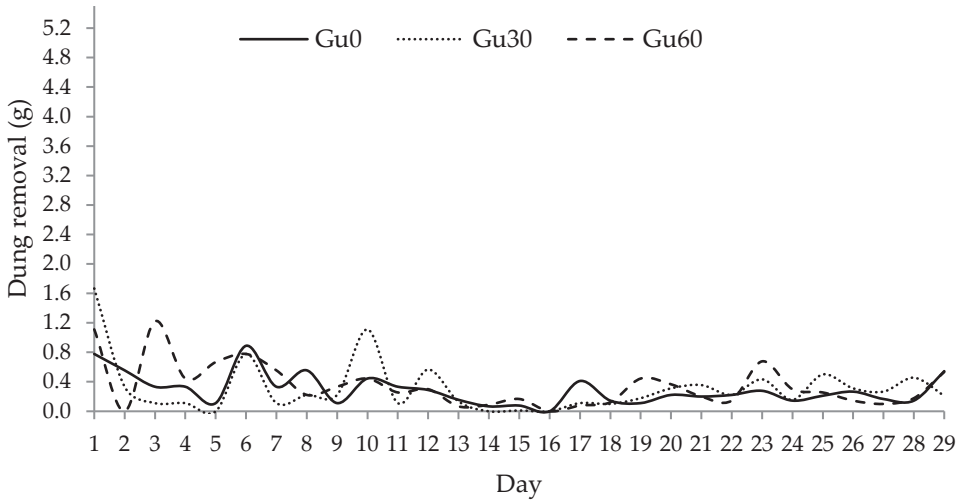

Figure 1. Dung removal (g d^{-1}) by *Canthon leechi* in treatments Gu0 (100 % grass [*Megathyrsus maximus* Jacq. cv. Cuba 22]), Gu30 (70 % grass and 30 % *Guazuma ulmifolia* Lam.), and Gu60 (40 % grass and 60 % *G. ulmifolia*).

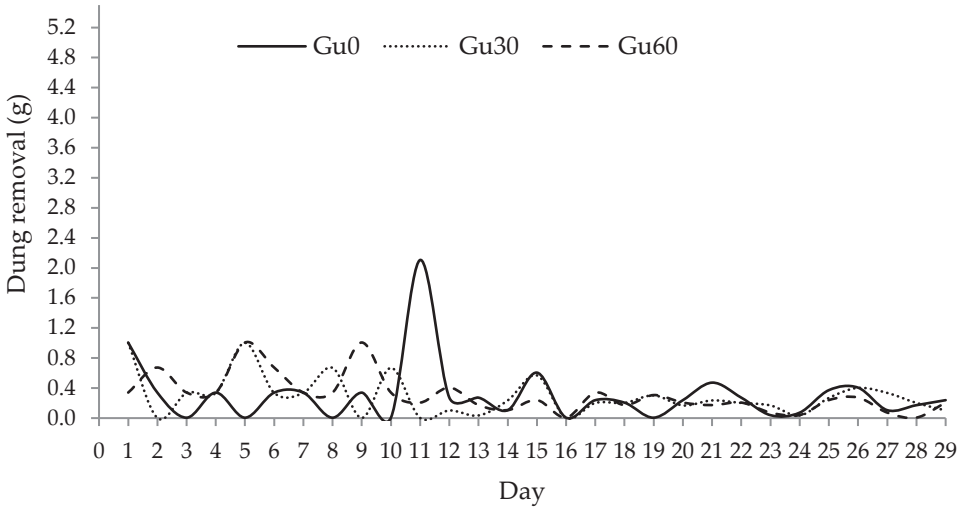

Figure 2. Dung removal (g d^{-1}) by *Canthidium pseudopuncticolle* in treatments Gu0 (100 % grass [*Megathyrsus maximus* Jacq. cv. Cuba 22]), Gu30 (70 % grass and 30 % *Guazuma ulmifolia* Lam.), and Gu60 (40 % grass and 60 % *G. ulmifolia*).

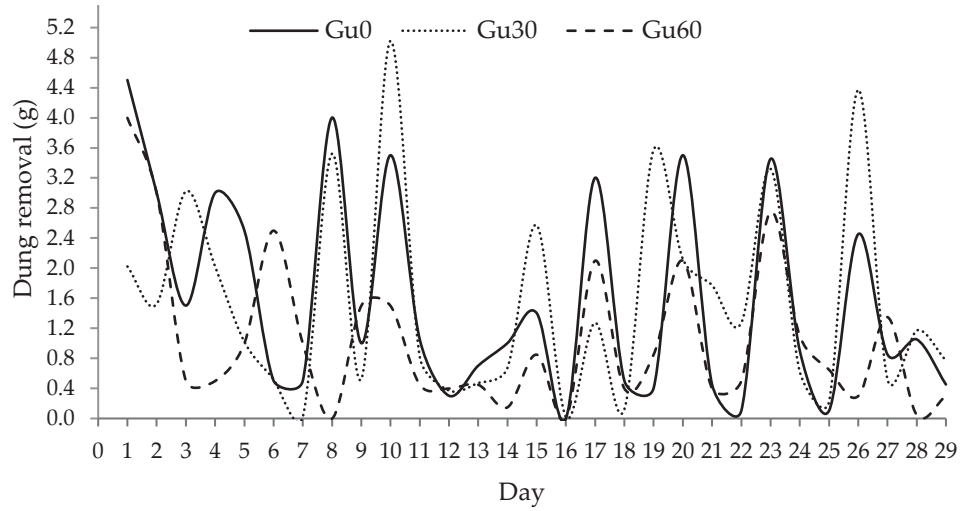

Figure 3. Dung removal (g d^{-1}) by *Canthon chiapas* in treatments Gu0 (100 % grass [*Megathyrsus maximus* Jacq. cv. Cuba 22]), Gu30 (70 % grass and 30 % *Guazuma ulmifolia* Lam.), and Gu60 (40 % grass and 60 % *G. ulmifolia*).

of *C. leechi* (df = 12, X^2 = 22.9, p = 0.028) was not independent of the type of manure removed because couples, males, and females, were seen interchangeably several times on the surface; only on the Gu60 diet were males seen on the surface fewer times than males in the other treatments. The presence of dung balls and gallery entrances

Table 3. Frequency of activities performed by the dung beetle species *Canthon leechi*, *Canthidium pseudopuncticolle*, and *Canthon chiapas* assigned to treatments Gu0 (100 % grass [*Megathyrsus maximus* Jacq. cv. Cuba 22]), Gu30 (70 % grass and 30 % *Guazuma ulmifolia* Lam.), and Gu60 (40 % grass and 60 % *G. ulmifolia*).

Type of observation	*C. leechi*			*C. pseudopuncticolle*			*C. chiapas*		
	Gu0	Gu30	Gu60	Gu0	Gu30	Gu60	Gu0	Gu30	Gu60
	Frequency of activities performed by the dung beetles								
MS	21	14	4	1	3	3	1	0	0
FS	38	61	49	10	7	6	4	4	0
CS	28	22	24	0	1	5	6	2	0
PDB	3	5	3	0	2	1	0	1	1
ET	14	9	16	4	5	2	3	1	8
DM	5	3	1	1	2	2	0	0	0
DF	1	3	1	0	1	2	0	0	0
	Frequency of dung condition in the terraria								
DFu	29	38	47	0	0	0	0	0	0
DD	50	59	39	2	16	10	1	5	0
BD	17	25	21	7	7	2	16	10	15

MS: male on the surface; FS: female on the surface; CS: couple on the surface; PDB: presence of dung balls; ET: entries to tunnels (holes on the surface); DM: dead male; DF: dead female; DFu: dung with fungi; DD: dispersed dung; BD: buried dung.

throughout the terraria was higher in Gu30. This observation could denote that those beetles were preparing for nesting using available feces. The presence of fungi in the food offered to this species was highly frequent, and disintegrated and buried dung was observed; however, the condition in which dung was found was independent of the diet (df = 4, $X^2 = 6.9$, $p = 0.144$).

The behavior of *C. chiapas* was not independent of diet (df = 12, $X^2 = 19.3$, $p = 0.013$), but a greater participation of females on the surface in treatments Gu0 and Gu30 and of couples in Gu0 was observed. There was a scarce presence of dung balls, more entries to galleries in Gu60, and no dead individuals. No fungi were observed in any treatment; however, dung condition is not independent of treatment (df = 2, $X^2 = 8.6$, $p = 0.013$). While there was more disintegrated manure in G30, more buried manure was observed in Gu0 and Gu60, using all the manure offered.

Finally, the activity of *C. pseudopuncticolle* was independent of the type of manure consumed (df = 12, $X^2 = 14.5$, $p = 0.272$). Although there was a greater presence of females on the surface in very similar frequencies among treatments, few dung balls, entries into galleries, and deaths were observed. The manure provided to this species did not develop fungi, but broken-down and buried dung were high (df= 2, $X^2 = 9.03$, $p \leq 0.01$).

Laboratory environmental conditions influenced removal behavior in all studied dung beetle species. The behavior of *C. leechi* and *C. pseudopuncticolle* was negatively correlated with temperature (τ = -0.32, p = 0.015 and τ = -0.29, p = 0.03, respectively) and positively correlated with humidity (τ = 0.33, p = 0.01 and τ = 0.43, p = 0.001, respectively); that is, their removal activity decreased as temperature increased but improved with increased relative humidity. This is because these species are native to tropical dry forests and have adapted to thrive in humid environments. On the contrary, the removal of *C. chiapas* showed a marginal negative correlation with temperature (τ = -0.24, p = 0.06) and did not have a significant correlation with humidity, which could be explained by the fact that this species is mostly present in pastures where solar radiation is high.

CONCLUSIONS

Guazuma ulmifolia foliage can be included up to 30% in sheep diets when offered integrated with other components of the diet, as it is well accepted by sheep and does not compromise voluntary intake. When integrated into the grass-based diet, the chemical-nutritional content of the mixture increased compared to the diet containing only grass. Although *G. ulmifolia* was used as a source of secondary metabolites for the purpose of this research, further evidence of the potential of this species to be integrated into sheep production systems was generated.

The results on the presence of phenolic compounds in feces are inconclusive because quantification must be done with other more appropriate methods that allow separation of these compounds from other products of ruminant digestion. The activity of dung beetles varied when exposed to sheep manure fed different proportions of *G. ulmifolia*. *Canthon chiapas* showed higher removal activity in all treatments, although it made greater use of the grass-only diet because it is a species adapted to consume the dung of cattle that feed on grass.

REFERENCES

AOAC (Association of Official Agricultural Chemistry). 1990. Official methods of analysis (15th edition). Washington, DC, USA. 500 p.

Basto-Estrella GS, Rodríguez-Vivas RI, Delfín-González H, Navarro-Alberto JA, Favila ME, Reyes-Novelo E. 2016. Dung removal by dung beetles (Coleoptera: Scarabaeidae) and macrocyclic lactone use on cattle ranches of Yucatan, Mexico. Revista de Biología Tropical 64 (3): 945–954. https://doi.org/10.15517/rbt.v64i3.21044

Basto-Estrella GS, Rodríguez-Vivas RI, Delfín-González H, Reyes-Novelo E. 2014. Dung beetle (Coleoptera: Scarabaeinae) diversity and seasonality in response to use of macrocyclic lactones at cattle ranches in the Mexican neotropics. Insect Conservation and Diversity 7 (1): 73–81. https://doi.org/10.1111/icad.12035

Chen B, Zhou J, Meng Q, Zhang Y, Zhang S, Zhang L. 2018. Comparative analysis of fecal phenolic content between normal and obese rats after oral administration of tea polyphenols. Food and Function 9 (9): 4858–4864. https://doi.org/10.1039/c8fo00609a

Clemensen AK, Provenza FD, Hendrickson JR, Grusak MA. 2020. Ecological implications of plant secondary metabolites - phytochemical diversity can enhance agricultural sustainability. Frontiers in Sustainable Food Systems 4: 547826. https://doi.org/10.3389/fsufs.2020.547826

Correa CMA, Puker A, Korasaki V, de Oliveira NG. 2013. Dung beetles (Coleoptera, Scarabaeinae) attracted to sheep dung in exotic pastures. Revista Brasileira de Entomologia 57: 113–116. https://doi.org/10.1590/s0085-56262013000100017

FAO (Food and Agriculture Organization). 2000. Quantification of tannins in tree foliage. Food and Agriculture Organization of the United Nations. International Atomic Energy Agency. Vienna, Austria. 26 p.

García DE, Medina MG, Clavero T, Humbría J, Baldizán A, Domínguez C. 2008. Preferencia de árboles forrajeros por cabras en la zona baja de los Andes venezolanos. Revista Científica 5 (5): 549–555.

García E. 2004. Modificaciones a la clasificación climática de Köppen (Quinta edición). Universidad Nacional Autónoma de México. Ciudad de México, México. 98 p.

Halffter G, Arellano L. 2002. Response of dung beetle diversity to human-induced changes in a tropical landscape. Biotropica 34 (1): 144–154. https://doi.org/10.1111/j.1744-7429.2002.tb00250.x

Hammer Ø, Harper DAT, Ryan PD. 2001. PAST: Paleontological statistics software package for education and data analysis. Palaeontologia Electronica 4 (1).

Lee HC, Jenner AM, Low CS, Lee YK. 2006. Effect of tea phenols and their aromatic fecal bacterial metabolites on intestinal microbiota. Research in Microbiology 157 (9): 876–884. https://doi.org/10.1016/j.resmic.2006.07.004

López J, Tejeda I, Vásquez C, Garza JD, Shimada A. 2004. Condensed tannins in humid tropical fodder crops and their *in vitro* biological activity: Part 1. Journal of the Science of Food and Agriculture 84 (4): 291–294. https://doi.org/10.1002/jsfa.1651

Manríquez-Mendoza LY, López-Ortiz S, Pérez-Hernández P, Ortega-Jiménez E, López-Tecpoyotl ZG, Villarruel-Fuentes M. 2011. Agronomic and forage characteristics of *Guazuma ulmifolia* Lam. Tropical and Subtropical Agroecosystems 14 (2): 453–463.

Márquez LD, Suárez LA, 2008. El uso de taninos condensados como alternativa nutricional y sanitaria en rumiantes. Revista Medicina Veterinaria 16: 87–109.

Martínez-Morales I, Cruz-Rosales M, Huerta-Crespo C, Montes de Oca-Torres E. 2015. La cría de escarabajos estercoleros. Secretaría de Educación de Veracruz. Instituto de Ecología A.C. Xalapa, México. 58 p.

Martínez-Morales I, Lumaret JP. 2022. Escarabajos estercoleros. Biología reproductiva y su regulación. Asociación Española de Entomología: León, España. 406 p.

Martínez-Morales MI, Montes de Oca E. 1994. Observaciones sobre algunos factores micro ambientales y el ciclo biológico de dos especies de escarabajos rodadores (Coleoptera, Scarabaeidae, *Canthon*). Folia Entomológica Mexicana 91: 47–59.

Morales-Trejo JJ, Dáttilo W, Zurita G, Arellano L. 2024. Duration of cattle ranching affects dung beetle diversity and secondary seed removal in tropical dry forest landscapes. Insects 15 (10): 749. https://doi.org/10.3390/insects15100749

Nava-Pérez E, García-Gutiérrez C, Camacho-Báez JR, Vázquez-Montoya EL. 2012. Bioplaguicidas: una opción para el control biológico de plagas. Ra Ximhai 8 (3b): 17–29.

Nervo B, Tocco C, Caprio E, Palestrini C, Rolando A. 2014. The effects of body mass on dung removal efficiency in dung beetles. PLoS ONE 9: e107699. https://doi.org/10.1371/journal.pone.0107699

Ortega-Martínez I, Moreno CE, Arellano L, Castellanos I, Rosas F, Ríos-Díaz CL. 2021. The relationship between dung beetle diversity and manure removal in sheep grazed grasslands and forest sites. Community Ecology 22 (2): 135–145. https://doi.org/10.1007/s42974-021-00043-w

Pereira GA, Araujo NMP, Arruda HS, Farias DP, Molina G, Pastore GM. 2019. Phytochemicals and biological activities of mutamba (*Guazuma ulmifolia* Lam.): A review. Food Research International 126: 108713. https://doi.org/10.1016/j.foodres.2019.108713

Provenza DF, Scott CB, Phy TS, Linch JJ. 1996. Preference of sheep for foods varying in flavors and nutrients. Journal of Animal Science 74 (10): 2355–2361. https://doi.org/10.2527/1996.74102355x

Rafi M, Meitary N, Septaningsih DA, Bintang M. 2020. Phytochemical profile and antioxidant activity of *Guazuma ulmifolia* leaves extracts using different solvent extraction. Indonesian Journal of Pharmacy 31 (3): 171–180.

Ríos-Díaz CL, Moreno CE, Ortega-Martínez IJ, Zuria I, Escobar F, Castellanos I. 2021. Sheep herding in small grasslands promotes dung beetle diversity in a mountain forest landscape. Journal of Insect Conservation 25 (1): 13–26. https://doi.org/10.1007/s10841-020-00277-5

Rivera-Cervantes LE, Halffter G. 1999. Monografía de las especies mexicanas de *Canthon* del subgénero *Glaphyrocanthon* (Coleoptera: Scarabaeidae: Scarabaeinae). Acta Zoológica Mexicana 77: 23–150. https://doi.org/10.21829/azm.1999.77771693

Sepúlveda-Vázquez J, Torres-Acosta JF, Sandoval-Castro CA, Martínez-Puc JF, Chan-Pérez JI. 2018. La importancia de los metabolitos secundarios en el control de nematodos gastrointestinales en ovinos con énfasis en Yucatán, México. Journal Selva Andina Animal Science 5 (2): 79–95.

SMN (Servicio Meteorológico Nacional). 2010. Normales climatológicas por estado. Gobierno de México. Comisión Nacional del Agua. Servicio Meteorológico Nacional. Ciudad de México, México. https://smn.conagua.gob.mx/es/climatologia/informacion-climatologica/normales-climatologicas-por-estado (Retrieved: January 2022).

Sosa-Rubio EE, Pérez-Rodríguez D, Ortega-Reyes L, Zapata-Buenfil BG. 2004. Evaluación del potencial forrajero de árboles y arbustos tropicales para la alimentación de ovinos. Técnica Pecuaria en México 42 (2): 129–144.

Tec-Pardillo R, Arellano L, López-Ortiz S, Jarillo-Rodríguez J, Mendoza Briseño MA, Vargas-Mendoza MC, Ortega-Martínez IJ. 2024. Different habitat condition proportions on farms affect the structure and diversity of dung beetle (Coleoptera: Scarabaeinae) communities. Tropical Zoology 37 (3–4): 42–63. https://doi.org/10.4081/tz.2024.150

Tonelli M. 2021. Some considerations on the terminology applied to dung beetle functional groups. Ecological Entomology 46 (4): 772–776. https://doi.org/10.1111/een.13017

Torres-Acosta JFJ, Alonso-Díaz MA, Hoste H, Sandoval-Castro CA, Aguilar-Caballero AJ. 2008. Efectos negativos y positivos del consumo de forrajes ricos en taninos en la producción de caprinos. Tropical and Subtropical Agroecosystems 9 (1): 83–90.

Villalba JJ, Provenza DF, Gibson N, López-Ortiz S. 2014. Veterinary medicine: The value of plant secondary compounds and diversity in balancing consumers and ecological health. *In* William BC, López-Ortiz S. (eds.), Issues in Agroecology, Vol 3. Sustainable Food Production Includes Human and Environmental Health. Springer: Dordrecht, Germany, pp: 165–190. https://doi.org/10.1007/978-94-007-7454-4_4

Vollmer M, Esders S, Farquharson FM, Neugart S, Duncan S, Schreiner M, Louis P, Maul R, Rohn S. 2018. Mutual interaction of phenolic compounds and microbiota: Metabolism of complex phenolic apigenin C- and kaempferol O-derivatives by human fecal samples. Journal of Agriculture and Food Chemistry 66 (2): 485–497. https://doi.org/10.1021/acs.jafc.7b04842.

Agrociencia

DRY MATTER YIELD AND TOTAL DIGESTIBLE NUTRIENT CONTENT OF MAIZE (*Zea mays* L.) VARIETIES IN ARID AREAS UNDER DIFFERENT MOISTURE REGIMES

Ricardo Alonso **Sanchez-Gutierrez**[1*], Francisco Guadalupe **Echavarría-Chairez**[1], Omar Ivan **Santana**[2], Jorge Alonso **Maldonado-Jaquez**[3], Edith **Ramírez-Segura**[4], Hector **Gutierrez-Bañuelos**[5], Alejandro **Espinoza-Canales**[5]

[1]Instituto Nacional de Investigaciones Forestales, Agrícolas y Pecuarias, Campo Experimental Zacatecas. Carretera Zacatecas-Fresnillo km 24.5, Calera de Víctor Rosales, Zacatecas, Mexico. C. P. 98500.
[2]Instituto Nacional de Investigaciones Forestales, Agrícolas y Pecuarias, Campo Experimental Pabellon.
[3]Instituto Nacional de Investigaciones Forestales, Agrícolas y Pecuarias, Campo Experimental La Laguna .
[4] Instituto Nacional de Investigaciones Forestales, Agrícolas y Pecuarias. Centro Nacional de Investigación Disciplinaria en Agricultura Familiar. Carretera Ojuelos-Lagos de Moreno, Ojuelos de Jalisco, Jalisco, Mexico. C. P. 47540.
[5]Universidad Autónoma de Zacatecas Francisco García Salinas. Unidad Académica de Medicina Veterinaria y Zootecnia. Carretera Zacatecas-Fresnillo km 31.5, El Cordovel, Enrique Estrada, Zacatecas, Mexico. C. P. 98500.
* Author for correspondence: rasanchez.gutiérrez@gmail.com

Citation: Sanchez-Gutierrez RA, Echavarría-Chairez FG, Santana OI, Maldonado-Jaquez JA, Ramírez-Segura E, Gutierrez-Bañuelos H, Espinoza-Canales A. 2025. Dry matter yield and total digestible nutrient content of maize (*Zea mays* L.) varieties in arid areas under different moisture regimes. **Agrociencia** 59(5): 646-656. https://doi.org/ 10.47163/agrociencia.v59i5.3252

Editor in Chief:
Dr. Fernando C. Gómez Merino

Received: September 13, 2024.
Approved: August 12, 2025.
Published in Agrociencia: August 13, 2025.

ABSTRACT

The inappropriate selection of maize varieties with higher water demand or a late growth cycle is a factor that reduces yield in rainfed conditions in Northern Mexico. This study aimed to evaluate the dry matter yield (DMY), total digestible nutrient content (TDN), and yield stability of eight maize (*Zea mays* L.) varieties under four moisture conditions in an arid region of Mexico. A randomized complete block design with a split-plot arrangement was used, with three replicates per treatment. The main plot factor was the soil moisture level (rainfed conditions only and rainfed plus one supplemental irrigation). Subplots consisted of eight maize varieties or genotypes. Data were analyzed through combined analysis of variance, additive main effects and multiplicative interaction (AMMI) modeling, principal component analysis (PCA), and biplot visualization to evaluate genotype stability. Under rainfed conditions, the varieties CHLHW09029, V-209, and CAFIME showed the highest DMY, while 35p12 had the highest TDN content. Under rainfed plus irrigation conditions, Ocelote exhibited the greatest DMY, and CHLHY02502, V-209, and VS-204 recorded the highest TDN. The AMMI model for DMY indicated that CAFIME, V-209, and CHLHY02502 were stable in Rain Y17, Rain Y18, and Rain + Irrigation Y18, respectively. For TDN, the compatibility of varieties with specific MLs was as follows: 35p12 was most suited to Rain Y17, VS-204 aligned with Rain Y18, and CHLHY02502 performed well under any irrigation treatment. The CAFIME genotype demonstrated consistently high performance in all moisture conditions. Given its adaptability

and the potential for seed reuse, it is recommended for smallholder farmers in arid and semi-arid regions of Mexico.

Keywords: hybrids, rainfed conditions.

INTRODUCTION

Maize (*Zea mays* L.) plays an important role in human food security and livestock systems. Due to its adaptability to different environmental conditions, it is one of the main crops cultivated worldwide. Under rainfed conditions, maize is the best alternative for farmers challenged by climate variability, as this crop usually presents scarce biomass loss from drought effects (Kumar *et al.,* 2019; Haarhoff *et al.,* 2020). In addition, maize has better water use efficiency than other forage crops, including Sudan grass, millet, soybean, common vetch, and oats, with an efficiency of up to 26.4 kg ha^{-1} mm^{-1} (Zhang *et al.,* 2018).

Maize is native to Mexico, where its cultivation is an important agricultural activity at the national level (Rasgado-Cabrera *et al.,* 2019; Martínez-Borrego and Vallejo-Román, 2019). In semi-arid areas of northern Mexico, the use of native varieties of maize for forage is still being adopted. Rivas-Jacobo *et al.* (2020) demonstrated that native maize produced similar yield and fibers to hybrid varieties in semiarid conditions, with a mean yield of 31 Mg ha^{-1}. Hernández *et al.* (2007) mentioned that achieving high yields under rainfed conditions requires implementing good management practices and varieties that present stability to the region.

The additive main effects and multiplicative interaction (AMMI) model allows to identify the stability of varieties and technologies under different environmental conditions or multiregional sites. This model uses analysis of variance and principal components to present an effective test, since it captures a large proportion of the sum of squares and accurately separates the main effects (genotype) from those corresponding to the interaction (genotypes × environment) (Crossa *et al.,* 1990; Legesse *et al.,* 2018). This model has helped other studies improve their interpretation of interactions (Božović *et al.,* 2020; Mousavi *et al.,* 2021).

In Zacatecas, Mexico, forage maize is grown in two agroecosystems: optimal and suboptimal, with the amount of precipitation being the primary distinguishing factor. Rainfall in optimal areas averages around 700 mm, with a forage maize area of 168 861 ha. In contrast, in the suboptimal area, the precipitation is around 450 mm, with an extended area of 1 471 613 ha planted to forage maize (Medina-García *et al.,* 2001). In 2019, 96 104 ha were planted under rainfed conditions in Zacatecas, but 24 % were reported as damaged, ranking first in damage at the national level (SIAP, 2019).

The inappropriate selection of varieties or hybrids with greater water demand or a late growth cycle is a factor that reduces yield; therefore, it is recommended to choose varieties adapted to the region. Nevertheless, in Zacatecas, there is scarce information about the yield performance of maize varieties for forage production and their

adaptability under different rainfed conditions. Hence, the objective of this study was to determine dry matter yield and total digestible nutrient content of eight varieties of maize, as well as to test their stability under four moisture level conditions in an arid region of Zacatecas, Mexico.

MATERIALS AND METHODS

The study was carried out in 2017 and 2018 at the Zacatecas Experimental Station of the National Institute of Forestry, Agricultural and Livestock Research (INIFAP) in Mexico, located at 22° 54′ N and 102° 39′ W, with an altitude of 2197 m, an annual average temperature of 14.6 °C and 333 mm of precipitation (Figure 1), mainly recorded from June to September (Medina-García and Ruiz-Corral, 2004).

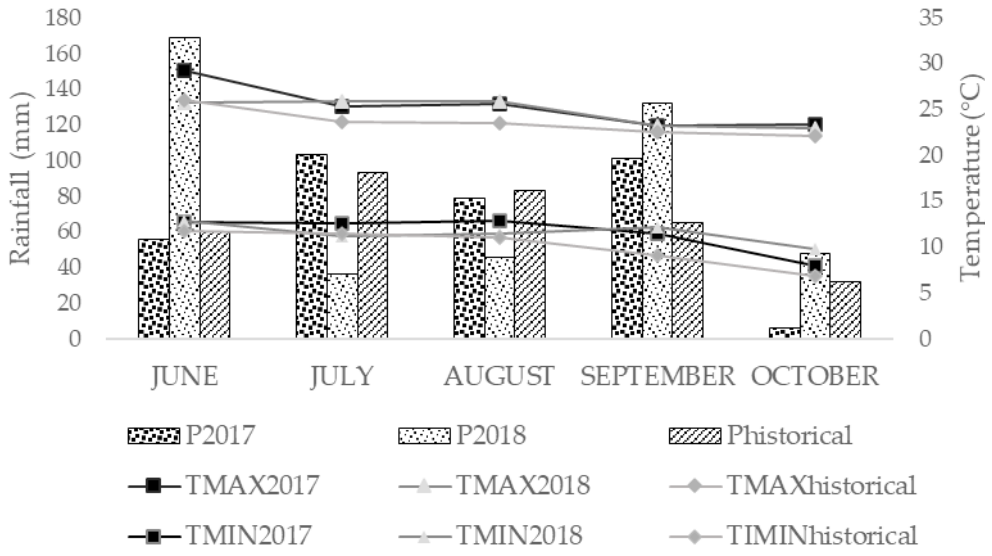

Figure 1. Monthly precipitation (mm) and temperature (°C, maximum and minimal) registered at the Zacatecas Experimental Station in 2017 and 2018.

The soil texture is clay loam, with a pH of 7.7, 1.6 % organic matter, and a bulk density of 1.4 g cm^{-3}. Planting was done manually in moist soil from rainfall at a seeding rate of 44 000 seeds per hectare on July 8, 2017, and July 1, 2018. A complete randomized block experimental design with three replicates under a split-plot arrangement was used annually. The main plots were assigned to two soil moisture treatments: 1) rainfed conditions and 2) rainfed plus a single irrigation event during the vegetative stage. Subplots included eight maize genotypes: 35P12 (Pioneer), Ocelote (Asgrow), CHLHY02502 (CIMMYT), CHLHW09029 (CIMMYT), VS-209 (INIFAP), VS-204 (INIFAP), VS-201 (INIFAP), and CAFIME (INIFAP). Each experimental unit consisted of four rows, 8 m in length and spaced 0.76 m apart. Data collection was performed

on the two central rows, with samples taken from 7 m of row length after excluding 0.5 m at each end.

Fertilization was carried out at sowing with a rate of 80 kg ha^{-1} of nitrogen (N) and 40 kg ha^{-1} of phosphorus (P). After plant emergence, a surface drip system was installed on plots with rainfed plus irrigation treatment. The separation between irrigation tapes was 76 cm, and the distance between emitters was 20 cm, with a discharge of 1 L h^{-1}. In 2017 and 2018, supplemental irrigation of 12 mm was applied 20 and 25 d after planting, respectively. This decision was based on the absence of rainfall during the 10 d preceding irrigation and a low probability of rainfall in the subsequent 5 d, as indicated by our internal forecasting system.

Harvest was carried out manually at the doughy grain stage. The measured variables included dry matter yield (DMY, kg ha^{-1}) and total digestible nutrient content (TDN, %), which was calculated based on the chemical composition determined through wet chemistry following AOAC methods. To assess DMY, the two central rows of each plot were cut at a height of 0.15 m and weighed to estimate fresh forage production. Additionally, two plants were randomly sampled and dried in a forced-air oven at 55 °C for 72 hours, or until constant weight, to determine dry matter content.

The chemical composition used to estimate TDN was obtained as follows: total nitrogen (N) was measured by dry combustion (FP-528, Leco Instruments, St. Joseph, MO, USA). Neutral detergent fiber (NDF), acid detergent fiber (ADF), and lignin content were determined sequentially using a fiber analyzer (A200, Ankom Tech., Macedonia, NY, USA). The NDF analysis included the use of α-amylase and sodium sulfite, ADF was determined using CTAB solution, and lignin was analyzed with 72 % sulfuric acid in beakers. Ash content was quantified by incinerating samples at 600 °C for 6 h. The ether extract value was assumed to be 2.89 (NRC, 2001). TDN values were calculated based on the NRC (2001) guidelines using the chemical composition data obtained.

Prior to statistical analysis, a normality test and homogeneity of variance test were applied to the dry matter yield dataset. The arcsine function was used to convert the total digestible nutrients. The total digestible nutrients were transformed using the arcsine function. A combined analysis of variance (ANOVA) was conducted to determine the main effects of year and varieties, as well as the interaction effect (Year × Genotype) under each moisture condition. Replication was nested within moisture level to improve precision (Fotso *et al*., 2018). To evaluate the stability of the varieties across moisture regimens, an AMMI analysis was performed. This included an ANOVA to assess the F-values associated with varieties, moisture regimes, and their interaction. Finally, a principal component (PC) analysis was conducted to derive eigenvectors and visualize the stability of the varieties in a biplot (SAS, 2011).

RESULTS AND DISCUSSION

Under rainfed conditions, dry matter yield (DMY) and total digestible nutrient content (TDN) showed statistically significant differences ($p \leq 0.05$) between years

and among varieties. However, no significant differences were observed for the Year × Genotype interaction ($p > 0.05$). Varietal performance was superior in 2017, with higher values for DMY (7664 kg ha^{-1}) and TDN (49 %) compared to 2018. Regarding varietal comparisons, the DMY reported for VS-204 (5485 kg ha^{-1}) was significantly surpassed ($p \leq 0.05$) by CHLHW09029, V-209, and CAFIME. In terms of TDN, the hybrid 35P12 achieved the highest mean value (50.45 %), followed by CHLHW09029, VS-204, and CAFIME, which showed similar percentages.

Results obtained under rainfed conditions plus one irrigation showed statistically significant differences ($p \leq 0.05$) across both years and varieties. However, no significant Year × Genotype interaction was detected ($p > 0.05$). Under these conditions, the year 2017 exhibited the best forage characteristics, with a DMY of 10 697 kg ha^{-1} and TDN of 70.83 %. The Ocelote hybrid recorded the highest DMY (11 302 kg ha^{-1}) and was superior ($p \leq 0.05$) to V-209 and VS-204, but there was no significant difference ($p > 0.05$) compared to the other varieties. The genotypes CHLHY02502, V-209, and VS-204 accumulated more than 70 % TDN and were statistically different from VS-201 (Table 1).

Table 1. Dry matter yield (DMY) and total digestible nutrient content (TDN) of eight maize varieties (*Zea mays* L.) under different moisture regimes, evaluated in 2017 and 2018 at the Zacatecas Experimental Station, Mexico.

Year	Soil moisture level condition			
	Rainfed		Rain + irrigation	
	DMY (kg ha^{-1})	TDN (%)	DMY (kg ha^{-1})	TDN (%)
2017	7664 a	49.6 a	10697 a	70.83 a
2018	6339 b	48.04 b	8907 b	68.06 b
Varieties				
35p12	6995 ab	50.45 a	10829 ab	69.34 ab
Ocelote	7070 ab	46.37 c	11302 a	68.64 ab
CHLHY02502	6472 ab	48.67 b	10758 ab	70.43 a
CHLHW09029	7528 a	49.49 ab	10651 ab	69.11 ab
V-209	7921 a	47.03 c	8667 bc	70.71 a
VS-204	5485 b	50.15 ab	7467 c	70.1 a
VS-201	6850 ab	48.88 b	9271 abc	67.33 b
CAFIME	7691 a	49.51 ab	9473 abc	69.92 ab
Year × Genotype (significance level)	0.4109	0.399	0.644	0.51

Ns: no significance.

During the evaluation years, total precipitation exceeded the historical average of 333 mm, with accumulations of 11.7 mm in 2017 and 98 mm in 2018. However, in 2018, the months of July (36 mm) and August (45 mm) received only 61 and 45 %

of their respective historical averages (Figure 1). Only 2017 showed a precipitation pattern comparable in both accumulation and distribution to the historical average. Due to the irregular rainfall distribution in 2018, yields under both moisture levels decreased by 18 to 20 %. This reduction aligns with previous reports suggesting that water restrictions during maize development can lead to yield losses of 15 to 20 % (Siatwiinda *et al*., 2021).

The amount of accessible water during the growing season is critical. Some authors have observed that water shortages from the tasseling to milk stage can reduce yield more severely than shortages during the vegetative stage (Gheysari *et al*., 2017; Marković *et al*., 2021). In both years, rainfall was concentrated in September, benefiting the tasseling stage (65 d after sowing), as rainfall exceeded the historical average. Therefore, the vegetative stage emerged as the critical period for water availability in this region.

To address this, auxiliary irrigation of approximately 12 mm was applied, resulting in yield increases equivalent to more than 2.4 Mg ha^{-1}. This additional forage could feed a 450 kg cow for 178 d during a drought period. Moreover, TDN, which indicates the projected energy content of a feedstuff (NRC, 2001), varied significantly between moisture treatments. Under rainfed conditions, TDN values ranged from 47 to 50.5 %, while the addition of irrigation increased TDN values to 67–70.4 %.

Water restriction during the vegetative stage can decrease photosynthetic rate, limiting leaf area and ear growth, and leading to increased fiber content and reduced digestibility (Gallo *et al*., 2014; Johansouz *et al*., 2014). Thus, the application of 12 mm of irrigation not only enhances yield but also significantly improves forage nutritional quality, contributing to the dietary requirements of cows from mid-gestation to delivery (van Die and Entz, 2022).

The AMMI analysis for DMY showed highly significant differences ($p \leq 0.0001$) for the moist level (ML), while the ML × Genotype interaction was not significant ($p > 0.05$). ML was the main factor affecting dry matter, resulting in 53.7 % of the total variation, while the other sources contributed less than 18 % (Table 2).

Table 2. Analysis of variance by the additive main effects and multiplicative interaction (AMMI) model for dry matter yield (DMY) under four moisture levels and eight maize varieties (*Zea mays* L.) evaluated in 2017 and 2018 in Zacatecas, Mexico.

Source of variation	Degrees of Freedom	Sum of squares	Percentage of sum of squares	F value
ML	3	276 526 506	53.77	26.1**
Rep(ML)	12	92 101 588	17.91	2.17*
Varieties	7	65 394 221	12.72	2.65*
ML × Genotype	21	80 215 544	15.60	1.08 Ns

ML: moisture level; Rep(ML): repetition by moisture level; ML × Genotype: interaction between moisture level and varieties; *($p \leq 0.05$); **($p \leq 0.0001$); [A]Ns: no significance.

Principal component analysis of DMY showed that the first and second components accounted for 51.05 and 32.43 % of the total variance, respectively, together explaining 83.49 % of the variation. The biplot analysis revealed notable differences in moisture levels, and the evaluated varieties exhibited distinct performance patterns for DMY, each occupying separate sectors. Among the varieties tested, CAFIME, VS-209, and CHLHY02502 displayed longer vectors and demonstrated stability under varying moisture conditions corresponding to Rain Y17, Rain Y18, and Rain + Irrigation Y18, respectively (Figure 2).

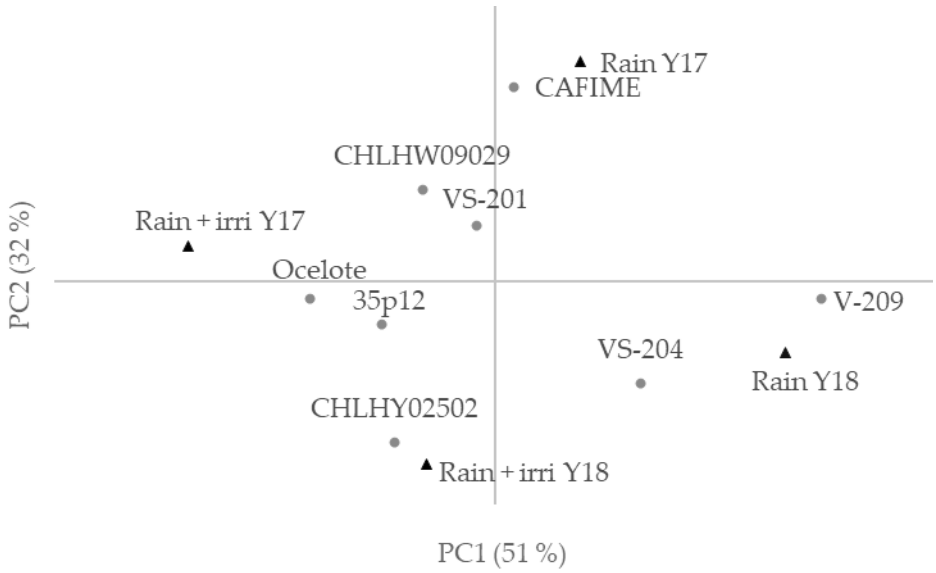

Figure 2. Biplot of dry matter yield of eight maize varieties (*Zea mays* L.) evaluated on four different moisture levels in Zacatecas, Mexico. Moisture level (▲); genotype (●).

Varieties CAFIME and V-209 performed particularly well under rainfed conditions (Rain Y17 and Rain Y18), suggesting they are suitable alternatives for smallholder farmers in north-central Zacatecas. According to Luna-Flores *et al*. (2005), these varieties have an early development cycle, reaching tasseling between 59 and 65 d, which facilitates seed production for future planting cycles. Additionally, Rumayor-Rodríguez *et al*. (2006) found that the V-209 genotype is beneficial in drought mitigation strategies in rainfed agriculture due to its lower risk of yield loss under water stress. Conversely, the Ocelote hybrid is better adapted to high soil moisture environments and is therefore recommended for the southwestern region of Zacatecas, where rainfall is more abundant and consistent (Medina-García and Ruiz-Corral, 2004).

The AMMY analysis for TDN revealed significant differences ($p \leq 0.0001$) in moisture levels. Furthermore, there were significant differences ($p \leq 0.05$) between varieties

and the ML × Genotype interaction. Moisture levels were the primary effect of TDN, accounting for 97.83 % of total variation; the remaining sources explained less than 2.2 % of the variation (Table 3).

Table 3. Analysis of variance of the additive main effects and multiplicative interaction (AMMI) model for the total digestible nutrient content (TDN) under different moisture levels and eight maize varieties (*Zea mays* L.) evaluated in 2017 and 2018 in Zacatecas, Mexico.

Source of variation	Degrees of freedom	Sum of squares	Percentage of sum of squares	F value
ML	3	9248.9	97.83	1007.5**
Rep(ML)	11	24.9	0.263	0.73 Ns
Genotype	7	76.8	0.81	3.57*
ML × Genotype	21	103.34	1.09	1.76*

ML: moisture levels; Rep(ML): repetition by moisture levels; ML × Genotype: interaction between moisture levels and varieties; *($p \leq 0.05$); **($p \leq 0.0001$); Ns: No significance.

Principal component analysis of TDN content revealed that the first (76.21 %) and second (16.23 %) components together account for 92.44 % of the total variance. The biplot analysis identified three distinct moisture level groupings based on TDN content. One of these moisture levels includes Rain + Irrigation Y17 and Rain + Irrigation Y18, as they are positioned in the same sector of the biplot. The remaining conditions, Rain Y1 and Rain Y2, each form independent moisture levels, being located in different sectors.

Regarding varietal performance, genotypes with the longest vectors and highest compatibility with specific moisture levels included 35P12 (under Rain Y17), VS-204 (close to Rain Y18), and CHLHY02502 (across all irrigation treatments) (Figure 3). Hybrids 35P12 and CHLHW09029 and the open-pollinated varieties VS-204 and CAFIME exhibited high TDN content under both irrigated and rainfed conditions. Among these, CAFIME produced a higher DMY than VS-204, making it the most suitable option for forage production under rainfed systems.

To enhance forage quality and fiber digestibility, the adoption of higher cutting heights at harvest is recommended, particularly for V-209 and potentially for CAFIME as well (Dejene *et al*., 2021; Kolar *et al*., 2022). Additionally, breeding efforts for V-209 should prioritize improvements in nutritional quality, as this genotype holds potential as a climate-resilient forage alternative for rainfed areas.

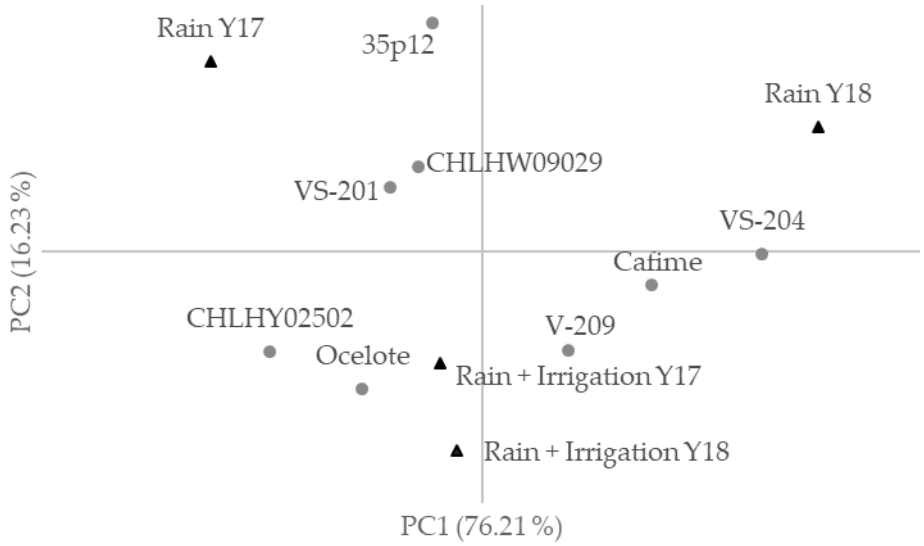

Figure 3. Biplot of total digestible nutrient content of eight genotypes evaluated on four different moisture levels in Zacatecas, Mexico. Moisture level (▲); genotype (●).

CONCLUSIONS

The additive main effects and multiplicative interaction (AMMI) analysis revealed high variability in moisture level conditions for both dry matter yield and total digestible nutrient (TDN) content. The genotypes CAFIME, VS-209, and CHLHW09029 exhibited stability in the environments Rain Y17, Rain Y18, and Rain + Irrigation Y18, respectively. Additionally, 35p12 performed best in Rain Y17, VS-204 in Rain Y18, and CHLHW09029 showed superior TDN content across all irrigation treatments. Although CAFIME did not display stability under certain conditions, its performance consistently matched or slightly exceeded the overall mean. Therefore, CAFIME is recommended for smallholder farmers, as it enables seed saving from their own harvests, contributing to self-sufficiency.

ACKNOWLEDGEMENTS

The authors thank students Angilberto Arturo Berumen González and Juan González Bañuelos for the collaborations on the field, and Julio Cesar González Márquez (certified technician in sustainable agriculture by CIMMYT) for donating seed of CIMMYT varieties for this study.

REFERENCES

AOAC. (Association of Official Analytical Chemists). 2000. Official methods of analysis of AOAC International (17th ed.). Association of Official Analytical Chemists, Gaithersburg, MD, USA.

Božović D, Popović V, Rajičić V, Kostić M, Filipović V, Kolarić L, Ugrenović V, Spalević V. 2020. Stability of the expression of the maize productivity parameters by AMMI models and GGE-biplot analysis. Notulae Botanicae Horti Agrobotanici Cluj-Napoca 48 (3): 1387–1397. https://doi.org/10.15835/nbha48312058

Crossa J, Gauch HG, Zobel RW. 1990. Additive main effects and multiplicative interactions analysis of two interactional maize cultivar trials. Crop Science 30 (3): 493–500. https://doi.org/10.2135/cropsci1990.0011183x003000030003x

Dejene M, Dixon RM, Walsh KB, McNeill D, Seyoun S, Duncan AJ. 2021. High-cut harvesting of maize stover and genotype choice can provide improved feed for ruminants and stubble for conservation agriculture. Agronomy Journal 114 (1): 187–200. https://doi.org/10.1002/agj2.20874

Fotso Ak, Hanna R, Kulakow P, Parkes E, Iluebbey P, Ngome FA, Suh C, Massussi J, Choutnji I, Wirnkar VL. 2018. AMMI analysis of cassava response to contrasting environments: case study of genotype by environment effects on pest and diseases, root yield, and carotenoids content in Cameroon. Euphytica 214 (9): 155. https://doi.org/10.1007/s10681-018-2234-z

Gallo A, Giuberti G, Masoero F, Palmonari A, Fiorentini L, Moschini M. 2014. Response on yield and nutritive value of two commercial maize hybrids as a consequence of a water irrigation reduction. Italian Journal of Animal Science 13 (3): 594–599. https://doi.org/10.4081/ijas.2014.3341

Gheysari M, Sadeghi SH, Loescher HW, Amiri S, Javad ZM, Majidi MM, Asgarinia P, Payero JO. 2017. Comparison of deficit irrigation management strategies on root, plant growth and biomass productivity of silage maize. Agricultural Water Management 182: 126–138. https://doi.org/10.1016/j.agwat.2016.12.014

Haarhoff SJ, Kotzé TN, Swanepoel PA. 2020. A prospectus for sustainability of rainfed maize production in South Africa. Crop Science 60 (1): 14–28. https://doi.org/10.1002/csc2.20103

Hernández AJA, Rosales NC, Beltrán LS, Loredo C. 2007. Variedades de forrajes anuales para temporal en el altiplano y zona media de San Luis Potosí. Instituto Nacional de Investigaciones Forestales, Agrícolas y Pecuarias. San Luis Potosí, México. 19 p.

Johansouz JM, Ashfar RK, Heidari H, Hashemi M. 2014. Evaluation of yield and quality of sorghum and millet as alternative forage crops to corn under normal and deficit irrigation regimens. Jordan Journal of Agricultural Sciences 10 (4): 699–715.

Kolar S, Vranić M, Božić L, Bošnjak K. 2022. The effect of maize crop cutting height and the maturity at harvest on maize silage chemical composition and fermentation quality in silo. Journal of Central European Agriculture 23 (2): 290–298. https://doi.org/10.5513/jcea01/23.2.3504

Kumar KM, Sridhara CJ, Hanumanthappa M, Marimuthu S. 2019. A Review of impact and mitigation strategies of climate change on dryland agriculture. Current Journal of Applied Science Technology 33: 1–12. https://doi.org/10.9734/cjast/2019/v33i430085

Legesse W, Tolera K, Berhanu T, Gezahegn B, Adefris T, Beyene A. 2018. Mega-environment targeting of maize varieties using AMMI and GGE biplot analysis in Ethiopia. Ethiopian Journal Agriculture Science 28: 65–84.

Luna-Flores M, Gutierrez-Sánchez JR, Peña-Ramos A, Echavarría-Chairez FG, Martinez-Gómez J. 2005. Behavior of early corn varieties in the semiarid and arid central-northern region of Mexico. Revista Fitotecnia Mexicana 28 (1): 39–45. https://doi.org/10.35196/rfm.2005.1.39

Markovic M, Šoštarić J, Josipović M, Rastija M, Matoša KM, Andrišić K. 2021. Yield and yield components of maize hybrids (*Zea mays* L.) as affected by irrigation. Journal of Agriculture and Food 9: 1–11.

Martínez-Borrego E, Vallejo-Román J. 2019. Pluriactividad, consumo y persistencia del maíz en dos municipios del noroeste del Estado de México. Revista Euroamericana de Antropología 7: 41–53. https://doi.org/10.14201/rea201974153

Medina-García G, Ruiz-Corral JA. 2004. Estadísticas climatológicas básicas del Estado de Zacatecas. Libro Técnico 3. Instituto Nacional de Investigaciones Forestales, Agrícolas y Pecuarias. Centro de Investigación Regional Norte Centro, Campo Experimental Zacatecas. Calera, México. 41 p.

Medina-García G, Salinas-González H, Rubio-Aguirre F. 2001. Potencial productivo de especies forrajeras en el Estado de Zacatecas, Libro técnico 1. Instituto Nacional de Investigaciones Forestales, Agrícolas y Pecuarias. Centro de Investigación Regional Norte Centro, Campo Experimental Zacatecas. Calera, México. 157 p.

Mousavi SMN, Bojtor C, Illés A, Nagy J. 2021. Genotype by trait interaction (GT) in maize hybrids on complete fertilizer. Plants 10 (11): 2388. https://doi.org/10.3390/plants10112388

NRC (National Research Council). 2001. Nutrient requirements of beef cattle (Seventh revised edition). National Academy Press: Washington, DC, USA.

Rasgado-Cabrera VE, Castañeda-Hidalgo E, Lozano-Trejo S, Pérez-León MI, Santiago-Martínez GM. 2019. Sustentabilidad de agroecosistemas de maíz de la planicie costera del Istmo, Oaxaca, México. Revista de la Facultad de Agronomía 118 (2). https://doi.org/10.24215/16699513e028

Rivas-Jacobo MA, Mendoza-Pedroza SI, Sangerman-Jarquín D, Sánchez-Hernández MÁ, Herrera-Corredor CA, Rojas-García AR. 2020. Forage evaluation of maize from various origins of Mexico in the semi-arid region. Revista Mexicana de Ciencias Agrícolas 24: 93–104. https://doi.org/10.29312/remexca.v0i24.2361

Rumayor-Rodríguez A, Medina-García G, Echavarría-Chairez F, Luna-Flores M, Vallejo-Díaz J. 2006. Estrategias de mitigación de la sequía en el estado de Zacatecas. *In* Bravo AG, Amador MD, Serna A, Medina G. (eds.), Sequía: Vulnerabilidad, Impacto y Tecnología para Afrontar en el Norte Centro de México. Instituto Nacional de Investigaciones Forestales, Agrícolas y Pecuarias, Campo Experimental Zacatecas: Zacatecas, México, pp: 231–267.

SAS Institute. 2011. SAS/STAT 9.3 User´s Guide. SAS Institute Inc. Cary, NC, USA.

SIAP (Servicio de Información y Estadística Agroalimentaria y Pesquera Información Agrícola). 2022. Avance mensual por estado. Estadísticas 2019. Gobierno de México. Secretaría de Agricultura y Desarrollo Rural. Servicio de Información y Estadística Agroalimentaria y Pesquera Información Agrícola. Ciudad de México, México. https://nube.agricultura.gob.mx/avance_agricola/ (Retrieved: June 2022).

Siatwiinda SM, Supit I, Hove B, Yerokun O, Ros GH, de Vries W. 2021. Climate change impacts on rainfed maize yields in Zambia under conventional and optimized crop management. Climatic Change 167 (3–4). https://doi.org/10.1007/s10584-021-03191-0

van Die M, Entz MH. 2022. Mid-summer annual forage performance in organic, grass-fed production. Canadian Journal of Plant Science 102 (3): 566–574. https://doi.org/10.1139/cjps-2021-0112

Zhang Q, Bell LW, Shen Y, Wish JPM. 2018. Indices of forage nutritional yield and water use efficiency amongst spring-sown annual forage crops in north-west China. European Journal of Agronomy 93: 1–10. https://doi.org/10.1016/j.eja.2017.11.003

Agrociencia

ADDITION OF YERBA MATE (*Ilex paraguariensis* A. St. Hil.) IN TILAPIA FEED FOR THE GROWTH OF THE MAYAN CICHLID (*Cichlasoma uropthalmus* Günther)

Irvin Jesús **Gómez-Hernández**[1], Martha Alicia **Perera-García**[1], Metodio Nicolas **Vite-García**[1], Carolina Esther **Melgar-Valdés**[2], Alfonso **Castillo-Domínguez**[2], Raúl Enrique **Hernández-Gómez**[2], Lenin **Rangel-López**[1]*

[1]Universidad Juárez Autónoma de Tabasco. División Académica de Ciencias Agropecuarias, Ingeniería en Acuacultura. Carretera Villahermosa-Teapa km 25 + 2, Ranchería La Huasteca Segunda Sección, Villahermosa, Tabasco, Mexico. C. P. 86298.
[2]Universidad Juárez Autónoma de Tabasco. División Académica Multidisciplinaria de los Ríos, Ingeniería en Acuacultura. Carretera Tenosique-Estapilla km 1, Tenosique, Tabasco, Mexico. C. P. 86901.
* Author for correspondence: lenin.rangel@ujat.mx

Citation: Gómez-Hernández IJ, Perera-García MA, Vite-García MN, Melgar-Valdés CE, Castillo-Domínguez A, Hernández-Gómez RE, Rangel-López L. 2025. Addition of yerba mate (*Ilex paraguariensis* A. St. Hil.) in tilapia feed for the growth of the Mayan cichlid (*Cichlasoma uropthalmus* Günther). **Agrociencia** 59(5): 657-666. https://doi.org/ 10.47163/agrociencia.v59i5.3417

Editor in Chief:
Dr. Fernando C. Gómez Merino

Received: April 07, 2025.
Approved: August 14, 2025.
Published in Agrociencia: August 13, 2025.

ABSTRACT

Native species with aquatic potential can be found in Southeastern Mexico, such as the Mayan cichlid (*Cichlasoma uropthalmus* Günther), which is commercially valuable and adaptable to farming conditions. The aim of this study was to evaluate the cytotoxicity and the effect of yerba mate (*Ilex paraguariensis* A. St. Hil.) on the growth parameters of the Mayan cichlid when added to a balanced tilapia feed. Dried, lightly toasted, and crumbled yerba mate from the ROSAMONTE brand was used. The cytotoxicity test was carried out using a bioassay with *Artemia salina* L. Serial dilutions from the yerba mate aqueous extract (0.78–100 mg mL^{-1}) were used to determine the mortality of the nauplii after 24 h of exposure and to calculate the lethal dose (DL50). The fish were distributed at random in nine interconnected fish tanks within a recirculation system, with 10 fish per unit. For 45 d, the fish were fed with a commercial tilapia diet (PURINA), homogenously mixed with non-pelletized yerba mate. Three replicates were established per treatment, corresponding to diets with 0, 1, and 2 % yerba mate (treatments T1 to T3). The feed was offered until the fish were satiated three times a day. A probit analysis was carried out to evaluate DL50. The productive parameters were evaluated with normality and homogeneity tests and arcsine transformation for the percentage data, followed by a one-way analysis of variance (ANOVA) and a Tukey test ($p < 0.05$). The DL50 obtained was 42.42 mg mL^{-1}, indicating a lack of toxicity. No significant differences were found in the productive parameters ($p > 0.05$). The best values were recorded in T3 for final weight (0.53 ± 0.04 g), food conversion rate (2.69 ± 0.06), and condition factor (1.86 ± 0.43), and in T2 for weight gain (0.43 ± 0.06 g) and specific growth rate (4.16 ± 0.89 %). The highest survival rate was obtained in T1 (93.3 ± 11.51 %) and T3 (93.3 ± 5.77 %). Yerba mate is not toxic and can be added to the diets of *C. urophthalmus*, although it does not significantly improve their growth.

Keywords: feed additive, cytotoxicity, growth parameters.

INTRODUCTION

The Mayan cichlid (*Cichlasoma uropthalmus* Günther) is a fish from the cichlid family. Its distribution ranges from the Coatzacoalcos River to Isla Mujeres in Mexico and includes Belize, Guatemala, Honduras, and Nicaragua (Villarreal *et al*., 2011). The species is promoted (Calzada-Ruiz *et al*., 2019) and introduced into aquaculture programs (Jiménez-Martínez *et al*., 2009), based on research on its reproduction, fecundity, nutrition, and population density (Jiménez-Martínez *et al*., 2012).

Yerba mate (*Ilex paraguariensis* A. St. Hil.) is consumed on a daily basis as an infusion in South American countries such as Argentina, Paraguay, Brazil, and Uruguay (Avena-Álvarez *et al*., 2019). This plant contains several active compounds, such as xanthines, from which caffeine, theophylline, and theobromine are derived (Messina *et al*., 2015). Additionally, it contains polyphenols, caffeoyl derivatives, saponins, triterpenes, and basic metabolic minerals, all considered beneficial due to their antioxidant and hypolipidemic effects, with benefits to the central nervous system (Cuesta *et al*., 2018). It also contains tannins, which increase the efficiency of food intake and are also considered beneficial for health (Ramírez *et al*., 2022). On the other hand, Pozebon *et al*. (2015) determined the presence of other elements such as aluminum (Al), barium (Ba), calcium (Ca), copper (Cu), iron (Fe), potassium (K), magnesium (Mg), manganese (Mn), phosphorous (P), strontium (Sr), and zinc (Zn).

Kuropka *et al*. (2021) administered a yerba mate hydroalcoholic extract to mice at a concentration of 10 mg kg^{-1} of body weight per day and found that it has a kidney protective effect and reduces high cholesterol. In turn, Lobo *et al*. (2020) fed lambs a 2 % yerba mate extract, favoring the intake of dry matter and reducing fat thickness, as well as producing an increase in the final weight and in white blood cells and lymphocytes. Barbato *et al*. (2019) obtained a difference of 1.79 L in milk produced in cows supplemented with 500 g of yerba mate a day in comparison with the cows fed normally.

The addition of plants rich in active compounds to the feed of farmed fish can favor their growth parameters, as shown with *Ulva lactuca* L. and *Lemna gibba* L., obtaining the greatest weight in young tilapia with the addition of 20 % of these plants (Aguilera-Morales *et al*., 2022). Hassan *et al*. (2018) found that by adding 1 % *Rosmarinus officinalis* Spenn., they obtained a greater growth rate in tilapia offspring. Salem and Abdel-Ghany (2018) obtained better growth results when they gave 2 g kg^{-1} of *Citrus sinensis* rind (L.) Osbeck. Cruz-Velázquez *et al*. (2014) obtained better growth in pacu (*Piaractus brachypomus*) and tilapia (*Oreochromis niloticus*) when they added 15 % *Lemna minor* L. and *Azolla filiculoides* Lam. to their feed. Therefore, the aim of this study was to evaluate the cytotoxicity and effect of yerba mate added to the tilapia feed on the growth of the Mayan cichlid.

MATERIALS AND METHODS

Plant material

Yerba mate (*Ilex paraguariensis* A. St. Hil.) from ROSAMONTE (Misiones, Argentina) was used. According to the product specifications, the leaves are dried, lightly toasted, crumbled, and packaged in paper bags. The nutritional information reports 4.7 g of carbohydrates, 0.6 g of proteins, 0 g of total and trans fats, 0 g of sodium, and an energy content of 21 kcal. Prior to analysis, the plant material underwent additional grinding to achieve a particle size of 0.35 mm, resulting in a flour-like texture.

Cytotoxicity test

For the cytotoxicity test, 0.1 g of artemia cysts (*Artemia salina* L.) were weighed and placed in a salt solution (38 g L^{-1}) to hatch. They were constantly ventilated for 24 h at temperatures from 25 to 29 °C. Subsequently, 100 mg of the yerba mate were weighed and placed in a microcentrifuge tube with a cover and 1 ml of the salt solution and left to stand for 48 h. In a 96-well plate, a serial microdilution was performed, where 100 µl of the yerba mate aqueous extract was placed, obtaining concentrations between 100 and 0.78 mg mL^{-1}. Straight afterwards, 10 to 15 artemia were added, with 100 µL of the salt solution. Tween 80 (Sigma P1754, St. Louis, MO, USA) was used as a positive control and salt solution as a negative control. The plate was incubated for 24 h, and the test was evaluated in triplicate. After this time period, a reading was taken from every well, where the living and dead artemia were counted to determine the percentage of mortality using the following formula (Rangel-López *et al*., 2022):

$$\text{Mortality} = \frac{\text{Number of dead nauplii}}{\text{Initial number of nauplii}} \times 100$$

In order to establish the level of toxicity, the criteria defined by Mentor *et al*. (2014) were applied, in which the values of over 1 mg mL^{-1} indicate the absence of toxic effects, values between 0.5 and 1 mg mL^{-1} indicate low toxicity, those between 0.1 and 0.5 mg mL^{-1} indicate medium toxicity, and values that do not surpass 0.1 mg mL^{-1} indicate high toxicity.

Preparation of the experimental feed

According to the manufacturer's information, PURINA (Mexico) commercial tilapia feed (0.35 mm) was used, with a protein content of 44 %, 12 % raw fat, 2.5 % raw fiber, 12 % humidity, and 12 % ash. The food was uniformly mixed with yerba mate (Table 1) and not pelletized.

Experimental design

The experiment was established in the aquaculture laboratory of the Academic Division of Farming Science at Juárez Autonomous University in Tabasco, Mexico (17° 78″ 59′ N, 92° 95″ 50′ W). A total of 120 fish were used, which were weighed

Table 1. Commercial feed and yerba mate (*Ilex paraguariensis* A. St. Hil.) content per treatment for Mayan cichlid consumption (*Cichlasoma uropthalmus* Günther).

Ingredients	T1: Control	T2: 1 % yerba mate	T3: 2 % yerba mate
Feed	100 g	99 g	98 g
Yerba mate	0 g	1 g	2 g
Total	100 g	100 g	100 g

and measured individually, for an average weight of 0.15 ± 0.11 g. The fish were distributed at random in nine tanks with a capacity of 80 L each, and 10 fish were placed in each tank. To maintain water quality in all treatments (water temperature of 28°C, dissolved oxygen of 5 ppm, pH of 8, and total ammonium below 0.1 mg L^{-1}), the tanks were linked together in a recirculation system. All treatments were carried out in triplicate. The feed for each corresponding treatment was given three times per day, at 8:00, 11:00, and 14:00, until satiation. The experimental period was 45 d long.

Growth parameters

Using an ichthiometer (mm) and a digital scale with an accuracy of 0.1 g (Ohaus Scout Pro SP601, Mexico), the initial biometrics for total length and weight were measured every 15 d. To determine the growth parameters, the formulas proposed by Arellano-Carrasco *et al*. (2023) were used:

$$\text{Survival (\%)} = \frac{\text{Number of final fish}}{\text{Number of initial fish}} \times 100$$

$$\text{Weight gain (g)} = \text{Final weight} - \text{Initial weight}$$

$$\text{Specific growth rate} = \frac{(\ln \text{Final weight} - \ln \text{Initial weight}}{\text{Days fed}} \times 100$$

$$\text{Feed conversion rate} = \frac{\text{Feed provided}}{\text{Weight increase}}$$

$$\text{Condition factor (k)} = \frac{\text{Final weight}}{(\text{Final length})^3} \times 100$$

Statistical analysis

The lethal dose values (DL50) of the yerba mate aqueous extract were analyzed with a probit analysis using the SAS version 9.0 software (SAS Institute, Cary, NC, USA). From the data obtained on the productive parameters, Kolmogórov-Smirnov normality tests and Bartlett's homogeneity tests were performed. For the parameters expressed as percentages, an arcsine square root transformation was applied. Subsequently, a one-way analysis of variance (ANOVA) was applied ($\alpha = 0.05$), as well as Tukey's test with a significance level of $p < 0.05$ to determine significant differences between treatments, using the package Minitab 18.

RESULTS AND DISCUSSION

Cytotoxicity of yerba mate

According to the criteria established for interpreting the results of the aqueous extract (Figure 1), yerba mate had a toxicity value of 42.42 mg mL^{-1}, indicating that it is nontoxic. Therefore, the use of this plant added to the tilapia feed is considered safe for fish intake. In comparison, Waghulde *et al*. (2019), who evaluated the aqueous extracts of *Annona reticulatatuvo* L. (18.92 mg mL^{-1}), *Allium fisolisum* L. (1846.55 mg mL^{-1}), and *Brassica oleraceaae* L. (64.83 mg mL^{-1}), determined that each species has a degree of toxicity. In turn, Alawi *et al*. (2018) determined that the aqueous *Acacia nilotica* (L.) Delile extract presents no toxicity at concentrations of 500 ppm.

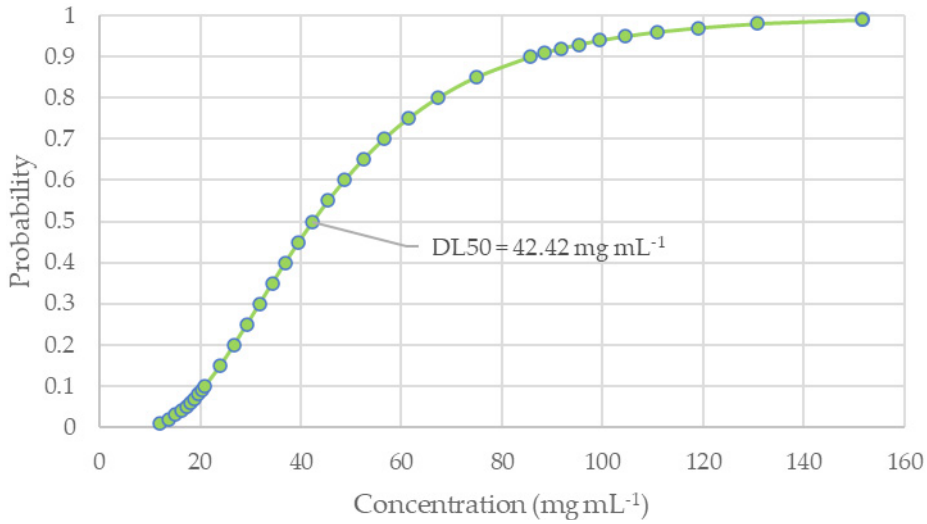

Figure 1. Cytotoxicity of the lethal dose (DL50) of the yerba mate (*Ilex paraguariensis* A. St. Hil.) aqueous extract.

Growth parameters

Experiments have been conducted on the incorporation or addition of plants to fish diets, including seed, leaf, and plant meals (Zetina-Córdoba *et al*., 2010), which may have immunostimulant properties and enhance fish growth (Akrami *et al*., 2015). The results of the growth parameters (Table 2) indicate that no significant differences were observed ($p > 0.05$) between treatments. However, in terms of final weight, treatment T3 (0.53 ± 0.04 g) stood out in comparison to the control. In contrast, Botello-León *et al*. (2011) substituted fish meal with sugarcane by-products, obtaining the best results in the treatments with 14 and 26 % protein.

Table 2. Growth parameters of the Mayan cichlid (*Cichlasoma uropthalmus* Günther) in the treatments evaluated.

Growth parameters	T1: control	T2: 1 %	T3: 2 %
Initial weight (g)	0.15 ± 0.11	0.15 ± 0.11	0.15 ± 0.11
Final weight (g)	0.46 ± 0.04^{A}	0.52 ± 0.04^{A}	0.53 ± 0.04^{A}
Survival (%)	93.3 ± 11.55^{A}	90.0 ± 10.0^{A}	93.3 ± 5.77^{A}
Weight gain (g)	0.31 ± 0.04^{A}	0.40 ± 0.09^{A}	0.38 ± 0.04^{A}
Specific growth rate (%)	2.52 ± 0.19^{A}	3.43 ± 1.35^{A}	2.80 ± 0.18^{A}
Feed conversion rate	3.07 ± 0.17^{A}	2.88 ± 0.48^{A}	2.69 ± 0.06^{A}
Condition factor	1.68 ± 0.16^{A}	1.75 ± 0.14^{A}	1.86 ± 0.43^{A}
Initial length (cm)	1.88 ± 0.07	1.86 ± 0.23	1.89 ± 0.05
Final length (cm)	3.08 ± 0.04^{A}	3.09 ± 0.05^{A}	3.07 ± 0.24^{A}

T1, T2, T3: treatments with yerba mate (*Ilex paraguariensis* A. St. Hil.) included in the diet. ^{ABC} Different letters in the rows indicate significant statistical differences ($p \leq 0.05$).

In terms of survival, the best results were obtained for treatments T1 and T3 (93.3 ± 11.55 and 93.3 ± 5.77 %). On the other hand, Kristiana *et al.* (2020) added noni (*Morinda citrifolia* L.) fruit to commercial tilapia feed with 40 % protein in various concentrations and obtained a survival rate of 100 % in all treatments. Villarreal *et al*. (2011) added soybean protein and wheat gluten to the feed and found that the treatments with higher percentages showed higher mortality. It is worth noting that the Mayan cichlid is considered to be aggressive and territorial, which increases its survival rate.

For weight gain, T2 (0.43 ± 0.06 g) produced the best yields. Emshaw *et al*. (2023) used *Pontederia crassipes* (Mart.) Solms fermentation in young tilapia and found that adding 10 % of the fermentation improved weight gain; however, their control group had similar results. Abidin *et al.* (2022) added neem (*Azadirachta indica* A. Juss.) extract to feed rainbow trout (*Oncorhynchus mykiss*) and found a greater weight gain in fish fed with a 7 % extract. In this study, the best feed conversion rate was obtained in T3 (2.69 ± 0.06). Dohaish *et al*. (2018) reported a feed conversion rate higher than that of this study when adding 5 % *Spirulina platensis* in the diets of *Oreochromis niloticus*.

The specific growth rate was best represented by T2 (4.16 ± 0.89). In comparison, Galeana-López *et al*. (2020) provided maize (*Zea mays* L.) ear leaf extract in the diets of *O. niloticus*, obtaining the best specific growth rate with the 200 mg kg^{-1} feed treatment. Specifically, no comparisons could be made with other authors, due to a total lack of investigations on fish using yerba mate. Regarding the condition factor, the best result was observed in treatment T (1.86 ± 0.43), which is similar to reports by Martínez-Santiago *et al*. (2022), who used oregano essential oil (*Lippia graveolens* Kunth) in tilapia feed.

Yerba mate has 9.5 % protein, 6.3 % lipids, and 7.04 % ash content (Berté *et al*., 2011; Cogoi *et al*., 2013; Frizon *et al*., 2013), as well as secondary metabolites such as methylxanthines, caffeine, theobromine, phenolic acids, chlorogenic acid (Valduga *et al*., 2016), saponins, triterpenes, flavonoids, and xanthines (García-Lázaro, 2023), tannins, carotenoids, and polyphenols (Najman *et al*., 2024). Lizárraga-Velázquez *et al*. (2018) mention that when polyphenols are added to or present in carnivorous fish feed, they can improve immune and antioxidant defenses. Ayutunde *et al*. (2016) mention that diets with leaf meals containing phenols, tannins, and saponins may hinder fish growth. Therefore, yerba mate could benefit fish by enhancing their immune system. However, it can affect the growth parameters of their offspring (Lobo *et al*., 2020).

CONCLUSIONS

Based on the cytotoxicity results with *Artemia salina*, it was determined that the plant can be included in the diet of *Cichlasoma uropthalmus* since it does not exhibit toxicity and therefore does not have a negative effect on its feeding. No variations were found in the growth parameters. Further research that includes a higher proportion of yerba mate in the diet and in pellet form is recommended, as well as studies to determine whether it has an impact on the immune system of the fish.

REFERENCES

Abidin ZU, Hassan HU, Masood Z, Rafique N, Paray BA, Gabol K, Shah MIA, Gulnaz A, Ullah A, Zulfiqar T, Siddique MAM. 2022. Effect of dietary supplementation of neem, *Azadirachta indica* leaf extracts on enhancing the growth performance, chemical composition and survival of rainbow trout, *Oncorhyncus mykiss*. Saudi Journal of Biological Sciences 29 (4): 3075–3081. https://doi.org/10.1016/j.sjbs.2022.01.046

Aguilera-Morales ME, Antonio-Cisneros CM, Flores-Ortíz CM. 2022. Effect of *Lemna gibba* and *Ulva Lactuca* on health and productive performance in juveniles of Nile tilapia (*Oreochromis niloticus*). Agrociencia 56 (6). https://doi.org/10.47163/agrociencia.v56i6.2497

Akrami R, Gharaei A, Mansour MR, Galeshi A. 2015. Effects of dietary onion (*Allium cepa*) powder on growth, innate immune response and hemato-biochemical parameters of beluga (*Huso huso* Linnaeus, 1754) juvenile. Fish and Shellfish Immunology 45 (2): 828–834. https://doi.org/10.1016/j.fsi.2015.06.005

Alawi SMA, Hossain MA, Abusham AA. 2018. Antimicrobial and cytotoxic comparative study of different extracts of Omani and Sudanese gum acacia. Beni-Suef University Journal of Basic and Applied Sciences 7 (1): 22–26. https://doi.org/10.1016/j.bjbas.2017.10.007

Arellano-Carrasco JG, Martínez-García R, Asiain-Hoyos A, Reta-Mendiola JL, Díaz-Rivera P, Frías-Gómez SA, Martínez-Burguete T, Asencio-Alcudia GG, Jiménez-Martínez LD, Guerrero-Zarate R, Sepúlveda-Quiroz CA, Álvarez-González CA. 2023. Dietary effects of sodium propionate supplementation on growth, digestive enzyme activity and immune system gene expression of tropical gar juveniles (*Atractosteus tropicus*). Research Square. https://doi.org/10.21203/rs.3.rs-2748665/v1

Avena-Álvarez V, Messina D, Corte C, Mussi-Stoizik J, Saez A, Boarelli P, Pérez-Elizalde R. 2019. Asociación entre el consumo de yerba mate y el perfil lipídico en mujeres con sobrepeso. Nutrición Hospitalaria 36 (6): 1300–1306.

Ayutunde EO, Ada FB, Udeh GN. 2016. Effect of partial replacement of fishmeal with *Moringa oleifera* leaf meal on the hematology, carcass composition and growth performance of *Clarias gariepinus* (Burchell 1822) fingerlings. International Journal of Fisheries and Aquatic Studies 4 (4): 307–311.

Barbato O, Holmes B, Filipescu IE, Celi P. 2019. Dietary supplementation of yerba mate (*Ilex paraguariensis*) during the dry period improves redox balance in lactating dairy cows. Antioxidants 8 (2): 38. https://doi.org/10.3390/antiox8020038

Berté KAS, Beux MR, Spada PKWDS, Salvador M, Hoffmann-Ribani R. 2011. Chemical composition and antioxidant activity of yerba-mate (*Ilex paraguariensis* A. St.-Hil., Aquifoluaceae) extract as obtained by spray drying. Journal of Agricultural and Food Chemistry 59 (10): 5523–5527. https://doi.org/10.1021/jf2008343

Botello-León A, Viana MT, Téllez-Girón E, Pullés-Ariza E, Cisneros-López M, Solano-Silveira G, Valdivié M, Miranda-Miranda O, Rodríguez-Valera Y, Cutiño-Espinoza M, Savón L, Botello-Rodríguez A. 2011. Sustitución de la harina de pescado por harina de caña proteínica para la engorda de tilapia roja. Agrociencia 45: 23–31.

Calzada-Ruiz D, Álvarez-González C, Peña E, Jiménez-Martínez LD, Alcantar-Vázquez J, Becerril-Morales F, Martínez-García R, Camarillo-Coop S. 2019. Lipid requirement using different oil sources in Maya cichlid *Cichlasoma urophthalmus* larvae (Percoidei: Cichlidae). Latin American Journal of Aquatic Research 47 (2): 331–341. https://doi.org/10.3856/vol47-issue2-fulltext-13

Cogoi L, Giacomino MS, Pellegrino N, Anesini C, Filip R. 2013. Nutritional and phytochemicas study of *Ilex paraguariensis* fruits. Journal of Chemistry 2013 (1): 750623. https://doi.org/10.1155/2013/750623

Cruz-Velázquez Y, Kijora C, Vergara-Hernández W, Schulz C. 2014. On-farm evaluation of cachama blanca and Nile tilapia fed fermented aquatic plants in a polyculture. Orinoquia 18 (2): 269–277.

Cuesta A, Guigou C, Varela A, Ferrero L, Charlin MC, Lluberas R. 2018. Efecto agudo del consumo de yerba mate (*Ilex paraguariensis*) sobre el ritmo cardíaco en pacientes derivados para estudio Holter. Archivos de Cardiología de México 88 (5): 468–473. https://doi.org/10.1016/j.acmx.2018.05.004

Dohaish BE, Al Dhahri M, Omar H. 2018. Potential application of the blue-green alga (*Spirulina platensis*) as a supplement in the diet of Nile tilapia (*Oreochromis niloticus*). Applied Ecology and Environmental Research 16 (6): 7883–7902. https://doi.org/10.15666/aeer/1606_78837902

Emshaw Y, Getahun A, Geremew A. 2023. Effect of different levels of fermented water hyacinth leaf meal on feed utilization and performance of juvenile Nile tilapia. Online Journal of Animal and Feed Research 13 (1): 55–62. https://doi.org/10.51227/ojafr.2023.9

Frizon C, Perussello C, Sturion J, Hoffmann-Ribani R. 2013. Novel beverages of yerba-mate and soy: Bioactive compounds and functional properties. Beverages 4 (1): 21. https://doi.org/10.3390/beverages4010021

Galeana-López JA, Hernández C, Leyva-López N, Lizárraga-Velázquez CE, Sánchez-Gutiérrez EY, Basilio HJ. 2020. Cor husk extracts an antioxidant additive in diets for Nile tilapia (*Oreochromis niloticus*) fingerlings: Effect on growth performance, feed intake and toxicity. Biotecnia 22 (2): 147–154.

García-Lázaro R. 2023. Dieta, química de la yerba mate y salud. Educación Química 34. https://doi.org/10.22201/fq.18708404e.2023.4.86129e

Hassan AAM, Yacout MH, Khalel MS, Hafsa SH, Ibrahim MAR, Mocuta DN, Turek Rahoveanu A, Dediu L. 2018. Effects of some herbal plant supplements on growth performance and the immune response in Nile tilapia (*Oreochromis niloticus*). Agriculture for Life, Life for Agriculture Conference Proceedings 1 (1): 134–141.

Jiménez-Martínez LD, Álvarez-González CA, Contreras-Sánchez WM, Márquez-Couturier G, Arias-Rodríguez L, Almeida-Madrigal JA. 2009. Evaluation of larval growth and survival in Mexican mojarra *Cichlasoma uropththalmus* and bay snook, *Petenia splendida*, under different initial stocking densities. Journal of the World Aquaculture Society 40 (6): 753–761. https://doi.org/10.1111/j.1749-7345.2009.00295.x

Jiménez-Martínez LD, Contreras RJ, Arias-Rodríguez L, Álvarez-González CA, Carmona-Díaz E, de la Cruz-Hernández NE. 2012. Efecto de la salinidad en larvas de la mojarra castarrica *Cichlasoma urophthalmus*. Kuxukab' 28 (34): 45–50.

Kristiana V, Mukti AT, Agustono. 2020. Increasing growth performance of Nile tilapia (*Oreochromis niloticus*) by supplementation of noni *Morinda citrifolia* fruit via diet. AACL Bioflux 13 (1): 159–166.

Kuropka P, Zwyrzykowska-Wodzinska A, Kupczynski R, Wlodarczyk M, Szumny A, Nowaczyk RM. 2021. The effect of *Ilex* × *meserveae* S. Y. Hu extract and its fractions on renal morphology in rats fed with normal and high-cholesterol diet. Foods 10 (4): 818. https://doi.org/10.3390/foods10040818

Lizárraga-Velázquez CE, Hernández C, González-Aguilar GA, Basilio-Herdia J. 2018. Propiedades antioxidantes e inmunoestimulantes de polifenoles en peces carnívoros de cultivo. CienciaUAT 12 (2): 127–136.

Lobo RR, Vincenzi R, Rojas-Moreno DA, Lobo AAG, da Silva CM, Benetel-Junior V, Ghussn LR, Mufalo VC, Berndt A, Gallo SB, Pinheiro RSB, Bueno ICS, Faciola AP. 2020. Inclusion of Yerba mate (*Ilex paraguariensis*) extract in the diet of growing lambs: Effects on blood parameters, animal performance and carcass traits. Animals 10 (6): 961. https://doi.org/10.3390/ani10060961

Martínez-Santiago A, Martínez-García JA, Núñez-García LG, Arana-Magallón FC, Vázquez-Silva G, Díaz-Larrea J, Cabrera R. 2022. Efecto del aceite de orégano mexicano *Lippia graveolens* en el crecimiento y supervivencia de crías de la tilapia *Oreochromis niloticus*. Brazilian Applied Science Review 6 (6): 1558–1573. https://doi.org/10.34115/basr6n6-009

Mentor RH, Blagica J, Tatjana KP. 2014. Toxicological evaluation of the plant products using brine shrimp (*Artemia salina* L.) model. Macedonian Pharmaceutical Bulletin 60 (1): 9–18. https://doi.org/10.33320/maced.pharm.bull.2014.60.01.002

Messina D, Soto C, Méndez A, Corte C, Kemnitz M, Avena-Álvarez V, del Balzo D, Pérez-Elizalde R. 2015. Efecto hipolipemiante del consumo de mate en individuos dislipidémicos. Nutrición Hospitalaria 31 (5): 2131–2139.

Najman K, Rakjewski R, Sadowska A, Hallmann E, Buczak K. 2024. Changes in the physicochemical and bioactive properties of yerba mate depending on the brewing conditions. Molecules 29 (11): 2590. https://doi.org/10.3390/molecules29112590

Pozebon D, Dressler VL, Alexandre MCA, de Oliveira TC, Ferrão MF. 2015 Toxic and nutrient elements in yerba mate (*Ilex paraguariensis*). Food Additives and Contaminants: Part B 8 (3): 215–220. https://doi.org/10.1080/19393210.2015.1053420

Ramírez MR, Mohamad L, Alarcón-Segovia LC, Rintoul I. 2022. Effect of processing on the nutritional quality of *Ilex paraguariensis*. Applied Sciences 12 (5): 2487. https://doi.org/10.3390/app12052487

Rangel-López L, Rivero-Pérez N, Valladares-Carranza B, Olmedo-Juárez A, Delgadillo-Ruiz L, Vega-Sánchez V, Hori-Oshima S, Nassan MA, Batiha GES, Zaragoza-Bastida A. 2022. Antibacterial potential of *Caesalpinio coriaria* (Jacq.) will fruit against *Aeromonas* spp. of aquaculture importance. Animals 12 (4): 511. https://doi.org/10.3390/ani12040511

Salem M, Abdel-Ghany HM. 2018. Effects of dietary orange peel on growth performance of Nile tilapia (*Oreochromis niloticus*) fingerlings. Aquaculture Studies 18 (2): 127–134. http://doi.org/10.4194/2618-6381-v18_2_06

Valduga AT, Goncalves IL, Dartora N, Mielniczki-Pereira AA, de Souza LM. 2016. Phytochemical profile of morphologically selected yerba-mate progenies. Ciencia e Agrotecnologia 40 (1): 114–120. https://doi.org/10.1590/s1413-70542016000100011

Villarreal C, Gelabert R, Gaxiola G, Cuzon G, Amador LE, Guevara E, Brito R. 2011. Crecimiento de alevines de *Cichlasoma urophthalmus* con dietas basadas en diferentes niveles de inclusión de proteína de soya y gluten de trigo. Universidad y Ciencia 27 (1): 53–62.

Waghulde S, Kale MK, Patil VR. 2019. Brine shrimp lethality assay of the aqueous and ethanolic extracts of the selected species of medical plants. Proceedings 41 (1): 47. https://doi.org/10.3390/ecsoc-23-06703

Zetina-Córdoba P, Reta-Mendiola JL, Ortega-Cerrilla ME, Ortega-Jiménez E, Sánchez-Torres MTE, Herrera-Haro JG, Becerril-Herrera M. 2010. Utilización de la lenteja de agua (Lemnaceae) en la producción de tilapia (*Oreochromis* spp.). Archivos de Zootecnia 59 (232): 133–155. https://doi.org/10.21071/az.v59i232.4911

Agrociencia

STAKES ROOTING OF 'Biloxi' BLUEBERRY (*Vaccinium corymbosum* L.) PLANTS

Cristóbal **Guadarrama-Pérez**[1], Manuel **Sandoval-Villa**[1*], Vicente **Espinosa-Hernández**[1], Gregorio **Arellano-Ostoa**[2], César **San Martín-Hernández**[1]

[1]Colegio de Postgraduados Campus Montecillo. Programa de Edafología. Carretera México-Texcoco km 36.5, Montecillo, Texcoco, State of Mexico, Mexico. C. P. 56264.
[2]Colegio de Postgraduados Campus Montecillo. Programa de Fruticultura. Carretera México-Texcoco km 36.5, Montecillo, Texcoco, State of Mexico, Mexico. C. P. 56264.
* Author for correspondence: msandoval@colpos.mx

Citation: Guadarrama-Pérez C, Sandoval-Villa M, Espinosa-Hernández V, Arellano-Ostoa G, San Martín-Hernández C. 2025. Stakes rooting of 'Biloxi' blueberry (*Vaccinium corymbosum* L.) plants. **Agrociencia** 59(5): 667-681. https://doi.org/ 10.47163/agrociencia.v59i5.3310

Editor in Chief:
Dr. Fernando C. Gómez Merino

Received: September 27, 2024.
Approved: June 27, 2025.
Published in Agrociencia: July 03, 2025.

ABSTRACT

Blueberry (*Vaccinium corymbosum* L.), native to North America, has become one of the most important fruit crops in Mexico and the world due to its hardiness, flavor, and health benefits. The objective of this study was to evaluate the inductive capacity of naphthaleneacetic acid (NAA), salicylic acid (SAL), their combination, a *Plantago* spp. extract, and indolebutyric acid (IBA) in the rooting of semi-woody cuttings of 'Biloxi' blueberry. In a rooting chamber, 5 cm long cuttings with two apical leaves cut transversely were established and treated with different concentrations of NAA (0, 15, and 20 mg L^{-1}), SAL (0, 50, and 75 mg L^{-1}), and their combination, with three additional controls of *Plantago* spp. extract and IBA (4000 and 3000 mg L^{-1}). A completely randomized design with treatments in a factorial arrangement and three additional controls was used. No significant individual effects of NAA or SAL were detected. However, individual applications of 20 mg L^{-1} of NAA and 75 mg L^{-1} of SAL showed the best results for rooting percentage (93.75 %), number of first- (8.88 and 10.25) and second-order roots (72.38 and 65.13), length of first- (33.92 and 32.44 mm) and second-order roots (17.6 and 19.67 mm), and root volume (81.88 and 85.63 mm^3). These results were statistically equivalent to the 4000 and 3000 mg L^{-1} concentrations of IBA. In contrast, the combination of NAA and SAL, as well as the plant extract, resulted in low values in all the variables evaluated.

Keywords: indolebutyric acid, naphthaleneacetic acid, salicylic acid, plant extract.

INTRODUCTION

Blueberry (*Vaccinium corymbosum* L.) is a plant native to North America. Because of its hardiness, pleasant flavor, antioxidant, and anti-inflammatory properties, the fruit has captured the attention of many producers and consumers. Over the years, the number of hectares dedicated to its cultivation has increased (Tinoco-Plasencia *et al*., 2023). In Mexico, this crop has had an important impact; from 2012 to 2022, the harvested area and production increased from 885 to 5887 ha and from 7191 to 67 304 Mg, respectively (FAO, 2024). This crop can be propagated in two ways: sexually

through seeds and asexually through meristematic tissue. Rooting cuttings is an asexual propagation technique that focuses on multiplying plants from stem segments of a specific individual, which are subjected to induction for root development under specific environmental conditions, which guarantees a high percentage of genetic resemblance to the mother plant (López-Corona *et al*., 2019).

According to Ikeuchi *et al*. (2016) and Druege *et al*. (2019), the rooting process is divided into three stages: induction, initiation, and expression. The first stage involves molecular and biochemical processes that do not produce visible changes in the cutting, including cell reprogramming, during which competent cells from the vascular tissue give rise to root primordia. In some cases, cells must first be reprogrammed to perceive and respond to rooting signals. During the second stage, qualitative changes occur in cell structure, accompanied by cell division and the organization of dome-shaped root primordia resulting from the differentiation of new cell groups. Finally, in the third stage, the root primordia undergo further differentiation and growth, developing into root structures with distinct vascular bundles connected to the vascular cylinder of the cutting, ultimately leading to root emergence.

The time and percentage of rooting depend on the type of stake, as its regenerative capacity is determined by endogenous factors, such as the levels of carbohydrates, mineral salts, and plant hormones available, auxins being considered the most important (Hu *et al*., 2020). Similarly, the substrate plays a determining role, as it is responsible for supporting the cutting of the stake, providing a dark environment, and supplying water and air in the metabolic process of root induction and elongation (Hartmann *et al*., 1997). Similarly, external conditions such as temperature and light must be considered, as they regulate respiration, vegetative shoot development, and stake reserve conservation, whereas relative humidity influences leaf temperature and gas exchange. Microorganisms anchored to the plant material are also an external factor that increases the risk of contamination and death of the cuttings (Owen and Maynard, 2007). To reduce time and increase the percentage of rooting, it is necessary to add exogenous hormones (growth regulators), where auxins stand out, which play an important role in the induction and development of roots, such as indolebutyric acid and naphthaleneacetic acid (López-Corona *et al*., 2019).

Each species has a certain propagation capacity, so specific protocols are required to achieve the highest percentage of multiplication (Le *et al*., 2023). Ligarreto *et al*. (2013), Kim *et al*. (2014), and Leiva *et al*. (2023) obtained a higher rooting percentage when applying naphthaleneacetic acid in *Vaccinium meridionale* Swartz, *V. corymbosum* 'Bluecrop' and 'Sunrise', and *V. corymbosum* 'Biloxi', respectively. Salicylic acid, a phenolic compound, can function as an auxin cofactor (Pacholczak and Nowakowska, 2015). By using this compound, Sardoei *et al*. (2014) and Pacholczak and Nowakowska (2015) reported higher rooting percentages in *Euphorbia pulcherrima* Willd. and *V. corymbosum* 'Bluecrop' and 'Duke.'

Extracts of *Plantago major* L. and *P. lanceolata* L. possess antimicrobial, anti-inflammatory, and wound-healing properties, and contain several secondary metabolites (phenols,

flavonoids, saponins, and alkaloids) (Mazzutti *et al*., 2017), in addition to carbohydrates, indoleacetic acid, vitamins, and traces of salicylic acid (Berit, 2000). However, little is known about their use in agricultural practices. Because of their properties, they may be able to induce cutting rooting. A commonly used growth regulator is indolebutyric acid, such as in *V. corymbosum* 'Biloxi' (An *et al*., 2018), 'Powderblue' (Colombo *et al*., 2018), 'Woodard' (Higuchi *et al*., 2021), and wild blueberry (Tejada-Alvarado *et al*., 2021). However, information on growth regulators in rooting cuttings of this crop is scarce and ambiguous. Therefore, the objective of this research was to evaluate the inductive capacity of naphthaleneacetic acid, salicylic acid, the combination of both compounds, *Plantago* spp. extract, and indolebutyric acid on the rooting of 'Biloxi' blueberry cuttings.

MATERIALS AND METHODS

Location of the study area and plant material

This study was conducted in an experimental greenhouse of the Plant Nutrition area of the Postgraduate College Campus Montecillo in Texcoco, State of Mexico, Mexico. Eight-year-old *Vaccinium corymbosum* 'Biloxi' plants were fed a Steiner nutrient solution at half of its original concentration (Steiner, 1984), pH 5.5, and an ammonium:nitrate ratio of 75:25. A rooting chamber was constructed with white greenhouse plastic, where substrate temperature (30 ± 2 °C) and relative humidity (≥ 75 %) were controlled by circulating warm water (50 ± 3 °C) below the seedlings and water misting, respectively.

Experimental design and compounds evaluated

A completely randomized design with treatments in an increased factorial arrangement was used, where naphthaleneacetic acid (NAA) and salicylic acid (SAL) were evaluated at three levels (0, 15, and 20, and 0, 50, and 75 mg L^{-1}, respectively), with three additional controls corresponding to a plant extract from *Plantago* spp. and two concentrations of indolebutyric acid (IBA) (4000 and 3000 mg L^{-1}). Each treatment was carried out with four replicates, where the experimental units consisted of four cells (5 × 5 cm) of a seedbed with a blueberry stake.

Treatments and substrate preparation

NAA (Pacific Growers, Mexico) and SAL (Fagalab, Mexico) with 98 % purity were dissolved in 5 mL of 96 % alcohol at the specified concentration for each treatment and mixed with 95 mL of deionized water. A total of 100 mL of *Plantago* spp. extract was used, which was obtained by boiling 1 L of deionized water with 200 g of aerial parts of plants collected for 15 min and dried in the shade for 30 d. Similarly, the concentrations of 4000 and 3000 mg L^{-1} of IBA were prepared on a 4:6 and 3:7 volume basis from a commercial product containing 10 000 mg of IBA (Intercontinental Import Export S.A. de C.V., Mexico) and hypoallergenic talc (Mennen, USA).

The substrate was prepared in a 1:1 ratio of perlite and peat and saturated with deionized water. Before distribution, the substrate was sterilized three times in pressure pots (Presto, Mexico) with pressures ranging from 0.1 to 0.13 MPa for 3 h at 24-h intervals.

Stakes establishment

Two apical leaves were cut transversely from the apical portion of vegetative shoots of plants with a semi-lignified consistency to create multiple 5-cm-long cuttings, which were disinfested twice in agitation for 1 min in metalaxyl-M (1.7 mL L^{-1}) (Syngenta, Switzerland) and captan (2 g L^{-1}) (Adama, Israel). After 3 s of immersion in each solution, 1 cm of the stake stem was inserted into the designated seedbed alveolus. During the entire experiment (70 d), six fungicide applications were made at the base of the stem of the cuttings at 10-d intervals.

Acclimatization of rooted cuttings

Seventy days after establishment (DAE), the rooted cuttings were removed from the chamber seedbeds. To avoid poor root development and facilitate transplanting, their root system was pruned. The cuttings were immersed for 1 s in mancozeb (2 g L^{-1}) (Syngenta, Switzerland) before being transplanted in a 1:1 volume of perlite and peat substrate in 60-cavity unicell forest trays (Hydrocultura, Mexico), with cells measuring 182 cm^3. Propamocarb hydrochloride (2.5 mL L^{-1}) (Bayer, Germany) was applied at the base of the stem. Finally, each tray was covered with polypropylene plastic, and the plastic was cut weekly with scissors until the tray was completely free.

Study variables and statistical analysis

At the end of the experiment (70 DAE), the percentage of survival and rooting was obtained by considering the surviving and rooted cuttings over the total number of cuttings per experimental unit. The number of first- and second-order roots was recorded by counting the number of roots in the root system of the rooted cuttings. The diameter and length of first- and second-order roots were evaluated by measuring the diameter of the thickest root and the longest first- and second-order roots, using the digital processing program ImageJ version 1.8.0. Root volume was obtained by submerging the roots of each stake into a 500 μL (mm^3) syringe and comparing the initial water volume against the final volume.

The data obtained were subjected to a normality test (Shapiro-Wilk) ($p \geq 0.05$), homogeneity of variances (Bartlett) ($p \geq 0.05$), and independence of residuals; likewise, an analysis of variance corresponding to a randomized design with treatments in augmented factorial arrangement and a multiple comparison of means by using Fisher's least significant difference test ($p \leq 0.05$) were performed in the statistical program R version 4.3.2 and Microsoft Excel 2021.

RESULTS AND DISCUSSION

Survival and rooting rates

After 70 d of establishment, there were no significant effects on the survival percentage attributable to the additional factors, interactions, and controls (Table 1). In general, the survival percentages were high (87.5 to 100 %), which is attributed to the care given during this experiment, especially the disinfection of the substrate used, which is an important factor when establishing cuttings in an environment with high relative humidity (Badilla-Valverde and Murillo-Gamboa, 2005). In this regard, Li *et al*. (2021) state that in order to maintain live explants of *Vaccinium arboreum* Marshall, a humid environment inside chambers using nebulizers is required, a factor that allowed them to report a 100 % survival rate.

Table 1. Comparison of means using Fisher's least significant difference test for survival and rooting rates in cuttings of *Vaccinium corymbosum* L. 'Biloxi' with the effects of various treatments.

Treatment	Composition (mg L^{-1})	Survival percentage	Rooting percentage
1	0 NAA+ 0 SAL	93.75 a	75.00 ab
2	15 NAA+ 0 SAL	100.00 a	68.75 ab
3	20 NAA+ 0 SAL	100.00 a	93.75 a
4	0 NAA+ 50 SAL	93.75 a	62.50 b
5	0 NAA+ 75 SAL	100.00 a	93.75 a
6	15 NAA+ 50 SAL	87.50 a	62.50 b
7	15 NAA+ 75 SAL	100.00 a	62.50 b
8	20 NAA+ 50 SAL	87.50 a	62.50 b
9	20 NAA+ 75 SAL	87.50 a	56.25 b
10	*Plantago* spp.^{z}	100.00 a	56.25 b
11	4000 IBA^{z}	87.50 a	68.75 ab
12	3000 IBA^{z}	100.00 a	81.25 ab
F-NAA	0	95.83 a	77.08 a
	15	95.83 a	64.58 a
	20	91.67 a	70.83 a
F-SAL	0	97.92 a	79.17 a
	50	89.58 a	62.50 a
	75	95.83 a	70.83 a
Overall average number of treatments		94.79	70.31
CV (%)		12.03	30.93
p-value of treatments		0.4556^{ns}	0.0495*
p-value of F-NAA		0.5912^{ns}	0.5587^{ns}
p-value of F-SAL		0.1911^{ns}	0.4232^{ns}
$LSD_{0.05}$ of treatments		16.36	31.19
$LSD_{0.05}$ of factors		8.55	17.57

NAA: naphthaleneacetic acid; SAL: salicylic acid; IBA: indolebutyric acid; z: additional control; F-NAA: naphthaleneacetic acid factor; F-SAL: salicylic acid factor; CV: coefficient of variation; ^{ns}: not significant; *: significant differences; $LSD_{0.05}$: least significant difference. Values with the same letter are statistically similar according to Fisher's least significant difference test ($p \leq 0.05$).

Another important factor was the consistency of the stake. In general, a semi-lignified consistency stake was used, which resulted in greater resistance to dehydration (Badilla-Valverde and Murillo-Gamboa, 2005). On the other hand, the exposure time of the cuttings in the solution can affect their survival, since prolonged times can cause phytotoxicity and death of the cuttings. Similarly, this can be aggravated depending on the concentration and type of plant material used (Coimbra *et al*., 2016).

In this study, it was demonstrated that 3 seconds of exposure with NAA, SAL, and IBA at the concentrations used did not affect the survival of semi-lignified 'Biloxi' blueberry cuttings, as opposed to deionized water and *Plantago* spp. The survival rates were similar to those shared by Colombo *et al*. (2018), with 100 % survival in 5 cm cuttings of 'Powderblueberry' blueberry when applying 3000 mg L^{-1} of IBA in talc. On the other hand, other studies report high survival percentages with long exposure times, such as Sardoei *et al*. (2014) on cuttings with 300 mg L^{-1} of NAA for 24 h and Leiva *et al*. (2023) on 'Biloxi' blueberry nodal segments for 15 min. This shows that exposure time will depend on cultivar, stake consistency, and type of compound (Coimbra *et al*., 2016).

At the end of the experiment, there were no significant differences in the rooting rates between the NAA and SAL factors (Table 1). On the other hand, for the interactions and controls, the comparison of means indicated that the rooting rates reported when using 20 and 75 mg L^{-1} of NAA and SAL (93.75 %) were statistically equal to those achieved with deionized water (75 %), 15 mg L^{-1} of NAA (68.75 %), 4000 mg L^{-1} of IBA (68.75 %), and 3000 mg L^{-1} of IBA (81.25 %). However, these values were higher than those obtained with other compounds, with values between 56.25 and 62.5 % (Figure 1). The best rooting percentages in this experiment were considerably high (68.75 to 93.75 %), corresponding to the individual use of NAA and SAL, IBA, and deionized water.

In other studies, it was reported that the highest rooting percentage was achieved in 'Biloxi' blueberry cuttings with 100 mg L^{-1} of NAA (Leiva *et al*., 2023). With 300 mg L^{-1} of SAL, a 75 % rooting rate was obtained in semi-lignified cuttings of *Euphorbia pulcherrima* (Sardoei *et al*., 2014), and with various concentrations of IBA in blueberry 'Biloxi' (3000 mg L^{-1}) (An *et al*., 2018), 'Powderblue' (3000 mg L^{-1} IBA in talc) (Colombo *et al*., 2018), 'Woodard' (1000 mg L^{-1}) (Higuchi *et al*., 2021), and wild blueberry (2000 mg L^{-1}) (Tejada-Alvarado *et al*., 2021). Likewise, Isfendiyaroğlu and Özeker (2008) and Pacholczak and Nowakowska (2015), by combining IBA and SAL, achieved high rooting percentages in cuttings of *Olea europaea* L. 'Domat' and blueberry 'Bluecrop' and 'Duke,' respectively.

The positive effects of NAA, SAL, and IBA on the rooting of plant material are due to the versatility of these compounds in the accumulation of indoleacetic acid, which has an impact on the rooting speed of cuttings and root development (Hopkins and Hüner, 2008; Damodaran and Strader, 2019; Dong *et al*., 2020). However, in this research, the percentage of rooting obtained was statistically equal to the control with deionized water, which can be attributed to a greater production of endogenous auxins in stakes

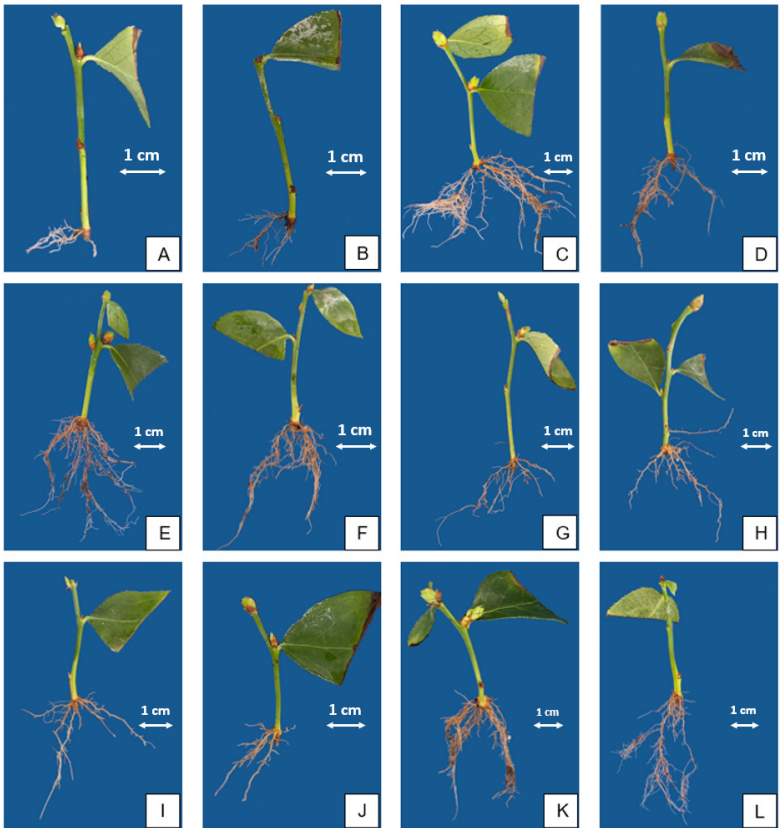

Figure 1. Rooted cuttings of *Vaccinium corymbosum* L. 'Biloxi' after 70 d of establishment with the effects of various treatments. A: deionized water; B: 15 mg L^{-1} naphthaleneacetic acid (NAA); C: 20 mg L^{-1} NAA; D: 50 mg L^{-1} salicylic acid (SAL); E: 75 mg L^{-1} SAL; F: 15 + 50 mg L^{-1} NAA and SAL; G: 15 + 75 mg L^{-1} NAA and SAL; H: 20 + 50 mg L^{-1} NAA and SAL; I: 20 + 75 mg L^{-1} NAA and SAL; J: extract of *Plantago* spp. K: 4000 mg L^{-1} of indolebutyric acid (IBA); L: 3000 mg L^{-1} of IBA.

without complete lignification, so that sometimes it is not necessary to add exogenous auxins to stimulate rooting (Shiembo *et al*., 1997). Therefore, it is possible that the conditions to which the cuttings were exposed were sufficient to stimulate rooting, even without the addition of growth regulators (Owen and Maynard, 2007).

On the other hand, it is likely that the low rooting percentage reported in the treatments where NAA and SAL were combined is due to an endogenous hormonal imbalance caused by the concentrations of these regulators (Haissig, 1970). This agrees with de Klerk *et al*. (1997), who found that SAL inhibits rooting produced by IBA and NAA in apple micro-cuttings. Likewise, Isfendiyaroğlu and Özeker (2008) emphasize that SAL should be applied in conjunction with auxins to avoid inhibiting root formation.

Number of first and second order roots

There are variables that are used as morphological indicators of the quality of root development, such as root number, length, diameter, and volume. These serve to evaluate root development, an important factor that reduces mortality in transplanting and acclimatization of cuttings (Colombo *et al*., 2018). According to the analysis of variance, no differences in the number of first- and second- order roots were reported in any of the factors (Table 2).

For the number of first-order roots, the comparison of means of the interactions and additional controls indicated that when 75 mg L^{-1} of SAL was applied, 10.25 first-order

Table 2. Comparison of means with Fisher's least significant difference test of the number of first and second order roots in cuttings of *Vaccinium corymbosum* L. 'Biloxi' with the effects of various treatments.

Treatment	Composition (mg L^{-1})	Number of roots			
		First order		Second order	
1	0 NAA+ 0 SAL	4.37	bc	16.50	d
2	15 NAA+ 0 SAL	3.25	c	14.50	d
3	20 NAA+ 0 SAL	8.87	ab	72.37	a
4	0 NAA+ 50 SAL	7.00	abc	45.50	abcd
5	0 NAA+ 75 SAL	10.25	a	65.12	ab
6	15 NAA+ 50 SAL	5.25	abc	35.50	bcd
7	15 NAA+ 75 SAL	5.62	abc	23.62	cd
8	20 NAA+ 50 SAL	4.62	bc	24.50	cd
9	20 NAA+ 75 SAL	7.62	abc	39.88	abcd
10	*Plantago* spp.^{z}	4.87	bc	20.25	cd
11	4000 IBA^{z}	9.37	ab	54.12	abc
12	3000 IBA^{z}	7.62	abc	45.62	abcd
F-NAA	0	7.20	a	42.37	a
	15	4.70	a	24.54	a
	20	7.04	a	45.58	a
F-SAL	0	5.50	a	34.46	a
	50	5.62	a	35.17	a
	75	7.83	a	42.87	a
Overall average number of treatments		6.56		38.12	
CV (%)		53.20		66.07	
p-value of treatments		0.0150	*	0.0097	**
p-value of F-NAA		0.1609	ns	0.1022	ns
p-value of F-SAL		0.1978	ns	0.6652	ns
$LSD_{0.05}$ of treatments		5.01		36.12	
$LSD_{0.05}$ of factors		2.83		21.06	

NAA: naphthaleneacetic acid; SAL: salicylic acid; IBA: indolebutyric acid; ^{z}: additional control; F-NAA: naphthaleneacetic acid factor; F-SAL: salicylic acid factor; CV: coefficient of variation; ^{ns}: not significant; *: significant differences; **: highly significant differences; $LSD_{0.05}$: least significant difference at a significance of 0.05. Values with the same letter are statistically similar according to Fisher's least significant difference test ($p \leq 0.05$).

roots developed, a value that only surpassed the means with deionized water (4.37), 15 mg L^{-1} of NAA (3.25), 20 + 50 mg L^{-1} of NAA and SAL (4.62), and with *Plantago* spp. (4.87) (Table 2). On the other hand, for the number of second-order roots, the analysis of variance showed significant effects in the interactions and the controls, where the comparison of means indicated that the treatment with 20 mg L^{-1} of NAA (72.37) was statistically equal to 50 mg L^{-1} of SAL (45.50), 75 mg L^{-1} of SAL (65.12), 20 + 75 mg L^{-1} of NAA and SAL (39.88), 4000 mg L^{-1} of IBA (54.12), and 3000 mg L^{-1} of IBA (45.62), but greater than the rest.

When speaking of the quality of root development, the rooting percentage usually takes second place, since in some cases there may be high percentages, but the root is slightly developed, i.e., with one or two roots, or *vice versa*. Such was the case of the treatment with deionized water, where its percentage was one of the highest (75 %), but its means were among the lowest in these variables, with 4.37 first-order roots and 16.5 second-order roots. The opposite case was the treatment with 20 + 75 mg L^{-1} of NAA and SAL, in which the rooting percentage was among the lowest (56.25 %), but it had a more developed root, with 7.62 first-order roots and 39.88 second-order roots. All of this was influenced by rooting time, as some treatments had cuttings with first-order roots after only 21 d of establishment, giving them more time to develop. This shows the effect of NAA and SAL applied individually on rooting induction and the rate of indoleacetic acid accumulation in the cuttings (Hopkins and Hüner, 2008; Dong *et al*., 2020).

These results are similar to those obtained by Sardoei *et al*. (2014), who obtained 11.6 roots in *E. pulcherrima* cuttings when applying 100 mg L^{-1} of SAL. Likewise, Coimbra *et al.* (2016) report eight roots in *Bertholletia excelsa* Humb. and Bonpl. cuttings when applying 3000 mg L^{-1} of IBA; An *et al*. (2018) obtained 19.09 roots in 'Biloxi' blueberry cuttings when applying 3000 mg L^{-1} of IBA; Colombo *et al*. (2018) obtained 4.59 roots when using 3000 mg L^{-1} of IBA in alcohol on blueberry cuttings 'Powderblue'; and Tejada-Alvarado *et al*. (2021) reported up to 2.95 roots in wild blueberry cuttings when applying 2000 mg L^{-1} of IBA. On the other hand, when applying 15 mg L^{-1} of NAA, means equal to those of the deionized water treatment were obtained, both in the percentage of rooting and in the number of first- and second-order roots. In this regard, it is likely that the concentration used was not sufficient to stimulate rooting, which unbalanced the endogenous hormone content (Haissig, 1970), inhibiting the rooting of cuttings (Hopkins and Hüner, 2008).

Root diameter and length

For root diameter and root length of first- and second-order of the root system, no statistical differences were found for the factors NAA and SAL, but they were found in the interactions and controls (Table 3). The diameter reported when applying 20 mg L^{-1} of NAA (0.68 mm) alone was larger than the means achieved by deionized water (0.51 mm), 15 mg L^{-1} of NAA (0.52 mm), and 3000 mg L^{-1} of IBA (0.5 mm). The greatest first-order root length was obtained when applying 20 mg L^{-1} of NAA (33.91 mm) in

Table 3. Comparison of means by Fisher's least significant difference test of root diameter and length of longest first and second order root in cuttings of *Vaccinium corymbosum* L. 'Biloxi' with the effects of various treatments.

Treatment	Composition (mg L^{-1})	Root diameter (mm)	Root length (mm)	
			First order	Second order
1	0 NAA+ 0 SAL	0.51 b	18.69 c	8.63 b
2	15 NAA+ 0 SAL	0.52 b	20.21 bc	8.44 b
3	20 NAA+ 0 SAL	0.68 a	33.91 a	17.60 ab
4	0 NAA+ 50 SAL	0.56 ab	29.60 abc	14.35 ab
5	0 NAA+ 75 SAL	0.58 ab	32.44 ab	19.67 a
6	15 NAA+ 50 SAL	0.58 ab	25.96 abc	13.67 ab
7	15 NAA+ 75 SAL	0.57 ab	23.27 abc	13.85 ab
8	20 NAA+ 50 SAL	0.55 ab	25.34 abc	9.51 b
9	20 NAA+ 75 SAL	0.65 ab	27.70 abc	12.42 ab
10	*Plantago* spp.^{z}	0.57 ab	21.65 abc	8.24 b
11	4000 IBA^{z}	0.65 ab	31.19 abc	16.77 ab
12	3000 IBA^{z}	0.50 b	25.52 abc	14.36 ab
F-NAA	0	0.55 a	26.91 a	14.22 a
	15	0.55 a	23.14 a	11.99 a
	20	0.63 a	28.99 a	13.18 a
F-SAL	0	0.57 a	24.27 a	11.56 a
	50	0.56 a	26.97 a	12.51 a
	75	0.60 a	27.81 a	15.32 a
Overall average number of treatments		0.57	26.29	13.12
CV (%)		19.08	34.76	51.73
p-value of treatments		0.0103 *	0.0176*	0.0298 *
p-value of F-NAA		0.1687 ^{ns}	0.2960^{ns}	0.7244 ^{ns}
p-value of F-SAL		0.7068 ^{ns}	0.6170^{ns}	0.3803 ^{ns}
$LSD_{0.05}$ of treatments		0.16	13.11	9.74
$LSD_{0.05}$ of factors		0.08	7.85	5.72

NAA: naphthaleneacetic acid; SAL: salicylic acid; IBA: indolebutyric acid; ^{z}: additional control; F-NAA: naphthaleneacetic acid factor; F-SAL: salicylic acid factor; CV: coefficient of variation; ^{ns}: not significant; *: significant differences; $LSD_{0.05}$: least significant difference at a significance of 0.05. Values with the same letter are statistically similar according to Fisher's least significant difference test ($p \leq 0.05$).

relation to that of deionized water (18.69 mm) and to the concentration of 15 mg L^{-1} of NAA (20.21 mm). On the other hand, the second-order root length reported with 75 mg L^{-1} of SAL alone was greater than that of deionized water, 15 mg L^{-1} of NAA, 20 + 50 mg L^{-1} of NAA and SAL, and the *Plantago* spp. extract (Table 3).

The results are different from those published by Sardoei *et al*. (2014), where SAL application was not needed to obtain the best root length in *E. pulcherrima* (28.1 cm). On the other hand, the results reported for the treatment with 15 mg L^{-1} of NAA differ from Das *et al*. (1997), who indicate that NAA can generate good sources of energy and carbon for root formation. This may be attributed to the concentration used, since

in other studies they applied concentrations of 100 and 4000 mg L^{-1} of NAA with good results in blueberry 'Biloxi' (Leiva *et al*., 2023) and *V. meridionale* (Ligarreto *et al*., 2013). These effects depend on the plant species used (López-Corona *et al*., 2019), which is reflected in the results shared by Kim *et al*. (2014), where the best root lengths were achieved with 500 mg L^{-1} of IBA in blueberry 'Bluecrop' (7.5 cm) and 'Duke' (7.6 cm), while in 'Sunrise', IBA did not present the same effect, since the best value was obtained with 500 mg L^{-1} of NAA (6.0 cm).

In this study, IBA did not stand out for these variables, as opposed to Coimbra *et al*. (2016), An *et al*. (2018), and Colombo *et al*. (2018), who achieved greater lengths when using 3000 mg L^{-1} of IBA on *B. excelsa* (7.0 cm), 'Biloxi' blueberry (4.0 cm), and 'Powderblue' blueberry (6.38 cm) cuttings, respectively. Likewise, Higuchi *et al*. (2021), when applying 1000 mg L^{-1} of IBA, reported a root length of 14.33 cm in 'Woodard' blueberry, while Tejada-Alvarado *et al*. (2021) obtained a root length of 27.51 mm when applying 2000 mg L^{-1} of IBA in wild blueberry.

Root volume

The analysis of variance showed that the factors had no significant effect on root volume (Table 4).

Likewise, for the interactions and controls, there were statistical effects on root volume, where the values reported for the treatments with 20 mg L^{-1} of NAA (81.87 mm^3) and 75 mg L^{-1} of SAL (85.62 mm^3) were statistically identical to the treatments with 50 mg L^{-1} of SAL (46.25 mm^3), 4000 mg L^{-1} of IBA (73.12 mm^3), and 3000 mg L^{-1} of IBA (46.25 mm^3), but evidently greater than the rest of the treatments (Table 4). Since this variable represents the space occupied by the developed root, it is inferred that with 20 mg L^{-1} of NAA, 75 mg L^{-1} of SAL, and 4000 mg L^{-1} of IBA, a greater number of roots was obtained.

The positive effects of NAA on rooting stimulation are due to the fact that NAA tends to accumulate indoleacetic acid faster (Hopkins and Hüner, 2008), coupled with an acceleration in starch hydrolysis, decreasing stake sugars, and generating large sources of energy and carbon for root formation (Das *et al*., 1997). In contrast, IBA is directly converted to indoleacetic acid, mainly by processes similar to β-oxidation of fatty acids (Damodaran and Strader, 2019). Dong *et al*. (2020) note that the use of SAL tends to increase endogenous levels of indoleacetic acid in the rooting zone by reducing its degradation through the intervention and inhibition of auxin-conjugating enzymes, thereby enhancing adventitious root development.

On the other hand, Colombo *et al*. (2018) found that optimal substrate physicochemical properties such as temperature, pH, aeration, and moisture retention promote root growth rate. In this regard, it can be concluded that using perlite and peat in a 1:1 volume ratio is a good option for rooting blueberry 'Biloxi' cuttings, as good root development was demonstrated. Other authors, such as Colombo *et al*. (2018), reported similar results when using 3000 mg L^{-1} IBA in rooting cuttings of blueberry 'Powderblueberry.'

Table 4. Comparison of means with Fisher's least significant difference test of root volume in cuttings of *Vaccinium corymbosum* L. 'Biloxi' with the effects of various treatments.

Treatment	Composition (mg L^{-1})	Root volume (mm^3)	
1	0 NAA+ 0 SAL	16.25	c
2	15 NAA+ 0 SAL	19.00	c
3	20 NAA+ 0 SAL	81.87	a
4	0 NAA+ 50 SAL	46.25	abc
5	0 NAA+ 75 SAL	85.62	a
6	15 NAA+ 50 SAL	35.00	bc
7	15 NAA+ 75 SAL	29.50	bc
8	20 NAA+ 50 SAL	33.75	bc
9	20 NAA+ 75 SAL	36.25	bc
10	*Plantago* spp.^{z}	25.62	c
11	4000 IBA^z	73.12	ab
12	3000 IBA^z	46.25	abc
F-NAA	0	49.37	a
	15	27.83	a
	20	50.62	a
F-SAL	0	39.04	a
	50	38.33	a
	75	50.46	a
Overall average number of treatments		44.04	
CV (%)		70.22	
p-value of treatments		0.0097	**
p-value of F-NAA		0.1422	ns
p-value of F-SAL		0.5642	ns
$LSD_{0.05}$ of treatments		44.35	
$LSD_{0.05}$ of factors		26.22	

NAA: naphthaleneacetic acid; SAL: salicylic acid; IBA: indolebutyric acid; ^{z}: additional control; F-NAA: naphthaleneacetic acid factor; F-SAL: salicylic acid factor; CV: coefficient of variation; ^{ns}: not significant; **: highly significant differences; $LSD_{0.05}$: least significant difference at a significance of 0.05. Values with the same letter are statistically similar according to Fisher's least significant difference test ($p \leq 0.05$).

CONCLUSIONS

The combination of naphthaleneacetic acid, salicylic acid, and the *Plantago* spp. extract decreased the rooting percentage and root volume of semi-lignified 'Biloxi' blueberry cuttings. Therefore, to obtain a greater number of rooted cuttings with good root development and guarantee their survival in transplanting and acclimatization, naphthaleneacetic acid, salicylic acid, and indolebutyric acid should be applied individually.

ACKNOWLEDGEMENTS

We thank the Colegio de Postgraduados, Campus Montecillo, for allowing the use of its facilities, and the Secretaría de Ciencia, Humanidades, Tecnología e Innovación (SECIHTI), for the financial support granted for the development of this research project.

REFERENCES

An H, Meng J, Xu F, Jiang S, Wang X, Shi C, Zhou B, Luo J, Zhang X. 2018. Rooting ability of hardwood cuttings in highbush blueberry (*Vaccinium corymbosum* L.) using different índole-butyric acid concentrations. HortScience 54 (2): 194–199. https://doi.org/10.21273/hortsci13691-18

Badilla-Valverde Y, Murillo-Gamboa O. 2005. Enraizamiento de estacas de especies forestales. Revista Forestal Mesoamericana Kurú 2 (6): 59–64.

Berit SA. 2000. The traditional uses, chemical constituents and biological activities of *Plantago major* L. A review. Journal of Ethnopharmacology 71 (1): 1–21. https://doi.org/10.1016/S0378-8741(00)00212-9

Coimbra CC, Iracema M, Alves LO, Oliveira FA, Wendling I. 2016. Enraizamiento de estacas juveniles de *Bertholletia excelsa* con diferentes concentraciones de ácido indol-butírico. Agrociencia 50 (2): 227–238.

Colombo RC, de Carvalho DU, da Cruz MA, Roberto SR. 2018. Blueberry propagation by minicuttings in response to substrates and indolebutyric acid application methods. Journal of Agricultural Science 10 (9): 450–458. https://doi.org/10.5539/jas.v10n9p450

Damodaran S, Strader LC. 2019. Indole 3-butyric acid metabolism and transport in *Arabidopsis thaliana*. Frontiers in Plant Science 10 (851): 9. https://doi.org/10.3389/fpls.2019.00851

Das P, Basak UC, Das AB. 1997. Metabolic changes during rooting in pre–girdled stem cuttings and air–layer of *Heritiera*. Botanical Bulletin of Academia Sinica 38: 91–95.

de Klerk G, Marinova S, Rouf S, Brugge J. 1997. Salicylic acid affects rooting of apple microcuttings by enhancement of oxidation of auxin. Acta Horticulturae 447 (53): 247–250. https://doi.org/10.17660/actahortic.1997.447.53

Dong CJ, Liu XY, Xie LL, Wang LL, Shang QM. 2020. Salicylic acid regulates adventitious root formation via competitive inhibition of the auxin conjugation enzyme CsGH3. 5 in cucumber hypocotyls. Planta 252 (75): 1–15. https://doi.org/10.1007/s00425-020-03403-4

Druege U, Hilo A, Pérez-Pérez JM, Klopotek Y, Acosta M, Shahinnia F, Zerche S, Franken P, Hajirezaei MR. 2019. Molecular and physiological control of adventitious rooting in cuttings: Phytohormone action meets resource allocation. Annals of Botany 123 (6): 929–949. https://doi.org/10.1093/aob/mcy234

FAO (Food and Agriculture Organization) 2024. FAOSTAT. Crops and livestock products. Food and Agriculture Organization of the United Nations. https://www.fao.org/faostat/es/#data/QCL (Retrieved: March 2024).

Haissig BE. 1970. Influence of indole-3-acetic acid on adventitious root primordia of brittle willow. Planta 95 (1): 27–35. https://doi.org/10.1007/bf00431118

Hartmann HT, Kester DE, Davies FT, Geneve RL. 1997. Plant propagation: Principles and practices (Sixth edition). Prentice Hall: Upper Saddle River, NJ, USA. 720 p.

Higuchi MT, Machado RLT, de Aguiar AC, Zeffa DM, Roberto SR, Koyama R. 2021. Methods of application of indolebutyric acid and basal lesion on 'Woodard' blueberry cuttings in different seasons. Revista Brasileira de Fruticultura 43 (5): 1–9. https://doi.org/10.1590/0100-29452021022

Hopkins WG, Hüner NPA. 2008. Introduction to plant physiology (Fourth edition). John Wiley and Sons: Kendallville, IN, USA. 528 p.

Hu H, Chai N, Zhu H, Li R, Huang R, Wang X, Liu D, Li M, Song X, Sui S. 2020. Factors affecting vegetative propagation of wintersweet (*Chimonanthus praecox*) by softwood cuttings. Horticultural Science 55 (11): 1853–1860. https://doi.org/10.21273/hortsci15289-20

Ikeuchi M, Ogawa Y, Iwase A, Sugimoto K. 2016. Plant regeneration: Cellular origins and molecular mechanisms. Development 143 (9): 1442–1451. https://doi.org/10.1242/dev.134668

Isfendiyaroğlu M, Özeker E. 2008. Rooting of *Olea europaea* 'Domat' cuttings by auxin and salicylic acid treatments. Pakistan Journal of Botany 40 (3): 1135–1141.

Kim E, Guak S, Joo KE, Seong HK. 2014. Effects of rooting agents and shading treatments on rooting and growth of highbush blueberry hardwood cuttings. Protected Horticulture and Plant Factory: 31–38. https://doi.org/10.12791/ksbec.2014.23.1.031

Le KC, Johnson S, Aidun CK, Egertsdotter U. 2023. *In vitro* propagation of the blueberry 'Blue Suede™' (*Vaccinium hybrid*) in semi-solid medium and temporary immersion bioreactors. Plants 12 (15): 2752–2765. https://doi.org/10.3390/plants12152752

Leiva MM, Toapanta AA, Ati TJD, Acosta TM. 2023. Efecto de diferentes tipos de sustratos y auxinas en el establecimiento *ex vitro* de segmentos nodales de arándano var. 'Biloxi'. Bionatura Journal 8 (3): 7. https://doi.org/10.21931/rb/2023.08.03.7

Li Q, Yu P, Lai J, Gu M. 2021. Micropropagation of the potential blueberry rootstock–*Vaccinium arboreum* through axillary shoot proliferation. Scientia Horticulturae 280. https://doi.org/10.1016/j.scienta.2021.109908

Ligarreto MGA, Torres AWS, Ariza CCA. 2013. Propagation of the neotropical fruit *Vaccinium meridionale* Swartz by air layering. Agronomía Colombiana 31 (2): 169–175.

López-Corona BE, Mondaca-Fernández I, Gortáres-Moroyoqui P, Holguín PJ, Meza-Montenegro MM, Balderas-Cortés JJ, Vargas-López JM, Rueda-Puente EO. 2019. Technique of cutting in agriculture: An alternative at the vanguard. Tropical Subtropical Agroecosystems 22 (2): 505–517. https://doi.org/10.56369/tsaes.2795

Mazzutti S, Riehl CAS, Ibáñez E, Ferreira SRS. 2017. Green-based methods to obtain bioactive extracts from *Plantago major* and *Plantago lanceolata*. The Journal of Supercritical Fluids 119: 211–220. https://doi.org/10.1016/j.supflu.2016.09.018

Owen JSJr, Maynard BK. 2007. Environmental effects on stem-cutting propagation: A brief review. Combined Proceedings International Plant Propagator's Society 57: 558–564.

Pacholczak A, Nowakowska K. 2015. The *ex-vitro* rooting of blueberry (*Vaccinium corymbosum* L.) microcuttings. Folia Horticulturae 27 (2): 145–150. https://doi.org/10.1515/fhort-2015-0024

Sardoei SA, Fahraji SS, Ghasemi H. 2014. Effect of salicylic acid on rooting of poinsettia (*Euphorbia pulcherrima*). International journal of Advanced Biological and Biomedical Research 2 (6): 1883–1886.

Shiembo PN, Newton AC, Leakey RRB. 1997. Vegetative propagation of *Ricinodendron heudelotii*, a West African fruit tree. Journal of Tropical Forest Science 9 (4):514–525.

Steiner AA. 1984. The universal nutrient solution. Sixth International Congress on Soilless Culture Proceedings. Lunteren, Netherlands, pp: 633–649.

Tejada-Alvarado JJ, Meléndez-Mori JB, Vilca-Valqui NC, Huaman-Huaman E, Oliva M. 2021. Rooting of wild blueberry (*Vaccinium* spp.) cuttings from the Peruvian northeast. Acta Agrobotanica 74: 7. https://doi.org/10.5586/aa.7413

Tinoco-Plasencia CJ, Zambrano-Casimiro LM, Roque-Paredes O, Chávez-Mayta RW, Maguiña-Vásquez BM, Espejo-Calderón JW. 2023. Los arándanos, generalidades y desarrollo en el mercado mundial: una revisión de literatura. Paideia XXI 13 (1): 125–140. https://doi.org/10.31381/paideia.v13i1.5674

Agrociencia

OPTIMIZED SUBSTRATE FORMULATION USING INDUSTRIAL INSTANT COFFEE RESIDUE FOR GROWING AMARANTH AND CHIA MICROGREENS

Erika **Piña-Moreno**[1], Otto Raúl **Leyva-Ovalle**[2], Mirna **López-Espíndola**[1], Adriana **Contreras-Oliva**[1], Emmanuel de Jesús **Ramírez-Rivera**[3], José Andrés **Herrera-Corredor**[1]*

[1]Colegio de Postgraduados – Campus Córdoba, Programa de Innovación Agroalimentaria Sustentable, Km. 348 Carretera. Fed. Córdoba-Veracruz, Amatlán de los Reyes, Veracruz México, C.P. 94946.
[2]Facultad de Ciencias Biológicas y Agropecuarias – Universidad Veracruzana, Josefa Ortiz de Domínguez s/n. Colonia Centro. Amatlán de los Reyes, Veracruz. México C.P. 94950.
[3]Tecnológico Nacional de México/ Instituto Tecnológico Superior de Zongolica, Km. 4 Carretera S/N Tepetitlanapa, 95005 Zongolica, Veracruz, México.
* Author for correspondence: jandreshc@colpos.mx

Citation: Piña-Moreno E, Leyva-Ovalle OR, López-Espíndola M, Contreras-Oliva A, Ramírez-Rivera EJ, Herrera-Corredor JA. 2025. Optimized substrate formulation using industrial instant coffee residue for growing amaranth and chia microgreens. **Agrociencia** 59(5): 682-700. https://doi.org/ 10.47163/agrociencia.v59i5.3439

Editor in Chief:
Dr. Fernando C. Gómez Merino

Received: April 03, 2025.
Approved: July 21, 2025.
Published in Agrociencia: July 28, 2025.

ABSTRACT

The objective of the study was to determine the potential of instant coffee residue as material for substrates in the production of amaranth and chia microgreens using the mixture experimental design methodology. The residue was mixed with sand and sawdust following a simplex centroid design. Sawdust was favorable for substrate aeration. Sand, sawdust, and coffee residue mixture improved the water-holding capacity of the mixture (74 %), whereas a mixture of coffee residue and sand resulted in an adequate pH substrate (6.7). Both, substrate bulk density and particle size were observed to influence plant development. The formulation composed entirely of sand (100%) demonstrated remarkable improvements in mean stem diameter, root length, and hypocotyl height compared to other mixtures, establishing it as the best substrate for amaranth and chia growth. This finding underscores the potential of this substrate to develop an efficient and environmentally friendly growing medium for microgreens, thus contributing to urban agriculture and sustainable organic waste management.

Keywords: Substrate, industrial coffee residue, mixture design, regression, microgreens.

INTRODUCTION

According to the United Nations, the world population is projected to reach approximately 9.7 billion by 2050, with a significant concentration of this growth occurring in urban areas. By 2050, it's estimated that 68% of the global population will reside in urban centers, compared to 55% today, adding an estimated 2.5 billion people to urban populations (Porras and González, 2016; Burgos, 2018). Population growth implies a higher demand for food and living space leading to the loss of agricultural land. The cultivation of microgreens is an alternative for fresh vegetable production

that has recently gained interest given its minimal space and time requirements for production in addition to its nutritional and sensory advantages (Di Gioia *et al.,* 2015). Microgreens are versatile in terms of cultivation, being able to be grown both at home and at complex agricultural facilities. Ebert (2022) indicated that cultivation of microgreens at home is completely viable. Nolan *et al.* (2018), pointed out that this variety of methods allows for different types of substrates to be used for expanding the options beyond conventional soil. Currently, peat moss, perlite, and coconut fiber have been used as substrates for growing microgreens. However, these can be expensive or difficult to access. The food industry produces organic waste when processing food. For example, in the production of instant coffee, a large amount of roasted coffee bean residues (spent coffee grounds) is generated after extraction. These coffee residues (CR) have no clear use and are usually deposited on large plots until they decompose. The use of mixture designs for the formulation of substrates can help identify a viable combination of these residues blended with other materials for growing microgreens. Coffee is one of the most popular beverages on the planet. Population growth suggests that coffee production and consumption will continue to increase in the future, including its by-products and residues. Its demand has grown significantly in recent years due to several factors such as urbanization, and economic and social development. Coffee is also one of the most important commodities in the international trade (Murthy and Naidu, 2012). The International Coffee Organization (ICO) in the 2023/2024 season projected a 5.8 % increase in world production, reaching 178 million 60 kg bags of parchment coffee (Johnson *et al*., 2021). In 2021, an increase in coffee demand was observed, with an annual growth of 2.4 %. Regarding coffee in Mexico, in 2016 there were consumed 87,300 Mg of roasted coffee beans, 35,339 Mg of ground coffee and 47,344 Mg of instant coffee. Out of instant coffee production, it is estimated that 45 % ends up as waste, which is equivalent to approximately 21,304.80 Mg (Euromonitor, 2017). Other coffee residues, such as husk and pulp (among others), have traditionally been used for agricultural or industrial purposes, such as fertilizers, animal feed, composting, or elimination of harmful substances to produce gibberellic acid. However, these uses only take advantage of a minimal part of the available residues (Antonio *et al.,* 2021). Residues from the industrial production of instant coffee (CR) have a high content of neutral detergent fiber (45.2 %), which includes hemicellulose, cellulose and lignin-bound substances, and acid detergent fiber (29.8 %), consisting of cellulose and lignin (Vardon *et al*., 2013). These characteristics suggest that it may be a viable substrate for microgreens production.

The production of microgreens has aroused interest in recent years. Their consumption has increased due to their high nutritional and functional value, as they are rich in phytochemicals, vitamins, and minerals (Kyriacou *et al.,* 2016). Microgreens stand out for their superior nutritional profile and represent a significant innovation in the field of fresh vegetables. A study by Di Gioia *et al.* (2015) examined twenty-five varieties of these plants revealed that, compared to traditional vegetables harvested at their optimum ripeness, microgreens contain significant antioxidant levels and vitamins

such as C, E, and K, as well as carotenoids such as β-carotene, lutein, and zeaxanthin, that can be up to twelve times higher (Xiao *et al.,* 2012). In addition, microgreens can be sustainably produced and can be adapted to different cultivation systems. They can be grown in greenhouses with hydroponic or soilless systems, or on a small scale at home for self-consumption (Renna *et al.,* 2018). These advantages, together with their attractive sensory properties, stimulate interest in their research.

The design of experiments with mixtures methodology is a variant of response surface methodologies. It is a tool that allows for optimizing substrate formulations based on specific objectives such as yield and plant development. Ceglie *et al*. (2015) successfully used this methodology to identify a replacement for peat in tomato, melon, and lettuce seedlings for transplanting. This methodology is based on varying the proportions of the components that make up a mixture to determine the synergistic effect of a combination of two or more components on a desired characteristic of the mixture. The study by Salamanca *et al.* (2015) highlights the use of blend design to optimize the manufacture of mango purees and contribute to the development of dairy products, such as yogurt. This process was supported by the application of sensory testing and experimental techniques for ingredient mixing. The objective of the study was to evaluate the potential of instant coffee residue as material for substrates in the production of amaranth and chia microgreens using the mixture experimental design methodology.

MATERIALS AND METHODS

Materials

Pine wood sawdust used in the study was purchased from a lumberyard in Córdoba, Veracruz, Mexico, with a particle size of approximately 2 mm. Sand was purchased from the local construction materials store in Córdoba, Veracruz, México. The residue from the industrial production of instant coffee (CR) was donated by Café Tostado de Exportación (CATOEX) Cordoba, Veracruz, Mexico.

Amaranth (*Amaranthus hypochondriacus* L.) seeds, Laura variety, grown in 2022, were purchased from a producer in Tlaxcala, Mexico. Chia seeds (*Salvia hispanica* L.) were purchased from a local natural products store (Naturista, located in Cordoba, Veracruz, Mexico).

Germination tests

According to the International Seed Testing Association (ISTA) the germination process was performed using an inter-folded towel (Sanitas, Kimberly-Clark S. A. B. de C. V. Mexico City, Mexico) which provided the necessary moisture for chia and amaranth seeds. The seeds (100) were placed on the distilled water-saturated paper before being rolled. The rolls were put in a polyethylene bag and stored at room temperature (26 °C) over a plastic tray. The first count was made on the third day visually identifying

the germinated seeds. The germination percentage was calculated with the formula (germinated seeds/total seeds) x 100. The test was performed in duplicate.

Chemical composition of mixture materials.

Chemical composition of coffee residue, sand, and sawdust (Table 1) used for the substrate formulation was determined at the FYPA Soil Analysis Laboratory in Fortín, Veracruz, Mexico. Moisture content, ashes, organic matter, total carbon, total nitrogen, and carbon/nitrogen ratio were determined according to the NMX-FF-109-SCFI-2008 (DOF, 2008) standard. Minerals were determined using an Atomic Absorption Spectrometer PERKIN ELMER AAnalyst-400 (Shelton, Connecticut, USA). Phosphorus was determined by UV-VIS using a PERKIN ELMER LAMBDA-25 UV-VIS Spectrometer (Shelton, Connecticut, USA).

Table 1. Chemical composition of mixture materials.

Variable	CR	SN	SD
Moisture (%)	2.33	0.0	15.5
Ashes (%)	0.78	98.0	0.25
Organic matter (%)	99.22	0.0	NA
Total carbon (%)	57.55	0.0	53.87
Total nitrogen (%)	0.90	0.0	0.35
Carbon/nitrogen ratio	63.94	0.0	153.9
Calcium (CaO) (%)	0.148	2.17	41.2
Magnesium (MgO) (%)	0.147	1.17	13.8
Sodium (Na_2O) (%)	0.044	1.51	1.1
Potassium (K_2O) (%)	0.159	0.0	26.5
Phosphorus (P_2O_5) (%)	0.017	0.18	3.9
Iron (Fe) (%)	0.0209	0.30	NA
Cupper (Cu) (%)	0.0050	0.0	NA
Zinc (Zn) (%)	0.0015	0.0	NA
Manganese (Mn) (%)	0.0036	0.0	NA

NA: Not available. SN=Sand, SD=Sawdust, CR=Coffee residue from industrial production of instant coffee.

Conditioning of industrial production of instant coffee residue (CR)

Before using the residue from the industrial production of instant coffee in the formulation of substrates for microgreens, a composting process was carried out to stabilize it. The composting process was carried out for 3 months according to the manual for aerobic composting (Navarro and De la Tierra, 2003).

Formulation of substrates for microgreens

Formulation of substrates using sand, sawdust, and CR followed a simplex mixture design with centroid. The proportions were based on weight. The codes assigned to the formulations and the percentages of each ingredient are presented in Table 2.

Table 2. Substrate formulations for microgreens production.

Formulation	Code	Sand (%)	Sawdust (%)	Coffee residue (%)
1	SN	100	0	0
2	SN/SD	50	50	0
3	SN/CR	50	0	50
4	SN/SD/CR	33.33	33.33	33.33
5	SD	0	100	0
6	SD/CR	0	50	50
7	CR	0	0	100

SN=Sand, SD=Sawdust, CR=Coffee residue from industrial production of instant coffee

Physical characterization of substrates

The characterization of substrates was carried out according to the Mexican Official Standard NOM-021-RECNAT-2000 (DOF, 2002), which establishes the standards for fertility, salinity, and soil classification. The analysis included the measurement of porosity, aeration capacity, water retention capacity, bulk density, and particle density.
2.7. pH and electrical conductivity (EC) of substrates

A pH meter was used to determine the pH of a suspension formed by the substrate and distilled water in a 1:2 ratio. To prepare the suspension, 30 g of substrate were weighed and mixed with 60 mL of distilled water in plastic cups. The suspension was then allowed to rest for at least 30 min and shaken again for 20 s before measuring pH with a Thermo Scientific™ Orion™ 3-star pH meter (©2010 Thermo Fisher Scientific Inc.) The electrical conductivity determination was carried out using a Hanna determinator model HI 9811-5, following the same procedure for pH.

Substrate sterilization

Before placing the seeds on the substrates, they were sterilized. A steamer with a 70 L capacity loaded with 2 L of water was used. Bags containing sand, sawdust, and CR were heat-treated at 70-80 °C for one hour to reduce microbial contamination. Finally, the ingredients were mixed according to Table 1 to formulate the substrates based on the simplex design with centroid.

Microgreens growing

Microgreen cultivation took place in a greenhouse with a transparent plastic cover at the Facultad de Ciencias Biológicas y Agropecuarias of the Universidad Veracruzana

(18° 51′ 38″ N, 96° 54′ 10″ W). In this setup, 55 cm x 28 cm x 6 cm trays were filled with 1.30 Kg of the substrate mixtures (formulations), reaching a height of 2.5 cm.

A disinfection solution was prepared with 1 L of water and 100 mL of chlorine (5 % initial concentration) in a 2 L container. The seeds, weighing 121.5 g, were immersed in this solution for 15 min, shaking them with a glass rod for an additional 5 min. They were then sieved and washed with distilled water to remove chlorine residues and dried at room temperature on absorbent paper. Nine grams of chia and amaranth seeds were sown. Seeds were distributed over the substrates and covered with black plastic layer for three days to facilitate germination (Di Gioia *et al.*, 2015). After germination, seedlings were nourished with a hydroponic SOLUPONICS® STANDARD A+B UNIVERSAL hydroponic solution (INVERFARMS Hidroponía Querétaro, Mexico,) applied daily by subirrigation (Di Gioia *et al.*, 2017). The pH was adjusted to 6.0 with nitric acid (65% purity) to neutralize the bicarbonates present. 0.054 mL L^{-1} of nutrient solution was used for this condition. The electrical conductivity was adjusted to 2300 mS cm^{-1}. The resulting osmotic potential was -0.083 MPa. (Table 3).

Table 3. Composition of the nutrient solution.

Nutriment	Soluponics formula (mmol L^{-1})	Water analysis (mmol L^{-1})	Nutritional contribution (mmol L^{-1})
NO_3^-	15	0	15
NH_4^+	1	0	1
PO_4^-	2	0	2
K^+	7	0	7
Ca^{2+}	5	1.23	6.23
Mg^{2+}	1.5	0.75	2.25
SO_4^{2-}	2	0	2
HCO_4^-	0	1.28	0.5
BO_3^-	13.9		
Fe-EDTA	28		
Zn-EDTA	3.3		
Cu-EDTA	1.7		
Mn-EDTA	15.2		
MoO_4^{2-}	0.7		

Microgreen growth assessment

The hypocotyl length of ten randomly selected seedlings per treatment was measured every 24 h after germination for 15 days. A ruler in centimeters was used to measure from the beginning of the hypocotyl to the cotyledonary leaves. Similarly, stem diameter and root length were measured in centimeters using a vernier and a ruler respectively every 24 hours for 15 days.

Microbiological analysis

The microbiological quality of the culture media and the microgreens produced in them were carried out according to NOM-113-SSA1-1994 (DOF, 1995) and NOM-110-SSA1-1994 (DOF, 1994) standards. Random samples of 10 g of microgreens were taken from each tray and from different substrates. Microgreens were cut with sterile scissors and serially diluted in sterile water. Then, they were seeded in duplicate on bile red violet agar for total coliform counts and on potato dextrose agar for fungal and yeast counts. The plates were incubated at 35 °C for 24 ± 2 h and 48 ± 2 h, respectively.

Statistical analysis

To analyze the effect of the formulation (as a whole) on the substrate characteristics (porosity, aeration, water retention, pH, EC, bulk, and particle densities), a completely randomized experimental design was used. Mean comparisons were performed using Tukey's test. Further analysis to identify the impact of formulation ingredients on physicochemical characteristics of substrates according to the mixture design were analyzed using a second-order mathematical model as follows.

$$Y=\beta_1 X_1 + \beta_2 X_2 + \beta_3 X_3 + \beta_{12} X_1 X_2 + \beta_{13} X_1 X_3 + \beta_{23} X_2 X_3 + \in.$$

Where: Y= the response variable (porosity, aeration, water retention, pH, EC, bulk, and particle densities); X1= proportion of sand in the mixture; X2 = proportion of sawdust in the mixture; X3 = proportion of coffee residue in the mixture, and ∈ = the error term. A factorial design with three factors: species (2 levels: amaranth and chia), formulation (7 levels = 7 formulations), days (15 levels) was used to analyze the evolution in the growth of microgreens of both species (chia and amaranth) through time.

All statistical analyses were conducted using a significance level α= 0.05 in R software ver. 4.3.2 with the integrated development environment R Studio ver. 2023.12.1.

RESULTS AND DISCUSSION

Germination tests

The amaranth germination percentage was 90 % after 72 h. According to Wang *et al*. (2023), amaranth has a high germination capacity at moderate temperatures. According to his results, 80-90 % of seeds germinated between 19 and 28 °C after 72 h. As for the germination percentage in chia, 93 % germinated after 72 h at room temperature. Differences in germination percentage between species could likely be due to genetic differences.

Physical characteristics of substrates

Table 4 shows the physical characteristics of the different formulations. The highest values of porosity were found in the formulations SN/SD/CR, SD, and CR. As expected,

Table 4. Results of physical analysis of substrates.

Formulation	Mixture	Porosity (%)	Aeration capacity (%)	Water retention capacity (%)	Bulk density (Mg m^{-3})	Particle density (Mg m^{-3})
1	SN	40.05±0.07^{e}	10.10±0.14^{b}	29.95±0.07^{d}	0.79±0.90^{a}	2.63±0.04^{a}
2	SN/SD	59.15±1.48^{c}	11.00±1.41^{b}	49.45±1.06^{c}	0.52±0.04^{a}	2.15±0.07^{b}
3	SN/CR	50.20±0.14^{d}	15.15±7.28^{b}	35.05±7.42^{d}	0.64±0.13^{a}	2.30±0.28^{ab}
4	SN/SD/CR	85.05±0.07^{a}	10.20±0.14^{b}	74.85±0.07^{a}	0.38±0.19^{a}	1.48±0.06^{c}
5	SD	80.90±0.57^{a}	30.45±0.64^{a}	50.45±1.20b^{c}	0.16±0.03^{a}	2.17±0.04^{ab}
6	SD/CR	70.05±0.07^{b}	20.15±0.07^{ab}	49.90±0.14^{c}	0.26±0.05^{a}	1.34±0.06^{c}
7	CR	82.75±3.46^{a}	20.20±0.14^{ab}	62.55±3.61^{ab}	0.45±0.06^{a}	0.44±0.05^{d}
Pr(>F)		<0.0001*	<0.0001*	<0.0001*	<0.0001*	<0.0001*

Mean of three replicates ± standard deviation. *Significant α= 0.05. Means within the same column followed by different letters are significantly different (Tukey, $P < 0.05$). SN=100 % sand; SD/SN=50 % sawdust+50 % sand; SN/CR=50 % sand + 50 % residue from industrial production of instant coffee; SN/SD/CR= 33.3 % sand + 33.3 % sawdust + 33.3 % residue from industrial production of instant coffee; SD= 100 % sawdust; CR/SD= 50 % residue from industrial production of instant coffee + 50 % sawdust, CR= residue from industrial production of instant coffee 100 %.

the formulation composed of 100 % sand had the lowest porosity value. Martínez and Roca (2011) reported that organic substrates typically exhibit porosity values above 85 %. This parameter is critical to ensure adequate aeration and water retention in the substrate which are essential factors for optimal plant development. Regarding aeration capacity, the highest value was observed for the SD formulation, whereas the lowest values corresponded to the SN, SD/SN, CR/SN and SN/SD/CR formulations. According to Martínez and Roca (2011), the optimum range of aeration capacity is between 20 and 30 %; presented by CR, SD/CR and SD formulations. The formulations for water retention in substrates revealed significant data. The SN/SD/CR formulation showed the highest value, highlighting its efficiency in water retention. On the other hand, the SN formulation registered the lowest water retention and, the general range of water retention oscillates between 29.95 and 74.85 %. The SD formulation presented the lowest bulk density value, whereas the SN formulation showed the highest value. The results obtained in the measurement of the particle density of the substrates indicate that the SN formulation had the highest real density. The results are consistent with the parameters published by Martínez and Roca (2011), except in the case of the CR formulation.

Chemical properties of substrates

Chemical properties of substrates are presented in Table 5. The formulations were found located in an acidic pH range. According to Di Gioia *et al.* (2015), a suitable substrate for the cultivation of microgreens should have a pH ranging between 5.5 and 6.5. In addition, it is crucial that the electrical conductivity is less than 500 mS cm^{-1}, thus indicating that the amount of nutrients present in the substrate is not excessive

Table 5. Chemical properties of substrates.

Formulation	Mixture	pH	Electrical conductivity (mS cm^{-1})
1	SN	5.53±0.09c	0.62±0.02e
2	SN/SD	5.80±0.11bc	92.10±0.14a
3	SN/CR	6.70±0.18a	11.00±0.00de
4	SN/SD/CR	5.61±0.10bc	103.00±1.41a
5	SD	5.72±0.04bc	27.50±2.12cd
6	SD/CR	5.81±0.02^{bc}	38.00±16.97bc
7	CR	5.96±0.06^{b}	59.00±0.00b
Pr(>F)		<0.0001*	<0.0001*

Mean of three replicates ± standard deviation. *Significant α= 0.05. Means within the same column followed by different letters are significantly different (Tukey, $P < 0.05$). SN=100 % sand; SD/SN=50 % sawdust+50 % sand; SN/CR=50 % sand + 50 % residue from industrial production of instant coffee; SN/SD/CR= 33.3 % sand + 33.3 % sawdust + 33.3 % residue from industrial production of instant coffee; SD= 100 % sawdust; CR/SD= 50 % residue from industrial production of instant coffee + 50 % sawdust, CR= residue from industrial production of instant coffee 100 %.

and that it has the right conditions for healthy microgreens growth (Di Gioia *et al.*, 2015). All the formulations used in this study were found to have an adequate EC.

The simplex coordinate system in mixture design allows for visual identification of the change in the property of interest as a function of the ingredient proportions in the mixture (Figure 1). In the case of porosity (Figure 1a), the evenly spaced lines in the triangle suggest that soil porosity was homogeneously distributed but decreased when increasing the sand content in the mix. This is reasonable given that sand is a compact and dense material whereas sawdust and CR are more porous. According to Moreno-Reséndez and Valdés-Perezgasga (2005), the use of sand in combination with vermicompost is effective in replacing other substrates. They found that vermicompost mixed with different levels of sand resulted in a rich and complete nutritional composition capable of integrally satisfying the nutritional needs of plants during their development. This alternative also promotes healthy plant growth due to the diversity of essential nutrients it offers. In case of aeration (Figure 1b), a clustering of curved lines towards sawdust indicated a rapid increase in substrate aeration. Regarding water retention (Figure 1c), a reduced variability was found increasing gradually towards sawdust and CR content. According to Morales-Maldonado and Casanova-Lugo (2015) sawdust particle size has a significant impact on air porosity and water holding capacity. Depending on their size, they can increase porosity while reducing water holding capacity, or vice versa. Formulation SN showed an increase in bulk density with a value of 0.8. On the other hand, formulation 5 with SD indicates a lower particle density, as shown by the clustering of lines near the lower vertex, reflecting lower values in this measure, specifically a value of 0.2. It is common to observe that as particle size decreases, both bulk and particle densities tend to increase.

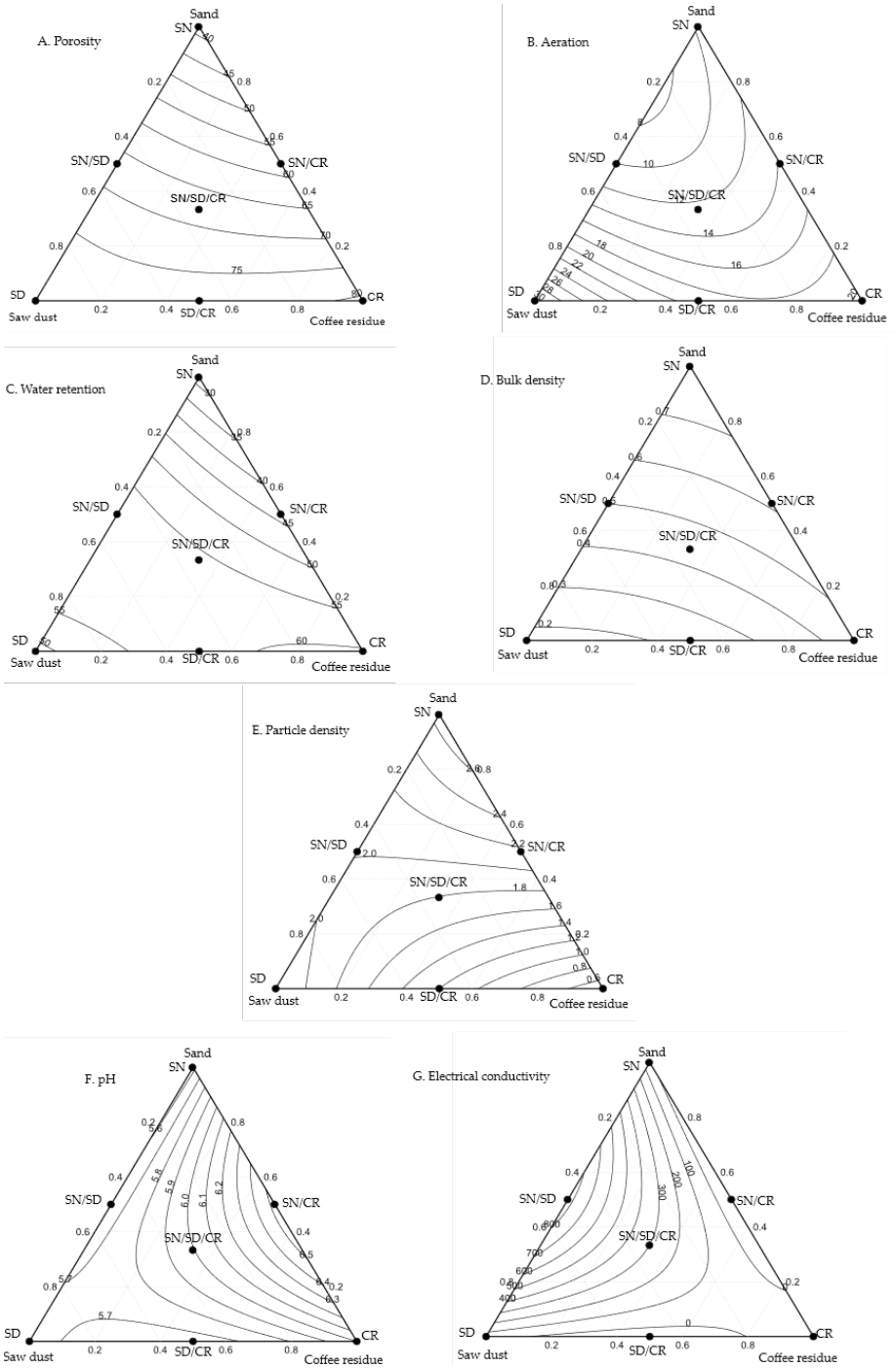

Figure 1. Use of the Simplex Coordinate System for Visualization of the impact of ingredients on the physicochemical characteristics of substrates. SN=100 % sand; SD/SN=50 % sawdust+ 50 % sand; SN/CR=50 % sand + 50 % residue from industrial production of instant coffee; SN/SD/CR= 33.3 % sand + 33.3 % sawdust + 33.3 % residue from industrial production of instant coffee; SD= 100 % sawdust; CR/SD= 50 % residue from industrial production of instant coffee + 50 % sawdust, CR= residue from industrial production of instant coffee 100 %.

This is because smaller particles can settle more densely and reduce the proportion of pores between them, resulting in a higher bulk density value.

In relation to pH, an increase (6.5) in this value was found to be oriented towards a combination of 50 % sand and 50 % CR (Formulation 3) and a lower value (5.7) towards the sawdust content in the mixture. This effect is attributed to the presence of acidic compounds in the mixture that have an adverse impact on complete plant growth. Regarding electrical conductivity, the lowest values were found in formulation SN (100 % sand) whereas the highest values were found in formulation SN/SD/SR composed of 33.3 % sand + 33.3 % sawdust + 33.3 % residue from industrial production of instant coffee.

Microgreen growth

In general, it was found that the substrate formulation significantly influenced microgreen growth variables such as stem diameter, root length and hypocotyl height (Table 6) with p values less than 0.0001.

In formulation SN showed a stem diameter of 0.21 mm, which was significantly different compared to formulations SN/SD, SN/CR and CR. In addition, the root length of formulation SN was 2.34 cm, marking a difference with formulations SN/CR, SN/SD/CR and CR. These differences may be indicative of how each formulation affects plant development in different aspects of growth. The hypocotyl height of formulation SN was 3.01 cm, also distinguishing it from formulations SN/SD, SN/CR and CR. These results suggest that formulation SN has a unique effect on plant growth, which could be crucial to better understand the influence of formulation variables on plant morphology.

Table 6. Average growth variables by formulation.

Formulation	Mixture	Stem diameter (mm)	Root length (cm)	Hypocotyl height (cm)
1	SN	0.21±0.11a	2.34±1.09a	3.01±1.24a
2	SN/SD	0.08±0.04bc	1.83±1.16b	1.29±0.78b
3	SN/CR	0.07±0.05cd	0.98±0.94c	0.77±0.66c
4	SN/SD/CR	0.10±0.02b	2.35±1.11a	1.44±0.64b
5	SD	0.09±0.05b	2.05±1.27ab	1.22±0.61b
6	SD/CR	0.09±0.03b	1.80±1.12b	1.27±0.69b
7	CR	0.05±0.05d	0.91±1.04c	0.75±0.78c
Pr(>F)		<0.0001*	<0.0001*	<0.0001*

Mean of three replicates, standard deviation. *Significant α= 0.05. Means within the same column followed by different letters are significantly different (Tukey, $P < 0.05$). SN = 100 % sand; SD/SN= 50 % sawdust+50 % sand; SN/CR=50 % sand + 50 % residue from industrial production of instant coffee; SN/SD/CR= 33.3 % sand + 33.3 % sawdust + 33.3 % residue from industrial production of instant coffee; SD= 100 % sawdust; CR/SD= 50 % residue from industrial production of instant coffee + 50 % sawdust, CR = residue from industrial production of instant coffee 100 %.

This pattern was confirmed from a multivariate perspective (Figure 2) where it was found that, according to the map of individuals (Figure 2a), formulation SN was located far away from the other formulations in the highest position of dimension 1, which represents the highest variability (84.23 %). Formulations SN/SD, SN/SD/CR,

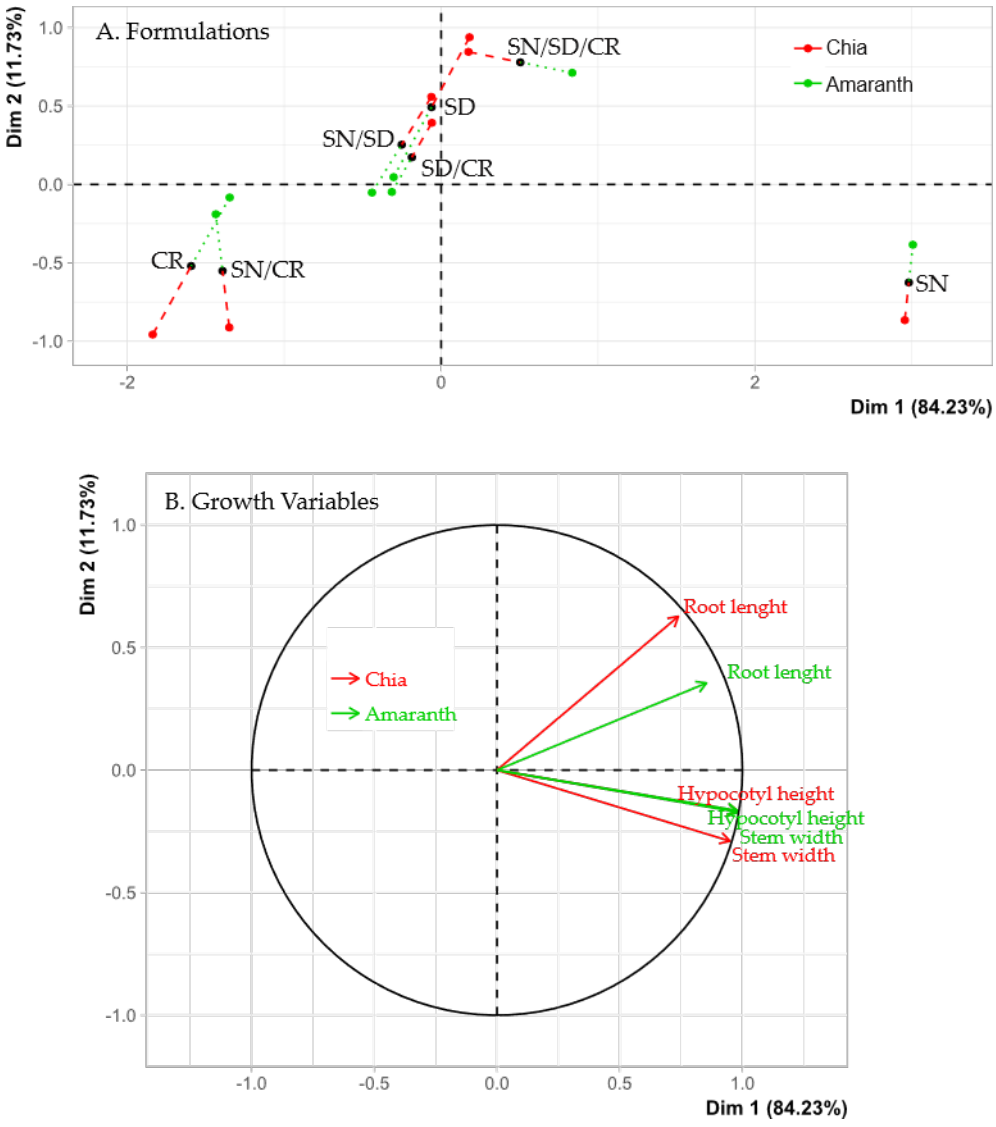

Figure 2. Comparison between species in terms of formulations and growth variables. SN=100 % sand; SD/SN=50 % sawdust+50 % sand; SN/CR=50 % sand + 50 % residue from industrial production of instant coffee; SN/SD/CR= 33.3 % sand + 33.3 % sawdust + 33.3 % residue from industrial production of instant coffee; SD= 100 % sawdust; CR/SD= 50 % residue from industrial production of instant coffee + 50 % sawdust, CR= residue from industrial production of instant coffee 100 %.

SD, and SD/CR also clustered in a central position of dimension 1. These formulations were characterized by being located towards the sawdust content in the mixture in the simplex coordinate system. Finally, formulations SN/CR and CR were in the lowest position in dimension 1 and are those oriented towards CR content. Regarding the correlation between variables (determined by the angle formed by these variables in Figure 2b), it was similar for both species. Hypocotyl height and stem diameter were found to be closely correlated, whereas the correlation of these variables with root length was lower. These results suggest that both species had higher growth of hypocotyl and stem diameter in the substrate composed only with sand whereas formulations SN/SD, SN/SD/CR, SD, and SD/CR had higher root growth in the formulations composed with sand and sawdust. Mineral nutrition from chemical sources, such as Steiner solution, becomes truly relevant and is utilized by seedlings once the first true leaves appear and metabolism shifts to autotrophic. Before this point, application of the nutrient solution has little effect and can be counterproductive if used at normal concentrations. In the case of chia (*Salvia hispanica* L.), the appearance of true leaves occurred between 7 and 14 days after sowing. In amaranth (*Amaranthus hypochondriacus* L.), this occurred between 15 and 17 days. Once the true leaves have appeared, the nutrient solution may have the following influence: promoting a more robust and less etiolated stem; the roots will develop and branch more; and the hypocotyl will be shorter and more robust. According to Table 2, if substrates containing coffee grounds (CR) and pine sawdust (SD), as well as their formulations, were watered only with water after the first true leaves appeared, the seedlings would grow more than those using sand as a substrate, due to the elements contained in each.

The magnitude of the differences in the growth variables is presented in Table 7. The values for chia indicate that this species had a significantly higher stem diameter than amaranth. For root length, chia significantly exceeded the amaranth in this variable. For hypocotyl height, as with the other variables, chia has a significantly higher hypocotyl height than amaranth. These data suggest that chia tends to have more robust growth compared to amaranth under the study conditions.

Figure 3 shows the effect of significant interactions among factors (time, formulation, and species) for growth variables. Figure 3a shows that formulation SN favored an increase in stem diameter, reaching 0.3 mm, in contrast to the other formulations that

Table 7. Comparison of growth variables by species.

Species	Stem diameter (mm)	Root length (cm)	Hypocotyl height (cm)
Amaranth	0.09±0.07[b]	1.29±0.97[b]	1.22±0.96[b]
Chia	0.11±0.07[a]	2.21±1.29[a]	1.56±1.13[a]
Pr(>F)*	<0.0001	<0.0001	<0.0001

*Mean of three replicates ± standard deviation. Means within the same column followed by different letters are significantly different (Tukey, $P < 0.05$).

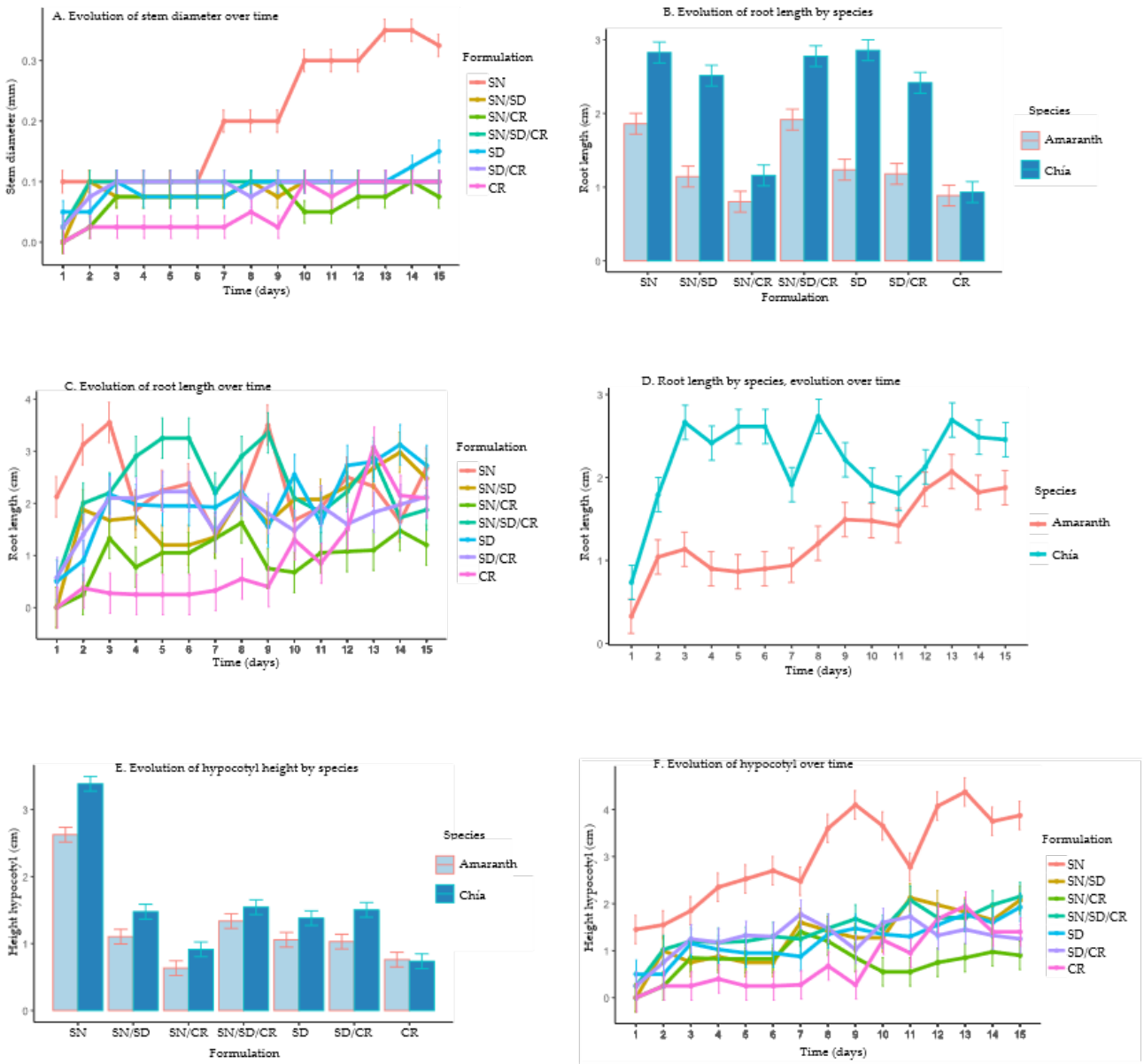

Figure 3. Growth variables of microgreens in amaranth and chia as a function of significant interactions (Tukey, $P < 0.05$) between time, species, and formulation factors. SN=100 % sand; SD/SN=50 % sawdust+50 % sand; SN/CR=50 % sand + 50 % residue from industrial production of instant coffee; SN/SD/CR= 33.3 % sand + 33.3 % sawdust + 33.3 % residue from industrial production of instant coffee; SD= 100 % sawdust; CR/SD= 50 % residue from industrial production of instant coffee + 50 % sawdust, CR= residue from industrial production of instant coffee 100 %.

remained at 0.1 mm. In Figure 3b, formulations SN, SN/SD/CR and SD, promoted root growth in the chia species, reaching 2 to 3 cm, whereas formulations SN/CR and CR were not as effective. In the case of amaranth, formulations SN and SN/SD/CR promoted root growth of 2 cm. Figure 3c revealed that, overall, formulations SN and SN/SD/CR promoted more pronounced root growth over time, with roots reaching 3 cm, comparatively superior to the other formulations that ranged between 1 and 2 cm in length. The decrease in root length concurs with the appearance of true leaves, which could encourage their branching. This can be attributed to the physical and chemical characteristics of each of the substrates evaluated, which plays an essential role in plant development. Figure 3d shows that chia had higher root length with values between 2 and 3 cm, surpassing amaranth, which root length varied in a range of 1 to 2 cm. Figure 3e formulation SN proved to be the most effective achieving hypocotyl growth between 2.5 and 3 cm in the species tested (amaranth and chia), in contrast to formulations SN/CR and CR, where the growth was less than 1 cm. According to Figure 3f, the same formulation SN excels in terms of hypocotyl height of the microgreens, achieving 4 cm, whereas formulations SN/SD, SN/SD/CR and SD present a height of 2 cm. These results agreed with the study of Flores-Pacheco *et al.* (2016) who found the increase in plant height is due to the capacity of the sand substrate to retain nutrients. Sand allows for a better accumulation of nutrients that are essential for microgreen growth. This is due to high nutrient retention of sand in hydroponic systems is due to a combination of surface nutrient uptake by the sand particles; precise control of irrigation and nutrient solution delivery; and rapid root uptake that prevents excessive leaching. Under overwatering conditions, its retention capacity will be limited.

Microbiological analyses

Microbiological results (Table 8) showed that formulations SN/SD/CR and SD had high levels of bacterial CFU. On the other hand, formulation SN registered the lowest number of bacteria. A notable presence of fungi was observed in the formulation SN/SD/CR, with a count of 40.45 $X10^2$ CFU g^{-1}. This increase could be related to the high-water retention shown in Table 1. So, this could create optimal conditions for fungi growth. Regarding microgreens, chia microgreens showed a microbial density of 127.09 X 10^{13} CFU g^{-1}, whereas amaranth microgreens showed a lower density with 11.02 X 10^{13} CFU g^{-1}. These findings are consistent with Chandra *et al.* (2012) who indicate that bacteria can easily grow in young and delicate tissues such as those of microgreens. It has also been noted that bacterial growth can be stimulated by sugars and other organic substances released during endosperm decomposition at germination. According to the regulatory framework proposed by the U. S. Environmental Protection Agency (EPA) and the European Union (EU), the tolerance for total coliforms is 100 UFC g^{-1} (Alimentarius, 2003). In a study Castagnino *et al.* (2020) found that 'rapini' (*Brassica rapa* L.) sprouts may contain high levels of bacteria due to the organic media used in their cultivation. These bacteria can cause a disease

Table 8. Microbiological analysis.

Formulation	Mixture	Moisture (%)	Bacteria (UFC g^{-1})	Fungi (UFC·g^{-1})
1	SN	13.52	14.45 X 10	Negative
2	SN / SD	53.00	51.22 X 10^2	Negative
3	SN / CR	45.59	31.43 X 10^3	Negative
4	SN/ SD /CR	45.62	98.38X 10^3	40.45 X10^2
5	SD	78.53	81.27 X 10^3	Negative
6	SD/CR	56.88	27.48 X 10^3	Negative
7	CR	46.84	39.31 X 10^3	Negative
	Chia microgreens	93.75	127.09 X 10^{13}	Negative
	Amaranth microgreens	89	11.02 X 10^{13}	Negative

SN=100 % sand; SD/SN=50 % sawdust+50 % sand; SN/CR=50 % sand + 50 % residue from industrial production of instant coffee; SN/SD/CR= 33.3 % sand + 33.3 % sawdust + 33.3 % residue from industrial production of instant coffee; SD= 100% sawdust; CR/SD= 50 % residue from industrial production of instant coffee + 50 % sawdust, CR= residue from industrial production of instant coffee 100 %.

known as soft rot which significantly reduces the shelf life of these fresh vegetables and may favor the development of pathogens.

CONCLUSIONS

The use of experimental mix design methodologies to optimize substrate composition is a strategy that has proven to be effective. The mixture with a higher percentage of sand shows a decreased in porosity. Sawdust improved the aeration of the substrate, although this also led to an increase in the variability of water retention capacity, particularly when the proportion of sawdust and CR increased in the mixture. With respect to pH, a balanced mixture of 50 % sand and 50 % CR resulted in an adequate pH of 6.7 for microgreens production. This study revealed that the best substrate for chia and amaranth microgreen growth was sand when irrigated with a nutrient solution. Coffee residue seemed not to be adequate for growing chia or amaranth microgreens. However, the possibility of combining it with other materials to improve its properties is a promising avenue that deserves further research. This sustainable approach not only facilitates waste management, but also promotes the production of local, fresh, and nutritious food, thus supporting a more sustainable and efficient agriculture.

ACKNOWLEDGMENTS

The authors would like to extend their gratitude to the Consejo Nacional de Humanidades, Ciencias y Tecnologías (CONAHCYT) for their invaluable support and the scholarship awarded

to the first author. Their contribution has been instrumental in the project's success. We also express our sincere thanks to the Colegio de Postgraduados, Campus Córdoba, for the support and training provided throughout these years of study, which have been crucial to our academic and professional development.

REFERENCIAS

Alimentarius C. 2003. Codex alimentarius commission. Code of practice for food quality. Rome: FAO/WHO.

Antonio CG, Romero LAR, Trejo JFG, Pérez AAF. 2021. Revaluation of coffee crop wastes: Towards a circular economy. Digital Ciencia@ UAQRO 4 (6): 71–79.

Burgos ME. 2018. Los desafíos del futuro: crecimiento poblacional y desarrollo. Journal of Social Sciences 6 (11): 179–185. https://doi.org/10.18682/jcs.v0i11.900.

Castagnino A, Marina J, Benvenuti S, Marin CMA. 2020. Microgreens and sprouts, two innovative functional foods for a healthy diet in Km 0. Horticultura Argentina 39 (100): 55–95.

Ceglie FG, Bustamante MA, Ben Amara, M Tittarelli F. 2015. The challenge of peat substitution in organic seedling production: optimization of growing media formulation through mixture design and response surface analysis. PLoS One 10 (6): e0128600. https://doi.org/10.1371/journal.pone.0128600

Chandra D, Kim JG, & Kim YP. 2012. Changes in microbial population and quality of microgreens treated with different sanitizers and packaging films. Horticulture, Environment, and Biotechnology. 53: 32–40. https://doi.org/10.1007/s13580-012-0075-6

Diario Oficial de la Federación. 1994. Preparación y dilución de muestras de alimentos para su análisis microbiológico. Norma Oficial Mexicana. https://dof.gob.mx/nota_detalle.php?codigo=4883170&fecha=16/10/1995#gsc.tab=0. (Retrieved: May 2024)

Diario Oficial de la Federación. 1995. Norma Oficial Mexicana que establece el método para la cuenta de microorganismos coliformes totales en placa.. https://www.dof.gob.mx/nota_detalle.php?codigo=4880115&fecha=25/08/1995#gsc.tab=0. (Retrieved: June 2024)

Diario Oficial de la Federación. 2000. Norma Oficial Mexicana que establece las especificaciones de fertilidad, salinidad y clasificación de suelos.. https://dof.gob.mx/nota_detalle.php?codigo=717582&fecha=31/12/2002#gsc.tab=0(Retrieved: January 2024)

Diario Oficial de la Federación. 2008. Norma Oficial Mexicana que establece las especificaciones para humus de lombriz (lombricomposta)-especificaciones y métodos de prueba. https://www.dof.gob.mx/nota_detalle.php?codigo=5044562&fecha=10/06/2008#gsc.tab=0. (Retrieved: March, 2024)

Di Gioia F, Mininni C, Santamaria P. 2015. Come coltivare micro-ortaggi. In F. Di Gioia & P. Santamaria (Eds.), Microgreens: Novel fresh and functional food to explore all the value of biodiversity (pp. 51–80). ECO-logica. Bari, Italy.

Di Gioia F, De Bellis P, Mininni C, Santamaria P, Serio F. 2017. Physicochemical, agronomical and microbiological evaluation of alternative growing media for the production of rapini (*Brassica rapa* L.) microgreens. Journal of the Science of Food and Agriculture 97 (4): 1212–1219. https://doi.org/10.1002/jsfa.7852

Ebert AW. 2022. Sprouts and microgreens-Novel food sources for healthy diets. Plants. 11(4), 571. https://doi.org/10.3390/plants11040571

Euromonitor C. 2017. Analysis of the coffee consumption market in Mexico 2016. Report of the study conducted by Euromonitor International. https://amecafe.org.mx/. (Retrieved: March, 2024)

Flores-Pacheco, JA Pacheco, C F Murillo, Y Oporta, R Alemán Y. 2016. Hydroponic production of tomato (*Solanum lycopersicum*) and chiltoma (*Capsicum annuum*) with inert substrates. Revista Científica de FAREM-Estelí, 20: 73–81. https://doi.org/10.5377/farem.v0i20.3069

Johnson SA, Prenni JE, Heuberger AL, Isweiri H, Chaparro JM, Newman SE, Uchanski ME, Omerigic HM, Michell KA, Bunning M, Foster MT, Thompson HJ, Weir TL. 2021. Comprehensive Evaluation of Metabolites and Minerals in 6 Microgreen Species and the Influence of Maturity. Current Developments in Nutrition 5 (2): https://doi.org/10.1093/cdn/nzaa180

Kyriacou MC, Rouphael Y, Di Gioia F, Kyratzis A, Serio F, Renna M, De Pascale S, Santamaria P. 2016. Micro-scale vegetable production and the rise of microgreens. Trends in Food Science and Technology 57: 103–115. https://doi.org/10.1016/j.tifs.2016.09.005

Martínez PF, Roca D. 2011. Sustratos para el cultivo sin suelo. Materiales, propiedades y manejo. In: Flórez R., V.J. (Ed.). Sustratos, manejo del clima, automatización y control en sistemas de cultivo sin suelo. Bogotá: Editorial Universidad Nacional de Colombia. pp: 37–77.

Morales-Maldonado, ER & Casanova-Lugo F. 2015. Organic and inorganic substrate mixtures, particle size and ratio. Agronomía Mesoamericana, 26(2):365–372. https://doi.org/10.15517/am.v26i2.19331

Moreno Reséndez A, & Valdés Perezgasga MT. 2005. Tomato development on vermicompost/sand substrates under greenhouse conditions. Agricultura Técnica, 65 (1): 26–34. https://doi.org/10.4067/S0365-28072005000100003

Murthy PS, Naidu MM. 2012. Sustainable management of coffee industry by-products and value addition-A review. Resources, Conservation and Recycling 66: 45–58. https://doi.org/10.1016/j.resconrec.2012.06.005. (Retrieved: April 2024)

Navarro R, de la Tierra CA. 2003. Manual for aerobic composting. CESTA, Friends of the Earth El Salvador, pp: 2–5.

Nolan C, Overpeck JT, Allen JR, Anderson PM, Betancourt JL, Binney HA, Brewer S, Bush M B, Chase BM, Cheddadi R, Djamali M, Dodson J, Edwards ME, Gosling WD, Haberle S, Hotchkiss SC, Hntley B, Ivory SJ, Kershaw AP, Kim S-H, Latorre C, Leydet M, Lézine A-M, Liu K-B, Liu Y, Mcglone AVL, Marchant RA, Momohara A, Moreno PI, Müller S, Otto-Bliesner, B Shen C, Stevenson J, Tahahara H, Tarasoy PE, Tipton J, Vincens A, Wend C, Xi O, Zheng Z, Jacksom ST. 2018. Past and future global transformation of terrestrial ecosystems under climate change. Science 361 (6405): 920–923. https://doi.org/10.1126/science.aan5360

Porras ÁC, González AR. 2016. Aprovechamiento de residuos orgánicos agrícolas y forestales en Iberoamérica. Academia y Virtualidad 9 (2): 90–107. http://dx.doi.org/10.18359/ravi.2004.

Renna M, Castellino M, Leoni B, Paradiso V M, Santamaria P. 2018. Microgreens production with low potassium content for patients with impaired kidney function. Nutrients 10 (6): 675. https://doi.org/10.3390/nu10060675

Salamanca G, Méndez LMR, Osorio M, Arias NR. 2015. Experimental design of mixtures as a tool for the optimization of mango cremolacteos. Colombian Journal of Agroindustrial Research 2 (1): 16–24.

Vardon DR, Moser BR, Zheng W, Witkin K, Evangelista RL, Strathmann TJ, Rajagopalan K, Sharma B K. 2013. Complete Utilization of spent coffee grounds to produce biodiesel, bio-oil, and biochar. ACS Sustainable Chemistry & Engineering 1 (10): 1286–1294. https://doi.org/10.1021/sc400145w.

Wang, J., Li, J., Liu, W., Zeb, A., Wang, Q., Zheng, Z. and Liu, L. 2023. Three typical microplastics affect the germination and growth of amaranth (*Amaranthus mangostanus* L.) seedlings. Plant Physiology and Biochemistry, *194*, 589–599. https://doi.org/10.1016/j.plaphy.2023.01.012

Xiao Z, Lester GE, Luo Y, Wang Q. 2012. Assessment of Vitamin and Carotenoid Concentrations of Emerging Food Products: Edible Microgreens. Journal of Agricultural and Food Chemistry 60 (31): 7644–7651. https://doi.org/10.1021/jf300459b

Agrociencia

IMPACT OF CLIMATE CHANGE ON *Pinus hartwegii* Lindl. FOREST ECOSYSTEMS AS A SUBJECT OF INTERINSTITUTIONAL AND INTERNATIONAL STUDIES

Marlín **Pérez-Suárez**[1], Jorge Enrique **Ramírez-Albores**[2*], J. Jesús **Vargas-Hernández**[3], Philippe **Rozenberg**[4]

[1]Universidad Autónoma del Estado de México. Instituto de Ciencias Agropecuarias y Rurales. Carretera El Cerrillo-Piedras Blancas s/n, Toluca, State of Mexico, Mexico. C. P. 50090.
[2]Universidad Autónoma Agraria Antonio Narro. Departamento de Botánica. Calzada Antonio Narro 1923, Colonia Buenavista, Saltillo, Coahuila, Mexico. C. P. 25315.
[3]Colegio de Postgraduados, Campus Montecillo. Postgrado en Ciencias Forestales. Carretera México-Texcoco km 36.5, Montecillo, Texcoco, State of Mexico, Mexico. C. P. 56230.
[4]Institut National de Recherche pour l'Agriculture l'Alimentation et l'Environnement. UMR 0588 BioForA INRAE Val de Loire. Avenue de la Pomme de Pin 2163, Cedex 2, Orleans, France. C. P. 45075.
* Author for correspondence: jorgeramirez22@hotmail.com

Citation: Pérez-Suárez M, Ramírez-Albores JE, Vargas-Hernández JJ, Rozenberg P. 2025. Iimpact of climate change on *Pinus hartwegii* Lindl. forest ecosystems as a subject of interinstitutional and international studies. **Agrociencia** 59 (5): 701-714. https://doi.org/ 10.47163/agrociencia.v59i5.3413

Editor in Chief:
Dr. Fernando C. Gómez Merino

Received: January 23, 2025.
Approved: June 23, 2025.
Published in Agrociencia: June 30, 2025.

ABSTRACT

Pinus hartwegii Lindl. is a low-temperature-adapted species that forms the highest elevation tree lines in the world, reflecting its tolerance to extreme high mountain conditions. Studying the mechanisms that determine the variation of tree lines in different regions helps to more accurately assess the impact of climate change on forest ecosystems. Thus, assessing its impact on the ecological features that affect *P. hartwegii* is critical, as is identifying and defining information gaps that may lead to new, important, and significant research lines. In this work, an intensive literature search on the impact of climate change on *P. hartwegii* was carried out in Scopus and other specialized databases. The information was grouped and analyzed in VOSviewer by year of publication, institution, research topics, and study area. Scientific publications on *P. hartwegii* have increased exponentially since its first publication, reaching a total of 281 scientific papers until 2024. More than 66 % of all studies were conducted in protected areas such as Iztaccíhuatl-Popocatépetl, Nevado de Toluca, and Cofre de Perote in Mexico. The most studied topics were forest management, climate change, dendrochronology, and population dynamics. The high heterogeneity in the number of studies suggests that there is an uneven distribution of interinstitutional and international resources or research interests. This study highlights the need to intensify research on the ecology and biology of the species, as well as to foster inter-institutional collaboration and coordination to increase studies in specific areas to deepen the understanding of the adaptive capacity of *P. hartwegii* populations in the face of the current climate crisis.

Key words: Cofre de Perote, Trans-Mexican Volcanic Belt, Iztaccíhuatl-Popocatépetl, alpine tree line, Nevado de Toluca, high altitude pine.

INTRODUCTION

Mountain ecosystems are inhabited by highly specialized and endemic plants that are particularly sensitive to climatic changes (Cavieres *et al*., 2021). Recent studies show that rising mountain temperatures encourage species distributions to move upward along altitudinal gradients (Aitken *et al*., 2008; Cavieres *et al*., 2021; Petrov *et al*., 2024). This would eventually put them at risk of extinction, given the difficulty of adapting their life and migration cycles at a slower rate than temperature changes (Aitken *et al*., 2008). Because of the tangible and intangible benefits that mountain ecosystems have on human societies, it is imperative to understand the ecological processes that regulate abiotic and biotic pressures on these ecosystems.

Pinus hartwegii Lindl., also known as the pine of the heights or white ocote, is a species of great ecological value that has captured international attention in recent years (Pérez-Suárez *et al*., 2022), being the subject of national and international studies. This species is reported to be the most widely distributed pine at the highest elevations in the world (Alfaro-Ramírez *et al*., 2020; Pérez-Suárez *et al*., 2022). It is characterized by the formation of tree lines due to its high tolerance to low temperature extremes and ability to withstand adverse environmental conditions such as high diurnal temperature variation, high precipitation, high winds, low soil quality, high UV intensity, and short growing season length (Richardson and Friedland, 2009).

According to Körner and Paulsen (2004) and Berdanier (2010), tree lines are associated with altitude or climatic conditions that limit the growth of arboreal life forms. Those individuals that exceed these lines grow stunted or structurally deformed, with a twisted trunk being the most common feature (krummholz). In the case of *P. hartwegii*, a diffuse line of trees is formed in krummholz (Alfaro-Ramírez *et al*., 2017), with a gradual decrease in the diameter, height, and density of individuals. The physiology, biology, and ecology of this species are closely related to low temperatures, highlighting its potential sensitivity to temperature increases resulting from global warming (Manzanilla-Quiñonez *et al*., 2019; Alfaro-Ramírez *et al*., 2020; Pérez-Suárez *et al*., 2022).

Several studies have focused on assessing the trend of changes in spatial distribution under different climate change scenarios (Malek and Verburg, 2021; Crespi *et al*., 2023). Most studies agree that its range will decrease by up to 69 % in the next 50 years (Alfaro-Ramírez *et al*., 2020). However, the underlying mechanisms that would lead to such a significant range reduction and whether these are shared locally or at the level of individual populations are unknown. The effects of high temperatures are not necessarily direct or immediate, as they are not simultaneous responses to stressors but the result of long processes of change in which several complex interacting factors come together, including the impact of human activities and topography, as well as their integration along elevation gradients (Gray and Brady, 2016; Balfagón *et al*., 2020). Human activities play an important role in the degradation and anthropogenic pressure on these populations, so that a spatial distribution map does not provide the reason for the reduction or the dominant factor causing this process. In the case of

P. hartwegii, local and regional demand for the species as a raw material for furniture manufacture, among others, is a factor that significantly reduces its populations throughout its range. At the regional level, temperature regulates ecological processes in high mountain forests. However, other local site-specific factors must also be considered, as they can influence the potential impact of climate change or variability on forest ecosystems (Albrich *et al*., 2020; Thakur *et al*., 2021).

In this context, the generation of knowledge on the impact of climate change on forest ecosystems is a challenge that must be addressed from multidisciplinary and interdisciplinary approaches, where the efforts of different institutions are combined to carry out complementary rather than duplicated work, allowing for the efficiency of material and human resources. This provides the necessary tools to identify the causes and take action to mitigate the loss of *P. hartwegii* in support of its conservation, in addition to maintaining the multiple services that its forest cover provides to society (Pérez-Suárez *et al*., 2022; Wang *et al*., 2024) and the recreational and cultural activities that are carried out throughout the species' range (Varo-Rodríguez *et al*., 2019).

The biological, geological, and chemical processes that occur in the ecosystems inhabited by this species benefit both local communities in the mountains and those settling lower down, including the more populated valleys in central Mexico. This includes regulating water flows, local and regional temperature, carbon sequestration, and providing forest biomass for various economic activities such as furniture and fuelwood production. (Franco-Maass *et al*, 2006; Endara-Agramont and Herrera-Tapia, 2016; Martínez-Luna *et al*., 2020).

Predicting how temperature increases will affect *P. hartwegii* forest cover requires taking into account the majority of its range. This species has not received enough research, and little attention has been paid to how it relates to climatic factors. This limits the ability to draw conclusions at different levels of organization (species, population, etc.) (Pérez-Suárez *et al*., 2022) and reduces the accuracy in predicting the effects of various global change factors on its biology, ecology, and adaptability. In this context, it is important to know the position of the climate change approach in studies on *P. hartwegii*, what the interest of institutions in studies on this species is, and which areas have been studied throughout its distribution in order to identify and delimit information gaps that can lead to new lines of research with greater relevance and impact. This is possible through collaborative work involving different institutions that will lead to the establishment of adequate and efficient strategies for the management and conservation of *P. hartwegii*.

MATERIALS AND METHODS

An intensive literature search on ecological aspects of *Pinus hartwegii* was conducted in Scopus (Elsevier; available at https://www.scopus.com/) and complemented with other specialized databases, such as Web of Science (Clarivate Analytics; https://clarivate.com/), SciELO (https://www.scielo.org/es/), Publons (https://publons.com/),

and Redalyc (https://www.redalyc.org/). To ensure the completeness and scientific reliability of the literature reviewed, a list of scientific publications was created that included synonyms and words related to the topic, or a combination of them, in the title, abstract, or keywords. Key words for the search were '*Pinus hartwegii*' OR '*Pinus rudis*' OR 'Hartwegs Pine' OR 'mountain pine' OR 'white ocote' OR '*Pinus*' OR 'highland pine' AND 'climate change.'

A database was constructed and purified, considering only scientific articles related to *P. hartwegii*, specifically those related to climate change and its impact on ecological aspects such as forest management, population dynamics, dendrochronology, climate change, hydrological cycle, conservation, phenology, histopathology, symbiosis, population genetics, fire ecology, systematics, physiology, community ecology, carbon capture and sequestration, forest health, biogeographical patterns, environmental pollution, nutrient flow, taxonomy, phytosociology, human impact, ethnobotany, and evolution. In addition, theses, books or book chapters, technical reports, and presentations or full-length papers from scientific meetings were excluded, as well as papers that did not address any ecological or biological aspect other than the occurrence of the species. References in the revision process or incomplete references were also excluded.

The final information contained in the database was grouped by year of publication to subsequently carry out an orderly review that would facilitate the identification of those areas with a lack of scientific studies related to *P. hartwegii*. The VOSviewer software (van Eck and Waltman, 2010, 2017) was used, which represents a high-performance solution with numerous bibliometric network visualization options. In this software, keyword co-occurrence networks, co-authorship relationships between institutions (or affiliations), and co-occurrence between main research topics and geographical areas (or study areas) are observed.

RESULTS AND DISCUSSION

Bibliometric aspects

A total of 281 scientific publications related to *P. hartwegii* were found, using 844 keywords (Figure 1). The most prominent words close to *P. hartwegii* were 'Mexico,' 'climate change,' and 'pine.' These words appeared most frequently within the papers as co-occurring keywords (Figure 1A and 1B). The more intense colors show areas with a higher density of co-occurrence between outstanding keywords that are more closely related to *P. hartwegii*, with 'climate change' again being the most prominent, while lighter colors indicate areas where terms are less frequent or have weaker connections to each other (Figure 1C and 1D).

Scientific work was published from 1962 to 2024 (Figure 2), showing an exponential growth over time. From 2000 to 2024, more than 80 % of the registered papers were published, with a total of 234 articles. In addition, 154 studies (54.8 %) were published

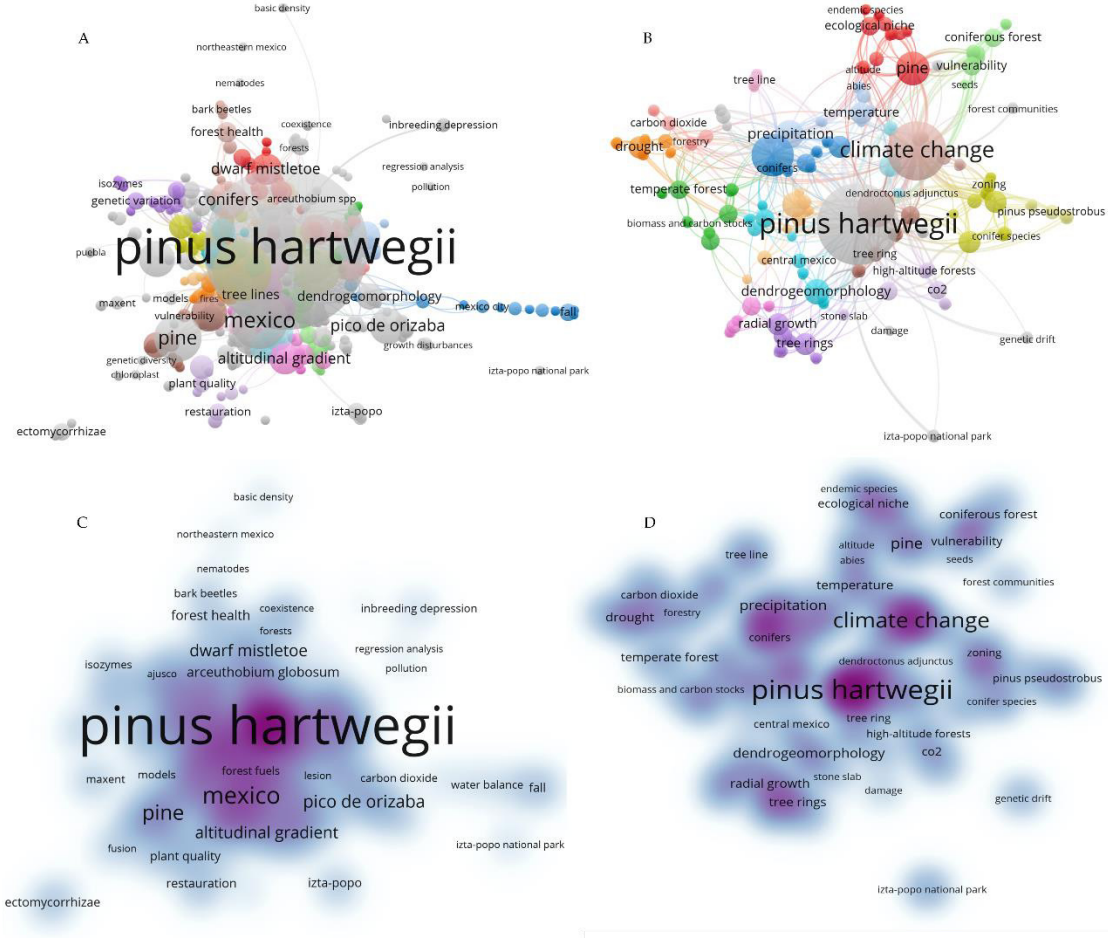

Figure 1. Bibliometric analysis of keywords in scientific publications on *Pinus hartwegii* Lindl. A: co-occurrence of total keywords; B: co-occurrence of keywords related to climate change; C: total keyword density map; D: density map of keywords related to climate change publications.

in national journals and 127 (45.1 %) in international journals (Figure 1). As for the topic of climate change, out of the total number of publications, only 77 corresponded to this topic; however, the proportion of publications in national journals was lower (25; 32.4 %) compared to that in international journals (52; 67.5 %) (Figure 2).

One of the most important aspects of the analysis was to find 135 institutions that have focused on the study of *P. hartwegii*. These institutions have established major collaborative networks with other institutions, both national and international. The Postgraduate College (COLPOS), the National Institute of Forestry, Agricultural, and Livestock Research (INIFAP), Autonomous University of Chapingo, University of Veracruz (UV), and the National Autonomous University of Mexico (UNAM) stand out the most and have the strongest relationship with other institutions in studies on *P. hartwegii*. All of them together carried out more than 75 % of the published research.

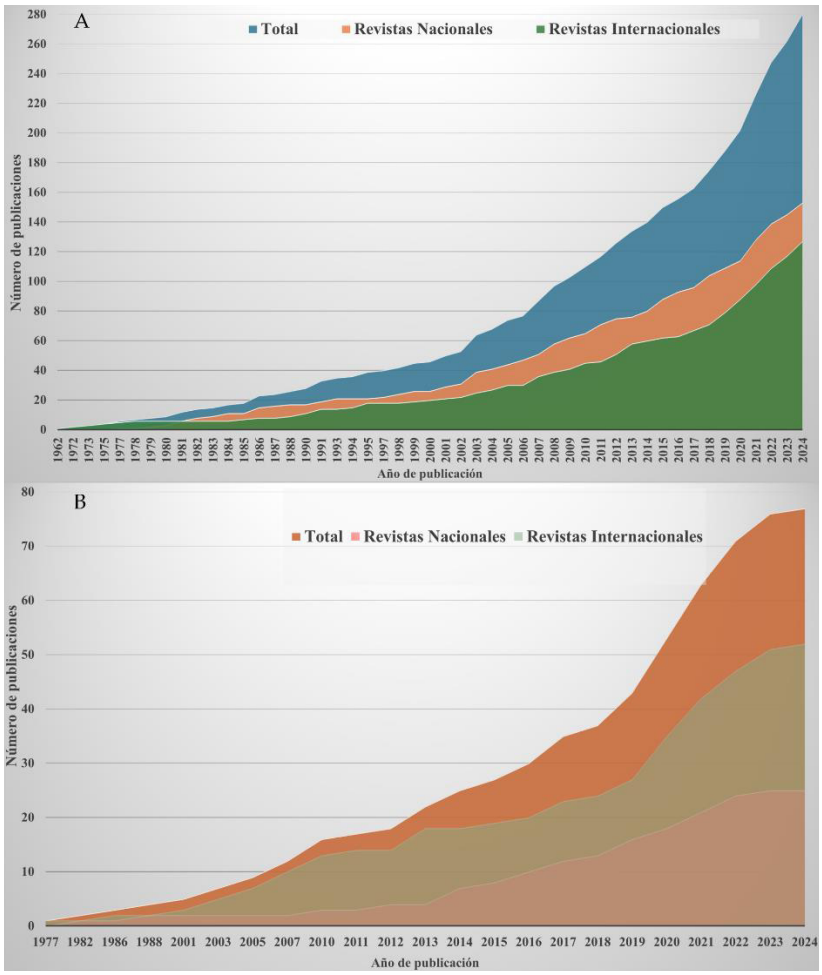

Figure 2. Trend of scientific publications analyzed in the time period from 1962 to 2024. A: total number of scientific publications on *Pinus hartwegii* Lindl.; B: number of publications on climate change.

The same pattern was found for climate change, with a total of 58 institutions having researched this topic (Figure 3B). Stronger colors show areas with a higher frequency of collaboration between institutions and which are more closely related to each other, while lighter colors indicate areas where collaboration between institutions is less frequent or has a low connection (Figure 3C and 3D).

In terms of the research topics studied, a total of 24 different topics were found (Figure 4). The more prominent and the closer they are, the greater the relationship between topics and the greater the number of documents with keywords that were linked together (Figure 4A and 4B), with forest management (103 papers), climate change (77 papers), population dynamics (58 papers), and dendrochronology (46 papers) standing out, while the rest of the topics had less than 30 publications.

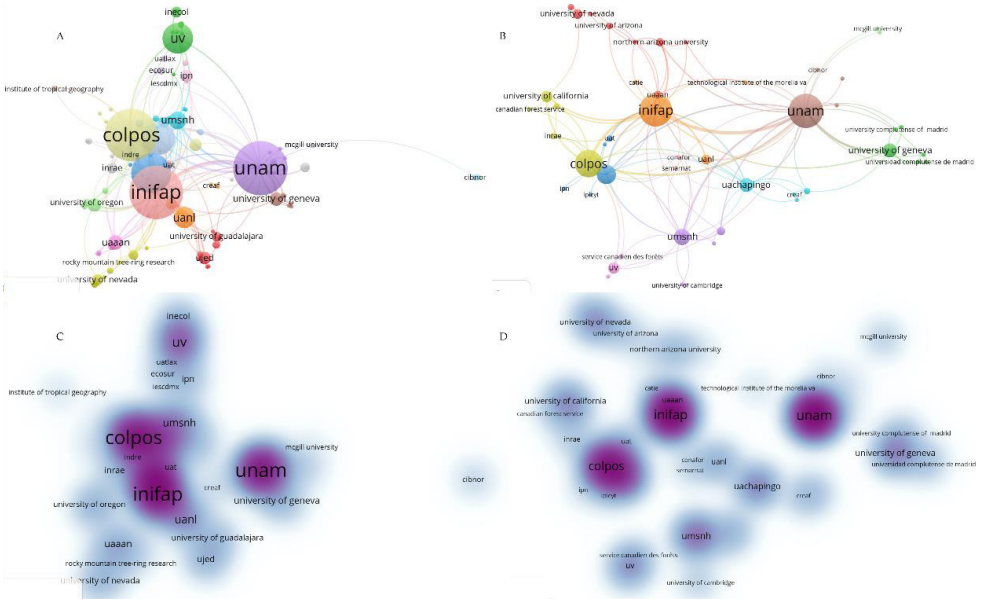

Figure 3. Bibliometric analysis of institutions (or affiliations) in scientific publications on *Pinus hartwegii* Lindl. from 1962 to 2024. A: network map of institutions; B: network map of institutions related to climate change; C: total density map of institutions; D: density map of institutions related to climate change.

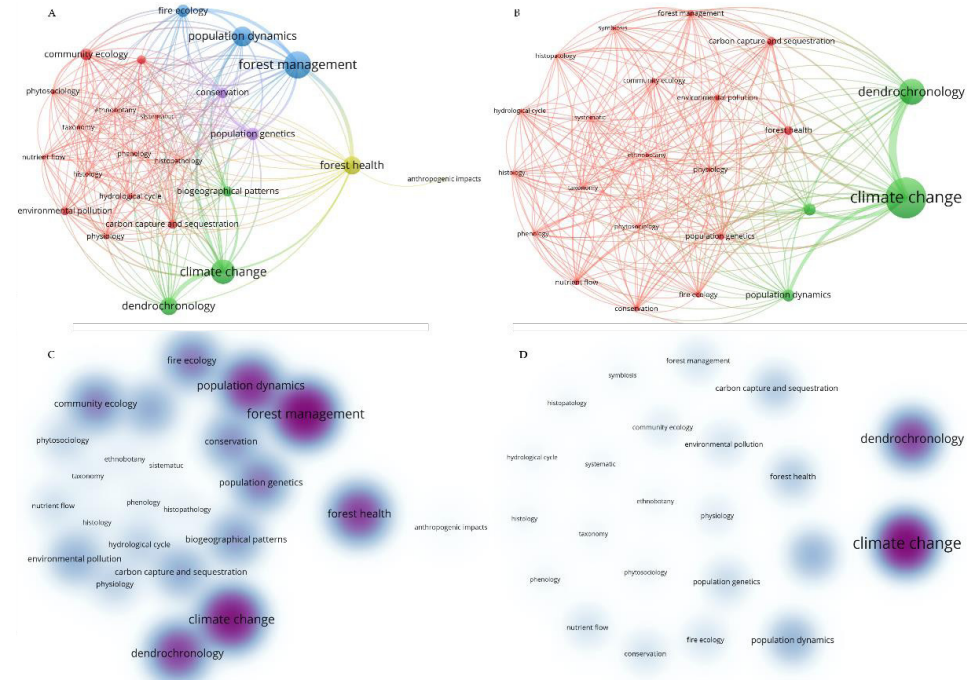

Figure 4. Bibliometric analysis of research topics in scientific publications on *Pinus hartwegii* Lindl. from 1962 to 2024. A: network map of research topics; B: network map of research topics related to climate change; C: total density map of research topics; D: density map of research topics related to climate change.

Recent publications have focused on climate change, nutrient flow, dendrochronology, hydrological cycle, ethnobotany, and systematics (Figure 4A). In terms of climate change, publications were focused on dendrochronology, population dynamics, and biogeography (Figure 4B). Stronger colors indicate areas with a higher density of co-occurrence between research topics, while lighter colors show areas with a lower density (Figure 4C and 4D). This can be explained by either emerging trends (which are yet to develop) or topics that are little frequented by researchers.

In relation to the most studied areas, the publications found show a concentration towards studies carried out in the Trans-Mexican Volcanic Belt, including the Iztaccíhuatl-Popocatépetl National Park (including Monte Tláloc and the Zoquiapan Experimental Forest Station), followed by the Nevado de Toluca Flora and Fauna Protection Area, Cofre de Perote National Park, Cumbres del Ajusco National Park, and Pico de Orizaba National Park (Figure 5A and 5B). Of these areas, an increasing trend was recorded on the survey of *P. hartwegii* populations found in both Iztaccíhuatl-Popocatépetl National Park and Nevado de Toluca Flora and Fauna Protection Area. Stronger colors show a higher frequency between study areas that are more closely related to each other, while softer colors indicate a lower frequency (Figure 5C).

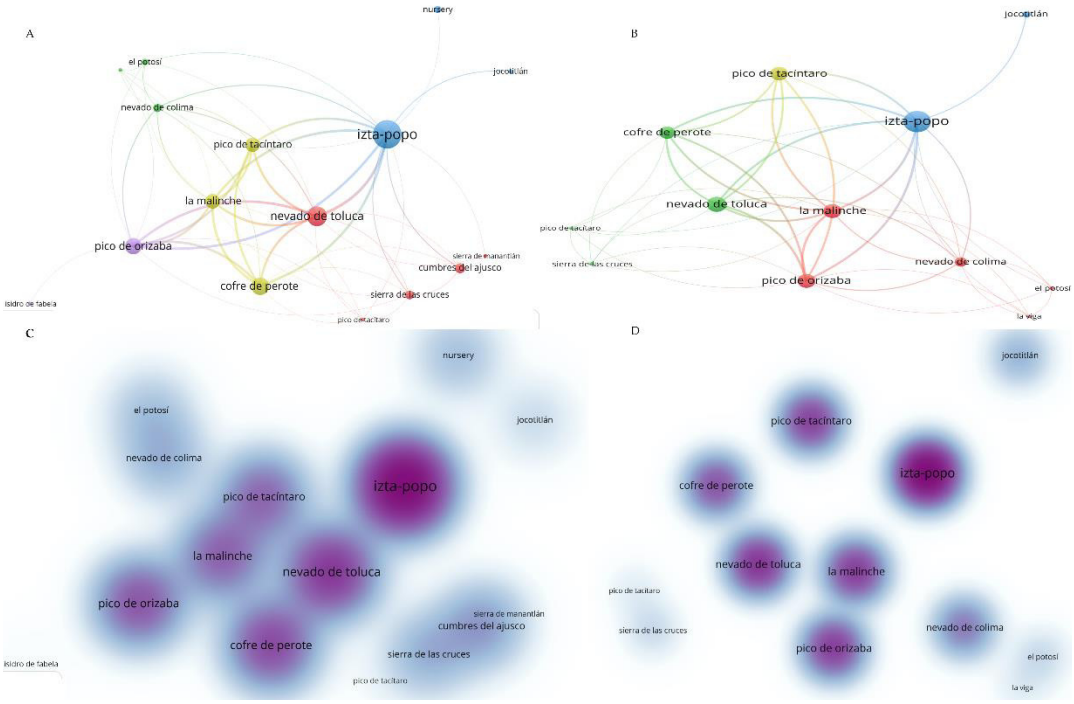

Figure 5. Bibliometric analysis of geographical areas (study areas) in scientific publications on *Pinus hartwegii* Lindl. from 1962 to 2024. A: network map of geographical areas; B: network map of geographical areas related to climate change; C: total density map of geographical areas; D: density map of geographical areas related to climate change publications.

This trend was also reflected for climate change and its proportion among these areas (Figure 5D). However, studies on population genetics and fire ecology were the exception, as these were more concentrated in Cofre de Perote National Park and fire ecology in Cumbres del Ajusco National Park, respectively. This emphasizes the need to consider populations of *P. hartwegii* located in other parts of its range, as well as study particularly important issues in terms of its adaptation to new environmental conditions, not only at the local level but throughout the species' range.

The results show a heterogeneity and frequency in the topics addressed in scientific publications throughout the distribution area of *P. hartwegii*, as well as the institutions that have contributed most to the generation of information. An exponential increase in scientific interest in *P. hartwegii* since 2000 was observed, with climate change being the main focus of most of these publications. This has also led to greater inter-institutional collaboration in the studies carried out.

Research topics

High mountain systems are characterized by the concentration of different transition zones in a relatively small area (Körner and Paulsen, 2004; Holtmeier and Broll, 2005), with the upper forest boundary ecotone being one of the best known (Franco-Ramos and Vázquez-Selem, 2017). Since the plant species present in the high mountains are highly adapted to low temperature conditions, extreme for many biological processes (Körner, 1995; Holtmeier and Broll, 2005), they have become ideal sites for analyzing the effects of climate change (Arriaga and Gómez, 2004; Körner and Paulsen, 2004).

Pinus hartwegii is the pine species that has been recorded at the highest altitude in the world, around 4200 m (Alfaro-Ramírez *et al*., 2017, 2020), generating great interest in its structure, composition, and response to environmental changes. However, the problem with tree species that are part of the upper limit of high mountain forests is that there is not much surface area available to migrate upwards, and the natural migration speed would be too slow (Aitken *et al*., 2008). Towards the lower boundary, climate change promotes increasingly unfavorable water stress conditions, increasing competition with other forest species that tend to benefit from higher temperatures.

The elevational movement of *P. hartwegii* has been evaluated (Alfaro-Ramírez *et al*., 2017, 2020), concluding that populations of this species at different elevations will respond differently and at different rates to the impacts of climate change (Franco-Ramos and Vázquez-Selem, 2017). Under unfavorable climate scenarios (Arriaga and Gómez, 2004), it could migrate to higher altitudes or latitudes in search of sites with favorable conditions for its survival (Gómez-Mendoza and Arriaga, 2007; Alfaro-Ramírez *et al*., 2020).

Some aspects have been little explored and go beyond the reduced surface area on mountain peaks, among which are the limitations of support and nutrition imposed by the shallow and poorly developed soils characteristic of volcanic areas (Körner and Paulsen, 2004). Biological interactions with other species that promote the establishment and survival of *P. hartwegii*, especially in early stages, also influence its population

structure (Almeida-Leñero *et al*., 2004; Iglesias-Andeu and Tivo-Fernández, 2006), in addition to the potential migration of individuals of this species under the context of climate change (Franco-Ramos and Vázquez-Selem, 2017).

Finally, extreme scenarios such as extinction and adaptation are displayed. In the first case, it is predicted that this species could reach local extinction (Gutiérrez and Trejo, 2014), so that the remaining populations would have the same effect in the long term; the second case would involve the adaptation of the physiological processes of *P. hartwegii* to the new environmental conditions through phenotypic plasticity mechanisms (Arzate-Fernández *et al*., 2016). However, the scientific information to predict with certainty which pathway to follow is not yet available. Therefore, it is necessary to study several aspects, such as genetic diversity and gene flow among its populations (Viveros-Viveros *et al*., 2009; Arzate-Fernández *et al*., 2016; Pérez-Suárez *et al*., 2022). In addition, there is insufficient information on the mechanisms that regulate the presence of each population and how resilient they may be to climate change (Arriaga and Gómez, 2004; Pérez-Suárez *et al*., 2022), nor on their ability to modify or conserve an ecological niche in the long term (Gómez-Mendoza and Arriaga, 2007; Gutiérrez and Trejo, 2014).Another aspect in which scientific interest has increased the most is the health status of forest cover, given that it depends on various abiotic factors such as temperature, humidity, and nutrient availability. Increases in global temperature have a strong impact on the susceptibility of forest species to pest incidence (Hawksworth and Wiens, 1996; Queijeiro-Bolaños *et al*., 2011). *Pinus hartwegii* is no exception, as its biology and ecology are closely dependent on the temperature extremes that dominate along its elevational distribution gradient. Thus, this pine species is considered particularly susceptible to the direct and indirect impact of ambient temperature increases.

Currently, an increased incidence of pests has been recorded, mainly mistletoes such as *Arceuthobium globosum* and *A. vaginatum* (Mathiasen *et al*., 2008; Queijeiro-Bolaños *et al*., 2011; Queijeiro-Bolaños and Cano-Santana, 2016). Among the main recorded effects of these pests on *P. hartwegii* are the reduction in growth and survival of infested individuals (Mathiasen *et al*., 2008; Queijeiro-Bolaños and Cano-Santana, 2016). However, some authors point out that this interaction has an important ecological role, particularly in forest regeneration (Queijeiro-Bolaños and Cano-Santana, 2016), arguing that mistletoe reduces the number of susceptible individuals, giving way to more resistant individuals (Queijeiro-Bolaños *et al*., 2011). However, there is no precise information on the infestation ranges that *P. hartwegii* can tolerate or the physiological mechanisms that cause mistletoe damage and death in trees.

Another pest affecting *P. hartwegii* is *Dendroctonus adjunctus* (Billings *et al*., 2004). This bark beetle causes high mortality of pine individuals in susceptible stands (Biondi *et al*., 2005), causing severe damage to pine populations. However, as in the case of mistletoe, there is very little information on the infestation mechanisms, the factors that promote it, the population dynamics of this insect in *P. hartwegii*, and the impact that the increase or modification of climatic conditions could have on the intensity

and speed of infestation. All these questions have generated growing scientific interest in this species, both nationally and internationally. This is evidenced not only by the increase in publications but also by the increase in the number of study topics and the number of institutions involved.

Several questions remain to be addressed: (*i*) whether there is variability in tree exposure to temperature; (*ii*) the effect of climate variability on biogeochemical cycles and on the dynamics of plant communities at both the upper and lower distributional limits, as well as along the entire distribution gradient; (*iii*) the impact of densification on the regenerative dynamics of trees and the redistribution of resources; (*iv*) seed viability throughout the species' distribution range; and (*v*) the characteristics of microsites that influence germination, establishment, and growth. Addressing these questions will be essential in the future to understand, at the population level, the impact of climate change on this species more clearly. Such understanding would support the implementation of management and conservation strategies with a higher likelihood of success.

CONCLUSIONS

Interest in the study of *Pinus hartwegii* has led to an exponential increase in scientific publications, particularly in recent years, with forest management, climate change, population dynamics, and dendrochronology being the main topics addressed in these publications. The locations where most of these studies have been carried out include the Trans-Mexican Volcanic Belt, mainly in the Iztaccíhuatl-Popocatépetl National Park and the Nevado de Toluca Flora and Fauna Protection Area. It is necessary to conduct more studies that cover its entire distribution area in order to better represent populations and gain knowledge of the species and its interactions with various biotic and abiotic factors, so that conclusions can be reached at the species level that allow for prediction of its behavior in the face of new environmental conditions.

ACKNOWLEDGEMENTS

MP-S is grateful to the Secretariat of Science, Humanities, Technology, and Innovation (SECIHTI) for funding the project (No. 219696) in which this work is carried out.

REFERENCES

Aitken SN, Yeaman S, Holliday JA, Wang T, Curtis-McLane S. 2008. Adaptation, migration or extirpation: Climate change outcomes for tree populations. Evolutionary Applications 1 (1): 95–111. https://doi.org/10.1111/j.1752-4571.2007.00013.x

Albrich K, Rammer W, Seidl R. 2020. Climate change causes critical transitions and irreversible alterations of mountain forest. Global Change Biology 26 (7): 4013–4027. https://doi.org/10.1111/gcb.15118

Alfaro-Ramírez FU, Arredondo-Moreno JT, Pérez-Suárez M, Endara-Agramont AR. 2017. Ecotono del límite superior del bosque de *Pinus hartwegii* Lindl.: estructura y límites altitudinales en el Nevado de Toluca, México. Revista Chapingo Serie Ciencias Forestales y del Ambiente 23 (2): 261–273. https://doi.org/10.5154/r.rchscfa.2016.10.055

Alfaro-Ramírez FU, Ramírez-Albores JE, Vargas-Hernández JJ, Franco-Maass S, Pérez-Suárez M. 2020. Potential reduction of Hartweg´s pine (*Pinus hartwegii* Lindl.) geographic distribution. PLoS One 15 (2): e0229178. https://doi.org/10.1371/journal.pone.0229178

Almeida-Leñero L, Giménez-de Azcárate J, Cleef AM, González-Trápaga MA. 2004. Las comunidades vegetales del zacatonal alpino de los volcanes Popocatépetl y Nevado de Toluca, Región Central de México. Phytocoenologia 34 (1): 91–132. https://doi.org/10.1127/0340-269x/2004/0034-0091

Arriaga L, Gómez L. 2004. Posibles efectos del cambio climático en algunos componentes de la biodiversidad de México. *In* Martínez J, Fernández A. (eds.), Cambio Climático: una Visión desde México. Instituto Nacional de Ecología y Cambio Climático: Ciudad de México, México, pp: 255–265.

Arzate-Fernández AM, Gutiérrez-González G, Heredia-Bobadilla RL. 2016. Diversidad genética de dos especies de coníferas en el Nevado de Toluca: una alternativa de conservación. Universidad Autónoma del Estado de México. Toluca, México. 136 p.

Balfagón D, Zandalinas SI, Mittler R, Gómez-Cárdenas A. 2020. High temperatures modify plant responses to abiotic stress conditions. Physiologia Plantarum 170 (3): 335–344. https://doi.org/10.1111/ppl.13151

Berdanier AB. 2010. Global treeline position. Nature Education Knowledge 3 (10): 11.

Billings RF, Clarke SR, Espino-Mendoza V, Cordón-Cabrera P, Meléndez-Figueroa B, Ramón-Campos J, Baeza G. 2004. Bark beetle outbreaks and fire: A devastating combination for Central America's pine forests. Unasylva 217 (55): 15–21.

Biondi F, Hartsough PC, Galindo-Estrada I. 2005. Daily weather and tree growth at the tropical treeline of North America. Arctic, Antarctic and Alpine Research 37 (1): 16–24. https://doi.org/10.1657/1523-0430(2005)037[0016:dwatga]2.0.co;2

Cavieres L, Valencia G, Hernández C. 2021. Calentamiento global y sus efectos en plantas de alta-montaña en Chile central: una revisión. Ecosistemas 30 (1): 2179. https://doi.org/10.7818/ecos.2179

Crespi A, Renner K, Zebish M, Schauser I, Leps N, Walter A. 2023. Analysing spatial patterns of climate change: Climate clusters, hotspots and analogues to support climate risk assessment and communication in Germany. Climate Services 30: 100373. https://doi.org/10.1016/j.cliser.2023.100373

Endara-Agramont AR, Herrera-Tapia F. 2016. Deterioro y conservación de los bosques del Nevado de Toluca y el rol de los actores locales. Ciencia Ergo-Sum 23 (3): 247–257.

Franco-Maass S, Regil-García HH, Ordoñez-Díaz JAB. 2006. Dinámica de perturbación-recuperación de las zonas forestales en el Parque Nacional Nevado de Toluca. Madera y Bosques 12 (1): 17–28. https://doi.org/10.21829/myb.2006.1211247

Franco-Ramos O, Vázquez-Selem L. 2017. Trabajo de campo dendrocronológico para estudios de geografía física. Experiencias en los volcanes Popocatépetl e Iztaccíhuatl, 2006–2017. Investigaciones Geográficas 94: 1–13. https://doi.org/10.14350/rig.59574

Gómez-Mendoza L, Arriaga L. 2007. Modeling the effect of climate change on the distribution of oak and pine species of Mexico. Conservation Biology 21 (6): 1545–1555. https://doi.org/10.1111/j.1523-1739.2007.00814.x

Gray SB, Brady SM. 2016. Plant developmental responses to climate change. Developmental Biology 419 (1): 64–77. https://doi.org/10.1016/j.ydbio.2016.07.023

Gutiérrez E, Trejo I. 2014. Effect of climatic change on the potential distribution of five species of temperate forest trees in Mexico. Revista Mexicana de Biodiversidad 85 (1): 179–188. https://doi.org/10.7550/rmb.37737

Hawksworth THFG, Wiens D. 1996. Dwarf mistletoes: Biology, pathology and systematics. U.S. Department of Agriculture, Forest Service: Washington, DC, USA. 410 p.

Holtmeier FK, Broll G. 2005. Sensitivity and response of northern hemisphere altitudinal and polar treelines to environmental change at landscape and local scales. Global Ecology and Biogeography 14 (5): 395–410. https://doi.org/10.1111/j.1466-822X.2005.00168.x

Iglesias-Andeu LG, Tivo-Fernández Y. 2006. Caracterización morfométrica de la población de *Pinus hartwegii* Lindl. del Cofre de Perote, Veracruz, México. Ra Ximhai 2: 449–468. https://doi.org/10.35197/rx.02.02.2006.08.li

Körner C, Paulsen J. 2004. A world-wide study of high altitude treeline temperatures. Journal of Biogeography 31 (5): 713–732. https://doi.org/10.1111/j.1365-2699.2003.01043.x

Körner C. 1995. Alpine plant diversity: A global survey and functional interpretations. *In* Chapin FS, Körner C. (eds.), Arctic and Alpine Biodiversity: Patterns, Causes and Ecosystem Consequences. Springer: Berlin, Germany, pp: 45–62. https://doi.org/10.1007/978-3-642-78966-3

Malek Ž, Verburg PH. 2021. Representing responses to climate change in spatial land system models. Land Degradation and Development 32 (17): 4954–4973. https://doi.org/10.1002/ldr.4083

Manzanilla-Quiñones U, Aguirre-Calderón OA, Jiménez-Pérez J, Treviño-Garza EJ, Yerena-Yamallel JI. 2019. Distribución actual y futura del bosque subalpino de *Pinus hartwegii* Lindl. en el Eje Neovolcánico Transversal. Madera y Bosques 25 (2): e2521804. https://doi.org/10.21829/myb.2019.2521804

Martínez-Luna JE, Carrillo-Anzures F, Acosta-Mireles M, Romero-Sánchez ME, Pérez-Miranda R. 2020. Ecuaciones alométricas para estimar carbono en brinzales de *Pinus hartwegii* Lindl. Revista Mexicana de Ciencias Forestales 11 (60): 1–16. https://doi.org/10.29298/rmcf.v11i60.726

Mathiasen RL, Nickrent DL, Shaw DC, Watson DM. 2008. Mistletoes. Pathology, systematics, ecology and management. Plant Disease 92 (7): 988–1006. https://doi.org/10.1094/pdis-92-7-0988

Pérez-Suárez M, Ramírez-Albores JE, Vargas-Hernández JJ, Alfaro-Ramírez FU. 2022. A review of the knowledge of Hartweg's pine (*Pinus hartwegii* Lindl.): Current situation and the need for improved future projections. Trees 36 (1): 25–37. https://doi.org/10.1007/s00468-021-02221-9

Petrov D, Ocokoljić M, Galečić N, Skočajić D, Simović I. 2024. Adaptability of *Prunus cerasifera* Ehrh. to climate changes in multifunctional landscape. Atmosphere 15 (3): 335. https://doi.org/10.3390/atmos15030335

Queijeiro-Bolaños ME, Cano-Santana Z, Castellanos-Vargas I. 2011. Distribución diferencial de dos especies de muérdago enano sobre *Pinus hartwegii* en el área natural protegida "Zoquiapan y Anexas", Estado de México. Acta Botánica Mexicana 96: 49–57. https://doi.org/10.21829/abm96.2011.258

Queijeiro-Bolaños ME, Cano-Santana Z. 2016. Growth of Hartweg's pine (*Pinus hartwegii*) parasitized by two dwarf mistletoe species (*Arceuthobium* spp.). Botanical Sciences 94 (1): 51–62. https://doi.org/10.17129/botsci.218

Richardson AD, Friedland AJ. 2009. A review of the theories to explain arctic and alpine treelines around the world. Journal of Sustainable Forestry 28 (1–2): 218–242. https://doi.org/10.1080/10549810802626456

Thakur S, Negi VS, Dhyani R, Satish KV, Bhatt ID. 2021. Vulnerability assessment of mountain forest ecosystems: A global synthesis. Trees, Forest and People 6: 100156. https://doi.org/10.1016/j.tfp.2021.100156

van Eck NJ, Waltman L. 2010. Software survey: VOSviewer, a computer program for bibliometric mapping. Scientometrics 84 (2): 523–538. https://doi.org/10.1007/s11192-009-0146-3

van Eck NJ, Waltman L. 2017. Citation based clustering of publications using CitNetExplorer and VOSviewer. Scientometrics 111 (2): 1053–1070. https://doi.org/10.1007/s11192-017-2300-7

Varo-Rodríguez R, Ávila-Akerberg V, Gheno-Heredia J. 2019. Uso tradicional de la fitodiversidad de los bosques de *Pinus hartwegii* en dos comunidades mexicanas de alta montaña. Caldasia 41 (2): 327–342. https://doi.org/10.15446/caldasia.v41n2.69477

Viveros-Viveros H, Sáenz-Romero C, Vargas-Hernández JJ, López-Upton J, Ramírez-Valverde G, Santacruz-Varela A. 2009. Altitudinal genetic variation in *Pinus hartwegii* Lindl.: Height growth, shoot phenology and cold damage in seedlings. Forest Ecology and Management 257 (3): 836–842. https://doi.org/10.1016/j.foreco.2008.10.021

Wang Z, Wang T, Zhang X, Wang J, Yang Y, Sun Y, Guo X, Wu Q, Nepovimova E, Watson AE, Kuca K. 2024. Biodiversity conservation in the context of climate change: Facing challenges and management strategies. Science of the Total Environment 937: 173377. https://doi.org/10.1016/j.scitotenv.2024.173377

Agrociencia

PRODUCT PRICE FORECAST FOR BANANA GROWERS IN THE STATE OF COLIMA, MEXICO

Mario Salvador **Gonzalez-Rodriguez**[1], José de Jesús **Brambila-Paz**[1*], Jaime Arturo **Matus-Gardea**[1], María Magdalena **Rojas-Rojas**[2], Verónica **Perez-Cerecedo**[1], Silvia Xóchilt **Almeraya-Quintero**[1]

[1]Colegio de Postgraduados Campus Montecillo. Posgrado en Economía. Carretera México-Texcoco km 36.5, Montecillo, Texcoco, State of Mexico, Mexico. C. P. 56264.
[2]Universidad Autónoma Chapingo. Posgrado en Ciencia y Tecnología Agroalimentaria, Departamento de Ingeniería Agroindustrial. Carretera México-Texcoco km 38.5, Chapingo, Texcoco, State of Mexico, Mexico. C. P. 56230.
* Author for correspondence: jbrambilaa@colpos.mx

Citation: Gonzalez-Rodriguez MS, Brambila-Paz JJ, Matus-Gardea JA, Rojas-Rojas MM, Perez-Cerecedo V, Almeraya-Quintero SX. 2025. Product price forecast for banana growers in the state of Colima, Mexico. **Agrociencia** 59(5): 715-727. https://doi.org/ 10.47163/agrociencia.v59i5.3152

Editor in Chief:
Dr. Fernando C. Gómez Merino

Received: December 23, 2024.
Approved: July 21, 2025.
Published in Agrociencia: August 08, 2025.

ABSTRACT

Banana (*Musa* spp.) is the fourth most important food in the world, after corn, beans, and rice. It contributes to food security in several countries, and in Mexico, it is the most cultivated tropical fruit. The goal of this work was to project real banana prices for the next 10 years using a non-homogeneous linear second-order difference equation of moving equilibrium, which would serve as a basis for the design of marketing strategies by banana organizations in the state of Colima, Mexico. An autoregressive econometric model was built with real monthly banana prices for the period from January 2014 to February 2020. It was identified that the behavior of the banana market in the state of Colima corresponds to a complex structure, with a cyclical behavior and a duration of nine months. This market tends to converge; therefore, it will reach equilibrium and continue to grow.

Key words: value chain, marketing, dynamic models, *Musa* AAA.

INTRODUCTION

The banana (*Musa* AAA subgroup Cavendish) is native to Southeast Asia, whose cultivation is widely extended in the world. In 2021, bananas were the most produced fruit worldwide, with a total of 125 million Mg (FAO, 2021). The leading banana-producing countries were India (24.1 %), China (23.8 %), and Indonesia (6.4 %) (FAO, 2021). In Mexico, the main cultivated varieties include Dominico, Valery, Pera, Tabasco, Morado, Manzano, Cavendish Gigante or Grand Naine (giant dwarf), and Macho. Due to its availability in the domestic market, bananas are among the most demanded fruits in the country, with a per capita consumption of 14.2 kg (SIAP, 2023). Around 30 % of national production was exported to 43 world markets, with an estimated value of USD 272 million (SIAP, 2023). Mexico's main banana export destinations included the USA, Japan, the United Kingdom, South Korea, Russia, Italy, and New Zealand (SADER, 2020).

In 2022, Mexico ranked 19th in global banana production with a volume of 2 593 025 Mg. Cultivation took place in 16 states (SADER, 2021), with Chiapas (664 156 Mg), Tabasco (622 175 Mg), Veracruz (335 238 Mg), Colima (324 133 Mg), Jalisco (202 743 Mg), and Michoacán (179 220 Mg) producing the most. The Central-West region contributed 27 % of the national volume. Colima stood out as the fourth largest producer, accounting for 12.5 % of total production. The total value of national banana production was MXN 10 547 million, of which Colima contributed 18.9 %, surpassing Chiapas (15.1 %) and ranking just below Tabasco (21.3 %). Together, these three states contributed 55.3 % of the national production value (SIAP, 2024). At the state level, Colima has a harvested area of 9555.5 ha. The primary producing municipalities are Tecomán (66 %), Manzanillo (29 %), and Armería (4 %) (SIAP, 2024). The banana agri-food chain is the third most important among the priority agricultural chains of the state (SADER, 2019).

The growth rate of the banana plant and the development of its fruit are influenced by ambient temperature, which directly affects physiological processes. Temperature determines the duration of the growth cycle and the weight of the bunch by influencing the leaf emission rate, root development, floral differentiation, and bunch formation (Robinson and Galán-Saúco, 2012). Ramírez *et al*. (2011) pointed out that the environmental conditions directly impact banana productivity, the length of the production cycle, and fruit quality, factors that are crucial for producers in terms of profits, food security, and market supply.

Banana cultivation is characterized by seasonality, with production dependent on ambient temperature. Ramírez *et al*. (2011) noted that higher temperatures increase production, leading to imbalances such as shortages or surpluses at different times of the year. This seasonality also affects Colima, causing fluctuations in field prices. A typical pattern emerges, with higher production volumes that correlate with lower prices, directly impacting producers' incomes. These conditions enable individual banana traders (coyotes) to speculate on both the field price and the market price offered to buyers across national supply chains. Consequently, producer income is negatively affected, and investment in technological improvements is reduced, diminishing the quality of the fruit marketed. According to the State Council of Banana Producers of Colima A.C., producer prices have increased in recent years but remain highly volatile.

The central hypothesis of this research is that the price paid to banana producers will continue to rise over the next 10 years and that it will be influenced by temperature-driven changes in production. Specifically, prices will tend to be lower in warmer months when production increases and higher in cooler months when production decreases. Therefore, the objective of this study is to project real banana prices for the next 10 years using a non-homogeneous linear second-order difference equation of moving equilibrium. This projection aims to provide a basis for designing effective marketing strategies for banana organizations in the state of Colima.

MATERIALS AND METHODS

The research study is quantitative, prospective, and longitudinal. A database with monthly product prices paid to the producer in the field during the period from January 2015 to February 2020 was provided by the State Council of Banana Producers of Colima A.C. based on field surveys by González-Rodríguez (2025). Nominal prices were deflated with the National Consumer Price Index (INPC) (based on February 2020) (INEGI, 2022) to place them in real terms according to Brambila-Paz (2011).

Actual prices

The actual prices were calculated according to the following expression (Equation 1):

$$p_r = \frac{Pn}{INPCb} \times 100 \quad (1)$$

where *Pr* is the actual price (in MXN); *Pn* is the nominal price (in MXN); and *INPCb* is the National Consumer Price Index, based on February 2020 (= 100).

The Dickey Fuller (DF) test was used on the data to test the statistical presence of stochastic trend behavior in the time series of the variables using a hypothesis test (Lizarazu-Alanez and Villaseñor-Alva, 2007), which met with an asymptotic *p* value of 0.000697, which is less than the significance value of the model ($p = 0.05$).

Econometric model

For this study, an econometric model was formulated using real monthly banana prices (*Pt*). As exploratory variables, two-time lags of the price variable (p_{t-1}, p_{t-2}), a dummy variable, and a discrete time variable were introduced. The dummy variable was considered since the production cycle is affected by climate throughout the year. At higher temperatures, plants and fruit ripen and grow faster, resulting in an oversupply of the product (Ramírez *et al.*, 2011). As a result, producer prices decrease. For this purpose, the value D = 1 was assigned to the cold months (January, February, March, October, November, and December) and D = 0 to the warm months (April, May, June, July, August, and September). a_1 y a_2 are the coefficients of the model, as shown in the following expression (Equation 2).

$$P_t = \beta + a_1 P_{t-1} + a_2 P_{t-2} + \beta_1 D + t \quad (2)$$

A trend variable (*t*) was added to the model, which was considered a discrete time variable, since the value of the variable y_i changes only when *t* goes from one integer value to the next, such as $t = 1$ to $t = 2$. The values of *t* are known as "periods," where $t = 1$ denotes period 1 and $t = 2$ denotes period 2, then y_i is considered to have a unique value for each period (Chiang and Wainwright, 2006).

The model was estimated using the ordinary least squares methodology to obtain the intercept and the coefficients (Equation 3).

$$y_i = \beta_0 + \beta_1 x_1 + \beta_2 x_2 \ldots + \beta_k x_k + \varepsilon_i \quad (3)$$

where y_i is the explained variable, x_k is the explanatory variable, β_k is the parameter that quantifies the relationship between the explained variable and each explanatory variable, and ε_i is the error (Gujarati and Porter, 2010).

The model is based on a second-order difference equation, which was analyzed dynamically using the difference equation techniques described by Chiang and Wainwright (2006). This model was used to determine the projection of future banana prices for the next 10 years (scenario 1). A second scenario was also estimated, where the minimum price acceptable to producers was taken as the banana production cost (MXN 3.19 kg^{-1}), corresponding to November 2022 (González-Rodríguez *et al*., 2025); this value was added as a restriction to the model. The Gretel software was used to calculate the model.

Dynamic analysis

The starting point was a second-order difference equation (Equation 4), expressed by the general model (Equation 1).

$$y_{t+2} + a_1 y_{t+1} + a_2 y_t = c \quad (4)$$

The variable p_t was renamed by y_t. The y_t variables were cleared and pre-multiplied by y_2 which is the order of the equation, and c is a constant variable. It was assumed that the market tends to reach balance eventually; therefore, $y^* = y_{t+1} = y_{t+2} = y_t$. The y^* variable was factored and cleared to obtain the particular solution from the general model (Equation 5), then it was equaled to zero to start with the calculation of the complementary equation (Equation 6).

$$y^* = \beta + \beta_1 D + \beta_2 t \quad (5)$$

$$y_{t+2} + a y_{t+1} + a_2 y_t = 0 \quad (6)$$

$Y_t = A(b)^t$ was renamed by $Y_{t+n} = A(b)^{t+n}$, therefore, for $Y_{t+n} = A(b)^{t+n}$, A is the initial condition of the banana price when $t = 0$; the common factor Ab^t (different from 0) was cancelled to obtain the following expression:

$$b^2 + a_1 b + a = 0 \quad (7)$$

The quadratic function (Equation 7) has two characteristic roots (b). The value of b was determined using the general formula, where the complex roots correspond to the next expressions:

$$b_1 = h \pm v_i \tag{8}$$

$$b_2 = h \pm v_i \tag{9}$$

The cyclic behavior of the function is presented by a complex number. When plotted in an Argand diagram (Brambila-Paz, 2011) (Figure 1), the real values (h) are located on the horizontal axis and the imaginary values (v_i) on the vertical axis, and M is the modulus or absolute value of the complex number $h + v_i$.

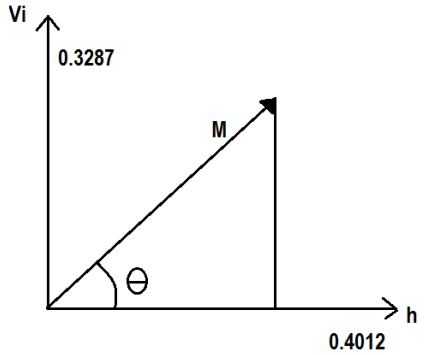

Figure 1. Argand diagram

To determine the modulus of Equations 8 and 9 and define market behavior, the Pythagorean theorem was used (Equation 10), which indicates a market is cyclical but convergent when $M < 1$, cyclical but convergent when $M > 1$, and cyclical but convergent when $M = 1$.

$$M = \sqrt{h^2 + vi^2} \tag{10}$$

To calculate the angle θ, the following (Equations 11 and 12) were used to estimate the cycle length, which is equivalent to 360° / θ.

$$cos\ \theta = \frac{h}{M};\ \theta = cos^{-1}\left(\frac{h}{M}\right) \tag{11}$$

$$sen\ \theta = \frac{h}{M};\ \theta = sin^{-1}\left(\frac{h}{M}\right) \tag{12}$$

where M is the modulus, and h is the real part of the complex number.

Using Moivre's theorem (Chiang and Wainwright, 2006), the complementary solution was obtained (Equation 13).

$$Y_t = r^t[A1\ cos(\theta_t) + A2\ sen(\theta_t)] \quad (13)$$

where Y_t is the projected price, r^t equals module M, $A1$ is the first long-run multiplier, θ_t is the angle, and $A2$ is the second long-run multiplier.

The total solution (Equation 14) was obtained from the sum of the particular solution (Equation 5) and the complementary solution (Equation 13). This expression made it possible to project prices for the next 10 years.

$$Y_t = M^t[A1\ cos(\theta_t) + A2\ sen(\theta_t)] + \beta + \beta_1 D + \beta_2 t \quad (14)$$

where Yt is the projected future price; M^t is the modulus of the equation that defines the behavior of the banana market; $A1$ is the first long-term multiplier; $\cos(\theta^t)$ is the cosine of angle θ; $A2$ is the second long-term multiplier; $\sin(\theta^t)$ is the sine of the angle θ; β is the intercept of the econometric model; β_1 is the intercept that relates the dummy variable to the model; D is the dummy variable that relates the influence of temperature on price at different times of the year; β_2 is the intercept that relates the time variable to the model; and t is the discrete time trend variable.

RESULTS AND DISCUSSION

The second order difference equation (Equation 15) was formulated to understand the structure and behavior of the banana market. The statistic results of the variables used in this dynamic model (Table 1) were used to determine the trajectory and projection of future banana prices for the next 10 years.

$$P_t = 1.1373 + 0.8025P_{t-1} - 0.2691P_{t-2} + 0.4888D + 0.0150t \quad (15)$$

Table 1. Statistical results of the econometric model (Equation 15) for real banana prices projection from January 2015 to February 2020.

Variable	Coefficient	Standard deviation	*t* statistic	*p* value	
Intercept	1.1373	0.6219	1.829	0.0729	*
$P_{(t-1)}$	0.8025	0.1321	6.077	<0.0001	***
$P_{(t-2)}$	-0.2691	0.1378	-1.954	0.0558	*
D	0.4888	0.4445	1.100	0.2762	
t	0.0150	0.01223	1.229	0.2243	

D: dummy variable; *t*: time variable; $P_{(t-1)}$: lagged price variable on the first period; $P_{(t-2)}$: the lagged price variable on the second periods; *not statistically significant, **** statistically significant.

Market structure

From the mathematical transformations described in methodology and applied to Equation 15, Equation 16 was obtained, which has two characteristic roots. The value of b was determined using the general formula, where the complex roots correspond to the values b_1 and b_2.

$$b^2 - 0.8025b + 0.2691 = 0 \tag{16}$$

where:

$$b_1 = 0.4012 + 0.3287i$$

$$b_2 = 0.4012 - 0.3287i$$

The module value (Equation 10) is $M = 0.5186$; therefore, since the model has a negative root, the market has a complex structure. As $M < 1$, the market behaves cyclically and tends to converge, allowing long-term projections (Brambila-Paz, 2011).

The following expressions were used to calculate the angle θ (Equations 17 and 18). The cycle length equals 360° / θ.

$$cos\ \theta = \frac{h}{M}; \theta = cos^{-1}\frac{0.4012}{0.5186};\ \theta = 39.3217 \tag{17}$$

$$sen\ \theta = \frac{h}{M}; \theta = sin^{-1}\frac{0.3287}{0.5186};\ \theta = 39.3310 \tag{18}$$

360° / 39.321 = 9.153 months; the prices used in the model were presented on a monthly basis, which means that the cycle of price increases and decreases was estimated in nine months.

The most important variables involved in banana price consolidation are related to supply and demand, which in turn are defined by external and internal factors, such as weather conditions and resource allocation in the case of supply. In terms of demand, the most important factors affecting the price of fruit are the tastes and preferences of consumers, who are looking for a better-quality product and are willing to pay a higher price. For this reason, the quality of the fruit is very important for the international market.

In regions where seasonal transitions are well defined, the trend in banana consumption is generally of a seasonal nature, with drops in consumption occurring during the summer and at the end of the year, which coincides the prices observed in the field by González-Rodríguez (2025). This coincides with an increase in the supply and demand of seasonal fruits, since temperature attracts consumers to other products,

coupled with the low school activity due to holiday periods. On the other hand, banana consumption peaks in autumn and early spring (April, May, and October), thanks to favorable temperatures for the production and consumption of this fruit (Martínez-Solórzano and Rey-Brina, 2021).

The increase or decrease in the price depends on the amount of fruit harvested, although this often does not correspond to actual production. In addition, there is the variability in market prices of products used as inputs for production, transportation, and even exchange rate fluctuations (Erazo-Berrú *et al*., 2021).

Price projections

The price projection for the first scenario was calculated using Equation 14, and the multipliers *A1* and *A2* of the equation were estimated when $D = 1$ and $D = 0$. $Y_0 = 5.2$ (first real price of the data series) and $Y_1 = 4.61$ (second real price of the data series) were considered (Table 2 y 3). Also, a non-negativity restriction was established for the model so that in case of a negative value in the price estimation, the previous

Table 2. Calculation of multipliers A1 and A2, when D = 1.

$$Y_t = 0.5186^t[A1\ cos(39.3217t) + A2\ sen(39.3310t)] + 2.4374 + 1.0475D + 0.0321t$$

Variable	Value	Variable	Value
Y_0	5.20	Y_1	4.61
t	0	t	1
D	1	D	1
$A1$	1.7151	$A2$	1.2321

D: dummy variable; t: time variable; Y_0: first real price of the data series; A1: first long-term multiplier; Y_1: second real price of the data series; A1: second long-term multiplier. D = 1 when estimating prices during the cold months (January, February, March, October, November, and December).

Table 3. Calculation of multipliers A1 and A2, when $D = 0$.

$$Y_t = 0.5186^t[A1\ cos(39.3217t) + A2\ sen(39.3310t)] + 2.4374 + 1.0475D + 0.0321t$$

Variable	Value	Variable	Value
Y_0	5.20	Y_1	4.61
t	0	t	1
D	0	D	0
$A1$	2.7626	$A2$	3.1412

D: dummy variable; t: time variable; Y_0: first real price of the data series; A1: first long-term multiplier; Y_1: second real price of the data series; A1: second long-term multiplier. D = 0 when estimating prices during the warm months (April, May, June, July, August, and September).

positive value is taken. This restriction is based on the commercial strategy taken by the producers in the area, who stop the banana harvest when the price is very low, with the purpose of pressuring the marketers. This allows the producer to obtain a better sale price.

The total solution expression (Equation 14) was used to estimate real monthly banana prices for the next 10 years (Table 4).

Table 4. Real banana prices for the years 2021–2030 (MXN kg^{-1}).

Month	2021	2022	2023	2024	2025	2026	2027	2028	2029	2030
January	5.62	2.99	2.86	6.65	5.01	3.49	7.33	7.05	4.47	7.74
February	5.10	2.02	4.20	6.71	3.71	4.49	7.97	5.65	4.96	8.86
March	3.87	1.92	5.60	5.86	3.03	5.94	7.66	4.52	6.20	9.15
April	1.23	1.92	7.05	4.13	3.03	7.10	6.97	1.09	6.67	9.45
May	1.23	2.25	7.47	1.42	1.77	8.63	4.21	1.70	9.06	7.14
June	1.23	5.06	6.03	1.42	4.54	8.31	1.77	3.94	9.92	4.34
July	1.23	6.95	3.40	1.42	7.14	6.28	1.77	6.81	8.88	2.34
August	2.40	7.07	3.40	1.86	8.41	3.49	1.66	9.02	6.41	2.05
September	5.14	5.38	3.40	4.69	7.79	1.21	4.08	9.59	3.66	3.63
October	5.92	3.49	2.99	6.85	5.53	3.70	7.45	7.54	4.78	7.81
November	5.53	2.41	4.27	7.06	4.18	4.59	8.23	6.16	5.12	9.03
December	4.37	2.16	5.70	6.33	3.37	6.01	8.07	4.95	6.27	9.46
Annual Average	3.57	3.64	4.70	4.53	4.79	5.27	5.60	5.67	6.37	6.75

For the analysis and price projection for the period from January 2021 to December 2030, the dummy variable (D = 1 cold months and D = 0 hot months) explains the projected prices. This is due to the fact that the average prices for the cold months were higher than the hot months, which coincides with the amount of fruit harvested during these two periods of the year. The hot months are the peak season for fruit production (more supply). Therefore, the selling price is lower, while during the cold months, the supply of fruit decreases and the price increases.

The projected average annual price was estimated to increase by 68.32 % over the entire period (January 2021 to December 2030). Regardless of the fact that the banana market behaves in cycles of highs and lows (Figure 2), prices showed an upward trend for the following years.

For the second scenario, the production cost was taken as a reference, which was calculated for November 2022 and is equivalent to MXN 3.19 kg^{-1}. This value was added as a constraint to the model. It was assumed that producers would implement a commercial strategy that would allow them to obtain a minimum price at the time of sale equivalent to this production cost (Figure 3).

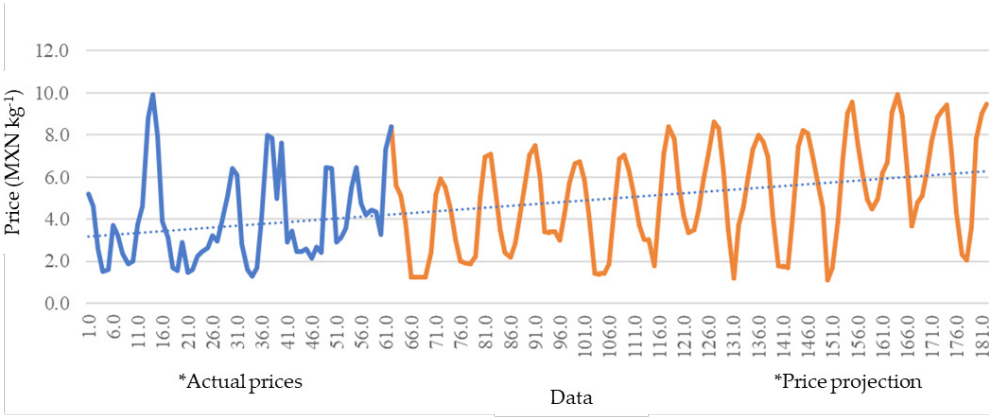

Data 1 to 62 = observed price.
Data 61 to 181 = projected price within the analyzed period.

Figure 2. Projected real banana prices, 2021–2030 (MXN kg^{-1}).

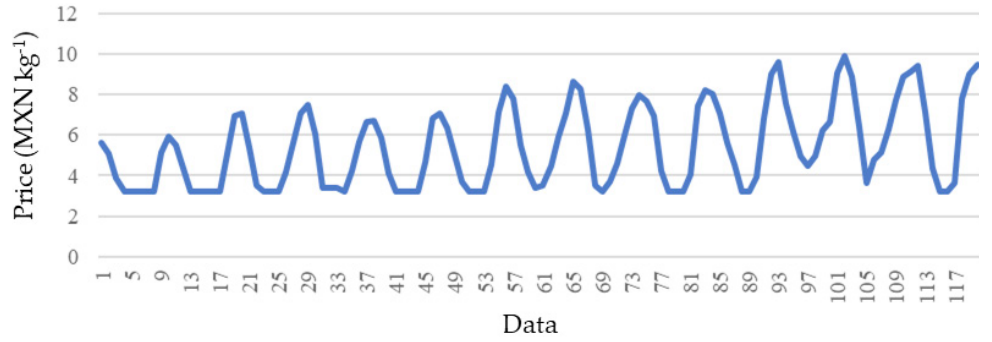

Data 1 to 62 = observed price.
Data 61 to 181 = projected price within the analyzed period.

Figure 3. Projection of real banana prices for 2021–2030, with the assumption of receiving the cost of production (MXN kg^{-1}).

In Ecuador, an analysis of banana price variation was conducted for the period 2015-2020. Erazo-Berrú *et al*. (2021) conclude that the variation of the price has mostly been increasing. However, between 2017 and 2018, there was a decrease of six cents in its price, corresponding to -0.96 %. In 2020, the highest price was USD 6.4 per box, despite the fact that it was a year with high risks in the world economy due to the COVID-19 pandemic, which paralyzed many industries.

In addition to the limitations derived from the pandemic, factors such as increases in the price of production inputs (fertilizers and packaging materials) and transportation costs, shortages of refrigerated containers, low production due to adverse weather conditions and plant diseases, strict limitations on maximum residue levels in some important markets, and slightly lower demand in import markets affected world trade in bananas (FAO, 2022). All of the above hinder prices and profit margins along the value chain, as well as the ability of producers and exporters to supply bananas in adequate quantities and meet the quality requirements of export markets. In most of the main import markets, banana prices have shown an upward trend. The European Commission (2022) notes that prices for this fruit produced in the European Union grew by 33 % over the 2018–2021 period. Meanwhile, import prices from African, Caribbean, and Pacific countries increased by 13.6 % from 2012 to 2021.

So far, no studies provide a previous reference of the use of this dynamic economic analysis tool in price projection for banana cultivation as in the present article. However, Mendoza-Rodríguez *et al*. (2016) implemented this methodology of using superior difference equations to analyze the egg market in Mexico and estimate the amount of egg per capita to be consumed for 2013–2020. The egg market did not behave cyclically like the banana market; however, both markets tend to converge.

Brambila-Paz *et al*. (2015) also used this methodology to measure the technological effort required and increase the yields of different agricultural products such as corn, lemon, wheat, avocado, potato, egg, and milk, to cover the demand of the Mexican population and its projected trend for the year 2025.

CONCLUSIONS

Real banana price projections showed an upward trend, with a cumulative growth rate of 89 % over the period from January 2021 to December 2030. This validates the hypothesis that the product price paid to the producer will continue to rise over the next 10 years, influenced by the effect of ambient temperature on plant production. The structure of the banana market is complex, cyclical, and convergent. The cycle period has a duration of 9 months. This implies that the market will reach equilibrium and is expected to continue growing.

ACKNOWLEDGMENTS

To the State Council of Banana Producers of Colima A.C. for the data provided and to Eng. Marco Antonio Sinécio Moreno, general manager of AgoColima Saludable S.C.C. who assisted in the management of the price database to develop the model.

REFERENCES

Brambila-Paz JJ, Martínez-Damián MÁ, Rojas-Rojas MM, Pérez-Cerecedo V. 2015. Medición del esfuerzo tecnológico necesario para aumentar el rendimiento de productos agropecuarios en México. Revista Mexicana de Ciencias Agrícolas 6 (4): 841–854.

Brambila-Paz JJ. 2011. Bioeconomía: instrumentos para su análisis económico. Secretaría de Agricultura, Ganadería, Desarrollo Rural, Pesca y Alimentación: Ciudad de México, México. 312 p.

Chiang AC, Wainwright K. 2006. Métodos fundamentales de economía matemática (Cuarta edición). McGraw-Hill: Ciudad de México, México. 688 p.

Erazo-Berrú MA, Prado-Carpio E, Cervantes-Álava A, Vite-Cevallos H. 2021. Análisis de regulación del precio de la caja de banano en Ecuador periodo 2015-2020. Revista Metropolitana de Ciencias Aplicadas 4 (S1): 210–217. https://doi.org/10.62452/brtj3939

European Commission. 2022. COM(2022) 427 final. Report from the Commission to the European Parliament and the council on the situation of the Union market for bananas and the state of Union banana producers after the expiry of the stabilization mechanism for bananas including a preliminary assessment of the functioning of the 'Programme d'Options Spécifiques à l'Éloignement et l'Insularité' (POSEI) in preserving the banana production in the Union. Brussels, Belgium. https://data.consilium.europa.eu/doc/document/ST-11960-2022-INIT/en/pdf (Retrieved: April 2022).

FAO (Food and Agriculture Organization). 2021. Agricultural production statistics 2000–2021. FAOSTAT Analytical Brief 60. Rome, Italy. https://openknowledge.fao.org/server/api/core/bitstreams/58971ed8-c831-4ee6-ab0a-e47ea66a7e6a/content (Retrieved: April 2022).

FAO (Food and Agriculture Organization). 2021. FAOSTAT. FAO Database on food and agriculture. United Nations Food and Agriculture Organization. Rome, Italy. https://www.fao.org/statistics/en/ (Retrieved: April 2022).

FAO (Food and Agriculture Organization). 2022. Banana market review, preliminary results 2021. Rome, Italy. https://openknowledge.fao.org/handle/20.500.14283/cb9411en (Retrieved: April 2022).

González-Rodríguez MS, Brambila-Paz JJ, Matus-Gardea JA, Rojas-Rojas MM, Pérez-Cerecedo V, Almeraya-Quintero SX. 2025. Caracterización del proceso productivo, postcosecha y comercial de la cadena de valor del plátano en Cerro de Ortega. Agricultura, Sociedad y Desarrollo 22 (2). https://doi.org/10.22231/asyd.v22i2.1676

Gujarati DN, Porter DC. 2010. Econometría (Quinta edición). McGraw-Hill: Ciudad de México, México. 921 p.

INEGI (Instituto Nacional de Estadística y Geografía). 2022. Sistema de consulta. Índice nacional de precios al consumidor. Ciudad de México, México. https://www.inegi.org.mx/temas/inpc/ (Retrieved: May 2022).

Lizarazu-Alanez E, Villaseñor-Alva JA. 2007. Efectos del rompimiento bajo la hipótesis nula de la prueba de Dickey-Fuller para la raíz unitaria. Agrociencia 41 (2): 193–196.

Martínez-Solórzano GE, Rey-Brina JC. 2021. Bananos (Musa AAA): Importancia, producción y comercio en tiempos de Covid-19. Agronomía Mesoamericana 32 (3): 1034–1046. https://doi.org/10.15517/am.v32i3.43610

Mendoza-Rodríguez YY, Brambila-Paz JJ, Arana-Coronado JJ, Sangerman-Jarquín DM, Molina-Gómez JN. 2016. El mercado de huevo en México: tendencia hacia la diferenciación en su consumo. Revista Mexicana de Ciencias Agrícolas 7 (6): 1455–1466.

Ramírez J, Jarvis A, van den Bergh I, Staver C, Turner D. 2011. Changing climates: Effects on growing conditions for banana and plantain (*Musa* spp.) and possible responses. *In* Crop Adaptation to Climate Change. John Wiley and Sons: Hoboken, NJ, USA, pp: 426–438.

Robinson JC, Galán-Saúco V. 2012. Plátanos y bananas. Editorial Mundiprensa: Ciudad de México, México. 321 p.

SADER (Secretaría de Agricultura y Desarrollo Rural). 2019. Compendio de indicadores 2018 Colima. Programa de concurrencia con las entidades federativas. Secretaría de Agricultura y Desarrollo Rural. Gobierno de Colima. Colima, México. 123 p.

SADER (Secretaría de Agricultura y Desarrollo Rural). 2020. Blog de publicaciones. Plátano: la fruta tropical más cultivada en México. Gobierno de México. Secretaría de Agricultura y Desarrollo Rural. Ciudad de México, México. https://www.gob.mx/agricultura/articulos/hoy-dia-del-platano?idiom=es (Retrieved: May 2022).

SADER (Secretaría de Agricultura y Desarrollo Rural). 2021. Prensa/Noticias/Comunicado. Aumentó 2.9 por ciento producción de plátano mexicano en 2020. Gobierno de México. Secretaría de Agricultura y Desarrollo Rural. Ciudad de México, México. https://www.gob.mx/agricultura/prensa/aumento-2-9-por-ciento-produccion-de-platano-mexicano-en-2020?idiom=es (Retrieved: May 2022).

SIAP (Sistema de Información Agroalimentaria y Pesquera). 2023. Panorama agroalimentario 2023. Gobierno de México. Secretaría de Agricultura y Desarrollo Rural. Sistema de Información Agroalimentaria y Pesquera. Ciudad de México, México. https://www.gob.mx/siap/acciones-y-programas/panorama-agroalimentario-258035 (Retrieved: September 2023).

SIAP (Sistema de Información Agroalimentaria y Pesquera). 2024. Sistema de información agroalimentaria de consulta (SIACON). Gobierno de México. Secretaría de Agricultura y Desarrollo Rural. Sistema de Información Agroalimentaria y Pesquera. Ciudad de México, México. https://www.gob.mx/siap/documentos/siacon-ng-161430 (Retrieved: May 2022).

Agrociencia

SECTORIAL ANALYSIS OF WATER FEES AND USE IN TULANCINGO, HIDALGO, MEXICO

Fidel **Bautista-Mayorga**[1], José Alberto **García-Salazar**[1]*

[1]Colegio de Postgraduados Campus Montecillo. Programa de Socioecnomía Estadística e Informática-Economía. Carretera México-Texcoco km 36.5, Montecillo, Texcoco, State of Mexico, Mexico. C. P. 56264.
*Author for correspondence: jsalazar@colpos.mx

Citation: Bautista-Mayorga F, García-Salazar JA. 2025. Sectorial analysis of water fees and use in Tulancingo, Hidalgo, Mexico. **Agrociencia** 59(5): 728-740. https://doi.org/ 10.47163/agrociencia.v59i5.3213

Editor in Chief:
Dr. Fernando C. Gómez Merino

Received: November 28, 2024.
Approved: June 16, 2025.
Published in Agrociencia: June 19, 2025.

ABSTRACT

Water is an important element for the development of productive activities, though its scarcity will make it more difficult to supply the growing demand of different consumer sectors. The aim of this article was to analyze the water demand of the household, commercial, industrial, agricultural irrigation, and livestock sectors using economic instruments such as water and electricity fees in order to reduce water consumption and achieve rational resource use. A double-log multiple linear regression model was estimated to analyze water demand in the aforementioned sectors using annual data from the municipality of Tulancingo in Hidalgo, Mexico, from 2005 to 2023. The results indicate that, in order to reduce water use by 30 %, the water fee in the household, commercial, and industrial sectors should increase by 54.6, 11.1, and 12.8 %, respectively, whereas to achieve the same reduction in electricity use, the fee in the household, commercial, industrial, agricultural, and livestock sectors must increase by 93.5, 75.4, 35.1, 229, and 71.6 %, indicating that the commercial and industrial sectors are more sensitive to water fees and that the commercial, industrial, and livestock sectors are more sensitive to electricity fees. It is feasible to implement increases in water and electricity fees to reduce water use, particularly in the commercial and industrial sectors.

Keywords: Water scarcity, household sector, commercial and industrial sectors, farming sector, water fees, electricity fees.

INTRODUCTION

According to the National Water Commission and the National Statistics and Geography Institute, in 2020, Mexico had 461 640 hm^3 of renewable water, 126 million people, and a real gross domestic product (GDP) of 20.9 billion MXN (CONAGUA, 2021). The regions of the southeast had 23 % of the population, 68 % of the water, and provided 18 % of the country's GDP. The regions of the north, center, and northwest had 32 % of the country's renewable water, 77 % of the population, and provided 82 % of the GDP. The relevance of these data lies in the regional inequality of the water distribution, the concentration of the population, and the economic activity, which could aggravate the overuse of the country's water resources.

The Tulancingo municipality has a total surface of 290.4 km^2. It is located in the southeast of the state of Hidalgo (20° 05′ 09′′ N and 98° 21′48′′ W) and borders the municipalities of Metepec to the north, Acaxochitlán and Cuautepec to the east, Acatlán and Singuilucan to the west, and Santiago Tulantepec to the south. Its mean annual temperature is 14 °C, and total annual rainfall ranges from 500 to 553 mm. The municipality has two rivers, four bodies of water, one dam, and the Tulancingo Valley aquifer, which is a part of the Golfo Norte basin organism (PMD, 2016; CONAGUA, 2023a).

The Tulancingo municipality contains 8881 economic units, with retail trade, manufacturing industry, temporary accommodation, and food and beverage preparation services being predominant. The economic units employ 29 041 people. The industrial field, with a long-standing tradition that dates back to the early 20th century, stands out mostly in textiles, focused on the manufacturing of clothing, knit fabrics, and acrylic yarn production (PMD, 2016).

In the farming sector, 9272 ha are dedicated to agricultural activities, out of which 60.4 % (5599 ha) are irrigated and 39.6 % (3673 ha) are rainfed (SIAP, 2023). The predominant crops under irrigation are maize grain, grasses and prairies, alfalfa, green forage maize, and green forage oats, whereas the predominant crops under rainfed conditions are grain maize, green forage oat, and grain barley. Likewise, 7292 ha are used for livestock, with the main species being raised are dairy and beef bovines, sheep, pork, and poultry (PMD, 2016).

Water demand in the municipality has grown significantly. Between 2005 and 2023, the number of water connections increased from 5733 to 12 002; commercial connections rose from 1119 to 2620; and industrial connections grew from 146 to 606. These increases represent 109, 134, and 315 % compared to the year 2005 (PNT, 2024).

Droughts in the municipality started becoming constant in 2018 under abnormally dry conditions; in May of 2022, conditions became moderately dry; in October of that same year, they turned into a severe drought; in January and February of 2023, the conditions turned into extreme drought; from that date until February of 2024, it was characterized as a severe drought, and in March of 2024, it became an extreme drought once more (SMN, 2024).

Along with this problem, there is an overuse of the Tulancingo Valley aquifer, which is a water source for the municipalities of Santiago Tulantepec, Acatlán, Cuautepec, Metepec, Tulancingo, Huasca de Ocampo, Singuilucan, and others. This aquifer has an annual underground water deficit of 20.93 hm^3, indicating that there is more water being extracted than replenished through recharging (CONAGUA, 2023a). Water scarcity will make it harder to supply this resource to different consumer sectors, and as a result, it will increase over time.

Some authors have studied the water demand in the household sector (Gam and Rejeb, 2021), the commercial sector (Almendarez-Hernández *et al*., 2015), the industrial sector (Rendón-Contreras *et al*., 2021), and the farming sector (Castro-Ramírez *et al*., 2017). The results of these studies indicate that more efficient water use can be made with the

implementation of policies and that an increase in water and electric energy fees can reduce the demand for the resource in the consumer sectors.

Population growth and the economic activity of the Tulancingo Valley will increase the demand for water in the future, and the more severe drought, along with the overuse of the aquifer, will make it harder to satisfactorily supply water. Considering this problem, the aim of the investigation was to analyze the water demand for the household, commercial, industrial, irrigation agriculture, and livestock sectors with economic instruments, such as water and electricity fees, to help reduce water use and reach a rational use of the resource. The hypothesis indicates that the rises in water and electric energy fees reduce water use in these sectors.

MATERIALS AND METHODS

The series of household, commercial, and industrial use and fee data from 2005 to 2023 were provided by the director of the Water and Sewage Commission of the Municipality of Tulancingo (AWUMT) via the National Transparency Platform (PNT, 2024). The average water use in the irrigation agriculture sector (supplied with underground water from springs and wells) was obtained from the National Water Commission (CONAGUA, 2023b). The average water use in the livestock sector was estimated as follows: a) the number of heads of livestock population (bovines, pigs, goats, sheep, and poultry) was multiplied by the per capita use of each species (liters of water a day); b) the result was divided by 1000 to obtain the figure (in m^3); and c) the annual use was obtained by multiplying the daily use by 365 days.

The data on livestock population and the price of beef were taken from the Agri-food and Fisheries Information Service (SIAP, 2023) and the per capita use of each species was taken from the United Nations Food and Agriculture Organization (FAO, 2013). Regarding the water fees for agricultural and livestock use, there is no price as such. However, price of the electricity used to pump water for irrigated agriculture was used as a proxy variable for the water tariff in both sectors. The electricity fee for household, commercial, industrial, and agricultural use for the 2005–2016 period was obtained from the National Institute of Statistics and Geography (INEGI, 2024a), and for 2017–2023, from the Energy Regulation Commission (CRE, 2020).

To measure the income, proxy variables were used. In the household sector, the general minimum wage was used, as it is the income one person earns per day; in the industrial, agricultural, and livestock sectors, the GDP of the secondary activities, agriculture, and livestock breeding and production (including the value of cattle, pigs, goats, sheep, and poultry), respectively, were used. The general minimum wage came from the National Minimum Wage Commission (CONASAMI, 2023), and the GDP came from INEGI (2024b). Temperature and rainfall data were taken from the National Weather Service (SMN, 2024). The average prices of pesticides were retrieved from FAO (2024). The monetary variables were deflated using the National Consumer Price Index (INEGI, 2024b) on a 2018 basis.

Model structure and statistical validation

A double-log Cobb-Douglas model was used so that the parameters associated with the explanatory variables would indicate their respective elasticities (Gujarati and Porter, 2010). The Cobb-Douglas function is stochastically expressed as follows:

$$Y_t = \beta_1 X_{2t}^{\beta_2} X_{3t}^{\beta_3} e^{u_t} \quad (1)$$

The relationship between the dependent variable (Y_t) and the explanatory variables (X_{2t} and X_{3t}) is not linear; therefore, Equation 1 is transformed by applying the natural logarithm to each variable. This gives the multiple linear regression model (Equation 2):

$$lnY_t = ln\beta_1 + \beta_2 lnX_{2t} + \beta_3 lnX_{3t} + u_t \quad (2)$$

The formulation of the models proposed to estimate water demand was based on economic theory and empirical evidence. The determining factors of the demand for a good were the price of the good itself, the price of related goods (complements and substitutes), income, and others (Barkley and Barkley, 2013). Empirically, the work by Guzmán-Soria *et al*. (2013) was considered, which was composed of weather variables, electric energy fees as a complementary good to water in demand in different sectors, and other variables that improve agricultural and livestock productivity as determinants of water demand.

For the household sector, the model was as follows:

$$lnHWU_t = \beta_1 + \beta_2 lnHRWF_t + \beta_3 lnHREF_{t-2} + \beta_4 lnGMW_t + \beta_5 lnTE_t + u_t \quad (3)$$

where, for year *t*, *HWU* is the household average water use (in m^3); *HRWF* is the real average water fee for household use (in MXN m^{-3}); *HREF* is the average real electric energy fee for household use (in MXN kW^{-1} h^{-1}, with a 2-year delay); *GMW* is the general minimum wage (in MXN d^{-1}); *TE* is the temperature (in °C); and *u* is the random error.

For the commercial sector:

$$lnCWU_t = \beta_1 + \beta_2 lnCRWF_{t-3} + \beta_3 lnCREF_{t-3} + \beta_4 lnCWU1_{t-1} + u_t \quad (4)$$

where, for year *t*, *CWU* is the average commercial water use (in m^3); *CRWF* is the real average water fee for commercial use (in MXN m^{-3}, with a three-year delay); *CREF* is the real average electric energy fee for commercial use (in MXN kW^{-1} h^{-1}, with a three-year delay); *CWU1* is the delayed average commercial water use (in m^3, with a three-year delay); and *u* is the random error.

For the industrial sector:

$$lnIWU_t = \beta_1 + \beta_2 lnIRWF_{t-3} + \beta_3 lnIREF_{t-3} + \beta_4 lnGDPSA_t + \beta_5 lnTE3_t + u_t \quad (5)$$

where, for year *t*, *IWU* is the average industrial water use (in m^3); *IRWF* is the real average water fee for industrial use (in MXN m^{-3}, with a three-year delay); *IREF* is the real average electric energy fee for industrial use (in MXN kW^{-1} h^{-1}, with a three-year delay); *GDPSA* is the real GDP of secondary activities (in millions of MXN); *TE3* is the temperature (in °C); and *u* is the random error.

For the agricultural irrigation sector:

$$lnAWU_t = \beta_1 + \beta_2 lnAEF_{t-1} + \beta_3 lnGDPA_{t-3} + \beta_4 lnPRP_t + \beta_5 lnPP1_{t-1} + u_t \quad (6)$$

where, for year *t*, *AWU* is the average water use for agricultural use under irrigation (in thousands of m^3); *AEF* is the average fee for electric energy for agricultural use (in MXN kW^{-1} h^{-1}, with a one-year delay); *GDPA* is the real GDP of agriculture (in millions of MXN, with a three-year delay); *PRP* is the real average price for pesticides (in MXN Mg^{-1}); *PP1* is rainfall (in mm, with a one-year delay); and *u* is the random error.

For the livestock sector:

$$lnLWU_t = \beta_1 + \beta_2 lnLREF_t + \beta_3 lnGDPL_{t-3} + \beta_4 lnPBEEF_{t-2} + \beta_5 lnPP_t + u_t \quad (7)$$

where, for year *t*, *LWU* is the average water use for the livestock sector (in m^3); *LREF* is the real average electric energy fee for agricultural use (in MXN kW^{-1} h^{-1}, with a three-year delay); *GDPL* is the real GDP for the raising and exploitation of livestock (in millions of MXN, with a three-year delay); *PBEEF* is the price of beef (in MXN kg^{-1}, with a two-year delay); *PP* is rainfall (in mm), and *u* is the random error.

The parameters were estimated by Ordinary Least Squares (OLS) with robust standard deviations, using the R software (R Core Team, 2023). The results were economically and statistically validated, considering the following criteria: a) the estimated parameters were proven to display the expected sign according to the economic theory, and b) statistical tests were carried out, such as Student's *t* and Fisher's test (F), to determine the global significance of the parameters, the Shapiro-Wilk (SW) test for the normality of the residues, the Breusch-Pagan (BP) test for the absence of heteroscedasticity, and the Durbin-Watson (DW) and Breusch-Gofrey (BG) statistics for the absence of first-order and serial autocorrelation, respectively.

The models were validated by comparing the estimated values of the dependent variable with the value observed in reality. A difference of less than 10 % was considered useful to create predictive scenarios in which the water demand of different consumer

sectors decreases by 10, 20, and 30 %. Similarly, the degree to which water and electric energy fees must rise in order to achieve such reductions in water use was determined.

RESULTS AND DISCUSSION

From the point of view of the economic theory, the relationship that must exist between the dependent and independent variables of the method was fulfilled. The coefficients of determination (R^2) vary from 0.71 to 0.94, indicating an acceptable goodness-of-fit between the observed values and those predicted by the model. Similarly, the Student *t* statistic was greater than the unit in absolute terms, indicating that the estimated parameters are significant at the individual level. Considering a 5 % statistical significance ($p \leq 0.05$), the probabilities of the other statistical tests (F, SW, DW, BG, and BP) displayed the following statements in all models: a) that there is global significance of the parameters and at least one of the parameters is different from zero; b) that the errors have a normal distribution; c) that there are no self-correlation issues, no first-order or serial issues; and d) that there are no heteroscedasticity problems (Table 1).

Due to the above, the models proposed were valid, both economically and statistically, and can be used to predict behaviors of the use of water in each of the sectors (endogenous variables of the model) in the face of any change in their exogenous variables.

If a 1 % increase is considered for exogenous variables *HRWF*, *HREF*, *GMW*, and *TE*, *ceteris paribus*, the effects on the water use for households (*HWU*) are as follows: 0.55 % reduction, 0.32 % reduction, 0.93 % increase, and 0.74 % increase, respectively (Table 1). These results indicate that household water use is inelastic against water fees. Additionally, they suggest that water is a complementary good of electric energy, since the use of household appliances such as washing machines and dishwashers, which simplify household chores, is associated with a greater use of water.

According to Reynaud *et al*. (2018), the price elasticity of the demand for household water is -0.7. On the other hand, Bautista-Mayorga *et al*. (2023) estimated elasticity coefficients of -0.588 for water use in regard to the use of household electric energy and 0.235 in regard to the income. Likewise, Reynaud *et al*. (2018) found an elasticity of 0.776 between water use and the mean temperature. Altogether, these findings help conclude that water is a normal good, given that its use increases with income. In addition, temperature is confirmed as a relevant factor in the household use of water.

In commercial use of water (*CWU*), a 1 % change in the exogenous variables *CRWF*, *CREF*, and *CWU1*, *ceteris paribus*, leads to the following changes in use: 2.69 % reduction, 0.4 % decrease, and 0.71 % increase, respectively. In earlier studies, Gracia-de Rentería *et al*. (2021) reported price elasticities related to activities in the tertiary sector of -1.08 for professional services and -1.24 for real estate. In turn, Gómez-Ugalde *et al*. (2012) found a price elasticity of water demand for commercial use of -1.03, as well as an elasticity regarding electric energy of -0.25. Although the latter study did not determine the elasticity associated with the endogenous variable with one year of delay (*t*-1), a direct effect on the use of water was identified in the current period (*t*).

Table 1. Elasticity of water use in the household, commercial, industrial, agricultural, and livestock sectors in the municipality of Tulancingo in Hidalgo, Mexico.

Endogenous variables	Intercept	Exogenous variables				Probabilities					
						R^2	F	SW	DW	BG	BP
		HRWF	*HREF*	*GMW*	*TE*						
HWU	8.52	-0.55	-0.32	0.93	0.74	0.90	0.000	0.24	0.90	0.07	0.22
Standard error	1.63	0.24	0.09	0.28	0.81						
t statistic	5.23	-2.27	-3.65	3.35	0.91						
		CRWF	*CREF*	*CWU1*							
CWU	9.70	-2.69	-0.40	0.71		0.94	0.000	0.11	0.22	0.34	0.49
Standard error	1.95	0.60	0.12	0.07							
t statistic	4.98	-4.49	-3.37	9.87							
		IRWF	*IREF*	*GDPSA*	*TE3*						
IWU	-28.85	-2.35	-0.85	3.31	2.57	0.71	0.006	0.67	0.14	0.30	0.77
Standard error	13.63	1.64	0.53	0.97	1.84						
t statistic	-2.12	-1.43	-1.62	3.43	1.39						
		AEF	*GDPA*	*PRP*	*PP1*						
AWU	11.61	-0.13	0.32	-0.25	-0.33	0.73	0.004	0.91	0.75	0.79	0.14
Standard error	1.77	0.06	0.20	0.06	0.11						
t statistic	6.54	-2.08	1.61	-4.13	-2.99						
		LREF	*GDPL*	*PBEEF*	*PP*						
LWU	-16.09	-0.42	2.84	2.32	-0.96	0.81	0.001	0.26	0.15	0.08	0.57
Standard error	7.52	0.09	0.72	0.40	0.30						
t statistic	-2.14	-4.41	3.96	5.86	-3.22						

Endogenous water use variables: *HWU*: household use; *CWU*: commercial use; *IWU*: industrial use; *AWU*: for agricultural irrigation; *LWU*: livestock use. Exogenous variables: *HRWF*: real average water fee for household use; *HREF*: real average electric energy fee for household use; *GMW*: general minimum wage; *TE*: mean atmospheric temperature; *CRWF*: real average water fee for commercial use; *CREF*: real average electric energy fee for commercial use; *CWU1*: delayed average commercial use of water; *IRWF*: real average industrial use of water; *IREF*: average industrial use of electric energy; *GDPSA*: real gross domestic product (GDP) of secondary activities; *TE3*: mean atmospheric temperature; *AEF*: average electric energy fee for agricultural use; *GDPA*: real agriculture GDP; *PRP*: average pesticide price; *PP1*: rainfall; *LREF*: real average electric energy fee for agricultural use; *GDPL*: real GDP of the raising and exploitation of livestock; *PBEEF*: price of beef; *PP*: rainfall. Probabilities: F: Fisher's test; SW: Shapiro-Wilk; BP: Breusch-Pagan; DW: Durbin-Watson; BG: Breusch-Gofrey.

Differences were observed in the magnitude of the coefficients of elasticity related to the price of water and electric energy, particularly in relation to the price elasticity of the demand. These differences may be attributed to the treatment of the data and the method used in the estimations. However, despite these discrepancies, all studies coincide in the same conclusions: the use of water in the commercial sector displays an elastic behavior, and electric energy acts as a complementary good to water. Therefore, water use is sensitive to changes in price, which suggests that the amount used can be reduced with an adequate price policy.

In the water use for industry (*IWU*), a 1 % change in the exogenous variables *IRWF*, *IREF*, *GDPSA*, and *TE3*, *ceteris paribus*, would have the following effects: 2.35 % reduction, 0.85 % reduction, 3.31 % increase, and 2.57 % increase, respectively. Tobarra-González (2018) reported a water price elasticity for the paper industry of -3.17, displaying a high sensitivity of the consumer to price variations. On the other hand, Bautista-Mayorga *et al*. (2023) identified coefficients related to electric energy, income, and temperature of -0.156, 0.104, and 0.911, respectively.

Significant differences were observed between coefficients in this study and those reported by the authors cited, which may be due to the method used and specific special factors. Nevertheless, the water for industrial use is confirmed to respond elastically to the price of water. Additionally, there is clear evidence of a strong inverse relationship between water consumption and electricity consumption, suggesting that these are complementary goods. The *GDPSA*, used as an approximation of income in this sector, allows water to be classified as a normal good. On the other hand, temperature also plays a crucial part in the use of water. Consequently, the use of water and electric energy fees is suggested as economic policy instruments to incentivize the reduction of water use in the industrial sector. Regarding the variables of income and temperature, their control is more limited since they depend on the general economic surroundings and on the local weather conditions.

For water use in agriculture (*AWU*), a 1 % change in the exogenous variables *AEF*, *GDPA*, *PRP*, and *PP1*, *ceteris paribus*, leads to the following variations in this use: 0.13 % reduction, 0.32 % increase, 0.25 % reduction, and 0.33 % reduction, respectively. Several studies back these findings; Bruno and Jessoe (2021) found a price elasticity in the demand for water agriculture of -0.15, indicating that this demand is inelastic to variations in price. Likewise, Torres-Sombra *et al*. (2013) identified a direct relation between the GDP per capita and the demand for water in agriculture: for every MXN that GDP increases, the demand for water in Sinaloa rises by 0.447 hm^3. Guzmán-Soria *et al*. (2010) found an elasticity regarding the use of fertilizers of -0.315. On the other hand, Khorchani *et al*. (2024), using a correlation matrix, found a positive relation of 0.67 between the yield of rainfed maize and the contribution of water (rainfall plus irrigation).

These results suggest that the use of water in agriculture responds inelastically to the electric energy fee, which is used as a proxy variable for the price of water due to the lack of specific price data over the period of analysis. Additionally, a direct relation is observed with the agricultural GDP (*GDPA*), which helps classify water as a normal good. On the other hand, the reverse relation between the average price of pesticides and agricultural water use suggests that if the price of pesticides decreases, farmers may be incentivized to grow more crops in a larger plot, which would increase water use. By contrast, an increase in the price of pesticides could reduce their use, thus reducing productivity and leading farmers to plant less, reducing water use. Finally, the weather is one of the factors with the greatest repercussions on the yield of agricultural crops, as well as being one of the elements that generates the most uncertainty in terms of decision-making (Khorchani *et al*., 2024).

Finally, a 1 % increase in the exogenous variables *LREF*, *GDPL*, *PBEEF*, and *PP*, *ceteris paribus*, brings about the following changes in the water use for livestock (LWU): 0.42 % reduction, 2.84 % increase, 2.32 % increase, and 0.96 % reduction, respectively. Torres-Sombra *et al.* (2013) found elasticities related to the price of water and electric energy in this sector of -0.065 and 0.051, which are different from the results found and which may be due to the methods used. Guzmán-Soria *et al.* (2010) found an elasticity in milk of 0.0001 and point out that the final products (milk and meat) impact the use of water in the livestock sector.

In the period of study, the agricultural, household, and commercial sectors used 12.5 million, 790 and 263 thousand m^3 of water, whereas the livestock and industrial sectors demanded 105 and 87 thousand m^3 of water (Table 2). With a total demand of approximately 13.8 hm^3 of water, the situation of the aquifer of the municipality of Tulancingo is one of overuse, indicating that a reduction in demand is required.

Table 2. Increase scenarios in water and electricity fees to reduce water use in Tulancingo municipality in Hidalgo, Mexico.

Indicator	Water use per sector (m^3)				
	Household	Commercial	Industrial	Agricultural	Livestock
Observed use	790 353	263 030	87 038	12 515 110	105 789
Estimated use	815 832	285 788	90 859	12 242 000	95 417
Difference	25 479	22 758	3821	-273 110	-10 372
Difference (%)	3.2	8.7	4.4	-2.2	-9.8
Reduction in use (%)	Increase in water fee (%)				
10	18.2	3.7	4.3		
20	36.4	7.4	8.5		
30	54.6	11.1	12.8		
Reduction in use (%)	Increase in electricity fee (%)				
10	31.2	25.1	11.7	76.3	23.9
20	62.3	50.3	23.4	152.7	47.7
30	93.5	75.4	35.1	229.0	71.6

The validation of the models revealed differences of less than 10 % between estimated and observed values. A difference with a positive/negative sign indicates that the model overestimated or underestimated water use in comparison to the observed value (Table 2). Thus, it was possible to develop scenarios to determine the water and electricity fees required to reduce water consumption. If the goal is to reduce household water consumption by 10, 20, or 30 % in terms of estimated value, the fee must rise by 18.2, 36.4, and 54.6 %, respectively. To achieve these commercial water use reductions, water fees must increase by 3.7, 7.4, and 11.1 %. Similarly, to reduce industrial use, the fee must be increased by 4.3, 8.5, and 12.8 %, respectively (Table 2).

The use of water in each sector can be reduced by raising the electric fee. To reduce household water consumption by 10, 20, and 30 %, electricity rates must rise by 31.2, 62.3, and 93.5 %, respectively. For the commercial sector, the fee must increase by 25.1, 50.3, and 75.4 %. Finally, in order to reduce industrial water use, the fee must increase by 11.7, 23.4, and 35.1 %, respectively. For agricultural water use, the fee must increase by 76.3, 152.7, and 229 %. Similarly, the fee for using water for livestock must increase by 23.9, 47.7, and 71.6 %, respectively (Table 2).

Other authors found that increasing the water fee can lead to a decrease in water consumption. According to Bautista-Mayorga *et al*. (2023), in order to reduce water consumption by 10 and 20 % in the household and industrial sectors, the household sector fee must increase by 53.1 and 106.3 %, respectively, while the industrial sector fee must increase by 57.7 and 115.4 %. According to Gómez-Ugalde *et al*. (2012), a 10 % increase in water fees would result in a 10.3 % bimonthly decrease in commercial water demand. Bruno and Jessoe (2021) found a price elasticity of -0.15 for agricultural water use, implying that a 66.7 % increase in price would be required to reduce water use by 10 %. Torres-Sombra *et al*. (2013) observed that reducing water in the livestock sector by 5 % would result in a 76.9 % increase in price.

The authors below found that increasing the electric energy fee makes it possible to reduce water use. Bautista-Mayorga *et al*. (2023) discovered that in order to reduce water use in the household and industrial sectors by 10 and 20 %, respectively, the electricity fee in the household sector must rise by 17 and 34 %, and in the industrial sector by 64.3 and 128.6 %. Gómez-Ugalde *et al*. (2012) discovered an elasticity associated with electric energy of -0.25, implying that in order to reduce water use by 10 and 20 %, the price of electric energy must rise by 40 and 80 %, respectively.

An economic policy would be most effective in the commercial and industrial sectors if water fee increases were considered, and in the commercial, industrial, and livestock sectors if electricity fee increases were considered. This is because the price and cross-price elasticity coefficients were determined to be elastic. Water and electric energy fees in the household sector were higher than in previous sectors, which can be attributed to the critical importance of water and the lack of price elasticity in its demand. The agricultural sector saw significant increases in water fees, which could be attributed to the following: a) electric energy is subsidized in Mexico; b) the inelastic elasticity coefficient is associated with electricity (used as a proxy variable for the water fee); and c) the water use value in agriculture is lower than in other consumer sectors.

CONCLUSIONS

The analysis of water demand for the water-using sectors in the municipality of Tulancingo revealed that increasing water and electricity fees is a feasible way to reduce water consumption. The commercial and industrial sectors are especially sensitive to increases in water fees, while the commercial, industrial, and livestock sectors are more sensitive to increases in electricity fees. Reducing water use or

demand in drought-prone areas benefits future generations by allowing them to use water more wisely.

ACKNOWLEDGEMENTS

To the Secretariat of Science, Humanities, Technology, and Innovation (SECIHTI) for granting the first author a scholarship to carry out a postdoctoral academic stay. To Mr. Luis Alonso González Cruz, director of the Water and Sewage Commission of the Municipality of Tulancingo (AWUMT), for providing essential information to develop the present manuscript.

REFERENCES

Almendarez-Hernández MA, Avilés-Polanco G, Beltrán-Morales LF. 2015. Demanda de agua de uso comercial en la reserva de la biosfera El Vizcaíno, México: Una estimación con datos de panel. Nova Scientia 7 (15): 553–576.

Barkley A, Barkley PW. 2013. Principles of agricultural economics. Routledge: New York, NY, USA. 351 p.

Bautista-Mayorga F, García-Salazar JA, Mora-Flores JS. 2023. Econometric analysis of water demand in Tijuana, Mexico. Tecnología y Ciencias del Agua 14 (4): 268–304. https://doi.org/10.24850/j-tyca-14-04-06

Bruno EM, Jessoe K. 2021. Using price elasticities of water demand to inform policy. Annual Review of Resource Economics 13 (1): 427–441. https://doi.org/10.1146/annurev-resource-110220-104549

Castro-Ramírez JC, Cruz-Gutiérrez FV, Magaña-Zamora JD, Martínez-Atilano G, Reyes-Martínez A, Sainz-Zamora RO. 2017. La demanda del agua y su asignación eficiente en la agricultura: un caso en Guanajuato, México. Economía Coyuntural 2 (2): 145–180.

CONAGUA (Comisión Nacional del Agua). 2021. Estadísticas del agua en México 2021. Gobierno de México. Secretaría de Medio Ambiente y Recursos Naturales. Comisión Nacional del Agua. Ciudad de México, México. 349 p.

CONAGUA (Comisión Nacional del Agua). 2023a. Actualización de la disponibilidad media anual de agua en el acuífero Valle de Tulancingo (1377), Estado de Hidalgo. Ciudad de México, México. 28 p.

CONAGUA (Comisión Nacional del Agua). 2023b. Estadísticas agrícolas de los distritos de riego. Gobierno de México. Comisión Nacional del Agua. Ciudad de México, México. https://www.gob.mx/conagua/documentos/estadisticas-agricolas-de-los-distritos-de-riego (Retrieved: February 2024).

CONASAMI (Comisión Nacional de los Salarios Mínimos). 2023. Salarios mínimos generales y profesionales en la capital 1966-2022. Gobierno de México. Comisión Nacional de los Salarios Mínimos. Ciudad de México, México. https://datos.gob.mx/busca/dataset/salarios-minimos-generales-y-profesionales-en-la-capital-1966-2022 (Retrieved: February 2024).

CRE (Comisión Reguladora de Energía). 2020. Consulta las memorias de cálculo de las tarifas eléctricas. Gobierno de México. Comisión Reguladora de Energía. Ciudad de México, México. https://www.gob.mx/cre/articulos/consulta-las-memorias-de-calculo-de-las-tarifas-electricas?state=published (Retrieved: February 2024).

FAO (Food and Agriculture Organization). 2013. Captación y almacenamiento de agua de lluvia: opciones técnicas para la agricultura familiar en América Latina y el Caribe. Santiago, Chile. 270 p.

FAO (Food and Agriculture Organization). 2024. FAOSTAT. Food and agriculture data. Rome, Italy. https://www.fao.org/faostat/es/#home (Retrieved: February 2024).

Gam I, Rejeb JB. 2021. Micro-economic analysis of domestic water demand: Application of the pseudo-panel approach. Environmental Challenges 4: 100118. https://doi.org/10.1016/j.envc.2021.100118

Gómez-Ugalde SG, Mora-Flores JS, García-Salazar JA, Valdivia-Alcalá R. 2012. Demanda de agua para uso residencial y comercial. Terra Latinoamericana 30 (4): 337–342.

Gracia-de Rentería P, Barberán R, Mur J. 2021. Urban water demand for manufacturing, construction and service industries: a microdata analysis. AQUA—Water Infrastructure, Ecosystems and Society 70 (3): 274–288.

Gujarati DN, Porter DC. 2010. Econometría (Quinta edición). McGraw-Hill: Ciudad de México, México. 921 p.

Guzmán-Soria E, de la Garza-Carranza MT, Hernández-Martínez J, Rebollar-Rebollar S, González-Razo FJ, García-Salazar JA. 2010. Análisis econométrico sobre el consumo de agua subterránea por el sector agropecuario en Guanajuato, México. Ciencia Ergo Sum 17 (2): 159–164.

Guzmán-Soria E, de la Garza-Carranza MT, Rebollar-Rebollar S, Hernández-Martínez J, Terrones-Cordero A. 2013. Modelo econométrico del consumo urbano e industrial de agua subterránea en Guanajuato, México: 1980-2011. Tecnología y Ciencias del Agua 6 (3): 187–193.

INEGI (Instituto Nacional de Estadística y Geografía). 2024a. Publicaciones. Ciudad de México, México. https://www.inegi.org.mx/app/publicaciones/ (Retrieved: October 2023).

INEGI (Instituto Nacional de Estadística y Geografía). 2024b. Banco de información económica. Ciudad de México, México. https://www.inegi.org.mx/app/indicadores/?tm=0#divFV472180 (Retrieved: February 2024).

Khorchani M, Awada T, Schmer M, Jin V, Birru G, Dangal SRS, Suyker A, Freidenreich A. 2024. Long-term croplands water productivity in response to management and climate in the western US corn belt. Agricultural Water Management 291: 108640. https://doi.org/10.1016/j.agwat.2023.108640

PMD (Plan Municipal de Desarrollo). 2016. Plan municipal de desarrollo Tulancingo 2016-2020. Gobierno Municipal de Tulancingo de Bravo. Tulancingo, México. https://2016-2020.tulancingo.gob.mx/plan-municipal-de-desarrollo-tulancingo-2016-2020/ (Retrieved: January 2024).

PNT (Plataforma Nacional de Transparencia). 2024. Información pública. Ciudad de México, México. https://www.plataformadetransparencia.org.mx/ (Retrieved: January 2024).

R Core Team. 2023. R: A language and environment for statistical computing. R Foundation for Statistical Computing. Vienna, Austria. https://www.R-project.org/

Rendón-Contreras HJ, Chavoya-Gama JI, Morales-Hernández JC, Ramírez-Rodríguez H. 2021. Ciudades turísticas, el agua y su demanda: Escenario al año 2030, Puerto Vallarta, México. Investigación y Ciencia 29 (82): 72–85. https://doi.org/10.33064/iycuaa2021822576

Reynaud A, Pons M, Pesado C. 2018. Household water demand in Andorra: Impact of individual metering and seasonality. Water 10 (3): 321. https://doi.org/10.3390/w10030321

SIAP (Servicio de Información Agroalimentaria y Pesquera). 2023. Sistema de información agroalimentaria de consulta. Gobierno de México. Servicio de Información Agroalimentaria y Pesquera. Ciudad de México, México. https://www.gob.mx/siap/documentos/siacon-ng-161430 (Retrieved: February 2024).

SMN (Servicio Meteorológico Nacional). 2024. Climatología. Gobierno de México. Comisión Nacional del Agua. Servicio Meteorológico Nacional. Ciudad de México, México. https://smn.conagua.gob.mx/es/ (Retrieved: February 2024).

Tobarra-González MA. 2018. The value of water in the manufacture industry and its implications for water demand policies. The case of Chile. Estudios de Economía Aplicada 36 (3): 945–960. https://doi.org/10.25115/eea.v36i3.2561

Torres-Sombra J, García-Salazar JA, García-Mata R, Matus-Gardea J, González-Estrada E, Pérez-Zamorano A. 2013. Respuesta de la demanda de agua a cambios en el precio: un estudio por tipo de consumidor en el norte de Sinaloa, México. Agrociencia 47 (3): 293–307.

Agrociencia

ENVIRONMENTAL ATTITUDE DUE TO THE USE OF GLYPHOSATE IN AGRICULTURE IN THE LOWER BASIN OF THE JAMAPA RIVER IN VERACRUZ, MEXICO

María de Lourdes **Fernández-Peña**[1], Arturo **Pérez-Vázquez**[1*], María del Refugio **Castañeda-Chávez**[2], Pablo **Díaz-Rivera**[1], Eusebio **Ortega-Jiménez**[1], Gustavo **López-Romero**[1]

[1]Colegio de Postgraduados Campus Veracruz. Carretera Xalapa-Veracruz km 88.5, Tepetates, Manlio Fabio Altamirano, Veracruz, Mexico. C. P. 91700.
[2]Tecnológico Nacional de México. Instituto Tecnológico de Boca del Río. Carretera Veracruz-Córdoba km 12, Boca del Río, Veracruz, Mexico. C. P. 94290.
* Author for correspondence: parturo@colpos.mx

Citation: Fernández-Peña ML, Pérez-Vázquez A, Castañeda-Chávez MR, Díaz-Rivera P, Ortega-Jiménez E, López-Romero G. 2025. Environmental attitude due to the use of glyphosate in agriculture in the lower basin of the Jamapa river in Veracruz, Mexico. **Agrociencia** 59 (5): 741-753. https://doi.org/ 10.47163/agrociencia.v59i5.3240

Editor in Chief: Dr. Fernando C. Gómez Merino

Received: December 17, 2024.
Approved: June 16, 2025.
Published in Agrociencia: July 03, 2025.

ABSTRACT

Currently, there is a debate about the toxicity and consequences of glyphosate use on human health and the environment. The objective of this work was to estimate the level of use of this herbicide and the environmental attitude of farmers. The hypothesis was that glyphosate use is low in agriculture and the environmental attitude is unclear. For this purpose, a total of 103 questionnaires were distributed to farmers in Jamapa and Medellín in Veracruz, Mexico, to gather socioeconomic, technical-productive, and attitude data. The information was analyzed through descriptive statistics and parametric (*t*-student) and non-parametric (X^2) tests. According to the findings, farmers have an average age of 60 to 63 years, work in agriculture, and have an average level of education equivalent to incomplete primary school. The type of tenure of the production unit between municipalities was found to be statistically different ($p < 0.05$). In Jamapa and Medellín, the average land extension was 6 and 9 ha, respectively. The predominant crops are maize (*Zea mays* L.), beans (*Phaseolus vulgaris* L.), and grass (*Panicum maximum* Jacq. cv. Tanzania), mainly rainfed and for self-consumption or local and/or regional sale. Weeds are moderately affected when chemical herbicides are used, with glyphosate being the main herbicide for both agricultural and non-agricultural use. It was found that 94–98 % of farmers do not use safety measures and do not receive technical training. Glyphosate is used sparingly by farmers in agricultural practices. However, the general perspective is that it has a negative impact on the environment and people's health. There is a difference of opinion regarding the risk in the use of glyphosate and the environmental attitude in the disposal of containers and application of personal prevention measures.

Keywords: herbicide, agroecosystems, weeds, contamination.

INTRODUCTION

The use of agrochemicals such as fertilizers and pesticides is widely accepted in agriculture and has increased significantly since the "Green Revolution" model, which

aimed to boost agricultural productivity and profitability. However, its externalities caused serious consequences, including environmental degradation, human diseases, and socioeconomic effects, primarily on small farmers (Ceccon, 2008; Martínez-Centeno and Huerta-Sobalvarro, 2018).

Inadequate management and constant pesticide abuse endanger human and wildlife health. If this trend continues, it may lead to a food crisis and imminent damage to human health. The social and environmental damage caused by pesticide contamination was first described by Rachel Carson in her book "Silent spring," published in 1962, and today we face the problems described by this author as a result of the excessive and uncontrolled use of different types of pesticides. Soil degradation, loss of biodiversity, increase in human diseases, and contamination of food and water are notorious (Díaz-Vallejo *et al*., 2021).

Pesticide contamination is a global problem that persists. Products such as dichlorodiphenyltrichloroethane (DDT), chlorpyrifos, and paraquat are banned in some countries. In the case of Mexico, DDT is classified as a "restricted use" compound, while paraquat and chlorpyrifos are not restricted (COFEPRIS, 2024). In contrast, new pesticides are entering the market or are in the process of approval and/or prohibition due to the risk they represent. An example of this is glyphosate (N-phosphonomethylglycine, $C_3H_8NO_5P$), which was marketed under the trade name Roundup® in the 1970s and is now being debated globally due to its toxic effects (Fernández-Peña *et al*., 2023; Novotny, 2023).

Glyphosate has been associated with a decrease in soil microorganisms and pollinating insects such as bees (Cullen *et al*., 2023), which may have repercussions on the alteration of biogeochemical cycles and food production. In addition, several toxicological studies have identified damage to the development of aquatic organisms (Kale *et al*., 2023; Bellot *et al*., 2023). Glyphosate contamination alters both surface and groundwater quality; in addition, the use of this herbicide is a precursor of diseases, mainly in agricultural workers through direct contact (Rydz *et al*., 2021). However, another route of contact with the population is the consumption of contaminated food or drinking water (Gomes *et al*., 2020; Rampazzo *et al*., 2023). Glyphosate concentrations have been reported in the urine of workers and pregnant women, which is alarming because of the effects it could cause (Dou *et al*., 2023; Fuhrimann *et al*., 2023).

In Mexico, the presence of this compound has been reported in surface and groundwater, as well as commercial bottled water (Rendón-von Osten and Dzul-Caamal, 2017; Reynoso *et al*., 2020). Although its application is designed to increase agricultural efficiency, its presence can alter several natural processes in the ecosystem, affecting biodiversity and the quality of natural resources. In 2019, the Ministry of Environment and Natural Resources (SEMARNAT) of Mexico applied the "precautionary principle" to stop the importation of glyphosate. In 2020, a presidential decree was published, indicating the "gradual substitution" of glyphosate, which would conclude with its total ban by January 2024. However, in April of that year, the ban was postponed until a viable substitution could be found.

Therefore, the objective of this research was to estimate the level of glyphosate use and to statistically characterize the environmental attitude (degree of knowledge, perception, and behavior) expressed by farmers regarding the impact of glyphosate use on the environment and human health. It was hypothesized that glyphosate use in agriculture is low in the lower Jamapa River basin, and farmers' perceptions of the negative effects on the environment and human health are unclear.

MATERIALS AND METHODS

Study area

The Jamapa River basin is located on the Gulf of Mexico slope in the states of Veracruz and Puebla, between the La Antigua and Papaloapan River basins. It covers an area of 3918 km^2 and partially or totally covers 31 municipalities in the state of Veracruz. It includes two important streams, the Jamapa River as the main watershed and the Cotaxtla River as the main tributary. The watershed is divided into three zones according to its altitude and function: high (catchment zone), medium (accumulation-transport zone), and low (discharge zone) (PAMIC, 2017).

The lower basin covers an area of 1355 km^2 and has altitudes ranging from 0 to 400 m. It has a predominantly warm sub-humid climate with an average annual temperature of 26 °C. The region is characterized by its eminently agricultural activity, and to a lesser extent, subsistence fishing (INEGI, 2019). This work was carried out in the municipalities of Medellín de Bravo and Jamapa, located within the lower basin of the Jamapa River in the state of Veracruz, Mexico (Figure 1).

Questionnaire design and application

A questionnaire was created to collect information, and it was divided into four sections: the first one made a brief exposition of the purpose of the research, the second registered aspects related to the socioeconomic profile of the interviewee, the third compiled technical-productive characteristics of the production unit, and finally, the fourth consisted of a series of items established in an ordinal Likert scale to identify the attitude of farmers in relation to the environmental and human health impacts caused by the use of glyphosate, evaluating the cognitive (level of knowledge), affective (perception), and behavioral (way of acting in the face of certain events) components. Five response options were used for each item, assigning a numerical value for analysis: strongly disagree (1), disagree (2), neutral (3), agree (4), and strongly agree (5).

The questionnaire consisted of a total of 48 open and closed questions. Previously, a pilot test of the questionnaire was carried out (December 2021), and some pertinent adjustments were made. Finally, the questionnaire was validated by means of expert judgment, taking coherence, clarity, scale, and relevance as evaluation indicators (Escobar-Pérez and Cuervo-Martínez, 2008). The questionnaire was applied through personal interviews during the months of March to June 2022.

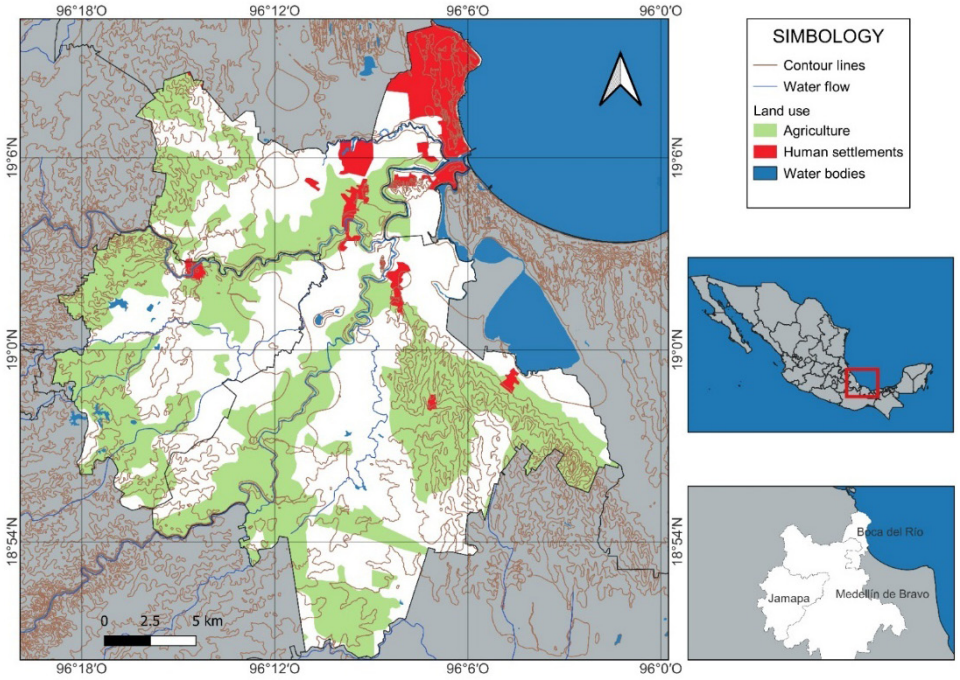

Figure 1. Location of the study area in the lower basin of the Jamapa River in the state of Veracruz, Mexico.

Sample size determination

To determine the sample size for the municipalities of Medellín de Bravo and Jamapa, the number of farmers registered in the Rural Development District (DDR) Veracruz was considered, which was 492 in both municipalities. The estimated sample size was 103 farmers with a confidence level of 95 %. The type of sampling was non-probabilistic, using the snowball technique (Hernández-Ávila and Carpio, 2019); therefore, initial information was obtained from one farmer and other farmers of interest were identified.

Data processing and analysis

The information was captured using Microsoft Excel. Subsequently, the data were analyzed using descriptive statistics and parametric (*t*-student) and non-parametric (chi-squared test) tests. The statistical programs used were Statistica version 7.0 (StatSoft Inc.), IBM SPSS V25 (IBM Statistics; Cary, NC, USA), and Microsoft Excel 2016. Through frequency analysis, the attitude graph by municipality was constructed.

RESULTS AND DISCUSSION

Farmer characterization

A total of 103 farmers were interviewed in both municipalities: Medellín de Bravo (50.4 %) and Jamapa (49.6 %). The farmer profile corresponded to people belonging to the elderly group. The average age in Medellín was 60 years (33–88), while in Jamapa it was 63 years (42–98). No statistically significant differences ($p > 0.05$) were found in the age of farmers between municipalities.

In terms of schooling, more than 60 % have not completed primary school. Most of their working lives have been dedicated to activities related to agriculture and livestock as their main activity, both in Jamapa (80.4 %) and Medellín (90.4 %). A small proportion reported that their primary work activity was permanent jobs in the region or their own businesses (sales of various products), with no statistical differences found between locations ($p > 0.05$).

Both municipalities were mostly represented by the male gender (> 90 %). In terms of agricultural activities, the participation and role of women is very low. However, Leyva-Trinidad (2019) noted that women participated significantly in agricultural activities, despite some social inequality between men and women.

Level of glyphosate use

The type of tenure of the production unit between municipalities was statistically different ($p < 0.05$). In Jamapa, the ejido type is predominant (74.5 %), while in Medellín de Bravo, the small property prevails (65.4 %). The average land area of farms in Jamapa was 6.3 ha and 9.7 ha in Medellín de Bravo. However, statistically, there were no differences ($p > 0.05$). Farmers in both municipalities use their agricultural land for planting and livestock management, mainly cattle.

The predominant crops in the Jamapa and Medellín region are maize (*Zea mays* L.), beans (*Phaseolus vulgaris* L.), and grass (*Panicum maximum* Jacq.), and to a lesser extent, fruit species such as pineapple (*Ananas comosus* (L.) Merr.), mango (*Mangifera indica* L.), and apple (*Byrsonima crassifolia* (L.) Kunth), and vegetables such as papalo (*Porophyllum ruderale* (Jacq.) Cass.) and chili (*Capsicum annuum* L.). However, the position of the predominant crops is reversed in the municipalities. In Jamapa, the main crop is maize, while in Medellín it is grass (Figure 2). The main cropping regime is rainfed. In June 2024, 757.52 ha of corn were planted in Jamapa and 100.18 ha in Medellín (SIAP, 2024). This may be related to the type of tenure of the production unit, the agricultural vocation, and the fact that the number of hectares per farmer is greater in Medellín than in Jamapa. It is important to note that much of what is harvested is for self-consumption and/or local or regional sales in smaller proportion.

The main herbicides used by farmers to control weeds in production units (agricultural use), as well as on the edges of plots, gaps, or roads (non-agricultural use) in both municipalities, are chemical herbicides, including glyphosate, paraquat (1,1'-dimethyl-4,4'-bipyridyl dichloride), and 2,4-D (2,4-dichlorophenoxyacetic acid) (Figure 3). Glyphosate is marketed under the names LaFam®, Faena Fuerte, Durango,

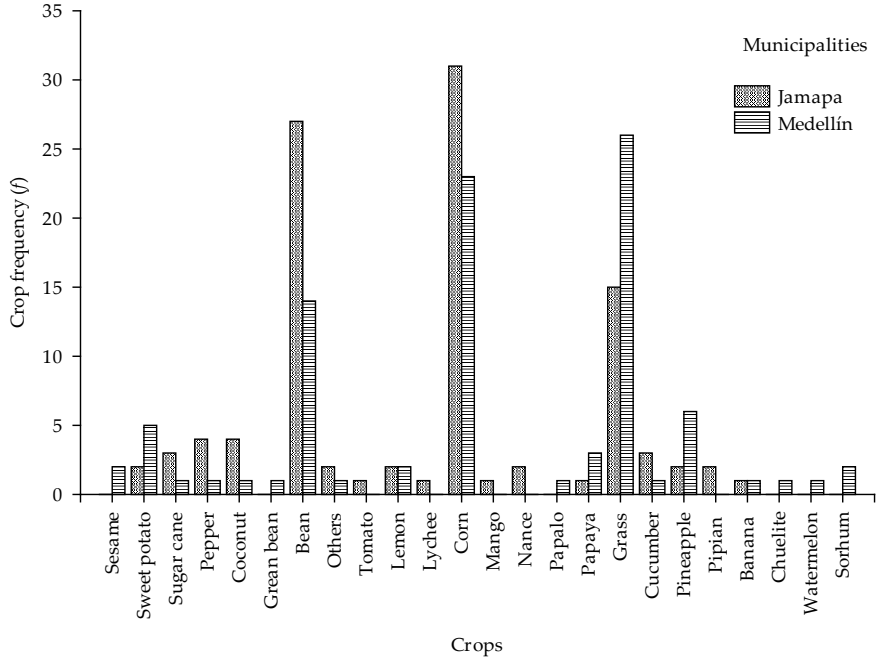

Figure 2. Frequency of predominant crops in the municipalities of Jamapa and Medellín de Bravo in Veracruz state, Mexico.

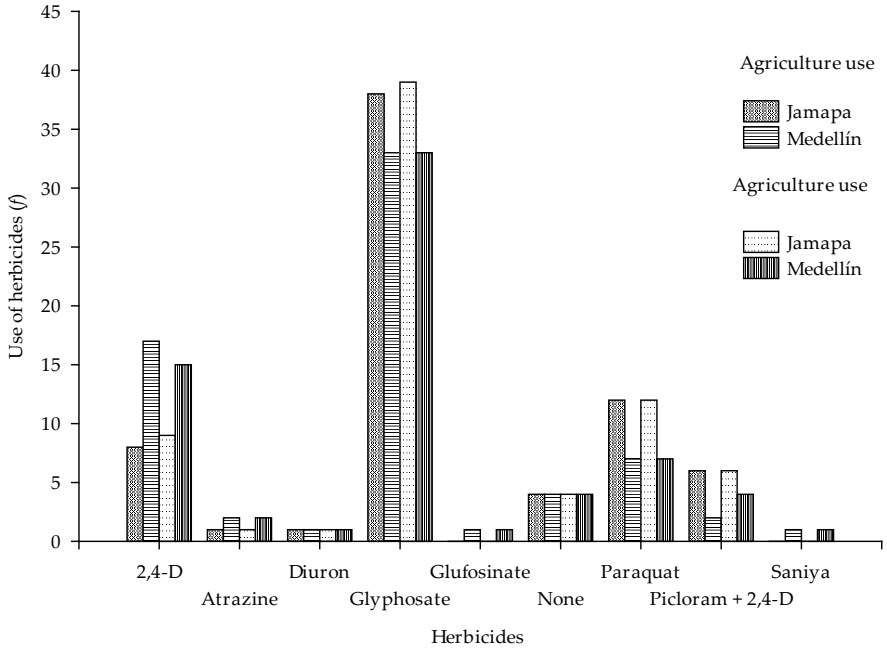

Figure 3. Herbicides used in production units for agricultural and non-agricultural use in the municipalities of Jamapa and Medellín de Bravo in Veracruz state, Mexico.

Glyphosate Technical, Glyfos, or Velfosate. The average dose they use is 1.8 L ha^{-1}, and the season they apply the most is during the rainy season (90 %), where the number of applications is one to three times per crop cycle, and, in general, the application is made in the morning (6 to 8 a.m.).

Farmers emphasize that herbicide applications depend on the growth and resistance of weeds, which are increasingly aggressive and present greater resistance to eliminate them. Alcántara-de la Cruz (2022) points out that the application of herbicides several times during an annual cycle generates the modification of genes in weeds that confer resistance. Therefore, it is important to take into account the type of weeds to be eliminated, rotate herbicides, and try alternatives that allow eliminating dependence on these products. One option could be intercropping, which, although some farmers in the municipalities report using it, there are still very few cases (15–20 %).

The glyphosate dose they apply is lower compared to that reported in northern states of the country or Campeche and Yucatan, where 3 to 5 L ha^{-1} and even more is applied, mainly in soybean, corn, citrus, and vegetable crops (Polanco-Rodriguez *et al*., 2019). However, it continues to be used despite the presidential decree published on December 31, 2020, establishing the gradual substitution and regulation of the acquisition, distribution, promotion, and importation of glyphosate (DOF, 2020). Ramírez-Mora *et al*. (2018) identified glyphosate as the primary herbicide used in the La Antigua irrigation district (DR035) near the study area, where sugarcane cultivation is prevalent. This herbicide has been used since 1995.

Inappropriate and excessive use of herbicides such as glyphosate leads to occupational exposure to pesticides. The safety of agricultural workers is inadequate when handling and applying pesticides. This issue is of vital relevance to human health, given that farmers do not receive training in the proper use of pesticides and measures to reduce the risk of exposure and intoxication. In Jamapa, 16 % of farmers have received technical assistance, while in Medellín only 12 % have received it. Most farmers report that they rely on the experience of other farmers, their own experience, or what is suggested to them in agrochemical stores regarding the type and amount of herbicide to use. This shows that training on the safe use of agrochemicals is a neglected issue where there is still much work to be done.

Regarding the safety measures used by farmers and/or agricultural workers, according to the indications on most pesticide labels and the International Code of Conduct on the Distribution and Use of Pesticides (FAO, 2013), at least a mask, gloves, overalls, and boots should be used. However, of the total number of interviewees, only 2 to 6 % follow what is established in the safety labels and the use of protective measures; the remaining group (94–98 %) only use one or two safety measures (mask covers and/or boots).

In the case of glyphosate, interviewees stated that they do not use safety precautions because it does not have unpleasant odors like other pesticides and that they have been using it for years with no health problems. Farmers reported headaches or rashes, but no other symptoms. Ramírez-Mora *et al*. (2019) reported that 50 % of farmers interviewed in DR035 have presented symptoms of acute intoxication during pesticide

application and that most (90 %) do not use safety measures. Sánchez-Alarcón *et al*. (2023) reported that a group of agricultural workers exposed to pesticides without the necessary protection at the time of preparation and/or application presented significant genotoxic damage.

The gradual reduction that would conclude with a total ban on the use of glyphosate in Mexico was postponed. Therefore, the use of glyphosate in agricultural fields will not be eliminated, and its application will continue despite the risks involved in its use. It is important to join efforts and implement training and orientation programs for farmers, since the risk of intoxication during exposure to herbicides such as glyphosate is serious. In addition, it is necessary to work and implement alternatives to reduce dependence on this and other types of pesticides, which will ultimately lead to a reduction in the impact on health and the environment.

Environmental attitude

A general Likert index value close to five indicates a favorable or positive attitude, while values close to one indicate an unfavorable or negative attitude. In the case of both municipalities, the attitude analysis indicates that farmers had a slightly positive attitude (Table 1) based on what they know, observe (cognitive component),

Table 1. Attitudes toward the impact of glyphosate in Jamapa and Medellín de Bravo, Veracruz, Mexico, measured using a Likert index.

Aspects on the impact of glyphosate	Key	Jamapa	Medellín
		IL*	IL*
1. The use of herbicides (glyphosate) affects the biodiversity of agricultural fields.	IGBIO	4.0	3.9
2. The use of herbicides (glyphosate) affects soil quality and fertility.	IGCFSUE	4.2	3.8
3. The use of herbicides (glyphosate) affects air quality.	IGCAIRE	4.0	3.8
4. The use of herbicides (glyphosate) affects water quality and properties.	IGCAGUA	4.0	3.7
5. Herbicide use affects people's health.	IGSALUDH	4.2	4.0
6. Herbicide use has a direct impact on the health of field workers.	IGSALUDTRA	4.2	4.0
7. The use of herbicides has a direct impact on the health of those who apply them.	IGSALUDAPLI	4.2	4.2
8. The water in the Jamapa River is clean and safe for domestic use.	PAUSODOM	4.2	4.0
9. The water in the Jamapa River is clean and suitable for irrigation.	PAUSORIEG	2.1	2.3
10. The water in the Jamapa River is clean and safe for livestock consumption.	PAUSOGAN	2.1	2.6
11. The water of the Jamapa River contains pesticide and herbicide residues from the surrounding area.	PCONTAPLAG	3.6	3.3
12. The water of the Jamapa River carries pesticide and herbicide residues that can be toxic if used for animal consumption.	PERTOXANIM	3.7	3.6
13. Glyphosate (herbicide) residues in the water reduce and eliminate aquatic organisms in the Jamapa River.	PERPERBIO	4.1	4.2
14. By discontinuing the use of glyphosate (herbicides), environmental and human health impacts are eliminated.	PERRESPROB	1.7	1.8
Overall Likert index		**3.5**	**3.7**

IL*: Likert index.

and perceive (affective component) of the negative impacts of glyphosate and other pesticides on human health and the environment (Figure 4).

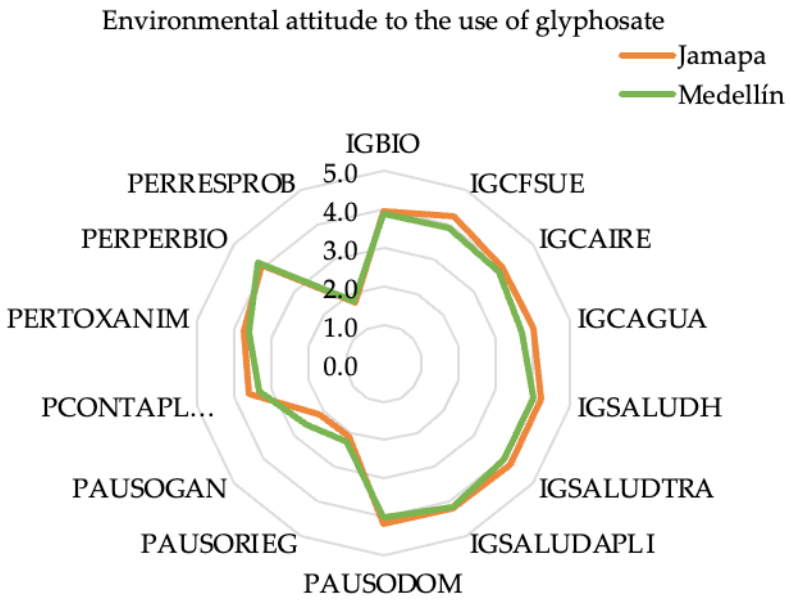

Figure 4. Environmental attitude of the farmers interviewed in the study municipalities in Veracruz, Mexico, by item evaluated (Table 1).

The interviewees have the notion that glyphosate and other herbicides negatively affect ecosystems in the short, medium, or long term, and even emphasized that in previous years (more than 20 years ago), the Jamapa Riverbed had a greater richness and abundance of fauna and flora species; in addition, the water was of good quality and was more reliable for human consumption and recreational activities. Unfortunately, today it can no longer be consumed, and there are fewer and fewer species for human consumption (mojarras, shrimp, among others).

Item 14 (Table 1) reflects that glyphosate is not the only agrochemical that harms the environment, since farmers perceive that there are other contaminants that trigger human health and environmental impacts and that eliminating the use of glyphosate will not end the negative impacts on the environment. Regarding the actions taken to avoid the use of chemical herbicides in Jamapa, 72 % answered that they use agricultural tools (machete, hoe, tarpala) and even weeding by hand; 23 % said none, and 5 % sometimes use agricultural machinery. In the case of Medellín, 60 % use agricultural tools, 23 % use no alternative, and 17 % use agricultural machinery.

They were asked, "What is the final disposal of empty agrochemical containers?" In both municipalities, producers first highlighted "burning," then "burying or throwing

away," and finally, only 20 % of farmers in Medellín and 2 % in Jamapa indicated that they collect them and take them to a special container located in the municipality of Manlio Fabio Altamirano. This practice is of concern in environmental and public health terms, so it is necessary to work and implement actions to mitigate this problem. One example is the placement of special collection containers (Clean Field Program) located in the municipalities of La Antigua and Ursulo Galván in the state of Veracruz, where bins are placed on the roadsides where farmers deposit the containers, and later, personnel from the Ministry of Agriculture collect them for proper disposal.

Both municipalities had similar attitudes toward the environment. Farmers demonstrated a level of knowledge and positive opinion, indicating that they are aware of and perceive the negative impact of glyphosate on the environment and even human health. It was found that there is a dissonance between the opinion and the way of acting, since their behavior is contrary to what was expressed, referring to the incorrect final disposal of empty agrochemical containers and the scarce personal prevention measures when handling and applying this or other products.

The results of this research regarding the environmental attitude towards the negative impacts of glyphosate, the disposal of empty containers, and farmer safety are similar to those reported by Ponce-Caballero *et al*. (2022), who pointed out that farmers do perceive the negative impacts of pesticides; however, they present deficiencies in terms of personal protection and disposal of empty containers, which they associate with age, level of schooling, lack of information, and technical training.

CONCLUSIONS

Farmers in the municipalities of Jamapa and Medellín are small-scale producers and use chemical herbicides to control weeds, with glyphosate being the most commonly utilized. Although the application rate is relatively low, it may be related to what they know or observe of the impacts of this or other pesticides. Based on their years of experience in the field, farmers know and have a positive and favorable environmental attitude. In terms of knowledge or perception of the impact of glyphosate or other agrochemicals, they are willing to use alternative methods (such as agricultural tools and machinery) to combat weeds in order to reduce the use of chemical herbicides. Although the problem may not be solved quickly, these actions could lead to gradual but significant progress in reducing the use of this herbicide.

On the other hand, despite being clear about the negative effects of glyphosate and other herbicides, farmers carry out unfavorable actions such as improper disposal of containers and do not use preventive personal protection measures when handling and applying this type of agrochemical. It is necessary for the sector's institutions to reach out to farmers and inform them of the risks they face. Given that agricultural workers are the most vulnerable to intoxication and disease, technical training programs and safety precautions must be implemented. To reduce the impact and contamination of natural resources, an environmental education program should be developed or expanded, similar to the Clean Field Program.

ACKNOWLEDGEMENTS

We thank the farmers of the municipalities of Jamapa and Medellín for their support and collaboration in this research, the Postgraduate College for funding this project; the Secretariat of Science, Humanities, Technology, and Innovation (SECIHTI) for the scholarship granted for postgraduate studies, and each of the co-authors for their support and guidance.

REFERENCES

Alcántara-de la Cruz R. 2022. Prevención, detección y manejo de la resistencia a herbicidas. Avances en Investigación Agropecuaria 26: 17–18. https://doi.org/10.53897/revaia.22.26.18

Bellot M, Carrillo MP, Bedrossiantz J, Zheng J, Mandal R, Wishart DS, Gómez-Canela C, Vila-Costa M, Prats E, Piña B, Raldúa D. 2023. From dysbiosis to neuropathologies: Toxic effects of glyphosate in zebrafish. Ecotoxicology and Environmental Safety 270: 115888. https://doi.org/10.1016/j.ecoenv.2023.115888

Ceccon E. 2008. La revolución verde tragedia en dos actos. Ciencias 1 (91): 21–29.

COFEPRIS (Comisión Federal para la Protección contra Riesgos Sanitarios). 2024. Consulta de registros sanitarios de plaguicidas, nutrientes vegetales y LMR. Gobierno de México. Comisión Federal para la Protección contra Riesgos Sanitarios. Ciudad de México, México. http://siipris03.cofepris.gob.mx/Resoluciones/Consultas/ConWebRegPlaguicida.asp (Retrieved: February 2024).

Cullen MG, Bliss L, Stanley DA, Carolan JC. 2023. Investigating the effects of glyphosate on the bumblebee proteome and microbiota. Science of the Total Environment 864: 161074. https://doi.org/10.1016/j.scitotenv.2022.161074

Díaz-Vallejo J, Barraza-Villarreal A, Yáñez-Estrada L, Hernández-Cadena L. 2021. Plaguicidas en alimentos: riesgo a la salud y marco regulatorio en Veracruz, México. Salud Pública de México 63 (4): 486–497. https://doi.org/10.21149/12297

DOF (Diario Oficial de la Federación). 2020. DECRETO por el que se establecen las acciones que deberán realizar las dependencias y entidades que integran la Administración Pública Federal, en el ámbito de sus competencias, para sustituir gradualmente el uso, adquisición, distribución, promoción e importación de la sustancia química denominada glifosato y de los agroquímicos utilizados en nuestro país que lo contienen como ingrediente activo, por alternativas sostenibles y culturalmente adecuadas, que permitan mantener la producción y resulten seguras para la salud humana, la diversidad biocultural del país y el ambiente. Gobierno de México. Presidencia de la República. Ciudad de México, México. https://www.dof.gob.mx/nota_detalle.php?codigo=5609365&fecha=31/12/2020#gsc.tab=0 (Retrieved: April 2024).

Dou JR, Zhou X, Pan XY, Miao RF, Zhou ML, Zhang F. 2023. Investigation on health status of workers exposed to glyphosate. Chinese Journal of Industrial Hygiene and Occupational Diseases 12: 517–522. https://doi.org/10.3760/cma.j.cn121094-20220329-00162

Escobar-Pérez J, Cuervo-Martínez A. 2008. Validez de contenido y juicio de expertos: una aproximación a su utilización. Avances de Medición 6 (1): 27–36.

FAO (Food and Agriculture Organization). 2013. Código internacional de conducta para la distribución y utilización de plaguicidas. Rome, Italy. 16 p.

Fernández-Peña ML, Pérez-Vázquez A, Castañeda-Chávez MR, Díaz-Rivera P, Ortega-Jiménez E, López-Romero G. 2023. Impacts of glyphosate (Roundup®) on the environment and on human health. Agrociencia 57 (4): 836–859. https://doi.org/10.47163/agrociencia.v57i4.2844

Fuhrimann S, Mueller W, Atuhaire A, Ohlander J, Mubeezi R, Povey A, Basinas I, van Tongeren M, Jones K, Sams C, *et al*. 2023. Self-reported and urinary biomarker-based measures of exposure to glyphosate and mancozeb and sleep problems among smallholder farmers in Uganda. Environment International 182: 108277. https://doi.org/10.1016/j.envint.2023.108277

Gomes MP, Rocha DC, Moreira de Brito JC, Tavares DS, Marques RZ, Soffiatti P, Sant'Anna-Santos BF. 2020. Emerging contaminants in water used for maize irrigation: Economic and food safety losses associated with ciprofloxacin and glyphosate. Ecotoxicology and Environmental Safety 196: 110549. https://doi.org/10.1016/j.ecoenv.2020.110549

Hernández-Ávila CE, Carpio N. 2019. Introducción a los tipos de muestreo. ALERTA Revista Científica del Instituto Nacional de Salud 2 (1): 75–79. https://doi.org/10.5377/alerta.v2i1.7535

INEGI (Instituto Nacional de Estadística y Geografía). 2019. Estudio de información integrada de la cuenca Ríos Actopan-Jamapa y otras. Ciudad de México, México. 117 p.

Kale OE, Adebesin AN, Kale TF, Oladoja F, Osonuga IO, Soyinka OO, Uwaezuoke D, Olajide O, Akinloye V, Adedugbe O, *et al*. 2023. Effects of glyphosate-based herbicide on gametes fertilization and four developmental stages in *Clarias gariepinus*. Heliyon 9 (4): e15048. https://doi.org/10.1016/j.heliyon.2023.e15048

Leyva-Trinidad DA. 2019. El rol de la mujer en el agroecosistema y su aporte a la producción de alimentos. Agro Productividad 12 (1): 47–52. https://doi.org/10.32854/agrop.v0i0.1337

Martínez-Centeno AL, Huerta-Sobalvarro KK. 2018. La revolución verde. Revista Iberoamericana de Bioeconomía y Cambio Climático 4 (8): 1040–1046. https://doi.org/10.5377/ribcc.v4i8.6717

Novotny E. 2023. ¿Glifosato: amigo o enemigo? Revista Formación Política 2: 10–26.

PAMIC (Plan de Acción de Manejo Integral). 2017. Cuenca del Río Jamapa. Secretaría de Medio Ambiente y Recursos Naturales. Instituto Nacional de Ecología y Cambio Climático. Ciudad de México, México. 108 p.

Polanco-Rodríguez AG, Magaña-Castro TV, Cetz-Luit J, Quintal-López R. 2019. Uso de agroquímicos cancerígenos en la región agrícola de Yucatán, México. Centro Agrícola 46 (2): 72–83.

Ponce-Caballero C, Cardeña-Echalaz F, Giácoman-Vallejos G, Vega-de Lille M, Góngora-Echeverría VR. 2022. Pesticide management and farmers perception of environmental and health issues due to pesticide use in the state of Yucatan, Mexico: A study case. Revista Internacional de Contaminación Ambiental 38: 289–300. https://doi.org/10.20937/rica.54134

Ramírez-Mora E, Pérez-Vázquez A, Landeros-Sánchez C, Martínez-Dávila JP, Villanueva-Jiménez JA, Lagunes-Espinoza LDC. 2018. Uso histórico de plaguicidas en caña de azúcar del DR035 La Antigua, Veracruz. Acta Universitaria 28 (4): 42–49.

Ramírez-Mora E, Pérez-Vázquez A, Landeros-Sánchez C, Martínez-Dávila JP, Villanueva-Jiménez JA, Lagunes-Espinoza LDC. 2019. Occupational exposure to pesticides in sugarcane agroecosystems in the central region of Veracruz state, Mexico. Revista BioCiencias 6 (1): e495. https://doi.org/10.15741/revbio.06.01.03

Rampazzo G, Gazzotti T, Zironi E, Pagliuca G. 2023. Glyphosate and glufosinate residues in honey and other hive products. Foods 12 (6): 1155. https://doi.org/10.3390/foods12061155

Rendón-von Osten J, Dzul-Caamal R. 2017. Glyphosate residues in groundwater, drinking water and urine of subsistence farmers from intensive agriculture localities: A survey in

Hopelchén, Campeche, Mexico. International Journal of Environmental Research and Public Health 14 (6): 595. https://doi.org/10.3390/ijerph14060595

Reynoso EC, Peña RD, Reyes D, Chavarin-Pineda Y, Palchetti I, Torres E. 2020. Determination of glyphosate in water from a rural locality in Mexico and its implications for the population based on water consumption and use habits. International Journal of Environmental Research and Public Health 17 (19): 7102. https://doi.org/10.3390/ijerph17197102

Rydz E, Larsen K, Peters CE. 2021. Estimating exposure to three commonly used, potentially carcinogenic pesticides (chlorolathonil, 2,4-D, and glyphosate) among agricultural workers in Canada. Annals of Work Exposures and Health 65 (4): 377–389. https://doi.org/10.1093/annweh/wxaa109

Sánchez-Alarcón J, Milic M, Bonassi S, Gómez-Arroyo S, Cortés-Eslava J, Flores-Márquez AR, Valencia-Sánchez RA, Valencia-Quintana R. 2023. Occupational exposure to pesticides: DNA damage in horticulturist from Nativitas, Tlaxcala in Mexico. Environmental Toxicology and Pharmacology 100 (5): 10414. https://doi.org/10.1016/j.etap.2023.104141

SIAP (Servicio de Información Agroalimentaria y Pesquera). 2024. Avance de siembras y cosechas. Gobierno de México. Servicio de Información Agroalimentaria y Pesquera. Ciudad de México, México. https://nube.siap.gob.mx/avance_agricola/ (Retrieved: July 2024).

Agrociencia

FACTORS AFFECTING THE ADOPTION OF SHADE CLOTH TECHNOLOGY IN APPLE PRODUCTION IN MEXICO

Abdiel **Menchaca-Aguilar**[1], José Saturnino **Mora-Flores**[1], José Alberto **García-Salazar**[1*], José Sergio **Escobedo-Garrido**[2], Roberto **García-Mata**[1]

[1]Colegio de Postgraduados Campus Montecillo. Posgrado en Socioeconomía Estadística e Informática-Economía. Carretera México-Texcoco km 36.5, Montecillo, Texcoco, State of Mexico, Mexico. C. P. 56264.
[2]Colegio de Postgraduados Campus Puebla. Posgrado en Estrategias para el Desarrollo Agrícola Regional. Boulevard Forjadores de Puebla 205, Ampliación Momoxpan, San Pedro Cholula, Puebla, Mexico. C. P. 72754.
* Author for correspondence: jsalazar@colpos.mx

Citation: Menchaca-Aguilar A, Mora-Flores JS, García-Salazar JA, Escobedo-Garrido JS, García-Mata R. 2025. Factors affecting the adoption of shade cloth technology in apple production in Mexico. **Agrociencia** 59(5): 754-767. https://doi.org/ 10.47163/agrociencia.v59i5.3275

Editor in Chief:
Dr. Fernando C. Gómez Merino

Received: November 24, 2024.
Approved: July 16, 2025.
Published in Agrociencia: July 21, 2025.

ABSTRACT

The vulnerability of apple tree (*Malus domestica* Borkh.) yield to changes in climatic variables justifies an examination of the determining factors in producer technology adoption. The main factors are age, orchard size, temperature, and the cost of shade cloth, fertilizers, and labor. The objective of this research was to analyze the factors that influence the adoption rate of shade cloth as protection for apple crops. Municipal-level data was used to estimate a grouped logistic model with the 24 municipalities in which shade cloth was used in 2022. The dependent variable was the adoption rate of shade cloth, and the independent variables were age, farm size, shade cloth price, fertilizers, labor, and temperature. The results show that when age, farm size, and temperature increase by 10 %, the probability of using shade cloth increases by 22.6, 15.7, and 7.6 %, respectively. A 10 % increase in the prices of shade cloth, fertilizers, and labor reduced the probability of shade cloth use by 1.7, 29.8, and 27.3 %, respectively. The adoption rate of shade cloth may increase as the size of the orchard expands through the rental or purchase of land, but it decreases to a greater extent with increases in fertilizer and labor prices. Among the benefits of using shade cloth are the protection of crops from excessive radiation and temperature increases.

Keywords: income per hectare, *Malus domestica* Borkh., logit model, probability, adoption rate, temperature.

INTRODUCTION

Apples (*Malus domestica* Borkh.) have become one of the most popular fruits in Mexico, thanks to changes in consumer tastes. The current trend toward healthy eating led to an increase in apple consumption from 643 698 to 1 112 246 Mg between 1994 and 2022. Over the last three decades, apple production in Mexico has increased from 487 698 to 817 806 Mg (Table 1). This was made possible by the transition from

Table 1. Evolution of the apple market (*Malus domestica* Borkh.) in Mexico from 1994 to 2022.

Year	Surface ha	Production Mg	Yield Mg ha^{-1}	Imports Mg	Exports Mg	FTB Mg	ADC Mg
	1	2	3	4	5	6 = 5 - 4	7 = 2 + 4 - 5
1994	61 472	487 698	7.93	156 110	110	-156 000	643 698
1999	64 474	449 867	6.98	136 380	300	-136 080	585 947
2004	59 095	572 906	9.69	154 050	243	-153 807	726 713
2009	56 992	561 493	9.85	222 208	253	-221 955	783 448
2014	55 447	716 865	12.93	235 502	305	-235 197	952 062
2019	52 981	761 483	14.37	252 223	606	-251 617	1 013 100
2022	54 959	817 806	14.88	295 183	743	-294 440	1 112 246
AAGR (%)	-0.40	1.86	2.27	2.30	7.06	2.33	1.97

FTB: foreign trade balance; ADC: apparent domestic consumption; AAGR: average annual growth rate for the period 1994–2022. The analysis was elaborated using data from SIAP (2024) and FAO (2023).

backyard orchards to technified orchards with traditional or introduced varieties and innovations in production management (Favret-Tondato, 2012).

Almost all the apples produced are destined for the domestic market. Production grew at an annual rate of 1.86 % from 1994 to 2022, which is lower than the consumption growth rate of 1.97 %. To satisfy domestic demand, imports increased from 156 110 in 1994 to 295 183 Mg in 2022; in turn, the share of imports for consumption increased from 21 to 26.5 % in the same period (FAO, 2023). Exports are minimal and account for only 0.06 % of total production; hence, the trade balance is in deficit (Table 1). Farmland has expanded over the last 20 years, which has led to an increase in agricultural production (Potapov *et al*., 2022). However, in the case of apples in Mexico, the area planted has decreased over the last 30 years, from 61 472 ha in 1994 to 54 959 ha in 2022. Therefore, the increase in production was due to an increase in yield per hectare, from 7.93 Mg ha^{-1} in 1994 to 14.88 Mg ha^{-1} in 2022 (SIAP, 2024).

Most apple production is concentrated in the north of the country. The states of Chihuahua and Coahuila account for 85 and 5.3 % of the total national production (SIAP, 2024). Puebla accounts for 4.4 %, but 66 % of the area is planted with native apples, which has an impact on producers' income, as the average rural price of native apples (4610.00 MXN Mg^{-1} in 2022) was 2.2 times lower than that of Golden Delicious apples (11 039.95 MXN Mg^{-1} in 2022) (SIAP, 2024). Production in the municipalities of Cuauhtémoc, Guerrero, and Namiquipa, Chihuahua, exceeds 23 Mg ha^{-1}. In Coahuila, apple trees are only planted in the municipality of Arteaga, and their irrigated yields reach 8.9 Mg ha^{-1} (SIAP, 2024). In the north of the country, integrated crop management is practiced, with varieties of higher market value developed according to the local climate. Some orchards are protected with shade cloth against solar radiation, hail, and late frosts (Favret-Tondato, 2012).

Socioeconomic, technological, and environmental factors influence the adoption rate of shade cloth. A study on the adoption of crop protection measures such as anti-hail netting conducted in India found that adoption is positively influenced by age, income, and property size, as producers have accumulated more wealth over time and find it easier to invest in crop protection (Prakash *et al*., 2021). In turn, Shashikala *et al*. (2022) found that income and property size are positively related to protective netting adoption rates, but age is negatively related. The adoption rate of shade cloth is limited by investment, production, and labor costs, so including government subsidies may be an alternative to increase their use (Prakash *et al*., 2020). The need to protect investment in perennial crops from temperature increases due to climate change also increases the likelihood for producers to adopt protective measures (Gunathilaka *et al*., 2018).

Currently, the global apple business faces challenges such as international competition and low product quality. Climate change affects the quantity and quality of natural resources due to variations in temperature, precipitation, winds, and water availability for crop growth and reproduction (Giacinti, 2003). Overexposure to sunlight and high temperatures affects plant and fruit development through physiological disorders (Severino *et al*., 2023). In South Africa, fruit quality problems have arisen due to sunburn, resulting from high temperatures with excessive solar intensity, leading to a decrease in export volumes of up to 50 % (Wand and Gindaba, 2005).

Porsch *et al*. (2018) point out that, in Germany, losses due to frost and hail are the most significant sources of risk in technified orchards and recommend the use of netting, even in places where hailstorms are not a regular occurrence. Protected agriculture in apple orchards is widely used in Europe and has spread throughout the world in the last 30 years. Depending on the type of protection, it fulfills various functions such as reducing sunburn, hail damage, and wind damage (Noè and Eccher, 1996).

In Brazil, do Amarante *et al*. (2011) found positive effects in the use of white netting in apple orchards to reduce sunburn and rot after cold storage. However, the fruit lost color and pulp firmness, and the starch index increased. In Mexico, low-tech producers are mainly affected by late frosts, with a loss of up to 70 % of the number of fruits per tree, because they are unable to mitigate the risk due to lack of resources and technical assistance (Ramírez-Legarreta *et al*., 2006).

It is believed that apple production and quality can be improved by adopting crop protection technologies. Therefore, this study aimed to analyze how population age, orchard size, temperature, and the prices of shade cloth, fertilizers, and labor affect the adoption rate of shade cloth technology in apple cultivation. The study was based on economic theory, so the hypothesis is that increases in age, size of the production units, and temperatures have positive effects on technology adoption. On the other hand, the price of shade cloth, fertilizers, and labor has negative effects as they add to the production cost.

MATERIALS AND METHODS

Based on Gujarati and Porter (2010), a grouped logit model (glogit) was formulated to determine the factors affecting the adoption rate of shade cloth technology in apple production, which was estimated using the Statistical Analysis System (SAS) 9.0 program (SAS Institute Inc., Cary, NC, USA). By using this model with municipal-level data, the proportion of shade cloth use can be estimated by adding the area that uses this technology and the area that does not. As a result, each observation (group) concentrates the total number of cultivated hectares where the technology is used or not; therefore, the total universe of municipalities that use shade cloth is considered. The dependent variable was the rate of adoption of shade cloth or, conversely, open-air planting. This was defined as the probability of using shade cloth in municipality *i* and was calculated following these steps (Equations 1 and 2):

$$P_i = TUMS_i = \frac{SMS_i}{ST_i} \tag{1}$$

$$1 - P_i = \frac{ST_i - SMS_i}{ST_i} \tag{2}$$

where, for municipality *i*, *Pi* is the probability of using shade cloth in *i* and 1-*Pi* is the probability of not using it (planting outdoors); $TUMS_i$ is the rate of shade cloth use in *i*; SMS_i is the area cultivated with shade cloth in *i*; and ST_i is the total area harvested in *i*. The grouped logit model was formulated, in which the qualitative dependent variable becomes an odds ratio. The proposed model is:

$$L_i = \ln\left(\frac{P_i}{1 - P_i}\right) = \beta_1 + \beta_2 EDA_i + \beta_3 TAM_i + \beta_4 PMP_i + \beta_5 PMO_i + \beta_6 PFE_i + \beta_7 TMI_i + u_i \tag{3}$$

where, for each municipality *i*, *Li* is the natural logarithm of the odds ratio [*Pi*/(1-*Pi*)], EDA_i is the average age of the population over 15 years (in years), TAM_i is the size of the orchard (in ha), PMP_i is the price of protective netting (in MXN ha^{-1}), PMO_i is the price of labor (in MXN per day), PFE_i is the price of fertilizer (in MXN Mg^{-1}), TMI_i is the average minimum temperature (in °C), and u_i is the error term, which is asymptotically normally distributed, with mean = 0 and variance = 1/[*STiPi*(*1-Pi*)], so the disturbance term in the glogit model is heteroscedastic (Theil, 1970).

To solve the problem of heteroscedasticity, Gujarati and Porter (2010) propose using weighted least squares; therefore, Equation 3 becomes:

$$\sqrt{w_i}L_i = \beta_1\sqrt{w_i} + \beta_2\sqrt{w_i}EDA_i + \beta_3\sqrt{w_i}TAM_i + \beta_4\sqrt{w_i}PMP_i + \beta_5\sqrt{w_i}PMO_i + \beta_6\sqrt{w_i}PFE_i + \beta_7\sqrt{w_i}TMI_i + \sqrt{w_i}u_i \quad (4)$$

or

$$L_i^* = \beta_1\sqrt{w_i} + \beta_2 EDA_i^* + \beta_3 TAM_i^* + \beta_4 PMP_i^* + \beta_5 PMO_i^* + \beta_6 PFE_i^* + \beta_7 TMI_i^* + v_i \quad (5)$$

where $\sqrt{w_i} = \sqrt{ST_i P_i(1-P_i)}$, EDA_i^* is the weighted average age of the population over 15 years of age, TAM_i^* is the weighted size of the orchard, PMP_i^* is the weighted price of protective netting, PMO_i^* is the weighted price of labor, PFE_i^* is the weighted price of fertilizer, TMI_i^* is the weighted average minimum temperature, and v_i is the weighted error term.

The model analysis was performed as an unweighted logit by dividing L_i^* by the weight $\sqrt{w_i}$. Subsequently, the ratio of predicted probabilities was obtained using the antilogarithm of L_i^* (Equation 6):

$$e^{\hat{L}_i} = \frac{\hat{P}_i}{1-\hat{P}_i} \quad (6)$$

The predicted probability of using shade cloth technology is obtained by solving for $\hat{P}_i$ in Equation 6, resulting in Equation 7:

$$\hat{P}_i = \frac{e^{\hat{L}_i}}{1-e^{\hat{L}_i}} \quad (7)$$

The unweighted and weighted estimated probabilities were obtained for each municipality. Using the latter, the total average probability of the adoption rate of shade cloth technology was calculated using Equation 8:

$$P_p = \sum_{i=1}^{I}\left[\hat{P}_i \times \delta_i\right] \quad (8)$$

where P_p is the total average probability of using shade cloth, $\delta_i = ST_i/ST$ is the share of region i in the total area planted with apple trees, and I is the total number of municipalities used in the model.

To obtain the total area planted with apple trees, municipal data reported by SIAP (2024) in 2022 was used. The area planted with shade cloth was obtained from the area planted with shade cloth for perennial crops in the 2022 Agricultural Census (INEGI, 2023). The procedure for obtaining the total planted area was as follows: a) The main apple-producing municipalities in the country were selected; b) The municipal area planted with shade cloth for perennial crops was obtained; and c) It was verified that the total area with shade cloth matched the state data reported in the census.

Using information from SIAP (2024), 340 producing municipalities were identified in the country, with a total planted area of 57 817 ha (Table 2). Municipalities with more than 100 ha planted were used as the grouping criterion. Of the 340 municipalities, 289 had an area of less than 100 ha, while 51 municipalities, distributed across Chihuahua, Coahuila, Durango, Nuevo León, Sonora, Zacatecas, Querétaro, Hidalgo, Veracruz, Puebla, and Chiapas, had an area greater than 100 ha (Table 2). According to the 2022 National Agricultural Census, shade cloth is used in 24 municipalities, so the model estimate was based solely on data from those municipalities (INEGI, 2023). The total area considered was 47 631 ha planted, representing 82.4 % of the national total, of which 9401 ha use shade cloth (Table 2). The adoption rate of shade cloth in these 24 municipalities is 19.7 %.

The average size of orchards at the municipal level was calculated using data from the 2022 Agricultural Census (INEGI, 2023). The area planted with perennial crops was divided by the number of production units. In municipalities that use shade cloth, 82 % of orchards are apple orchards, meaning they specialize in this crop. It was considered that apple producers can increase the size of their farms by renting or purchasing land from other apple producers, which means that the total area remains constant.

For the price of shade cloth, the price (MXN Mg^{-1}) of apples produced was used (Equation 9). The cost of the netting per hectare is fixed, as it is part of the orchard establishment and is the same regardless of the apples produced. Productivity (measured by yields) determines the price of shade cloth; that is, in orchards with low yields, the cost of the netting is higher and vice versa. In addition, different types of netting, the location of the municipalities, and the diversity of use determine the variability in prices. This way, the price reflects the effect of productivity and avoids price variability.

$$PMS_i = \frac{CMS}{R_i} \tag{9}$$

where, for municipality i, PMS_i is the price of shade cloth (in MXN Mg^{-1} in 2022), CMS is the cost of shade cloth quoted in Mexico City with a national distributor (in MXN ha^{-1}), and R_i is the yield level (in Mg ha^{-1} in 2022).

The price of labor was selected because of its importance in the apple production process, which is labor intensive, especially during the fruit thinning and harvesting phases. The data were obtained from the 2022 Agricultural Census daily wage data

Table 2. Area planted with apple trees (*Malus domestica* Borkh.) using shade cloth in Mexico by municipality in 2022.

Number	State	Municipality	Planted area (ha)	Surface with shade cloth (ha)	Number of municipalities	Adoption rate (%)
		Municipalities with more than 100 ha planted using shade cloth				
1	Chihuahua	Cuauhtémoc	10 581	4053	1	38.30
2	Chihuahua	Guerrero	8914	1647	1	18.48
3	Chihuahua	Namiquipa	5151	736	1	14.29
4	Chihuahua	Bachíniva	2763	212	1	7.67
5	Chihuahua	Cusihuiriachi	2599	1616	1	62.18
6	Chihuahua	Carichí	913	135	1	14.79
7	Chihuahua	Riva Palacio	700	261	1	37.29
8	Chihuahua	Gran Morelos	209	125	1	59.81
9	Chihuahua	Guachochi	129	1	1	0.78
10	Coahuila	Arteaga	5792	466	1	8.05
11	Durango	Canatlán	3057	26	1	0.85
12	Durango	Nuevo Ideal	1156	2	1	0.17
13	Durango	San Dimas	300	2	1	0.67
14	Durango	Pueblo Nuevo	256	9	1	3.52
15	Hidalgo	Acaxochitlán	151	1	1	0.66
16	Hidalgo	Zimapán	150	1	1	0.67
17	Nuevo León	Santiago	624	1	1	0.16
18	Nuevo León	Galeana	557	40	1	7.18
19	Puebla	Zacatlán	1882	25	1	1.33
20	Puebla	Tlachichuca	534	21	1	3.93
21	Puebla	Chignahuapan	422	15	1	3.55
22	Querétaro	San Joaquín	200	1	1	0.50
23	Sonora	Yécora	207	4	1	1.93
24	Veracruz	Jalacingo	384	1	1	0.26
Subtotal (1–24)	-	-	47 631	9401	24	19.74
		Municipalities with more than 100 ha planted without shade cloth				
Subtotal (25–51)	Several[†]	-	5571	0	27	0.00
		Municipalities with less than 100 ha planted (none use shade cloth)				
Subtotal (52–340)	Several[¶]	-	4615	0	289	0.00
Nationwide total	-	-	57 817	9401	340	16.26

[†]The 27 municipalities are located in the states of Chiapas, Chihuahua, Durango, Hidalgo, Puebla, Querétaro, Veracruz, and Zacatecas. [¶]The 289 municipalities are located in the states of Aguascalientes, Baja California, Chiapas, Chihuahua, Mexico City, Coahuila, Durango, Guanajuato, Guerrero, Hidalgo, Jalisco, State of Mexico, Michoacán, Morelos, Nuevo León, Oaxaca, Puebla, Querétaro, San Luis Potosí, Tlaxcala, Veracruz, and Zacatecas. Prepared with information obtained from INEGI (2023) and SIAP (2024).

(INEGI, 2023). For fertilizers, the frequent price for 2022 (SNIIM, 2024) at the nearest supply center in each producing municipality was used. Fertilizers are part of the technology bundle, which means that an increase in their price affects the adoption of the technology, as it raises the cost of production (García-Salazar *et al.*, 2023). For age,

the population average over 15 years of age from the 2020 Population and Housing Census (INEGI, 2021) was used. This variable includes apple producers, possible family labor, and wage earners involved in the production process.

To measure the effect of temperature on shade cloth adoption, the average annual minimum temperature for 2022 was used (CONAGUA, 2023). Temperature increases have different effects on apple tree development: in cold regions, flowering could be brought forward by late frosts, and in temperate climates, the cold period requirement would be incomplete, delaying the flowering phase and leading to poor fruit setting and final yield (Funes *et al*., 2016). Furthermore, rising temperatures increase the frequency of severe hailstorms, putting crops at risk (Martín *et al*., 2024).

For statistical analysis, the means, minimums, and maximums of each variable were used. For economic analysis, the following hypothetical scenarios were considered, taking into account the evolution of the independent variables over the last 10 years: a) An increase of 5, 10, and 15 % in the age of the population; b) An increase of 10, 20, and 30 % in the size of the property; and c) An increase of 5, 10, and 15 % in the price of shade cloth, fertilizers, labor, and temperature. The percentage of land suitable for integrating technology was estimated based on the share of irrigated land in the nationwide total.

RESULTS AND DISCUSSION

The model adequately explains the determining factors for the adoption of shade cloth technology. The coefficient of determination (R^2) was 0.95, indicating that the independent variables explain 95 % of the dependent variable, thus suggesting that there is little influence from other variables not explicitly included in the model. The Fisher significance test (F) had a value of 48.49 (Prob > F less than 0.05), so the correlation between the endogenous and exogenous variables is statistically significant and different from zero at $\alpha = 0.05$ (Table 3).

Table 3. Estimated statistical parameters of the glogit model for the adoption rate of shade cloth in apple orchards (*Malus domestica* Borkh.).

Variable	Parameter	Standard errors	*t* value	Prob > *t*
$\sqrt{w_i}$	5.19	4.10	1.27	0.22
*EDA**	0.07	0.04	1.83	0.09
*TAM**	0.11	0.02	7.13	<0.01
*PMP**	-0.0001	0.00004	-3.03	0.01
*PMO**	-0.02	0.01	-2.94	0.01
*PFE**	-0.0004	0.0001	-2.46	0.02
*TMI**	0.28	0.04	7.38	<0.01
R^2	0.95			
F	48.49	Prob > F	<0.01	

EDA*: average age of the population over 15 years old, TAM*: size of the orchard, PMP*: price of protective netting, PMO*: price of labor, PFE*: price of fertilizer, TMI*: average annual minimum temperature.

The model underwent statistical testing for validation. Based on the Breusch-Pagan test, it was concluded that there was no heteroscedasticity in the variance of the error term transformed to an $\alpha = 0.05$. The individual t-tests of the variables orchard size, netting and labor costs, fertilizers, and minimum temperature were significant at $\alpha = 0.05$, while population age was significant at $\alpha = 0.1$. The multicollinearity test was performed using the auxiliary regression method, and no significant collinearity between the independent variables was found. The coefficients of the independent variables had the expected sign. The parameters for producer age, orchard size, and temperature had a positive sign. The parameters for shade cloth prices, labor, and fertilizer have a negative sign.

Statistical analysis showed mixed results in terms of orchard size, mesh prices, fertilizers, and labor (Table 4). In municipalities where shade mesh is used, orchard size was 2.97 ha larger than the average for municipalities with more than 100 ha planted with apples. The minimum and maximum values indicate that there are still municipalities with small-scale backyard production as well as large-scale units. The average price of shade cloth in municipalities that use it was 18.6 % higher than the overall average, and the minimum price was obtained in highly productive units. The average price of fertilizers was 7.3 % lower in municipalities that use shade cloth compared to the overall average. The difference between the minimum and maximum values for this last aggregate was 98.2 %, indicating high variability in these prices at the municipal level. In apple-producing municipalities in the north, labor is paid higher than in the rest of the country. The highest daily wage was in Tamazula, Durango, while the lowest was in Chenalhó, Chiapas.

The model was validated with empirical data using the average probability of adoption by municipalities that use shade cloth (Table 5). The estimated total average probability (0.203) was close to the observed value (0.197). The estimated area of land cultivated with shade cloth was similar (9618 ha) to the observed area (9401 ha),

Table 4. Statistical indicators of the glogit model of the adoption rate of shade cloth (n = 24) in apple orchards (*Malus domestica* Borkh.).

Variable	Municipalities with over 100 ha planted			Municipalities using shade cloth		
	Average	Minimum value	Maximum value	Average	Minimum value	Maximum value
*EDA** (years)	39.94	33.55	48.79	40.84	36.85	48.79
*TAM** (ha)	5.59	0.25	32.61	8.56	0.33	32.61
*PMP**	11 616.00	1866.00	43 000.00	13 772.76	1866.32	43 000.00
*PMO** (daily MXN)	231.62	95.50	378.50	257.92	174.00	320.00
*PFE** (MXN Mg^{-1})	17 951.00	12 375.00	24 533.00	16 733.10	12 390.42	20 925.83
*TMI** (°C)	8.13	2.17	17.10	7.44	2.17	15.83

EDA*: average age of the population over 15 years, TAM*: orchard size, PMP*: price of protective netting, PMO*: price of labor, PFE*: price of fertilizer, TMI*: minimum annual average temperature.

Table 5. Effect of changes in independent variables on the adoption of shade cloth in apple cultivation (*Malus domestica* Borkh.).

Variable	Average total probability	Area cultivated with netting (ha)	Change† (%)	Area with potential (ha)	Cultivated area without netting (ha)	Change¶ (%)
Data observed	0.197	9401		38 535	29 134	-
Base scenario (estimated data)	0.203	9652		38 535	28 883	-
			Change in the independent variables			
EDA increases:						
5 %	0.222	10 595	9.773	38 535	27 940	-3.266
10 %	0.243	11 592	20.102	38 535	26 943	-6.717
15 %	0.265	12 640	30.959	38 535	25 895	-10.346
TAM increases:						
10 %	0.231	11 014	14.110	38 535	27 522	-4.715
20 %	0.261	12 450	28.992	38 535	26 085	-9.688
30 %	0.293	13 936	44.386	38 535	24 599	-14.832
PMP increases:						
5 %	0.201	9554	-1.016	38 535	28 981	0.340
10 %	0.199	9459	-1.999	38 535	29 076	0.668
15 %	0.197	9367	-2.954	38 535	29 168	0.987
PMO increases:						
5 %	0.157	7484	-22.462	38 535	31 051	7.506
10 %	0.119	5687	-41.084	38 535	32 849	13.729
15 %	0.089	4246	-56.009	38 535	34 289	18.716
PFE increases:						
5 %	0.166	7888	-18.271	38 535	30 647	6.106
10 %	0.134	6362	-34.088	38 535	32 174	11.391
15 %	0.106	5069	-47.484	38 535	33 467	15.868
TMI increases:						
5 %	0.218	10 382	7.568	38 535	28 153	-2.529
10 %	0.234	11 137	15.390	38 535	27 398	-5.143
15 %	0.250	11 914	23.431	38 535	26 622	-7.830

†Change relative to the netted area in the base scenario. ¶Change relative to the unnetted area in the base scenario. EDA*: average age of the population over 15 years old, TAM*: orchard size, PMP*: price of protective netting, PMO*: price of labor, PFE*: price of fertilizer, TMI*: average annual minimum temperature.

with a difference of 251 ha or 2.7 % of the observed value, allowing for the creation of scenarios to analyze the effects of changes in the adoption rate of shade cloth in response to changes in the explanatory variables.

The results showed a positive relationship between population age and the adoption of technology, as found by Adams *et al*. (2021) in Ghana. The average age in municipalities where shade cloth is used was 40.84 years, which is lower than the average of 48.6 years observed among agricultural workers (SE, 2024). According to the estimated average probabilities, with a 15 % increase in the age of the population in all apple-producing regions, the total average probability of adopting shade cloth increases from 0.203

to 0.265. In absolute terms, the protected area would increase to 12 640 ha, and the area without shade cloth would decrease by 11.62 %. In a study on apples in Puebla, Mexico, Peraza-Reyes *et al*. (2020) found a positive relationship between the age of producers and the decision to incorporate technological innovations. Younger farmers tend to be less risk-averse and are willing to try new technologies (Gelgo, 2016), so apple growers will find it easier to transition from open-air to protected agriculture.

The average size of the orchard is a variable that had a positive impact on the adoption of shade cloth. A 30 % increase in size would raise the probability of using shade cloth from 0.203 to 0.293; that is, the protected area would be 14 369 ha, and the unprotected area would decrease by 14.8 %. Kolady *et al*. (2021) found a positive relationship between the adoption rate of precision agriculture and farm size. This is because larger production units have more capacity to generate economies of scale by purchasing inputs in bulk and have easier access to credit, technology, and technical assistance. In addition, small associated producers can access better technologies, given that the small size of their production units makes access difficult (Ma *et al*., 2018).

The relationship between the price of the mesh and the adoption rate was negative. Given a 15 % increase in this variable in all municipalities, producers would stop purchasing shade mesh to protect their crops, which would reduce the utilization rate to 0.197. This would increase the area without shade mesh by 0.83 % compared to the base scenario. The results are consistent with García-Salazar *et al.* (2018), who found a negative relationship between the price of the technology and the adoption rate. In their analysis, a 15 % reduction in price would decrease the area without use of the technology by 5.3 %. This decline is caused by the law of demand, since increasing the price of shade cloth decreases the use of the product and therefore its adoption rate, and vice versa.

One of the most important factors in the adoption rate of shade cloth was the price of labor. According to the results, when labor costs increase by 15 %, the adoption rate drops to 0.089. Increases of this magnitude would reduce the adoption rate by up to 56 %. This variable has a negative impact on the adoption of this technology because administrative and labor costs limit producers' ability to incorporate technological innovations on their farms, especially when crops are labor-intensive (Fernández-Reyes and Restrepo-Franco, 2023), as is the case of apple production.

The price of fertilizers had an indirect relationship with the rate of technology adoption. A 10 % increase in price in all municipalities using shade cloth would reduce the average total probability of adoption to 0.134 and the protected area by 11.4 %. Similar results were reported by García-Salazar and Guzmán-Soria (2015), who found that a 10 % decrease in the price of inputs increases the rate of technology adoption by 17.5 %. Increases in input prices have a negative effect on the utilization rate because apple producers tend to prioritize their budget on the purchase of fertilizers rather than crop protection.

The use of shade cloth is a protective measure to control environmental factors in apple production. That is why temperature was a determining factor in the adoption

rate. The relationship between both variables was positive, where a 15 % increase in temperature increases the probability of use to 0.25. This decreased the area without shade cloth by 7.8 % compared to the base scenario. García-Salazar *et al*. (2023) found the same relationship between temperature and the adoption rate of technified irrigation systems in Mexico, although with more accentuated increases of up to 20 %. The effects of the variable on the use of shade cloth are modest, which may be due to growers' lack of knowledge of the advantages of using the correct shade cloth on plant physiology and yield. It is considered that, when faced with increases in temperature, producers take action to protect their investment in their crops.

CONCLUSIONS

The adoption rate of shade cloth technology in apple production is positively correlated with population age and orchard size. Young producers have easier access to this technology, and increasing the size of orchards through land acquisition (renting or purchasing) facilitates the use of shade cloth. The most significant barriers to the adoption of this technology are rising costs for shade cloth, labor, and fertilizers. In contrast, lower prices encourage the acquisition of this technology. The positive relationship between temperature and adoption rate of this technology suggests that apple growers should protect their crops from the effects of rising temperatures.

REFERENCES

Adams A, Jumpah ET, Caesar LD. 2021. The nexuses between technology adoption and socioeconomic changes among farmers in Ghana. Technological Forecasting and Social Change 173: 121133. https://doi.org/10.1016/j.techfore.2021.121133

CONAGUA (Comisión Nacional del Agua). 2023. Resúmenes mensuales de temperaturas y lluvia. Gobierno de México. Comisión Nacional del Agua. Ciudad de México, México. https://smn.conagua.gob.mx/es/climatologia/temperaturas-y-lluvias/resumenes-mensuales-de-temperaturas-y-lluvias (Retrieved: November 2023).

do Amarante CVT, Steffens CA, Argenta LC. 2011. Yield and fruit quality of 'Gala' and 'Fuji' apple trees protected by white anti-hail net. Scientia Horticulturae 129 (1): 79–85. https://doi.org/10.1016/j.scienta.2011.03.010

FAO (Food and Agriculture Organization). 2023. FAOSTAT. Statistical database, trade, detailed trade matrix. Food and Agriculture Organization of the United Nations. Rome, Italy. https://www.fao.org/faostat/es/#data/TM (Retrieved: May 2024).

Favret-Tondato RC. 2012. Manzaneros chihuahuenses. Trayectoria y organización. Colegio de Postgraduados: San Luis Huexotla, México. 149 p.

Fernández-Reyes DF, Restrepo-Franco GM. 2023. Evaluación de la adopción de buenas prácticas agrícolas en sistemas cafeteros con base en el análisis anual de costos de producción y sostenimiento. Inventum 18 (35): 29–49. https://doi.org/10.26620/uniminuto.inventum.18.35.2023.29-49

Funes I, Aranda X, Biel C, Carbó J, Camps F, Molina AJ, Herraldea F, Graua B, Savé R. 2016. Future climate change impacts on apple flowering date in a Mediterranean subbasin. Agricultural Water Management 164: 19–27. https://doi.org/10.1016/j.agwat.2015.06.013

García-Salazar JA, Bautista-Mayorga F, Reyes-Santiago E. 2023. Factores que condicionan la tasa de adopción de sistemas de riego tecnificados en México. Agronomía Mesoamericana 51202. https://doi.org/10.15517/am.v34i2.51202

García-Salazar JA, Borja-Bravo M, Rodríguez-Licea G. 2018. Consumo de fertilizantes en el sector agrícola de México: un estudio sobre los factores que afectan la tasa de adopción. Interciencia 43 (7): 505–510.

García-Salazar JA, Guzmán-Soria E. 2015. Factores que afectan la demanda de semilla mejorada de maíz en México. Revista Fitotecnia Mexicana 38 (3): 319–327.

Gelgo B, Mshenga P, Zemedu L. 2016. Analysing the determinants of adoption of organic fertilizer by smallholder farmers in Shashemene District, Ethiopia. Journal of Natural Sciences Research 6 (19): 35–44.

Giacinti MÁ. 2003. Pensamiento estratégico en el negocio mundial de manzanas. Agroalimentaria 8 (17): 49–60.

Gujarati D, Porter D. 2010. Econometría (Quinta edición). Interamericana Editores S.A. de C.V.: Ciudad de México, México. 921 p.

Gunathilaka RPD, Smart JC, Fleming CM. 2018. Adaptation to climate change in perennial cropping systems: Options, barriers and policy implications. Environmental Science and Policy 82: 108–116. https://doi.org/10.1016/j.envsci.2018.01.011

INEGI (Instituto Nacional de Estadística y Geografía). 2021. Programas de información. Censo de población y vivienda 2020. Ciudad de México, México. https://www.inegi.org.mx/programas/ccpv/2020/ (Recuperado: mayo 2024).

INEGI (Instituto Nacional de Estadística y Geografía). 2023. Programas de información. Programas de información. Censo Agropecuario 2022. Ciudad de México, México. https://www.inegi.org.mx/programas/ca/2022/ (Retrieved: May 2024).

Kolady DE, van der Sluis E, Uddin MM, Deutz AP. 2021. Determinants of adoption and adoption intensity of precision agriculture technologies: Evidence from South Dakota. Precision Agriculture 22 (3): 689–710. https://doi.org/10.1007/s11119-020-09750-2

Ma W, Renwick A, Yuan P, Ratna N. 2018. Agricultural cooperative membership and technical efficiency of apple farmers in China: An analysis accounting for selectivity bias. Food policy 81: 122–132. https://doi.org/10.1016/j.foodpol.2018.10.009

Martín ML, Calvo-Sancho C, Taszarek M, González-Alemán JJ, Montoro-Mendoza A, Díaz-Fernández J, Bolgiani P, Sastre M, Martín Y. 2024. Major role of marine heatwave and anthropogenic climate change on a giant hail event in Spain. Geophysical Research Letters 51 (6). https://doi.org/10.1029/2023GL107632

Noè N, Eccher T. 1996. 'Golden Delicious' apple fruit shape and russeting are affected by light conditions. Scientia Horticulturae 65 (2–3): 209–213. https://doi.org/10.1016/0304-4238(95)00850-0

Peraza-Reyes JD, Escobedo-Garrido JS, Pérez-Magaña A, Virginia-González M. 2020. La aceptabilidad tecnológica en los pequeños productores de manzana de José María Morelos, Tlachichuca, Puebla. Estudios Sociales. Revista de Alimentación Contemporánea y Desarrollo Regional 30 (56). https://doi.org/10.24836/es.v30i56.921

Porsch A, Gandorfer M, Bitsch V. 2018. Strategies to manage hail risk in apple production. Agricultural Finance Review 78 (5): 532–550. https://doi.org/10.1108/afr-07-2017-0062

Potapov P, Turubanova S, Hansen MC, Tyukavina A, Zalles V, Khan A, Song XP, Pickens A, Shen Q, Cortez J. 2022. Global maps of cropland extent and change show accelerated cropland expansion in the twenty-first century. Nature Food 3 (1): 19–28. https://doi.org/10.1038/s43016-021-00429-z

Prakash P, Kumar P, Kar A, Kishore P, Singh AK, Immanuel S. 2021. Protected cultivation in Maharashtra: Determinants of adoption, constraints, and impact. Agricultural Economics Research Review 34 (2): 217–228. https://doi.org/10.5958/0974-0279.2021.00031.8

Prakash P, Kumar P, Kar A, Singh AK. 2020. Status and impact of protected cultivation of horticultural crops in Maharashtra. Indian Journal of Horticulture 77 (3): 518–526. https://doi.org/10.5958/0974-0112.2020.00075.4

Ramírez-Legarreta MR, Jacobo-Cuéllar JL, Ávila-Marioni MR, Parra-Quezada RÁ. 2006. Pérdidas de cosecha, eficiencia de producción y rentabilidad de huertos de manzano con diversos grados de tecnificación en Chihuahua, México. Revista Fitotecnia Mexicana 29 (3): 215–222. https://doi.org/10.35196/rfm.2006.3.215

SE (Secretaría de Economía). 2024. Data México. Trabajadores en Actividades Agrícolas y Ganaderas. Gobierno de México. Secretaría de Economía. Ciudad de México, México. https://www.economia.gob.mx/datamexico/es/profile/occupation/trabajadores-en-actividades-agricolas-y-ganaderas (Retrieved: May 2024).

Severino V, Dogliotti S, Echeverría G, Frins E, González-Talice J, Yuri JA, Arias-Sibillotte M. 2023. Daño de sol y potencial hídrico de tallo y tejidos del fruto de manzanas (*Malus domestica*) 'Brasil Gala', 'Cripps Pink' y 'Granny Smith'. Agrociencia Uruguay 27 (NE1): e1213. https://doi.org/10.31285/agro.27.1213

Shashikala SR, Goudappa SB, Reddy BS, Shashidhara KK. 2022. Adoption level of farmers on protected cultivation technologies in Kalyana Karnataka region of Karnataka. The Pharma Innovation Journal 11 (6S): 1077–1081.

SIAP (Servicio de Información Agroalimentaria y Pesquera). 2024. Producción agrícola, acciones y programas. Gobierno de México. Secretaría de Agricultura y Desarrollo Rural. Servicio de Información Agroalimentaria y Pesquera. Ciudad de México, México. https://nube.siap.gob.mx/cierreagricola/ (Retrieved: February 2024).

SNIIM (Sistema Nacional de Información e Integración de Mercados). 2024. Mercados nacionales. Gobierno de México. Secretaria de Economía. Sistema Nacional de Información e Integración de Mercados. Ciudad de México, México. http://www.economia-sniim.gob.mx/nuevo/ (Retrieved: February 2024).

Theil H. 1970. On the estimation of relationships involving qualitative variables. American Journal of Sociology 76 (1): 103–154. https://doi.org/10.1086/224909

Wand SJE, Gindaba J. 2005. Controlling sunburn: What are the options? South African Fruit Journal 4: 24–26.

Agrociencia

DETERMINATION OF THE PRACTICAL CULTIVATION COEFFICIENT OR IRRIGATION FACTOR IN CHERIMOLIA ORCHARDS (*Annona cherimola* Mill.) USING SOIL SENSORS

Esteban Jesús **Gárate-Cortés**[1], Rodrigo Ignacio **Reyes-Sánchez**[1], Rodrigo Homero **Callejas-Rodríguez**[1*]

[1]Universidad de Chile. Facultad de Ciencias Agronómicas Santiago, Chile. Santa Rosa 11315, La Pintana, Santiago, Chile. C. P. 882 08 08.
* Author for correspondence: rcalleja@uchile.cl

Citation: Gárate-Cortés EJ, Reyes-Sánchez RI, Callejas-Rodríguez RH. 2025. Determination of the practical cultivation coefficient or irrigation factor in cherimolia orchards (*Annona cherimola* Mill.) using soil sensors. **Agrociencia** 59(5): 768-783. https://doi.org/ 10.47163/agrociencia.v59i5.3257

Editor in Chief:
Dr. Fernando C. Gómez Merino

Received: January 01, 2025.
Approved: August 04, 2025.
Published in Agrociencia: August 11, 2025.

ABSTRACT

Given the growing water scarcity and the need to make cherimoya (*Annona cherimola* Mill.) cultivation more sustainable, this study proposes using soil sensors to increase irrigation water use efficiency (EUAr) without compromising fruit yield or quality. The objective was to determine the practical crop coefficient (KcS) or irrigation factor by using capacitance probes to continuously determine the dynamics of water absorption from the soil by the crop. To this end, a completely randomized block design trial was conducted over two seasons, incorporating two irrigation treatments: the control (To) and cherimoya trees irrigated according to the FAO-56 Penman-Monteith (Kc-ETo) methodology, as established by the Food and Agriculture Organization of the United Nations (FAO). This approach utilized data obtained from soil sensors and the interpretation of management guidelines for efficient irrigation. Crop productivity and resource use efficiency were assessed. Likewise, relationships between crop phenology and changes in the normalized difference vegetation index (NDVI) were explored to determine curves that estimate the optimal KcS for the season. The use of sensors resulted in a notable increase in EUAr in both seasons, reaching a maximum of 68 % compared to the methodology proposed by FAO. No significant differences were detected between treatments in terms of yield or fruit size. The optimal mean and 70th percentile values of the crop coefficient (KcS) obtained were 0.43–0.47 for the flowering stage, 0.66–0.73 for the fruit set stage (start of fruit growth), and 0.43 for the fruit growth stage until harvest. Likewise, when reference evapotranspiration exceeded 2.25 mm per day, there was a clear difference in soil water depletion between levels above and below the irrigation threshold. Finally, it was observed that the crop absorbed the most water between 13:00 and 16:00 hours.

Keywords: Efficient irrigation, capacitance, water use efficiency, sustainability.

INTRODUCTION

Spain and Peru are the world's leading producers of cherimoya (*Annona cherimola* Mill.), producing 104 835 290 and 20 505 Mg annually, respectively (Larranaga *et al*., 2017; SIEA, 2018; MAPA, 2019; Vallejo, 2024). In Chile, annual production is around

3734.4 Mg per year, and the main production area is the Coquimbo Region in the north of the country, destined for export to the United States and the domestic market. However, due to the effects of climate change, this region has been subject to structural drought for more than 10 years (Pizarro *et al*., 2022a), prompting the need to develop strategies and adopt technological tools to reduce water consumption for irrigation in agriculture.

In technified orchards, crop water requirements are determined using the methodology proposed by the Food and Agriculture Organization of the United Nations (FAO) (Allen *et al*., 1998). In this way, crop evapotranspiration (ETc) can be obtained in millimeters per day (mm d^{-1}) from the product of reference evapotranspiration (ETo), determined using the Penman-Monteith method, and the crop coefficient (Kc), obtaining a dimensionless value (ETc = ETo × Kc). However, the value of Kc is not clearly defined for the soil and climate conditions of Chile's main production area.

In this context, Gardiazábal and Rosenberg (1993) proposed Kc values for orchards located in the Quillota area (central Chile, with a Mediterranean climate), establishing a minimum value of 0.2 for the period of lowest water consumption by the tree and a maximum value of 0.8 during its peak growth phase. Meanwhile, in Almuñécar, Spain, Rodríguez-Pleguezuelo *et al.* (2011) and Durán-Zuazo *et al*. (2019) estimated Kc values for cherimoya cultivation under conventional management in Mediterranean climate conditions. Both studies reported average Kc values between 0.62 and 0.63 during flowering, between 0.65 and 0.68 during fruit set, and between 0.5 and 0.55 during fruit growth. These studies confirm that the Kc value must be determined for each agroclimatic zone and even consider the existence of specific agronomic management practices, as these can significantly affect the ETc estimate (Calera *et al*., 2017; Domínguez-Niño *et al*., 2020).

Agriculture 4.0 is defined as the collection of technologies (equipment, sensors, and software) focused on the digitization of agricultural processes, big data analysis, and the use of the Internet of Things (IoT) to improve the production process from start to end, making it faster, cost-effective, and sustainable. The use of continuous reading soil sensors, such as capacitance probes or frequency domain reflectometry probes, has made it possible to generate more efficient irrigation strategies than those achieved using the FAO-56 Penman-Monteith methodology. These probes are currently considered one of the major technological advances for irrigation control in agriculture (Abioye *et al*., 2020; Hardie, 2020; Martínez-Gimeno *et al*., 2020).

The sensors continuously assess the volumetric water content in the soil at different depths, allowing the hourly or daily depletion caused by the root system to be determined. In addition, the information obtained from these measurements allows water balances to be calculated and deep percolation below the active root zone to be estimated (Coelho *et al*., 2021; Pizarro *et al*., 2022b), thus optimizing irrigation efficiency (da Silva, 2020). This approach also allows the determination of the so-called practical crop coefficient 'Kc probe' (KcS, dimensionless) (Callejas-Rodríguez and Seguel, 2021) or irrigation factor (IF) (Vera *et al*., 2019), which integrates variables such as vegetation

cover, location coefficient (Kr), and the efficiency of the irrigation system used. This strategy is particularly relevant at the farm level, as it represents a more practical and less costly alternative to the use of weighing lysimeters to obtain the Kc coefficient for the species.

In addition, KcS facilitates rational access to technology on medium-sized or large farms, characterized by a high number of irrigation sectors. Through categorized grouping (clustering) that considers variables such as variety, rootstock, soil types, and foliage expression (Callejas-Rodríguez and Seguel, 2021), and by determining the KcS or FI, it is feasible to manage multiple irrigation sectors belonging to the same cluster. This can be achieved from a single sector equipped with soil sensors and by adjusting the criteria using complementary technologies (satellite images, Scholander pressure pump, dendrometry, and other indicators), which reduces the investment in technology.

Given the limited information available to determine the water requirements of cherimoya cultivation, and considering the need to implement sustainable irrigation management systems to address water scarcity, the hypothesis was proposed that the use of soil sensors and the implementation of the concept of Agriculture 4.0 would increase irrigation water use efficiency (EUAr). In this context, the objective of the research was to determine a practical crop coefficient that maximizes water productivity without affecting the yield or export quality of the fruit.

MATERIALS AND METHODS

The study was conducted in northern Chile, in La Serena, Coquimbo Region, on commercial plots owned by HC Ltda., Fundo Corazón de María (29° 58.844' S, 71° 13.486' W, at an altitude of 100 m), during the 2019 and 2020 seasons. The study area has a climate classified as 'BMk' according to the Köppen-Geiger classification, corresponding to the coastal steppe or cloudy type, with an average annual temperature of 16 °C and approximate precipitation of 104 mm per year concentrated in the winter.

The study was conducted with 10-year-old cherimoya trees (*Annona cherimola* Mill.), "Concha Lisa" cultivar, planted at 5 x 2.5 m and formed into a cup shape. The irrigation system was located with two lines of emitters per tree and drippers every 0.5 m on the line with a flow rate of 2.8 L h^{-1}, whose precipitation from the equipment corresponded to 2.3 mm h^{-1}, with irrigation efficiency and a uniformity coefficient of 90 % each. The bulb was well defined, with a root system located mainly in the first 50 cm of the soil profile (Figure 1), with a high presence of fine and medium roots that decrease in depth, where the thick roots are located. The soil, with a high degree of evolution, has a sandy loam texture in the first 50 cm, a pH of 7.5, an electrical conductivity (CE) of 0.85 dS m^{-1}, an organic matter content of 0.97 %, and a stoniness of 3.7 %.

A completely randomized block design was used with two irrigation treatments and five replicates per treatment, considering four trees as the experimental unit. The first treatment was the control field (To), where trees were irrigated using the

Figure 1. Soil profile of "Concha Lisa" cherimoya trees (Annona cherimola Mill.) observed through a trial pit dug in the row, 50 cm from the tree trunk and in the area corresponding to the irrigation bulb.

methodology proposed by FAO (Allen *et al*., 1998). Crop evapotranspiration was obtained in millimeters per day (mm d^{-1}) using the expression $ETc = ET_0 \times Kc$, where ET_0 corresponds to reference evapotranspiration (mm d^{-1}), determined using the Penman-Monteith method, and Kc to the crop coefficient (dimensionless) proposed by Gardiazábal and Rosenberg (1993). Furthermore, a second treatment was considered, using capacitance probes with multisensors (Ts). The irrigation criterion was based on the evaluation of the dynamics of soil water content and its relationship with plant extraction, adjusting the frequency and timing of irrigation in accordance with the management guidelines for the use of soil sensors (Vera *et al*., 2019; Callejas-Rodríguez and Seguel, 2021).

The management lines used in the Ts treatment corresponded to: i) full level (NLL), which is the maximum water capacity that the soil can hold without producing deep percolation and where the sensor located at greater depth should not show activity (daily depletion); ii) probe field capacity (CCs), which refers to the water content in the soil evaluated with the probe after a heavy rainfall or irrigation event and being left to drain freely for 24 to 48 h (Zotarelli *et al*., 2019); and iii) recharge point (PR), equivalent to the irrigation threshold based on the capacitance probe technique, where, for the same atmospheric demand, a decrease in daily depletion is observed compared to the previous day, indicating that plants face greater difficulties in extracting water due to the progressive depletion of water resources (increased tension). The management

guidelines described and the data obtained by the sensors were interpreted in real time using the Irrimax Live platform (Sentek Technologies, Australia).

In both treatments, an SF model volumetric line meter (Arad, Israel) was installed to determine the volume of irrigation water used. An EnviroscanMR frequency domain reflectometry capacitance probe (Sentek Technologies, Australia) was also installed. The probe was calibrated for the study site and set 30 cm from the trunk of a representative plant, next to a dripper. Each probe had five sensors located at depths of 10, 20, 30, 50, and 80 cm in the soil profile. The readings from each sensor were recorded every 15 min. A Davis Vantage weather station (Davis Instruments, California, USA) was installed in the area to obtain temperature, reference evapotranspiration (ETo), and degree days (10 °C-based), with the biofix being the time of pruning (°DG).

To determine the apparent daily consumption of the trees (ETc), a water balance was performed, quantifying the inputs and outputs of the system according to the following equation:

$$ETc = R + P_{ef} + Ac - Es - P_{prof} - \Delta S$$

where ET_c is crop evapotranspiration (mm), R is irrigation quota (mm), P_{ef} is effective precipitation (mm), Ac is capillary rise (mm), Es is surface runoff (mm), P_{prof} is deep percolation (mm), and ΔS is the change in volumetric water content in the soil in the root zone (mm). Surface runoff was considered zero, as the orchard did not have a prominent slope, as was capillary rise, which was deemed insignificant for the balance. Deep percolation was calculated as the volume of water infiltrated below the last sensor in reference to NLL.

To calculate the practical crop coefficient (*KcS*), the 70th percentile of the data was used, and two assumptions were made: 1) The water content in the soil was adequate and not limiting for the plant; and 2) Outside irrigation periods, $ET_c = \Delta S$, because the daily variation in soil water content was due solely to evapotranspiration, with no percolation or water inputs, these values being zero. Finally, *KcS* was calculated from ET_c and its relationship with ET_o, using the formula:

$$KcS = \frac{ET_c \text{ or effective irrigation}}{ET_o}$$

Additionally, the following production variables were determined: i) fruit load, expressed as the total number of fruits harvested per tree; ii) average fruit weight, estimated from a subsample of 20 fruits per tree; and iii) total yield per tree. Likewise, vegetative growth was evaluated as the increase in trunk cross-sectional area (Δ ASTT) and the evolution of the normalized difference vegetation index (NDVI), based on images obtained with a multispectral imaging sensor (MSI) mounted on the Sentinel 2A and 2B satellites, with a spatial resolution of 10 m and a temporal resolution of

10 days. The bands used were B2, B3, B4, B8, B8a, and B11. The download format was L1-C from the top of the atmosphere (TOA), so the images were transformed to background surface reflectance (BOA) based on the two-step atmospheric correction method (Chávez, 1988). Moreover, to extrapolate irrigation protocols, the relationships between *KcS* obtained with NDVI and the accumulation of °DG for different periods in the season were explored. Finally, irrigation water use efficiency (EUAr) was determined as the ratio between yield and the volume of irrigation water used per hectare.

The data were analyzed using mixed linear models. The fixed effects are the irrigation treatments, and the random effects are the number of fruits harvested, fruit weight, yield per tree, and increase in trunk cross-sectional area. In cases where differences were detected between treatments, a Fisher's multiple comparison test was performed with $p \leq 0.05$, after verifying the assumptions of homogeneity of variance and normality of errors. Infostat and RStudio software were used.

RESULTS AND DISCUSSION

The evolution of the mean temperature and reference evapotranspiration in the trial sector was marked by the seasons of the year. In the case of temperature, the average maximum was 22 °C in January and the minimum was 7 °C in June. The maximum ET_o rose to 4.8 mm d^{-1} in summer and a minimum of 1.8 mm d^{-1} in winter (Figure 2). The total annual ETo was equivalent to 896.96 mm.

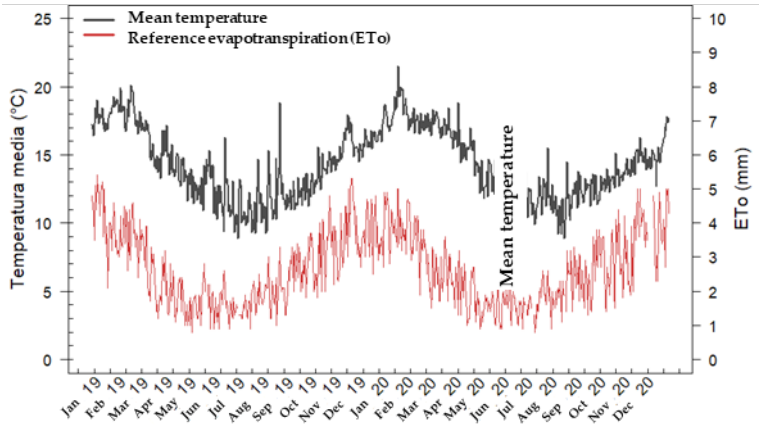

Figure 2. Evolution of the average ambient temperature (°C) and reference evapotranspiration (ETo) in the test area (southern hemisphere, La Serena, Coquimbo Region, Chile).

From pruning, it took approximately 314 calendar days to reach harvest, equivalent to around 1100 °DG for the fruit to ripen properly (Figure 3). Due to possible variations in mean temperatures in the area during the autumn and winter months (April, May,

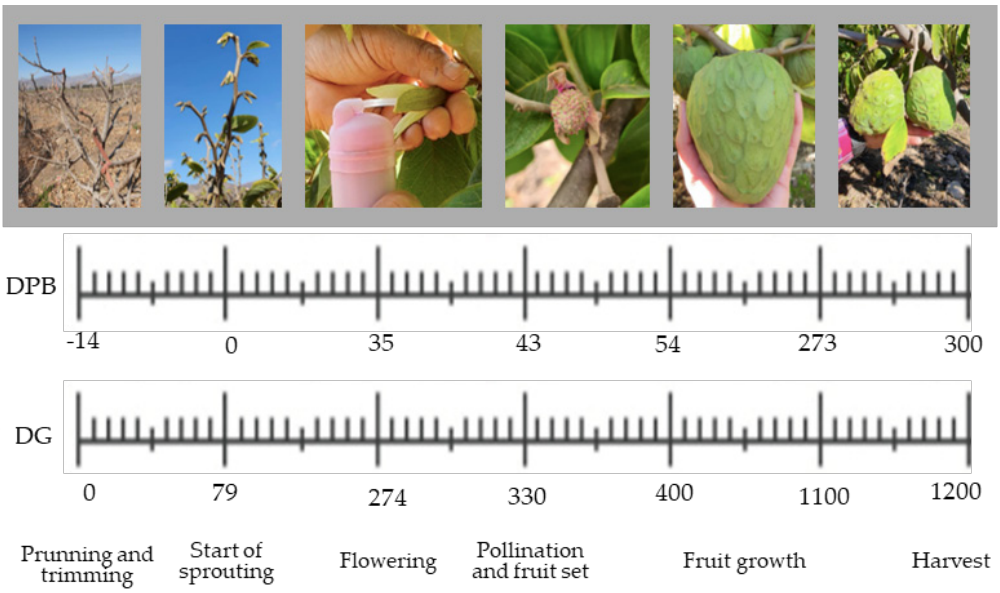

Figure 3. Estimation of duration (days after bud break, DAB) and accumulation of degree days (°DG), based on 10 °C, of phenological stages for the entire period (mean of both seasons), from the date of pruning of cherimoya plants (*Annona cherimola* Mill.).

June, and July), the harvest date for the same pruning date can vary between 20 and 15 calendar days. Pruning begins in late November (southern hemisphere, spring), with harvesting taking place in July-August of the following year (winter).

Water balance

The 2019 season saw low rainfall, with only 10.79 mm between the end of May and mid-June. These volumes did not exceed 80 cm in depth or NLL in the treatments, with the entire amount being considered effective precipitation. The percolation amounts attributed to irrigation management were higher in To, reaching 183.4 mm, while in Ts, 90.8 mm of percolation were recorded, distributed throughout the season. During the 2020 season, rainfall was 52 mm in two events in winter, with deep percolation observed only in To. The percolated amounts in the treatments were 167 mm and 28.7 mm for To and Ts, respectively (Figure 4), demonstrating more accurate programming, as pointed out by Gasque *et al*. (2016).

Treatment To showed greater inaccuracy in determining irrigation water requirements, with significant variations in ETc reported in many cases when comparing the results against the original unit in which it was developed (Pereira *et al*., 2021). Throughout the study, the Ts method allowed for a 65.9 % saving in deep percolation.

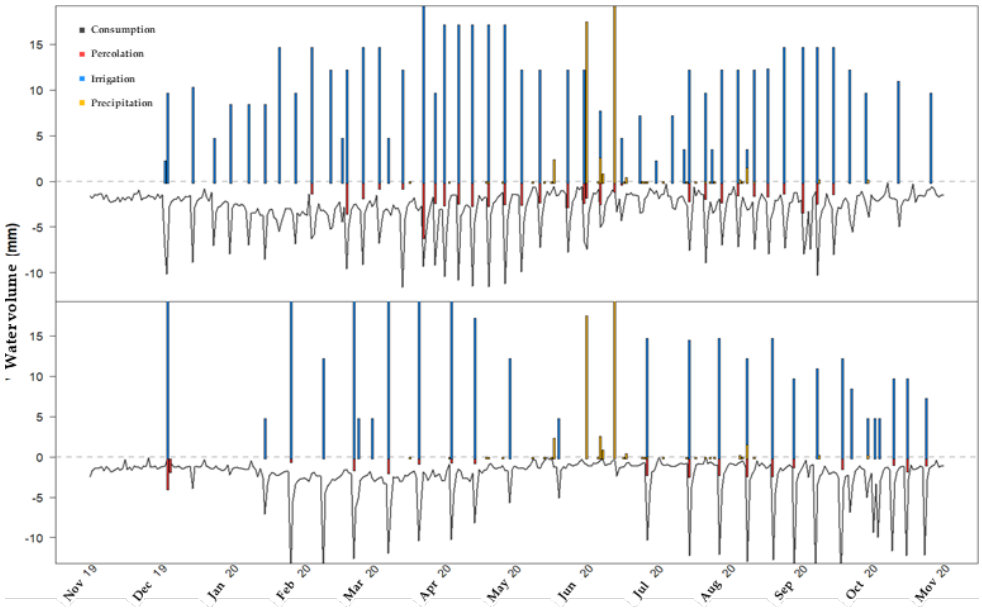

Figure 4. Temporal course of irrigation, precipitation, change in volumetric water content, and percolation in the control treatment (To, upper) and the treatment with capacitance probes (Ts, lower) during the 2020 season.

Practical crop coefficient (KcS) or irrigation factor

Using the information generated with Ts, KcS was calculated, from which three well-defined stages can be highlighted (Figure 5). For the 2019 season, the range of average values for the 70th percentile for the flowering, fruit set, and fruit growth stages evaluated was 0.63–0.75, 0.67–0.79, and 0.59–0.66, respectively. For the 2020 season, the average value ranges for the aforementioned stages were 0.43–0.47, 0.66–0.73, and 0.43, respectively, which were adjusted to a better definition of irrigation time and frequency based on the experience of the previous year. The possibility of continuously measuring irrigation water inflows and outflows at various intervals between irrigations for the estimation of KcS allows the equation to be simplified to the variation in daily water content, achieving results similar to the work carried out on peach trees by Vera *et al*. (2019), who also used capacitance probes.

The optimization of irrigation water use in the 2020 season is due to factors relevant to implementing this methodology: a) one year of experience allows for the stabilization of the initial variability of the data associated with the process of installing capacitance probes in the soil; and b) the optimization of irrigation criteria, after one year of information, is related to the adjustment of irrigation management lines. Moreover, irrigation criteria must be validated with optimal yield results, as well as the quality of export fruit. It is advisable to use other water status indicators to evaluate the irrigation schedule for the season, such as the water potential of the stem at solar noon (Vera *et*

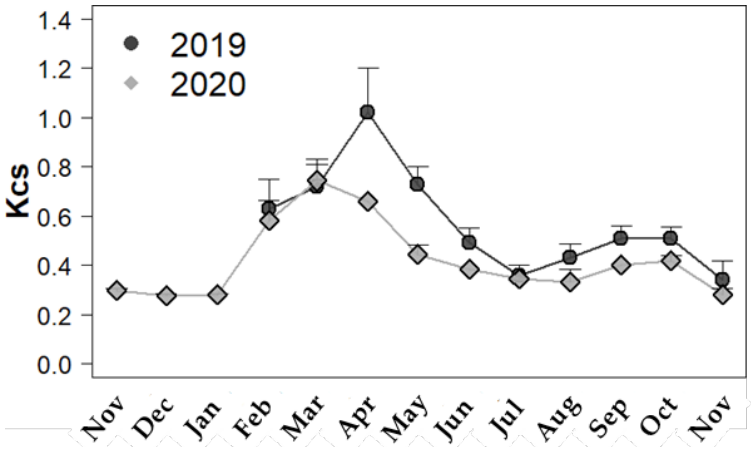

Figure 5. Average practical crop coefficient (KcS) of the 70th percentile per month for the 2019 and 2020 seasons, determined using information obtained from irrigation treatment with capacitance probes (Ts) in a cherimoya orchard (*Annona cherimola* Mill.). Vertical bars correspond to the 70th percentile.

al., 2019; Callejas-Rodríguez and Seguel, 2021). However, for the cherimoya crop, this was not feasible due to the thickness of the petiole and the excessive size of the leaves. The estimated KcS values for the 2020 season were compared with the Kc values proposed by other authors for this species in its different phenological stages obtained by other authors (Rodríguez-Pleguezuelo *et al*., 2011; Durán-Zuazo *et al*., 2019), and the means for the flowering, fruit set, and fruit growth stages were plotted (Figure 6).

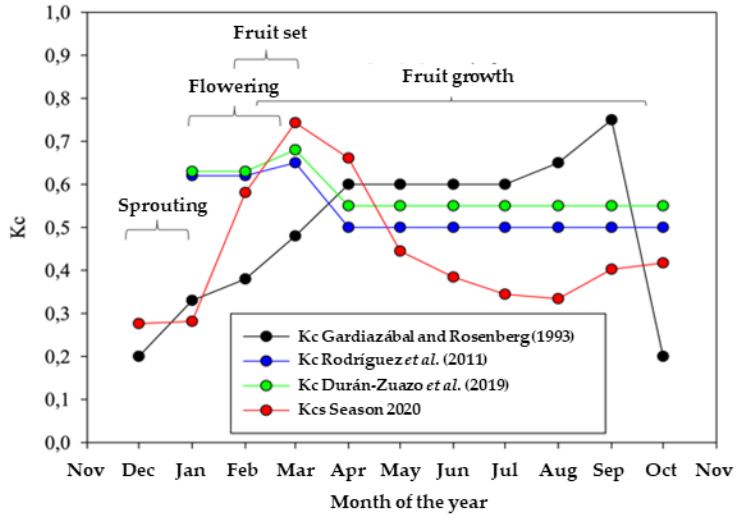

Figure 6. Estimation of the practical crop coefficient (KcS) for the 2020 season compared with different values proposed for the cultivation of cherimoya (*Annona cherimola* Mill).

During the summer (January and February), ETo ranged between 3.16 and 4.35 mm d^{-1}, dropping in winter to values between 0.56 and 2.26 mm d^{-1}. Devi and Reddy (2018) point out that, in autumn and winter, temperature and vapor pressure deficit decrease, and with them plant transpiration, generating low ETc values. This condition was observed in the dynamics of soil water content measured with capacitance probes, coinciding with Kirkham (2005), who points out that tree transpiration (water absorption by active roots) depends fundamentally on the volumetric water content in the soil when atmospheric demand is high. However, when it is very low, as in the study area, trees maintain a low transpiration rate regardless of the water content in the soil.

For cherimoya, an ETo below 2.25 mm d^{-1} does not have a clear effect on the daily moisture deficit monitored in the soil, both for optimal and suboptimal water availability conditions (Figure 7). However, once demand exceeds 2.5 mm d^{-1}, it is clear that low irrigation water availability (below the recharge point) is insufficient to compensate for this increase in atmospheric demand, a situation that occurs when the crop is not subject to limiting soil water conditions.

According to Higuchi *et al*. (1998), stomatal conductance in cherimoya leaves under 12 hours of daylight conditions shows two peaks according to the traditional schedule: one at 8:00 a.m. and another at 6:00 p.m., with the former being higher in the early morning. Considering that stomatal opening depends on solar radiation (Allen *et al*., 1998), it is important to note that in the test area, due to permanent cloud cover in the mornings, solar radiation values were low from sunrise until midday. Subsequently,

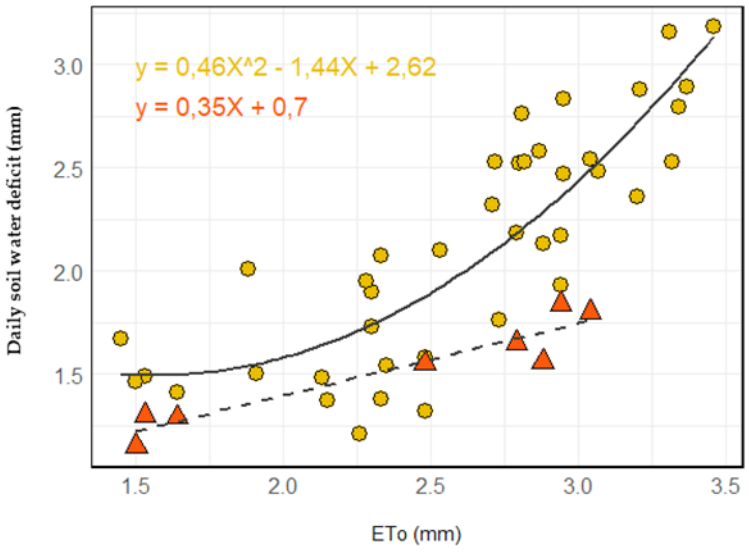

Figure 7. Relationship between reference crop evapotranspiration (ETo) and daily water deficit caused at root level in the area monitored with an Enviroscan sensor (depths of 20, 30, and 50 cm) for two soil moisture conditions: a) content between field probe capacity (CCs) and recharge point (PR) (yellow circles), and b) below PR or irrigation threshold (red triangles).

they increased (from 40 to 60 %) and remained so until 3:00 p.m., gradually decreasing thereafter. Therefore, it could be assumed that, as a result of low radiation and stomatal opening, the expected morning maximum did not occur, which would be reflected in the absorbent activity of the roots (Figure 8). This increased late, around midday, maintaining higher consumption until 4:00 p.m., the time when the production area traditionally clears up.

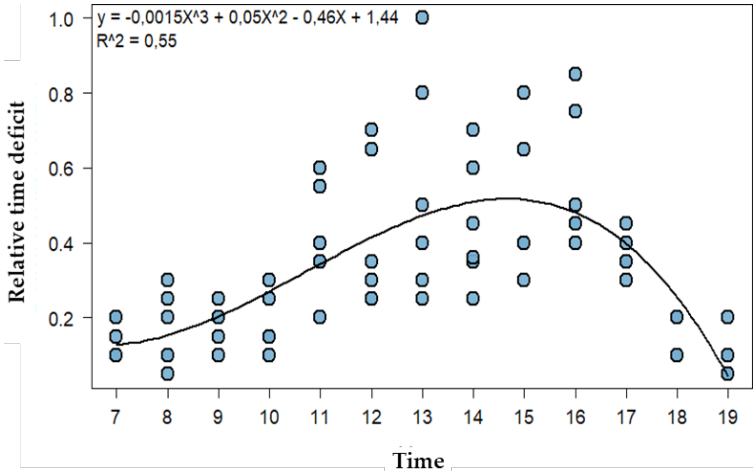

Figure 8. Hourly water deficit in the soil caused by cherimoya trees in the area monitored with an Enviroscan sensor (at depths of 20, 30, and 50 cm), according to the time of day.

These conditions contrast with those found in Andalusia, Spain, where the flowering-to-harvest period occurs in spring and summer with higher solar radiation, a mean annual temperature of 20 °C, high relative humidity (Rodríguez-Pleguezuelo *et al*., 2011), and up to 11 mm d^{-1} of ETo (Durán-Zuazo *et al*., 2019). With these climatic characteristics and proper irrigation, hypothetical explanations could be given for the possibilities of a higher transpiration rate and greater production potential, with yields of up to 40 Mg ha^{-1} (González and Cuevas, 2008) or fewer calendar days to harvest. Another determining factor that could partially explain the low KcS values in winter is the percentage of ground cover by trees, which would affect the location coefficient (Allen *et al*., 1998). An orchard with 70 % coverage by mature trees can result in a Kc value of less than one, as occurred in the trial, where the trees reached 59 % coverage. One of the commercial objectives of generating the practical crop coefficient on medium-sized or large farms is the possibility of extrapolating the experience of one irrigation sector to others that meet categorical criteria (cluster formation) (Callejas-Rodríguez and Seguel, 2021) that do not have soil sensors. With the information obtained from this study, two functions are proposed to define KcS (Table 1): function A, using days post-sprouting, and function B, using °DG as a cumulative predictor from pollination.

Table 1. Functions to determine the practical crop coefficient (*KcS*) based on the accumulation of degree days since pollination (°DG) or based on the days after sprouting (DPB) for the 2020 season.

Function	Variable		Equation	R^2
	Dependent	Independent		
A	*KcS*	DPB	$y = 9 \cdot 10^{-8}x^3 - 5 \cdot 10^{-5}x^2 + 0.0082x + 0.2303$	0.60
B	*KcS*	°DG	$y = 3 \cdot 10^{-9}x^3 - 6 \cdot 10^{-6}x^2 + 0.0032x + 0.2379$	0.77

Additionally, for the relationship between NDVI and KcS, three periods were identified, each with a different function (Table 2). The first period (C) ran from the start of the season to the beginning of autumn (590 accumulated °DG); the second (D) ran from autumn to the end of winter (750 accumulated °DG); and the third (E) ran from the start of spring (770 accumulated °DG) to the end of the season.

Table 2. Functions for determining the practical crop coefficient (*KcS*) from the normalized difference vegetation index (NDVI) for the periods from the start of the season to autumn (C), from autumn to the end of winter (D), and from the start of spring to the end of the season (E).

Funtion*	Variable		Equation	R^2
	Dependent	Independent		
C (590 °DG)	*KcS*	NDVI	$y = 0.8928x + 0.0213$	0.80
D (750 °DG)			$y = 0.8185x + 0.2844$	0.86
E (770 °DG)			$y = 0.3474x + 0.2043$	0.36

*The values in brackets indicate the cumulative degree days since pollination (°DG) for the start of each period.

The KcS values showed a high correlation with the NDVI values. As pointed out by Pôças *et al*. (2020), the use of vegetation indices may be a useful tool for irrigation management in the context of precision agriculture. A high correlation was also found with the accumulated °DG since pollination, which would allow for more efficient irrigation in areas without soil sensors.

In general, no significant differences were detected that could indicate that irrigation treatments would cause problems in fruit yield and quality (Table 3). An increase in the cross-sectional area of the trunk was only detected in the second season for Ts compared to To.

The use of soil sensors allowed for a significant reduction in irrigation water volumes compared to the FAO-56 Penman-Monteith (Kc-ETo) methodology (Table 4). In cherimoya orchards in Spain, the irrigation volume used was similar to that obtained with Ts (3970 m^3 ha^{-1}) (Durán-Zuazo *et al*., 2019), but clearly lower than that used

Table 3. Production parameters and increase in trunk cross-sectional area (Δ ASTT) obtained for each treatment and season.

Season and treatment	Fruit load (Number of fruits per tree)	Fruit weight (g)	Yield (kg tree^{-1})	Δ ASTT (cm^2 tree^{-1})
2019				
To	75.4	305.0	21.5	3.23
Ts	79.7	312.9	24.4	3.28
2020				
To	44.5	549.4	24.9	2.06b
Ts	45.1	600.2	26.6	5.32a

Different letters indicate significant differences between treatments for the same parameter and season ($p < 0.05$). To: control treatment; Ts: irrigation treatment with capacitance probes.

Table 4. Irrigation water volume, irrigation water use efficiency (EUAr), and resource savings achieved for each treatment.

Season and treatment	Irrigation (m^3 ha^{-1})	EUAr (kg m^{-3})	Water saving compared to To (m^3 ha^{-1})	Energy saving compared to To USD ha^{-1}
2019				
To	5916	2.9		
Ts	4255	4.6	1661 (28.1 %)	315.4
2020				
To	5169	3.8		
Ts	3360	6.4	1823 (35.3 %)	346.1

Different letters indicate significant differences between treatments for the same parameter and season ($p < 0.05$). To: control treatment.

by To. However, other studies in the same country have recorded volumes between 6000 and 7160 m^3 ha^{-1} year^{-1} (González and Cuevas, 2008; Soler and Cuevas, 2008), which are higher than both treatments. These results are consistent with authors who worked on other species, reporting that, when restoring water volumes lower than ETc, yields were the same as when 100 % of it was replaced (Centofanti *et al*., 2018).

Optimizing irrigation programming made it possible to increase EUAr by 63.5 % compared to the To treatment during the study period, thus validating it as a tool for addressing water stress situations without affecting crop yield. The value was higher than those recorded in Spain by Rodríguez-Pleguezuelo *et al*. (2011) and Durán-Zuazo *et al*. (2019), with 1.4 and 3.3 kg ha^{-1} m^{-3}, respectively. In addition, cost savings were

generated by reducing the amount of electricity used by about 300 USD ha^{-1} (Kaptein *et al*., 2019; Vera *et al*., 2019) (Table 4).

Finally, one of the difficulties in further analyzing the results is the limited availability of published information on this crop. The generation of the KcS, or irrigation factor, during two seasons of work made it possible to provide a new irrigation management tool for an area with particular conditions in Chile, whose final validation will be possible after several years of use and the correct categorization (clustering) of those irrigation sectors that do not have soil sensors.

CONCLUSIONS

The use of soil sensors, compared to the FAO-56 Penman-Monteith method (Kc-ETo), allowed for savings in irrigation water and electricity of up to 30 %, improving irrigation water use efficiency by up to 68 % without affecting yield or fruit size. By calculating a water balance, the use of probes made it possible to obtain values for the practical crop coefficient or irrigation factor, which vary between 0.27 and 0.74 for periods of lower and higher consumption, respectively.

Water depletion in the soil could only be clearly detected by the sensors when reference evapotranspiration (ETo) exceeded 2.25 mm per day, under conditions without water restrictions. Furthermore, the greatest relative hourly depletion by plants occurred between 1:00 p.m. and 4:00 p.m. This type of irrigation optimization strategy, which is site-specific and cost-effective, utilizes new technologies within the framework of Agriculture 4.0 to enable the development of more efficient irrigation management schemes in areas with particular conditions that differ from those under which the ETo-Kc methodology's parameters were established.

ACKNOWLEDGEMENTS

To Mr. Roberto Hernández Codoceo and Ismael Plácido Tomieli, from HC Ltda., La Serena, for their support in conducting the study.

REFERENCES

Abioye EA, Abidin MSZ, Mahmud MSA, Buyamin S, Ishak MHI, Rahman MKIA, Otuoze AO, Onotu P, Ramli MSA. 2020. A review on monitoring and advanced control strategies for precision irrigation. Computers and Electronics in Agriculture 173: 105441. https://doi.org/10.1016/j.compag.2020.105441

Allen RG, Pereira LS, Raes D, Smith M. 1998. Crop evapotranspiration: Guidelines for computing crop water requirements. Irrigation and Drainage Paper No. 56. Food and Agriculture Organization. Rome, Italy. 322 p.

Calera A, Campos I, Osann A, D'Urso G, Menenti M. 2017. Remote sensing for crop water management: From ET modelling to services for the end users. Sensors 17 (5): 1104. https://doi.org/10.3390/s17051104

Callejas-Rodríguez R, Seguel O. 2021. Paquete tecnológico UchileCrea para el control inteligente del riego en sistemas frutícolas. Aqua-LAC Volumen 13 (1): 128–142. https://doi.org/10.29104/phi-aqualac/2021-v13-1-09

Centofanti T, Bañuelos GS, Ayars JE. 2019. Fruit nutritional quality under deficit irrigation: The case of table grapes in California. Journal of the Science of Food and Agriculture 99 (5): 2215–2225. https://doi.org/10.1002/jsfa.9415

Chávez PSJ. 1988. An improved dark-object subtraction technique for atmospheric scattering correction of multispectral data. Remote Sensing of Environment 24 (3): 459–479. https://doi.org/10.1016/0034-4257(88)90019-3

Coelho EF, Campos MS, dos Santos MR, Fernandes RDM, Cruz JL. 2021. Soil water-balance-based approach for estimating percolation with lysimeter and in field with and without mulch under micro irrigation. Ambiente e Agua 16 (5): e2760. https://doi.org/10.4136/ambi-agua.2760

da Silva AO, da Silva BA, Souza CF, Azevedo BM, Bassoi LH, Vasconcelos DV, do Bonfi GV, Juárez JM, dos Santos AF, Carneiro FC. 2020. Irrigation in the age of agriculture 4.0: management, monitoring and precision. Revista Ciência Agronômica 51 (5): e20207695. https://doi.org/10.5935/1806-6690.20200090

Devi MJ, Reddy VR. 2018. Transpiration response of cotton to vapor pressure deficit and its relationship with stomatal traits. Frontiers in Plant Science 9: 1572. https://doi.org/10.3389/fpls.2018.01572

Domínguez-Niño JM, Oliver-Manera J, Girona J, Casadesús J. 2020. Differential irrigation scheduling by an automated algorithm of water balance tuned by capacitance-type soil moisture sensors. Agricultural Water Management 228: 105880. https://doi.org/10.1016/j.agwat.2019.105880

Durán-Zuazo V, Franco-Tarifa D, García-Tejero I, Gutiérrez-Gordillo S, Cermeño-Sacristan P, Pertiñez-Roldan JJ. 2019. Water use and leaf nutrient status for terraced cherimoya trees in a subtropical Mediterranean environment. Hoticulturae 5 (2): 46–56. https://doi.org/10.3390/horticulturae5020046

Gardiazábal F, Rosenberg G. 1993. El cultivo del chirimoyo. Universidad Católica de Valparaíso: Facultad de Agronomía. Valparaíso, Chile. 145 p.

Gasque M, Martí P, Granero B, González-Altozano P. 2016. Effects of long-term summer deficit irrigation on 'Navelina' citrus trees. Agricultural Water Management 169: 140–147. https://doi.org/10.1016/j.agwat.2016.02.028

González M, Cuevas J. 2008. Optimal crop load and positioning of fruit in cherimoya (*Annona cherimola* Mill.) trees. Scientia Horticulturae 115 (2): 129–134. https://doi.org/10.1016/j.scienta.2007.08.002

Hardie M. 2020. Review of novel and emerging proximal soil moisture sensors for use in agriculture. Sensors 20 (23): 6934. https://doi.org/10.3390/s20236934

Higuchi H, Utsunomiya N, Sakuratani T. 1998. High temperature effects on cherimoya fruit set, growth and development under greenhouse condition. Scientia Horticulturae 77 (1–2): 23–31. https://doi.org/10.1016/S0304-4238(98)00160-5

Kaptein ND, Light ME, Savage MJ. 2019. Review: Sensors for the improvement of irrigation efficiency in nurseries. Water SA 45 (3): 527–535. https://doi.org/10.17159/wsa/2019.v45.i3.6750

Kirkham MB. 2005. Principles of soil and plant water relations. Academic Press: Boston, MA, USA. 500 p. https://doi.org/10.1016/B978-0-12-409751-3.X5000-2

Larranaga N, Albertazzi FJ, Fontecha G, Palmieri M, Rainer H, van Zonneveld M, Hormaza JI. 2017. A Mesoamerican origin of cherimoya (*Annona cherimola* Mill.): Implications for the conservation of plant genetic resources. Molecular Ecology 26 (16): 4116–4130. https://doi.org/10.1111/mec.14157

MAPA (Ministerio de Agricultura, Pesca y Alimentación). 2019. Datos avances de frutales no cítricos y frutales secos año 2019. Gobierno de España. Ministerio de Agricultura, Pesca y Alimentación. Madrid, España. https://www.mapa.gob.es/es/estadistica/temas/estadisticas-agrarias/frutalesnocitricosysecosprovisionales2019_tcm30-537041.xls (Retrieved: July 2024).

Martínez-Gimeno MA, Jiménez-Bello MA, Lidón A, Manzano J, Badal E, Pérez-Pérez JG, Bonet L, Intrigliolo DS, Esteban A. 2020. Mandarin irrigation scheduling by means of frequency domain reflectometry soil moisture monitoring. Agricultural Water Management 235: 106151. https://doi.org/10.1016/j.agwat.2020.106151

Pereira LS, Paredes P, Hunsaker DJ, López-Urrea R, Jovanovic N. 2021. Updates and advances to the FAO56 crop water requirements method. Agricultura Water Management 248: 106697. https://doi.org/10.1016/j.agwat.2020.106697

Pizarro E, Galleguillos M, Barría P, Callejas R. 2022a. Irrigation management or climate change? Which is more important to cope with water shortage in the production of table grape in a Mediterranean context. Agricultural Water Management 263: 107467. https://doi.org/10.1016/j.agwat.2022.107467

Pizarro R, García-Chevesich P, McCray J, Sharp J, Valdés-Pineda R, Sangüesa C, Jaque-Becerra D, Álvarez P, Norambuena S, Ibáñez A, Vallejos C, Mendoza R. 2022b. Climate change and overuse: Water resource challenges during economic growth in Coquimbo, Chile. Sustainability 14 (6): 3440. https://doi.org/10.3390/su14063440

Pôças I, Calera A, Campos I, Cunha M. 2020. Remote sensing for estimating and mapping single and basal crop coefficients: A review on spectral vegetation indices approaches. Agricultural Water Management 233: 106081. https://doi.org/10.1016/j.agwat.2020.106081

Rodríguez-Pleguezuelo CR, Durán-Zuazo VH, Francia-Martínez JR, Muriel-Fernández JL, Tarifa DF. 2011. Monitoring the pollution risk and water use in orchard terraces with mango and cherimoya trees by drainage lysimeters. Irrigation and Drainage Systems 25 (2): 61–79. https://doi.org/10.1007/s10795-011-9112-3

SIEA (Sistema Integrado de Estadística Agraria). 2018. Anuario estadístico de producción agrícola. Ministerio de Desarrollo Agrario y Riego. Lima, Perú. http://siea.minagri.gob.pe/siea/sites/default/files/datos-excel-anuario-agricola-2018-070819.xls (Retrieved: July 2024).

Soler L, Cuevas J. 2008. Development of a new technique to produce winter cherimoyas. HortTechnology 18 (1): 24–28. https://doi.org/10.21273/horttech.18.1.24

Vallejo JA. 2024. Tenemos casi 50 millones de kilos de una fruta que no se cultiva en ningún otro lugar en Europa. Fresh Plaza. Tholen, Países Bajos. https://www.freshplaza.es/article/9395086/tenemos-casi-50-millones-de-kilos-de-una-fruta-que-no-se-cultiva-en-ningun-otro-lugar-en-europa/ (Retrieved: June 2024).

Vera J, Conejero W, Conesa MR, Ruiz-Sánchez MC. 2019. Irrigation factor approach based on soil water content: A nectarine orchard case study. Water 11 (3): 589–603. https://doi.org/10.3390/w11030589

Zotarelli L, Dukes MD, Morgan KT. 2023. Interpretación del contenido de la humedad del suelo para determinar capacidad de campo y evitar riego excesivo en suelos arenosos utilizando sensores de humedad. University of Florida: Gainesville, FL, USA. 11 p.

VOLUME 59, NUMBER 5 | July 01 - August 15, 2025 | MEXICO